UNIVERSIDADE ESTADUAL PAULISTA
“JULIO DE MESQUITA FILHO”

INTERAÇÃO ENTRE ALTA LIPOGÊNESE DECORRENTE DE CONDIÇÕES METABÓLICAS COM O COMPORTAMENTO DE OSTEOBLASTOS E DA CÉLULA ENDOTELIAL DESAFIADOS COM TITÂNIO

THAÍS SILVA PINTO

Prof. Dr. Willian Fernando Zambuzzi

Botucatu – SP
Fevereiro/2024

UNIVERSIDADE ESTADUAL PAULISTA

"JULIO DE MESQUITA FILHO"

INTERAÇÃO ENTRE ALTA LIPOGÊNESE DECORRENTE DE CONDIÇÕES METABÓLICAS COM O COMPORTAMENTO DE OSTEOBLASTOS E DA CÉLULA ENDOTELIAL DESAFIADOS COM TITÂNIO

THAÍS SILVA PINTO

Tese apresentada ao Instituto de Biociências, *Campus* de Botucatu, UNESP, para obtenção do título de Doutora, junto ao Programa de Pós-Graduação em Biotecnologia.

Prof. Dr. Willian Fernando Zambuzzi

Botucatu – SP

Fevereiro/2024

P659i

Pinto, Thaís Silva
Interação Entre Alta Lipogênese Decorrente de Condições Metabólicas Com o Comportamento de Osteoblastos e da Célula Endotelial Desafiados com Titânio / Thaís Silva Pinto. -- Botucatu, 2024
179 p.

Tese (doutorado) - Universidade Estadual Paulista (Unesp), Instituto de Biociências, Botucatu
Orientador: Willian Fernando Zambuzzi

1. Implantes de titânio. 2. Osseointegração. 3. Obesidade. 4. Célula endotelial. 5. Osteoblasto. I. Título.

Sistema de geração automática de fichas catalográficas da Unesp. Biblioteca do Instituto de Biociências, Botucatu. Dados fornecidos pelo autor(a).

Essa ficha não pode ser modificada.

UNIVERSIDADE ESTADUAL PAULISTA

Câmpus de Botucatu

ATA DA DEFESA PÚBLICA DA TESE DE DOUTORADO DE THAÍS SILVA PINTO, DISCENTE DO PROGRAMA DE PÓS-GRADUAÇÃO EM BIOTECNOLOGIA, DO INSTITUTO DE BIOCIÊNCIAS - CÂMPUS DE BOTUCATU.

Aos 23 dias do mês de fevereiro do ano de 2024, às 14:00 horas, no(a) Central de Aulas do Instituto de Biociências de Botucatu, realizou-se a defesa de TESE DE DOUTORADO de THAÍS SILVA PINTO, intitulada **Interação Entre Alta Lipogênese Decorrente de Condições Metabólicas Com o Comportamento de Osteoblastos e da Célula Endotelial Desafiados com Titânio**. A Comissão Examinadora foi constituida pelos seguintes membros: Prof. Dr. WILLIAN FERNANDO ZAMBUZZI (Orientador(a) - Participação Presencial) do(a) Departamento de Ciências Químicas e Bioquímicas / Instituto de Biociências de Botucatu - Unesp, Profa Dra CAMILA RENATA CORREA CAMACHO (Participação Presencial) do(a) Departamento de Patologia / Faculdade de Medicina de Botucatu - UNESP, Profa. Dra. CARMEN VERÍSSIMA FERREIRA HALDER (Participação Presencial) do(a) Departamento de Bioquímica e Biologia Tecidual / Instituto de Biologia - Unicamp, Prof. Dr. RODRIGO CARDOSO DE OLIVEIRA (Participação Presencial) do(a) Departamento de Ciências Biológicas / Faculdade de Odontologia de Bauru - USP, Prof. Dr. JOSÉ CAVALCANTE SOUZA VIEIRA (Participação Presencial) do(a) Química e Bioquímica / Instituto de Biociências de Botucatu - Unesp. Após a exposição pela doutoranda e arguição pelos membros da Comissão Examinadora que participaram do ato, de forma presencial e/ou virtual, a discente recebeu o conceito final: Aprovada. Nada mais havendo, foi lavrada a presente ata, que após lida e aprovada, foi assinada pelo(a) Presidente(a) da Comissão Examinadora.

Prof. Dr. WILLIAN FERNANDO ZAMBUZZI

Agradecimentos

Agradeço à minha Mãe, meu Pai e meu Irmão, que mesmo distantes, carrego sempre em meu coração e em meus pensamentos, e estão sempre me apoiando e me amparando. O amor que sinto por eles que me estabiliza e mantém firme para ir atrás dos meus sonhos. Agradeço também ao meu amado Padrasto que é meu segundo Pai e que também me apoia em tudo.

Ao Daniël Bruggeman, que tornou tudo mais fácil e leve desde que entrou na minha vida, e desde então está sempre me apoiando e torcendo por mim. De mãos dadas e com muito amor, juntos caminhamos na mesma direção.

Aos meus amigos e amigas de Taubaté por me permitirem dividir algumas das histórias mais fantásticas que vivi, em especial à Caroline Abou Hala Nunes e ao Marcos Rodrigo Mattje Fernandes.

Aos meus bons amigos da turma 6109R do Bacharel em Farmácia da Fundação Universitária Vida Cristã (Faculdade de Pindamonhangaba), bem como aos meus Professores da Graduação, por todos os momentos e ensinamentos. Em especial à Kátia Almeida.

Aos meus queridos amigos que fiz em Botucatu, sejam os da farmácia Universo Natural, da academia, da UNESP ou de qualquer outra origem, que não permitiram que eu me sentisse sozinha em nenhum momento, sempre me ajudaram como anjos e me proporcionaram momentos incríveis e inesquecíveis. Especialmente à Jéssica Leite Garcia e ao Felipe Prosdocini.

Ao Instituto de Biociências de Botucatu – UNESP, ao Coordenador do PPG em Biotecnologia, a todos os Professores, dos quais tive o privilégio e o prazer de aprender muito e de poder me inspirar. Aos colegas e funcionários do Setor de Química e Bioquímica pelas ajudas, risadas sem fim na cozinha, as comilanças nas confraternizações, pelo café nosso de cada dia e todos os momentos juntos.

Aos membros do Laboratório de Bioensaios e Dinâmica Celular (LaBIO) pela convivência durante todos esses 7 anos. Muito obrigada pela amizade, parceria e competência.

Vou levar em meu coração as boas amizades por toda minha vida. Em especial ao Anderson Moreira Gomes.

Ao meu orientador, Prof. Dr. Willian F. Zambuzzi, por ter me recebido tão bem em seu grupo, por ter me guiado e me encorajado durante todos esses anos, por todo o apoio e ajuda a todo momento. Por compartilhar seu rico conhecimento com brilhantismo e humildade. Cheguei acanhada e com medo em busca de crescimento profissional, mas fui surpreendida com oportunidades e conquistas incríveis que eu não acreditava ser capaz. Obrigada por me fazer seguir firme em busca dos meus sonhos. Agradeço imensamente por tudo!

À S.I.N. Sistema de Implantes, pela doação dos materiais utilizados em nossas pesquisas;

À CAPES, inclusive pela oportunidade de realizar o Programa de Doutorado Sanduíche no Exterior (PDSE). Aproveito e agradeço à Erasmus Medical Center, ao Prof. Dr. Maikel Peppelenbosch e a Prof.ª Dr.ª Gwenny Fuhler por me receberem tão bem em seus grupos de pesquisa durante esse período.

À Fundação de Amparo à Pesquisa do Estado de São Paulo – FAPESP (FAPESP: 2019/26854-2; 2014/22689-3).

Por último, o mais importante, agradeço à Deus pela maneira como conduz a minha vida, pela evolução tanto profissional como pessoal que adquiri nesse período e por me contemplar com tamanhas bençãos, oportunidades e realizações como essa. Me faltam palavras para expressar tanta alegria e gratidão.

“Mas eu confio na Tua benignidade; na Tua salvação, meu coração se alegrará.

Cantarei ao Senhor, porquanto me tem feito muito bem.”

- Sl 13,5s

Resumo

Biomateriais metálicos, especialmente o titânio, são utilizados como implantes odontológicos e ortopédicos, e dependem de processos como angiogênese e osteogênese para garantir o sucesso na implantação. Embora a utilização desses biomateriais seja bem estabelecida, profissionais de saúde enfrentam desafios, como a prolongada recuperação, sobretudo em indivíduos com metabolismo comprometido, como aqueles diagnosticados com obesidade e síndrome metabólica. O impacto dessas condições no processo de regeneração tecidual e osseointegração ainda é pouco compreendido. Estudos indicam que o metabolismo comprometido está associado a alterações na biologia óssea e vascular, prejudicando o microambiente peri-implante. Este estudo investigou as respostas de células endoteliais e osteoblastos ao titânio com diferentes modificações de superfície, como o duplo ataque ácido (DAE) e o revestimento de nanohidroxiapatita (nHA), em condições de alta lipogênese utilizando modelos com adipócitos, organoides de fígado e hepatócitos. Além disso, analisamos células mesenquimais (MSC) obtidas do fêmur de ratos obesos (Obese) e tratados com farelo de arroz (RB). Os modelos de alta lipogênese com adipócitos, organoides hepáticos e hepatócitos, demonstraram um aumento no número e no tamanho das gotículas de lipídeos intracelulares. A célula endotelial, quando exposta ao titânio e à condição adipogênica, mostrou modulações na expressão dos genes VEGF-R1, MAPKs e IL-6, assim como na proteína SRC. Os osteoblastos, quando diferenciados com meio condicionado por adipócitos, organoides de fígado e hepatócitos, exibiram gotículas de gordura intracelular e modulação na expressão de genes relacionados ao osso em resposta ao titânio. O gene RUNX2 foi amplificado nos osteoblastos tratados com titânio nHA em condições lipogênicas dos adipócitos e hepatócitos. Nas MSCs do fêmur de ratos obesos, observou-se um aumento na expressão do gene Runx2 e uma redução em Ppar-γ, Tgfb1 e Osx. Já o grupo Obese + RB elevou a expressão do gene Bglap. Na célula endotelial o titânio nHA estimulou a expressão de genes como VEGF, eNOS e AKT, resultando em uma maior angiogênese e migração celular, juntamente com um aumento no remodelamento da matriz extracelular. Os titânios testados influenciaram vias relacionadas à angiogênese dependente da via PI3K/AKT. Esta pesquisa apresenta contribuições importantes para o entendimento do impacto da alta lipogênese sobre a resposta de células endoteliais e osteoblastos ao titânio *in vitro*, assim como as alterações no perfil de expressão gênica das MSCs em um contexto *ex vivo* com ratos obesos tratados com farelo de arroz (Obese + RB), comprovando que os mecanismos envolvidos no microambiente peri-implantar são impactados nestas condições.

Palavras-chave: Osso; Titânio; Hidroxiapatita; Obesidade; Síndrome metabólica, Célula endotelial; Osteoblasto; Adipócito; Lipogênese.

Abstract

Metallic biomaterials, especially titanium, are widely used as dental and orthopedic implants, relying on processes such as angiogenesis and osteogenesis for successful implantation. Despite the well-established use of these biomaterials, healthcare professionals encounter challenges, such as extended recovery times, particularly in individuals with compromised metabolism, such as those diagnosed with obesity and metabolic syndrome. The impact of these conditions on tissue regeneration and the osseointegration process remains poorly understood. Studies indicate that compromised metabolism is linked to changes in bone and vascular biology, adversely affecting the peri-implant microenvironment. This study aimed to investigate the responses of endothelial cells and osteoblasts to titanium with different surface modifications, including double acid etching (DAE) and nanohydroxyapatite (nHA) coating, under conditions of high lipogenesis using models with adipocytes, liver organoids, and hepatocytes. Furthermore, we analyzed mesenchymal cells (MSC) obtained from the femur of obese rats (Obese) and treated with rice bran (RB). High lipogenesis models with adipocytes, liver organoids, and hepatocytes demonstrated an increase in the number and size of intracellular lipid droplets. The endothelial cell, when exposed to titanium and adipogenic conditions, showed modulations in the expression of VEGF-R1, MAPKs, and IL-6 genes, as well as in the SRC protein. Osteoblasts, when differentiated with medium conditioned by adipocytes, liver organoids, and hepatocytes, exhibited intracellular fat droplets and modulation in the expression of bone-related genes in response to titanium. The RUNX2 gene was amplified in osteoblasts treated with nHA titanium under lipogenic conditions of adipocytes and hepatocytes. In MSCs from the femur of obese rats, an increase in the expression of the Runx2 gene and a reduction in Ppar-γ, Tgfb1, and Osx were observed. The Obese + RB group increased the expression of the Bglap gene. In the endothelial cell, nHA titanium stimulated the expression of genes such as VEGF, eNOS, and AKT, resulting in greater angiogenesis and cell migration, along with an increase in the remodeling of the extracellular matrix. The tested titanium influenced pathways related to angiogenesis dependent on the PI3K/AKT pathway. This research presents important results for understanding the impact of high lipogenesis on the response of endothelial cells and osteoblasts to titanium in vitro, as well as changes in the gene expression profile of MSCs in an ex vivo context with obese rats treated with rice bran (Obese + RB), proving that the mechanisms involved in the peri-implant microenvironment are impacted under these conditions.

Keywords: Bone; Titanium; Hydroxyapatite; Obesity; Metabolic syndrome, Endothelial cell; Osteoblast; Adipocyte; Lipogenesis.

SUMÁRIO

LISTA DE FIGURAS

Capítulo 1:

Capítulo 2:

Capítulo 3:

LISTA DE TABELAS

LISTA DE ABREVIAÇÕES

18S - 18S ribosomal RNA
Actb - Actin beta
AKT – Protein Kinase B
ALP – Alkaline phosphatase
ANOVA – Analysis of Variance
Bglap - Bone gamma-carboxyglutamate protein
Bmpr1 - bone morphogenetic protein receptor 1
BMPs - bone morphogenetic proteins
BM-MSCs - Bone marrow-derived mesenchymal stem cells
BSA – Bovine Serum Albumin
$CaCl_2$ – Calcium chloride
CBO - Protein carbonylation
CDK2 – Cyclin Dependent Kinase 2
cDNA – Complementary DNA
CIDEB - cell death inducing DFFA like effector b
COX - cytochrome c oxidase
CPT1A – carnitine palmitoyltransferase 1A
CPT1B – carnitine palmitoyltransferase 1B
Ct - cycle threshold
CYTB – cytochrome b
DAE – Dual Acid Etched
DMEM – Dulbecco's modified Eagle's medium
DNA - Deoxyribonucleic acid
DNPH - 2,4-dinitrophenyl hydrazine
DTT – Dithiothreitol
ECL - Enhanced ChemiLuminescence
ECM – Extracellular Matrix
ECs – Endothelial cells
EGF - Epidermal growth factor
ELISA - Enzyme-Linked Immunosorbent Assay
eNOS - nitric oxide synthase 3
Erk – mitogen-activated protein kinase 1
FAK – Focal Adhesion Kinase
FBS – Fetal Bovine Serum
FFA – Free fatty acids
FGF - fibroblast growth factor
GADPH – Glyceraldehyde 3-phosphate dehydrogenase
GFAAS - Graphite Furnace Atomic Absorption Spectrometry
HA – Hidroxiapatite
HAnano® - surface blasted with nanosized hydroxyapatite
HCl - *Hydrochloric acid*
HGF *- Hepatocyte growth factor*
HGM – High Glucose Medium
hMSC – human mesenchymal stem cell
HSF - High-sugar fat
Huh7 - Human hepatocyte cell line
HUVEC - *Human umbilical vein endothelial cells*
IBMX - 3-isobutyl-1-methylxanthine
IL – Interleukin
iNOS - nitric oxide synthase 2
JNK – C-Jun N-terminal Kinase
LEM – Liver Organoids Expansion Medium
LPO – Lactate, Pyruvate, Octanoic acid
Mac – Machined (for implants surfaces)
MAPK – Mitogen-Activated Protein Kinase
MEC – Matriz extracelular
MMP – Matrix Metalloproteinase
MSC - mesenchymal stem cell
MTT - 3-(4,5-dimethyl-2-thiazolyl)-2,5-diphenyl-2H-tetrazolium bromide
MW - molecular weight
Myd88 - MYD88 innate immune signal transduction adaptor
NaCl - Sodium chloride
NAFLD - nonalcoholic fatty liver disease.
NaOH - sodium hydroxide
NFKB1 - nuclear factor kappa B subunit 1

nHA – surface blasted with nanosized hydroxyapatite
NO - Nitric oxide
OA – Oleic acid
OPG – Osteoprotegerin (TNF receptor superfamily member 11b)
OSX – Osterix
P38 - Mitogen-activated protein kinase 14
PA – Palmitic acid
PBS - *Phosphate-buffered saline*
PDGF - Platelet-derived growth factor
PFA - Paraformaldehyde
PI3K - phosphatidylinositol-4,5-bisphosphate 3-kinase
PKB – Protein Kinase B
PNPLA3 - patatin like phospholipase domain containing 3
PPARA – peroxisome proliferator activated receptor alpha
Pparg - Peroxisome proliferator activated receptor gamma
PVDF – Polyvinylidene difluoride
qPCR – Quantitative polymerase chain reaction
RANKL - TNF superfamily member 11
RB - Rice Bran
RNA - Ribonucleic acid
RP2 - RP2 activator of ARL3 GTPase
RPM - Revolutions per minute
RPMI – Cell culture growth medium (Roswell Park Memorial Institute)
RT - Room temperature
RT-qPCR – Real Time-quantitative Polymerase Chain Reaction
RUNX2 – Runt-Related Transcription Factor 2
SD - Standard deviation
SDS-PAGE – Sodium Dodecyl Sulfate Polyacrylamide Gel Electrophoresis
SEM – Standard Error of the Mean
Src – SRC proto-oncogene, non-receptor tyrosine kinase
SREBP1 - sterol regulatory element binding transcription factor 1
T2DM - Type 2 diabetes mellitus
TBS - Tris-buffered saline
TGFB1 - transforming growth factor beta 1 (TGF-β)
Ti – Titanium
TIMP - Tissue Inhibitor of Matrix Metalloproteinases
TiO_2 - Titanium dioxide
TM6SF2 - transmembrane 6 superfamily member 2
Tnf - Tumor necrosis factor (Tnfa; TNFα**)**
Tnfr1 - Tumor necrosis factor receptor superfamily, member 1A
Tnfr2 - TNF receptor superfamily member 1B
v/v – volume / volume
VEGF - Vascular endothelial growth factor
VEGFr1 - fms related receptor tyrosine kinase 1
VEGFr2 - kinase insert domain receptor
w/DAE – With Dual Acid Etched
w/v – weight / volume
wo/DAE – Without Dual Acid Etched
αMEM – Alpha Minimum Essential Media
γOz - Gamma-oryzanol

Capítulo 1

INTRODUÇÃO

Um aumento global significativo na prevalência da obesidade e das complicações metabólicas associadas vêm ocorrendo. Aproximadamente 40% da população mundial é afetada pela obesidade ou sobrepeso, sendo essa condição reconhecida como um fator de risco significativo da síndrome metabólica (X. Lin & Li, 2021). A síndrome metabólica compreende uma combinação de fatores de risco, incluindo obesidade abdominal, pressão arterial elevada, níveis aumentados de glicemia e dislipidemia. Esses fatores aumentam a probabilidade de desenvolvimento de doenças cardiovasculares, diabetes tipo 2, esteatose hepática e várias outras complicações de saúde (Huang, 2009). Notavelmente, distúrbios metabólicos como a obesidade são amplamente reconhecidos pela sua associação com danos no reparo e regeneração tecidual, incluindo em tratamentos com implantes metálicos, dificultando predominantemente o processo de cicatrização de feridas (Cheng, Ball, Gonzales, Schenk, & Hughes-Austin, 2020), isso ocorre provavelmente devido ao aumento da condição pró-inflamatória sistêmica e ao aumento do risco de complicações associadas ao implante, como de infecção, chamada peri-implantite (de Oliveira et al., 2020).

A obesidade é uma doença crônica multifatorial, caracterizada principalmente pelo acúmulo de gordura no tecido adiposo que com sua saturação acomete outros tecidos e que confere ao indivíduo o aumento de peso e um perfil metabólico pró-inflamatório e desregulado cronicamente (Engin, 2017). A prevalência dessa doença continua crescendo mesmo com avanços no conhecimento de sua fisiopatologia e com algumas opções terapêuticas (mas que sabidamente apresentam efeitos colaterais) (González-Muniesa et al., 2017). Devido ao crescente número de casos de obesidade no mundo (Fig.1) espera-se também o crescimento no número de pacientes obesos que receberão implante de titânio, passando a fazer parte de uma parcela importante da população que apresenta o metabolismo comprometido e que preocupa os profissionais da área da saúde (de Oliveira et al., 2020).

Embora existam várias métricas, o método predominante de diagnóstico da obesidade continua sendo o cálculo do Índice de Massa Corporal (IMC). O IMC é determinado pela relação entre o peso de um indivíduo em quilogramas e sua altura em metros quadrados (kg/m^2). Utilizando o IMC como ferramenta de medição e diagnóstico,

categoriza-se os indivíduos em três grupos principais: normais (<25 kg/m²), sobrepeso (entre 25 e 29 kg/m²) e obesos (>30 kg/m²) (Nuttall, 2015).

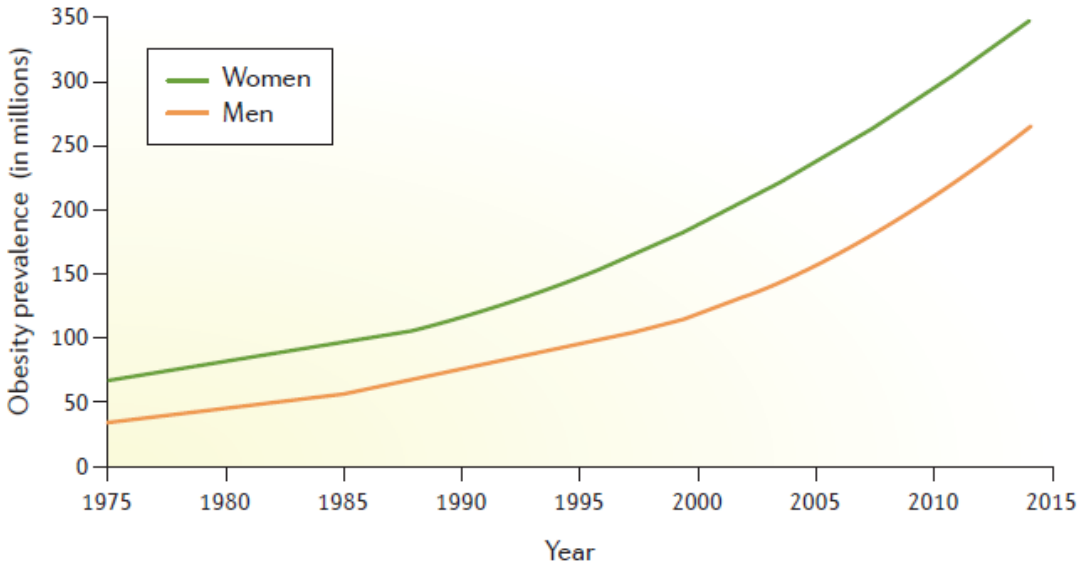

Fig. 1 Notável aumento na prevalência global da obesidade. De 1975 em diante, a incidência de obesidade quase triplicou em escala mundial, com taxas mais elevadas observadas em mulheres em comparação com homens. Além disso, o índice de massa corporal médio padronizado por idade global teve um aumento consistente, crescendo 0,4 kg/m² por década nos homens e 0,5 kg/m² nas mulheres de 1980 a 2008 (González-Muniesa et al., 2017).

O tecido adiposo serve principalmente ao propósito de armazenar energia através do acúmulo de gotículas de gordura intracelular nos adipócitos. Essas gotículas abrigam sobretudo o triacilglicerol, que é posteriormente quebrado em ácidos graxos e glicerol, e mobilizado quando o corpo necessita de energia adicional (Frühbeck, Méndez-Giménez, Fernández-Formoso, Fernández, & Rodríguez, 2014). O tecido adiposo é reconhecido não apenas como o principal reservatório para armazenamento de energia proveniente da ingestão alimentar, mas também como um órgão endócrino, exercendo atividades sistêmicas através de sinalização parácrina e endócrina (Feijóo-Bandín et al., 2020). Em períodos de balanço energético positivo, o tecido adiposo acumula energia excedente, armazenando triglicerídeos nas gotículas lipídicas dos adipócitos e esse armazenamento ocorre através de um aumento no número dessas células (hiperplasia) ou de um aumento no tamanho dos adipócitos existentes (hipertrofia) (Hausman, DiGirolamo, Bartness, Hausman, & Martin, 2001). Embora a ocorrência geral da obesidade esteja ligada a distúrbios metabólicos, propõe-se que a disfunção no tecido adiposo resultante da

hipertrofia desempenhe especificamente um papel significativo no aparecimento de condições metabólicas como a doença hepática gordurosa não alcoólica (DHGNA) (Kim et al., 2007; Machado & Cortez-Pinto, 2023). No contexto da obesidade, o acúmulo excessivo de gordura estimula a liberação de ácidos graxos livres na corrente sanguínea, agindo potencialmente como um fator crucial na formação da resistência à insulina (Boden, 2008; Perseghin, Ghosh, Gerow, & Shulman, 1997). Além disso, os ácidos graxos livres podem acessar diretamente o fígado através da circulação portal, e dessa forma, níveis elevados de ácidos graxos livres hepáticos contribuem para o aumento da síntese lipídica, gliconeogênese e resistência à insulina no fígado (Jung & Choi, 2014).

O acúmulo excessivo de gordura e a disfunção nos adipócitos levam à ruptura de numerosos fatores secretórios originados do tecido adiposo, observa-se assim, um desequilíbrio no perfil de liberação de moléculas sinalizadoras, como de interleucinas inflamatórias e nas adipocinas que atuam diretamente nos sistemas ou indiretamente via hipotálamo (Feijóo-Bandín et al., 2020).

A manutenção do equilíbrio metabólico surge da comunicação intrincada e bidirecional entre tecidos metabólicos cruciais, como tecido adiposo e fígado. Esta comunicação, convencionalmente facilitada por hormônios e metabólitos, sofre perturbações em condições como a obesidade, levando à desregulação (Luo & Liu, 2016). Um crescente conjunto de evidências indica que a inflamação persistente no tecido adiposo pode ser um fator crucial no início da disfunção metabólica associada à obesidade (Jung & Choi, 2014).

Como referido, a crescente epidemia mundial de obesidade é acompanhada por um aumento preocupante de indivíduos que enfrentam distúrbios hepáticos, principalmente a doença hepática gordurosa não alcoólica (DHGNA). A prevalência da DHGNA vem aumentando constantemente a uma taxa anual de 1%, já afetando 30% da população mundial (Machado & Cortez-Pinto, 2023).

A DHGNA está associada a fatores como obesidade, resistência à insulina e síndrome metabólica. Essa doença progride por estágios, começando com a esteatose simples, onde o excesso de gordura se acumula nas células do fígado, e pode avançar para a esteatohepatite não alcoólica, caracterizada por inflamação e danos às células do fígado. Se não for controlada, a esteatohepatite pode causar fibrose, cirrose e um risco aumentado de complicações relacionadas ao fígado (Paschos & Paletas, 2009). O fígado desempenha um papel fundamental no gerenciamento do metabolismo da gordura, orquestrando a integração de ácidos graxos produzidos internamente e obtidos externamente, e esse

acúmulo ou redução de gordura no fígado reflete o equilíbrio entre as vias que captam e eliminam ácidos graxos, que em condições comprometidas, como a DHGNA, esses papéis críticos no metabolismo da gordura podem ser afetados negativamente (Ipsen, Lykkesfeldt, & Tveden-Nyborg, 2018).

Como mencionado inicialmente, distúrbios metabólicos como a obesidade estão bem estabelecidos pela sua correlação com a reparação e regeneração tecidual prejudicada, afetando particularmente intervenções que envolvem implantes metálicos e impedindo significativamente o curso natural da cicatrização de feridas (Cheng et al., 2020). Vale destacar nesses processos a importância do suprimento sanguíneo adequado exercido pelos vasos sanguíneos, sendo que dentre as alterações vasculares iniciais observadas na obesidade, destaca-se a disfunção endotelial (Tran et al., 2023). Os mecanismos que impulsionam a disfunção endotelial estão principalmente associados à diminuição da produção e disponibilidade de óxido nítrico, juntamente com a presença de estresse oxidativo (Martínez-Martínez, Souza-Neto, Jiménez-González, & Cachofeiro, 2021). Por sua vez, uma crescente onda de relatos têm abordado implicações advindas da obesidade sobre o metabolismo ósseo, prejudicando processos naturais de formação e reabsorção óssea, bem como o processo de osseointegração frente a um implante, como os implantes de titânio (Cao, 2011; Greco, Lenzi, & Migliaccio, 2015; Monteiro, Pellizzer, Araújo Lemos, de Moraes, & do Egito Vasconcelos, 2019).

Por várias décadas o titânio é utilizado como dispositivo médico e biomaterial implantável nos diferentes tecidos, por exemplo, no tecido ósseo como *scaffolds*, e como *stents* tubulares, por exemplo, no endotélio vascular e no esôfago, mas mais comumente no tecido ósseo na área da ortopedia e na odontologia (Girón et al., 2021). O titânio possui importantes características que confere a esse biomaterial metálico adequada aplicabilidade, a citar, a sua elevada resistência à corrosão e força mecânica, boa biocompatibilidade, baixa toxicidade, entre outros, sendo assim o implante mais utilizado mesmo existindo outras opções de biomaterial metálico disponíveis comercialmente (Sidambe, 2014).

Ao longo dos anos o titânio veio sendo otimizado com o intuito de acelerar o processo de recuperação pós-cirúrgico bem como evitar complicações decorrentes do processo de implantação. Tais otimizações vão desde uma alteração no seu formato e apresentação até modificações de superfície que modulam a texturização ou que

adicionam algum revestimento (Bezerra et al., 2017; Fernandes et al., 2018; Sartoretto et al., 2020). As modificações de superfície têm o intuito de melhorar a osseointegração, o contato direto osso e implante e a adaptação do tecido peri-implante (Khosravi, Maeda, DaCosta, & Davies, 2018), sendo importante lembrar que o tecido peri-implante abrange não só o tecido ósseo, mas também o tecido endotelial (situado nos vasos sanguíneos que irrigam o local da lesão) e os tecidos moles (I, Noda, Ohba, Asahina, & Sumita, 2023).

Apesar do titânio ser bem estabelecido nas práticas clínicas, bem como suas alterações e otimizações, muito trabalho ainda precisa ser realizado já que vários desafios ainda são enfrentados pelos profissionais da área da saúde, como os casos de demasiada demora na recuperação, de rejeição tecidual e casos de infecção (peri-implantite), situações que apresentam maior risco de tratamento e que são mais comuns em pacientes com alterações sistêmicas e metabólicas, com potencial de resposta cicatricial comprometida (Coelho et al., 2018). Dentro dessa temática, pacientes com metabolismo não sadio, como os diagnosticados com síndrome metabólica, tem preocupado médicos e dentistas, por apresentarem metabolismo e sistemas comprometidos com consequente atividade celular disfuncional, podendo apresentar problemas no mecanismo de regeneração e reparo tecidual, bem como de osseointegração (de Oliveira et al., 2020).

Para enfrentar estes desafios, os esforços têm sido direcionados para melhorar o desempenho dos implantes de titânio para acelerar a recuperação pós-cirúrgica e mitigar potenciais complicações associadas ao procedimento de implantação. Isto envolve a otimização do titânio através de técnicas como modificações de superfície que alteram a topografia da superfície e/ou aplicam revestimentos com funcionalidades específicas (Bezerra et al., 2017; Fernandes et al., 2018; Sartoretto et al., 2020). Duas técnicas comuns para modificação de superfície são o duplo ataque ácido (*Dual Acid Etching*, *DAE*) e o jateamento com nanohidroxiapatita (nHA):

→ O duplo ataque ácido (DAE) envolve o tratamento da superfície do implante de titânio com uma combinação de ácidos fortes, normalmente uma mistura de ácido clorídrico (HCl) e ácido sulfúrico (H_2SO_4). Este processo cria uma textura superficial microrrugosa no implante, aumentando sua energia superficial e proporcionando um maior grau de molhabilidade. Esta microrrugosidade visa promover uma melhor adesão de proteínas e facilitar a fixação celular, apoiando em última análise os estágios iniciais da osseointegração. A superfície DAE é conhecida por sua capacidade de melhorar a fixação

biomecânica do implante e acelerar a cicatrização óssea (Al-Radha, 2016; Hung, Lin, & Feng, 2017).

→ A nanohidroxiapatita (nHA) é um material biocompatível, neste método de modificação de superfície, o implante de titânio, após receber o duplo ataque ácido, é jateado com partículas de hidroxiapatita (o componente mineral do osso natural) em nanoescala. Isso cria uma superfície com características nanométricas e uma camada de hidroxiapatita, proporcionando um ambiente biomimético que melhora a osteocondutividade do implante. A presença de hidroxiapatita estimula a formação de uma camada de fosfato de cálcio na superfície do implante, imitando a composição mineral óssea natural. Esta camada promove ainda mais a osseointegração, facilitando a interação entre o implante e o tecido ósseo circundante (Bezerra et al., 2017; A. Lin, Wang, Kelly, Gubbi, & Nishimura, 2009).

Tanto DAE quanto nHA visam melhorar a resposta biológica aos implantes de titânio, criando superfícies que promovem a fixação celular, adsorção de proteínas e subsequente formação óssea. A seleção entre essas técnicas depende de vários fatores, incluindo a aplicação específica, a rugosidade superficial desejada e a resposta biológica direcionada. Os profissionais de saúde encontram valor em testes e ensaios que identificam a abordagem mais adequada para um determinado público-alvo, contribuindo para a otimização do desempenho e o sucesso a longo prazo dos implantes de titânio em aplicações biomédicas (Bezerra et al., 2017; da Silva et al., 2020; Fernandes et al., 2018; Rossi et al., 2017).

Diante deste cenário e da problemática apresentada, há uma necessidade discernível de iniciativas de pesquisa que investiguem as influências metabólicas na saúde óssea e endotelial, decorrente da disponibilidade limitada de modelos *in vitro* cientificamente relevantes e translacionais para estudar os efeitos de condições como obesidade e DHGNA em implantes de titânio. O presente estudo emprega diferentes metodologias *in vitro* adaptadas especificamente para correlacionar as condições biológicas, especialmente aquelas associadas a esses estados patológicos. O objetivo principal é explorar de forma abrangente as interações potenciais entre condições metabólicas com elevada lipogênese, função das células endoteliais e a diferenciação de osteoblastos em resposta a um ambiente enriquecido com titânio. A investigação começa com um modelo de alta adipogenicidade utilizando adipócitos, examinando seu impacto

nas células endoteliais e na diferenciação de osteoblastos quando expostos a um meio enriquecido com titânio. Além disso, é proposto também um modelo validado de alta lipogênese *in vitro,* correlacionado com esteatose hepática, utilizando organoides de fígado e hepatócitos para observar seu impacto na diferenciação de osteoblastos na presença do titânio. E ainda, uma análise de um modelo *ex vivo* com células tronco mesenquimais extraídas do fêmur de ratos tratados com dieta rica em açúcar e gordura também é proposta.

No âmbito da pesquisa científica inúmeras metodologias *in vitro* que emulam ou aproximam cenários em sistemas biológicos têm sido projetadas, incluindo aqueles que envolvem patologias. A ciência básica e as fases pré-clínicas da investigação científica desempenham um papel fundamental na definição das etapas subsequentes, orientando principalmente o foco da investigação nas fases clínicas. Neste contexto, as metodologias que permitem um exame mais matizado dos eventos biológicos e o desenvolvimento de modelos preditivos para respostas sistêmicas têm merecido atenção. As análises *in vitro*, como o cultivo de células, apesar de suas limitações, oferecem vantagens notáveis, como garantir condições uniformes para todos os constituintes de um grupo de estudo. Isto contrasta com experimentos *in vivo* onde variações genéticas, fatores ambientais, hábitos e hormônios podem introduzir interferência. Além disso, o cultivo celular facilita a análise celular detalhada e fornece *insights* sobre a bioquímica de macromoléculas e sinalização celular implicada em alterações fenotípicas. As descobertas derivadas de técnicas *in vitro* podem posteriormente informar e refinar os objetivos dos estudos *in vivo* envolvendo animais experimentais, inclusive contribuindo com o princípio dos três erres da ciência (do inglês: *Replacement, Reduction and Refinement*), criado por Russel & Burch em 1959.

Tendo em mente os desafios associados à utilização de implantes de titânio na clínica médico-odontológica, particularmente no intricado meio molecular de indivíduos com obesidade e DHGNA, algumas questões específicas foram levantadas, dentre elas:

1. Como os distúrbios decorrentes da síndrome metabólica, especificamente a obesidade e a DHGNA, impactam os processos de reparo, regeneração e osseointegração tecidual na presença de titânio?

2. A angiogênese e a rede vascular que irriga o tecido são suscetíveis à interferência de moléculas circulantes associadas à obesidade?
3. Que moléculas específicas desempenham papéis fundamentais nestes processos complexos?

OBJETIVOS

Partindo desse contexto, o objetivo geral desta tese é provar a hipótese, por meio de modelos *in vitro*, do impacto da alta lipogênese, correlacionando com a obesidade e a doença hepática gordurosa não alcoólica (DHGNA), no comportamento das células endoteliais e de osteoblastos em resposta ao titânio utilizado como implante. Pretende-se com isso elucidar os mecanismos pelos quais a lipogênese alterada pode influenciar a integração de implantes, contribuindo futuramente para o desenvolvimento de estratégias terapêuticas mais eficazes na regeneração óssea e na osseointegração em pacientes obesos ou com DHGNA.

Capítulo 2

Adipogenesis-Related Metabolic Condition Affects Shear-Stressed Endothelial Cells Activity Responding to Titanium

Thaís Silva Pinto, Anderson Moreira Gomes, Paula Bertin de Morais and Willian F. Zambuzzi *

Lab. of Bioassays and Cellular Dynamics, Department of Chemical and Biological Sciences, Institute of Biosciences, UNESP—São Paulo State University, Botucatu 18618-970, SP, Brazil

* Correspondence: w.zambuzzi@unesp.br

ARTIGO PUBLICADO:

Pinto TS, Gomes AM, de Morais PB, Zambuzzi WF. Adipogenesis-Related Metabolic Condition Affects Shear-Stressed Endothelial Cells Activity Responding to Titanium. J Funct Biomater. 2023 Mar 17;14(3):162. doi: 10.3390/jfb14030162. PMID: 36976086; PMCID: PMC10052724.

Abstract

Purpose: Obesity has increased around the world. Obese individuals need to be better assisted, with special attention given to dental and medical specialties. Among obesity-related complications, the osseointegration of dental implants has raised concerns. This mechanism depends on healthy angiogenesis surrounding the implanted devices. As an experimental analysis able to mimic this issue is currently lacking, we address this issue by proposing an in vitro high-adipogenesis model using differentiated adipocytes to further investigate their endocrine and synergic effect in endothelial cells responding to titanium. Materials and methods: Firstly, adipocytes (3T3-L1 cell line) were differentiated under two experimental conditions: Ctrl (normal glucose concentration) and High-Glucose Medium (50 mM of glucose), which was validated using Oil Red O Staining and inflammatory markers gene expression by qPCR. Further, the adipocyte-conditioned medium was enriched by two types of titanium-related surfaces: Dual Acid-Etching (DAE) and Nano-Hydroxyapatite blasted surfaces (nHA) for up to 24 h. Finally, the endothelial cells (ECs) were exposed in those conditioned media under shear stress mimicking blood flow. Important genes related to angiogenesis were then evaluated by using RT-qPCR and Western blot. Results: Firstly, the high-adipogenicity model using 3T3-L1 adipocytes was validated presenting an increase in the oxidative stress markers, concomitantly with an increase in intracellular fat droplets, pro-inflammatory-related gene expressions, and also the ECM remodeling, as well as modulating mitogen-activated protein kinases (MAPKs). Additionally, Src was evaluated by Western blot, and its modulation can be related to EC survival signaling. Conclusion: Our study provides an experimental model of high adipogenesis in vitro by establishing a pro-inflammatory environment and intracellular fat droplets. Additionally, the efficacy of this model to evaluate the EC response to titanium-enriched mediums under adipogenicity-related metabolic conditions was analyzed, revealing significant interference with EC performance. Altogether, these data gather valuable findings on understanding the reasons for the higher percentage of implant failures in obese individuals.

Keywords: bone; wound healing; adipogenesis; obese; dental implants; titanium; failure; angiogenesis.

1. Introduction

Physiological changes in obese patients are widely studied due to their systemic complications. The comorbidities known to be associated with obesity include cardiovascular, pulmonary, renal, endocrine, and musculoskeletal problems (e.g., arthrosis, osteoarthritis, back and joint pain), as well as impaired wound healing [1]. It is known that the adipose tissue develops endocrine activity by secreting bioactive substances, named adipokines, that can reach all systems and develop important roles in metabolism [2]. In obese individuals there is a dysfunction of the adipose tissue, presenting higher adipogenesis (high number and size of adipocytes, as well as intracellular fat droplets) that directly affects the profiles of released adipokines, including an increase in proinflammatory interleukin secretion, which triggers different responses systemically, including in the cardiovascular system and vasculature [3].

The vasculature exerts an important function in supplying blood to the whole body, delivering oxygen, nutrients, and essential factors to ensure adequate physiologic and metabolic functioning, also guaranteeing adequate tissue regeneration and repair in cases of injuries, when the vasculature also provides undifferentiated cells [4]. In this context, the endothelial cells (ECs), present along the luminal surface of the blood vessels, develop a central role in vascular activity by perceiving and responding to the changes in chemical and mechanical factors in the blood [5–8]. It is important to mention that angiogenesis is a decisive event during tissue healing [9] and it has been shown that ECs differently respond to metallic implantable medical devices, such as titanium alloys [10–12].

Titanium is commonly used as a biomaterial in several dental and medical fields, e.g., implantology, orthopedics, cardiology, and gastroenterology [13]. This metallic alloy is considered the gold standard for these purposes because it possesses important properties such as mechanical and corrosion resistance and proper biocompatibility [14]. After biomaterial implantation, the reactional tissue surrounding the implants suffers adaptation processes that require blood supplements through the blood vessels, highlighting the importance of EC activities and angiogenesis [15]. In addition, studies have revealed that angiogenesis and osteogenesis are coupled processes, and shown that better osseointegration occurs by interfering with the process of appositional new bone growth [16]. This coupling between cells seems to be affected in specific metabolic conditions, such as diabetes and obesity.

In fact, obesity is related to severe complications in the process of bone healing and osseointegration, likely because it provokes a burst of pro-inflammatory involvement, and an increased risk of bone loss [17]. The explanation for the obesity-related tissue regeneration complications lies in the effects of the unbalanced adipose-derived proinflammatory cytokines and adipokines [18], however, the biology involved in this context is barely known.

Thus, studies exploring the metabolic effects of high adipogenicity on different systems are needed, as well as strategies and alternative technologies and methodologies to study these conditions and predict biological responses. In this context, in vitro methods and analyses, such as cell culture, have the relevant advantages, despite presenting a huge set of limitations in comparison to in vivo protocols arising from age, genetics, environments, habits, hormones, etc. Furthermore, many in vitro methodologies capable of mimicking or closely addressing scenarios in biological systems, as well as in the presence of pathologies, have been proposed and used to guide preclinical experiments.

Using in vitro methodologies, we investigated the potential crosstalk between adipogenicity-related metabolic conditions and ECs responding to a titanium-enriched medium. Specifically, we demonstrate the proof of concept of the creation of the high adipogenicity model using an adipocyte cell line, and observed its interference with EC activity. Altogether, these data gather new findings to understand the higher rate of failure of implants in obese individuals.

2. Methods

2.1. Implants

This experimental workflow was performed using two titanium surfaces, as follows: Dual Acid-Etched (DAE) and nanohydroxyapatite-coated surfaces (nHA). Both set of titanium discs were kindly provided by S.I.N.—Sistema Nacional de Implantes (Sao Paulo, SP, Brazil). The nHA titanium surface is described in more detail elsewhere by Gottlander et al. (1997) and Meirelles et al. (2008) [19,20].

2.2. Reagents

Dulbecco's modified Eagle's medium (DMEM), Fetal Bovine Serum (FBS), trypsin, penicillin, and streptomycin (antibiotics) were obtained from Nutricell (Campinas, Sao Paulo, Brazil). Trypan Blue (T6146), acetic acid glacial (695092), (3-

(4,5-dimethylthiazol-2-yl)-2,5-diphenyltetrazolium bromide) (MTT) (M2128), ethanol (459844), Oil Red O (O0625), 3-isobutyl-1-methylxanthine (IBMX) (I5879), Dexamethasone (D1756), β-glycerophosphate (G9422), glucose (G-5400) and insulin (I2643) were obtained from Sigma Chemical Co. (St. Louis, MO, USA). The antibodies #9102, #8690, #3700, and #2109 were obtained from Cell Signaling Technology (Beverly, MA, USA). TRIzol™ reagent (15596026), DNase I (18068015), and the High-Capacity cDNA Reverse Transcription Kit (4368814) were purchased from Thermo Fisher Scientific Inc. (Waltham, MA, USA). GoTaq qPCR Master Mix (A6002) was obtained from PROMEGA (Madison, WI, USA). Oligonucleotides for gene expression were purchased from Exxtend (Campinas, São Paulo, Brazil).

2.3. Cell Culture

Two cell lines were used in this study: both 3T3-L1 preadipocytes (passage < 10) and Human Umbilical Vein Endothelial Cells (HUVECs; ECs) (ATCC; CRL1730; passage < 10) were cultured in Dulbecco's modified Eagle's medium (DMEM—Nutricell, Campinas, Brazil) containing penicillin 100 U/mL, streptomycin 100 mg/mL, and 10% fetal bovine serum (FBS). The adipocyte differentiation is described below. Importantly, ECs were cultured subjected to a shear stress model, as is described in detail below. In all experiments, the cells were maintained at 37°C with a 5% CO_2 and 95% humidity environment.

2.4. Adipocyte Differentiation

The 3T3-L1 adipocyte cultures were maintained in 100 mm culture dishes in DMEM supplemented with 10% FBS and 1% penicillin/streptomycin at 37°C, 5% CO_2, and 95% humidity until reaching proper confluence. Then, adipocyte differentiation was induced by supplementing the cell culture medium with insulin (1 mg/mL), dexamethasone (1 mM), and 3-isobutyl-1-methylxanthine (IBMX) (0.5 mM), which was used to expose the cells for 3 days. The medium was changed to maintenance DMEM containing 10% FBS and insulin (1 mg/mL) for an additional 7 days (completing 10 days in toto), being changed every 2 days in the meantime. This differentiation process was followed under 2 separate experimental conditions; one under normal conditions (Ctrl), and the other subjected to a high-glucose medium (HGM) to induce higher adipogenesis, reaching a final glucose concentration of 50 mM. The cultures were maintained up to 10

days, at which point the cells were harvested and the conditioned medium collected to further expose ECs.

2.5. Shear Stress Model

ECs were seeded in the peripheral area of previously modified 100 mm culture dishes (Figure 1). The modification in the 100 mm culture dishes was made by using medical silicone to bond a 60 mm culture dish at the center-bottom of the 100 mm culture dishes. Thereafter, the modified dishes were sterilized using UV light for 30 min. To perform the model, the ECs were exposed to the tension forces induced by the circuit of shear stress triggered by the rotations of an orbital shaker (Scilogex, Rocky Hill, CT, USA) placed in the cell culture incubator, as in other experiments [21,22]. We calculated the maximal wall shear stress of ~3 Pa (physiological arterial shear stress = ~1–4 Pa) by using this equation: $\tau max = \alpha\sqrt{\rho\eta(2\pi f)}3$. This equation encompasses the τmax that is the shear stress (Pascal), α is the radius of orbital rotation (12 cm), ρ is the density of the cell culture medium (937.5 kg/m^3), η is the viscosity of the cell culture medium (7.5 x 10^{-4} Pa s), and f is the frequency of rotation.

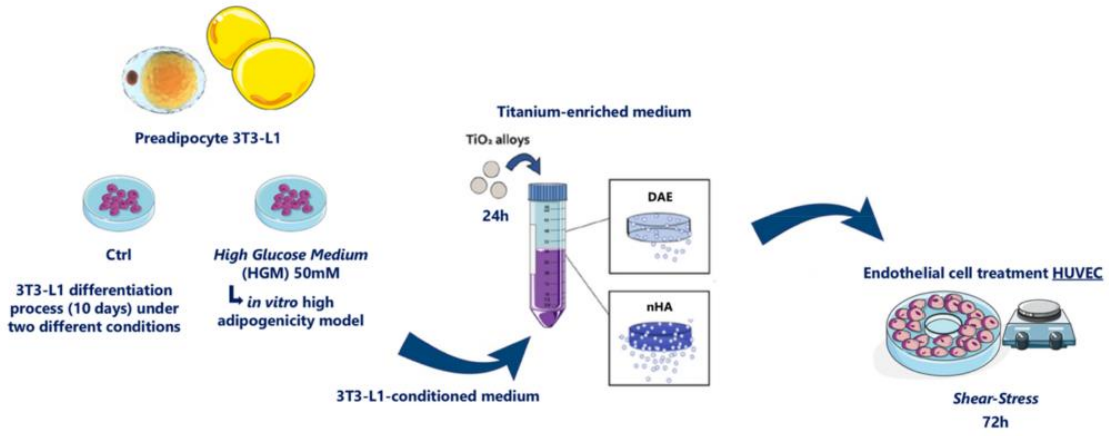

Figure 1. Outline and workflow. To evaluate the ECs behavior in response to titanium-enriched medium in concomitance with high adipogenesis conditions arising from 3T3-L1 adipocytes, we collected the medium conditioned by the adipocytes during their differentiation, which was later enriched with titanium for up to 24 h, as recommended by ISO 10993:2016. This conditioned medium was also further used to expose ECs for 72 h under shear stress mimicking blood flow, at which point the samples were collected to allow the molecular analysis.

2.6. Cell Viability Assay

The high-glucose medium was prepared previously at 50 mM final concentration. Concomitantly, the 3T3-L1 adipocytes were maintained on 96-well plates (5 x 10^4 cells/mL) and later incubated for up to 24 h. One group of cells was treated with the HGM to evaluate whether the high glucose concentration would affect cell viability. The control group contained cells under normal cell culture conditions. The cells were maintained in both treatments (Ctrl and HGM 50 mM) for up to 72 h, after which the cell viability was measured by adding 1 mg/mL of 3-(4,5-dimethyl-2-thiazolyl)-2,5-diphenyl-2H-tetrazolium bromide (MTT) to evaluate the mitochondrial dehydrogenase activity through the MTT reduction reaction after 3 h in a CO_2 incubator. During this reaction, the yellow-colored watersoluble tetrazolium salt MTT becomes the purple-colored soluble compound formazan proportional to mitochondrial activity. The dye of formazan was later dissolved in DMSO, and the absorbance was measured at 570 nm (Synergy II; BioTek Instruments,Winooski, VT, USA).

2.7. Oil Red O Staining

Previously, Oil Red O solution was obtained by dissolving the Oil Red O dye in propylene glycol (0.5%; w/v) in a heater at 95°C. By using a 0.45 μm syringe filter the Oil Red O solution was filtered to eliminate residual particulates from the solution and later used to stain the adipocytes. Adipocytes were differentiated for 10 days using a 24-well plate. At the end of differentiation, the medium was removed, the cells were washed with warm PBS, fixed in 4% paraformaldehyde for 10 min at room temperature, washed twice in deionized water, and then maintained in absolute propylene glycol for 5 min. The cells were stained in Oil Red O solution 0.5% up to 30 min at room temperature, then washed in 85% propylene glycol solution for 3 min. Finally, 3T3-L1 was washed twice in deionized water. Images were acquired using an inverted microscope (Axio Vert.A1, Carl Zeiss microscopy GMBH, Göttingen, Germany).

2.8. Titanium-Enriched Medium Obtaining

Adipocyte-related conditioned medium was later used to incubate both types of titanium disc for 24 h: DAE and nHA, in accordance with ISO 10993:2016 (0.2 g/mL w/v) with slight modification as suggested by Zambuzzi et al. [23–26]. The final conditioned medium was later used to expose ECs for 3 days under shear stress to mimic blood flow.

2.9. Western Blot

Both adipocytes and ECs were harvested using lysis buffer [Lysis Cocktail (50 mM Tris [tris(hydroxymethyl)aminomethane]–HCl [pH 7.4], 1% Tween 20, 0.25% sodium deoxycholate, 150 mM NaCl, 1 mM EGTA (ethylene glycol tetraacetic acid), 1 mM O-Vanadate, 1 mM NaF, and protease inhibitors [1 μg/mL aprotinin, 10 μg/mL leupeptin, and 1 mM 4-(2-amino-ethyl)-benzolsulfonylfluorid-hydrochloride])] for 2 h, after which the samples were cleared by centrifugation, and the protein concentration was measured using the Lowry method [27]. An equal volume of 2x sodium dodecyl sulfate (SDS) gel loading buffer (100 mM Tris-HCl [pH 6.8], 200 mM dithiothreitol [DTT], 4% SDS, 0.1% bromophenol blue, and 20% glycerol) was added to the samples and boiled for 5 min. Aliquots of protein extracts were resolved into SDS-PAGE (10 or 12%) and transferred to PVDF membranes (Millipore, Burlington, MA, USA). Membranes were blocked with either 5% fat-free dried milk dissolved in Tris-buffered saline (TBS)–Tween 20 (0.05%) and incubated overnight at 4°C with appropriate primary antibody at 1:1000 dilutions. After washing 3x TBS-Tween 20 (0.05%), those membranes were incubated with horseradish peroxidase-conjugated secondary IgGs antibodies, at 1:5000 dilutions, in a blocking buffer for 1 h. Thereafter, the bands were detected by enhanced chemiluminescence (ECL), or by fluorescence (ODYSSEY® CLx Infrared Imaging System).

2.10. Quantitative PCR Assay (qPCR)

The same experimental workflow was performed and the cells were harvested now in Ambion TRIzol Reagent (Life Sciences—Fisher Scientific Inc,Waltham, MA, USA), and treated with DNase I (Invitrogen, Carlsband, CA, USA). cDNA synthesis was performed using High-Capacity cDNA Reverse Transcription Kit (Applied Biosystems, Foster City, CA, USA) following the manufacturer's instructions. qPCR was performed on a total of 10 μL, containing PowerUp™ SYBR™ Green Master Mix 2x (5 μL) (Applied Biosystems, Foster City, CA, USA), 0.4 μM of each primer, and 50 ng of cDNA and nuclease-free H_2O. Data were expressed as relative amounts of each target gene normalized considering the expression of 18SrRNA and Gapdh genes, here used as housekeeping genes, using the cycle threshold (Ct) method. Specific primers and running details are described in Table 1.

Table 1. Sequences of the primers and conditions of the quantitative polymerase chain reaction cycle.

Genes	Primers	5′-3′ Sequences	Reaction's conditions
H-AKT	Forward	CAG CGC GGC CCG AAG GAC	95°C, 3 s; 55°C, 8 s; 72°C, 20 s
	Reverse	GAC GCT CAC GCG CTC CTC TC	
H-CDK2	Forward	CTT TGC TGA GAT GGT GAC TCG	95°C, 3 s; 55°C, 8 s; 72°C, 20 s
	Reverse	GCC TCC CAG ATT CCT CAT GC	
H-CDK4	Forward	CTC TCT AGC TTG CGG CCT G	95°C, 3 s; 55°C, 8 s; 72°C, 20 s
	Reverse	GCA GGG ATA CAT CTC GAG GC	
H-ERK	Forward	GCA GCG CCT CCC TTG CTA GA	95°C, 3 s; 55°C, 8 s; 72°C, 20 s
	Reverse	AAC AGC CTC TGG CCC ACC CAT	
H-IL1B	Forward	GGA GAA TGA CCT GAG CAC CT	95°C, 3 s; 55°C, 8 s; 72°C, 20 s
	Reverse	GGA GGT GGA GAG CTT TCA GT	
H-IL6	Forward	AGT CCT GAT CCA GTT CCT GC	95°C, 3 s; 55°C, 8 s; 72°C, 20 s
	Reverse	CTA CAT TTG CCG AAG AGC CC	
H-JNK	Forward	AAA GGT GGT GTT TTG TTC CCA GGT	95°C, 3 s; 55°C, 8 s; 72°C, 20 s
	Reverse	TGA TGA TGG ATG CTG AGA GCC ATT G	
H-P38	Forward	GAG AAC TGC GGT TAC TTA	95°C, 3 s; 55°C, 8 s; 72°C, 20 s
	Reverse	ATG GGT CAC CAG ATA CAC AT	
H-VEGF	Forward	TGC AGA TTA TGC GGA TCA AAC C	95°C, 3 s; 55°C, 8 s; 72°C, 20 s
	Reverse	TGC ATT CAC ATT TGT TGT GCT GTA G	
H-VEGFr1	Forward	CAG GCC CAG TTT CTG CCA TT	95°C, 3 s; 55°C, 8 s; 72°C, 20 s
	Reverse	TTC CAG CTC AGC GTG GTC GTA	
M-Gapdh	Forward	AGG CCG GTG CTG AGT ATG TC	95°C, 3 s; 55°C, 8 s; 72°C, 20 s
	Reverse	TGC CTG CTT CAC CAC CTT CT	
M-Il13	Forward	CAG TCC TGG CTC TTG CTT G	95°C, 3 s; 55°C, 8 s; 72°C, 20 s
	Reverse	CCA GGT CCA CAC TCC ATA CC	
M-Il18	Forward	ACT TTG GCC GAC TTC ACT GT	95°C, 3 s; 55°C, 8 s; 72°C, 20 s
	Reverse	GGG TTC ACT GGC ACT TTG AT	
M-Il1b	Forward	GAC CTT CCA GGA TGA GGA CA	95°C, 3 s; 55°C, 8 s; 72°C, 20 s
	Reverse	AGC TCA TAT GGG TCC GAC AG	
M-Il1r	Forward	ACC CCC ATA TCA GCG GAG CG	95°C, 3 s; 55°C, 8 s; 72°C, 20 s
	Reverse	TTG CTT CCC CCG GAA CGT AT	
M-Il33	Forward	CCT TCT CGC TGA TTT CCA AG	95°C, 3 s; 55°C, 8 s; 72°C, 20 s
	Reverse	CCG TTA CGG ATA TGG TGG TC	
M-Il6	Forward	AGT TGC CTT CTT GGG ACT GA	95°C, 3 s; 55°C, 8 s; 72°C, 20 s
	Reverse	CAG AAT TGC CAT TGC ACA AC	
M-Myd88	Forward	ATG GTG GTG GTT GTT TCT GAC GA	95°C, 3 s; 55°C, 8 s; 72°C, 20 s
	Reverse	GCA AGG GTT GGT ATA GTC GCA TAT A	
M-Nfkb	Forward	CAC CTG TTC CAA AGA GCA CC	95°C, 3 s; 55°C, 8 s; 72°C, 20 s
	Reverse	GGT TCA GGA GCT GCT GAA AC	
M-Pparg	Forward	TTT TCA AGG GTG CCA GTT TC	95°C, 3 s; 55°C, 8 s; 72°C, 20 s
	Reverse	AAT CCT TGG CCC TCT GAG AT	

M-Tnf	Forward	CCA CAT CTC CCT CCA GAA AA	95°C, 3 s; 55°C, 8 s; 72°C, 20 s
	Reverse	AGG GTC TGG GCC ATA GAA CT	

Note: H = Human; M = Mice.

2.11. Oxidative Stress Markers

After obtaining adipocytes, the cells were harvested in PBS and sonicated. Protein carbonylation (CBO) was measured by using DNPH (2,4-dinitrophenyl hydrazine) as derivatizing agent [28]. The experiment was performed in a dark chamber to prevent the light. Firstly, the samples (10 µL of the lysed cells) were incubated with DNPH 10 mM (100 µL) for 10 min, after which 50 µL of 6 M NaOH (sodium hydroxide) was added. The reaction was interrupted after 10 min. The CBO was estimated by reading the final solution coloration spectrophotometrically at 450 nm. Finally, the results were calculated using the molar extinction coefficient (22,000 M^{-1} cm^{-1}) of DNPH and expressed as nmol/mg protein.

2.12. Matrix Metalloproteinases (MMPs) Activities by Zymography

Differentiating adipocyte cell culture medium was collected to measure the activity of matrix metalloproteinases (MMPs). The conditioned medium was centrifuged at 14,000 rpm for 15 min to avoid cell debris, and the protein concentration was determined using the Lowry method [27]. The same concentration of protein was resolved into a 12% polyacrylamide gel containing 4% gelatin. The gelatinolytic activity of MMPs was determined in the resolved proteins (bands). The proteins' structures were renatured in Triton X-100 aqueous solution (2% w/v) for 40 min, followed by incubation for 18 h in proteolysis buffer (Tris-$CaCl_2$) at 37°C, when the gels were stained using Coomassie Blue R-250 dye solution 0.05% for 3 h. Thereafter, the stained gels were washed in a 30% methanol (v/v) and 10% glacial acetic acid solution (v/v). The opposite staining (clear bands) was obtained in the gels exactly where there was the gelatinolytic activity (bands) of MMP2 (~62 kDa) and MMP9 (~84 kDa), and then they were analyzed using the software ImageJ (Bethesda, MD, USA), as previously proposed [29].

2.13. Statistical Analysis

Data were expressed as mean ± standard error of the mean (SEM) of the replicates of each experiment (n = 3). The samples assumed a normal distribution, and they were subjected to Student's t-test (two-tailed) with $p < 0.05$ considered statistically significant.

In the experiment where there were more than two groups, the statistical analyses were performed using either analysis of variance (one-way ANOVA) combined with appropriate Bonferroni's correction post-test, or nonparametric analysis. A $p < 0.05$ was considered to be statistically significant. The software used was GraphPad Prism 7 (GraphPad Software, La Jolla, CA, USA).

3. Results

To better evaluate the molecular mechanism underlying EC response to high-adipogenesis conditions concomitant to a titanium-enriched medium, we proposed an *in vitro* experimental model subjecting adipocyte cell to differentiation under two conditions: Control cultures (Ctrl) and high-glucose treated cells (H_Adip). Furthermore, the adipocyte-obtained medium was enriched by titanium and then used to expose semiconfluent EC cultures dynamically responding to mechanotransduction mimicking blood flow [22]. Additionally, the titanium-enriched medium was obtained using two different titanium-modified surfaces: DAE, in which the discs were subjected to dual acid-etching, and nHA, in which DAE surfaces were covered by nano-hydroxyapatite [11,30,31], as we have shown previously.

3.1. Validation of the High-Adipogenesis Model

To validate the proposed high-adipogenesis model, we first analyzed classical biomarkers of adipocyte phenotype in cells responding to high-glucose exposition, which did not affect their viability (Figure 2A). Oxidative stress markers and fat droplet staining were analyzed and correlated with inflammatory profile and adipogenesis. Reactive oxygen species and concomitant oxidative stress in adipocytes was better investigated by evaluating the protein carbonylation profile. Our data show that this parameter was significantly affected in cells responding to the high-glucose exposure, with higher values than the conventional condition (Ctrl) (Figure 2B). Images acquired by using light microscopy show that adipocytes responding to the high-glucose medium presented a higher number of bigger-sized intracellular fat droplets stained by Oil Red O dye (Figure 2C).

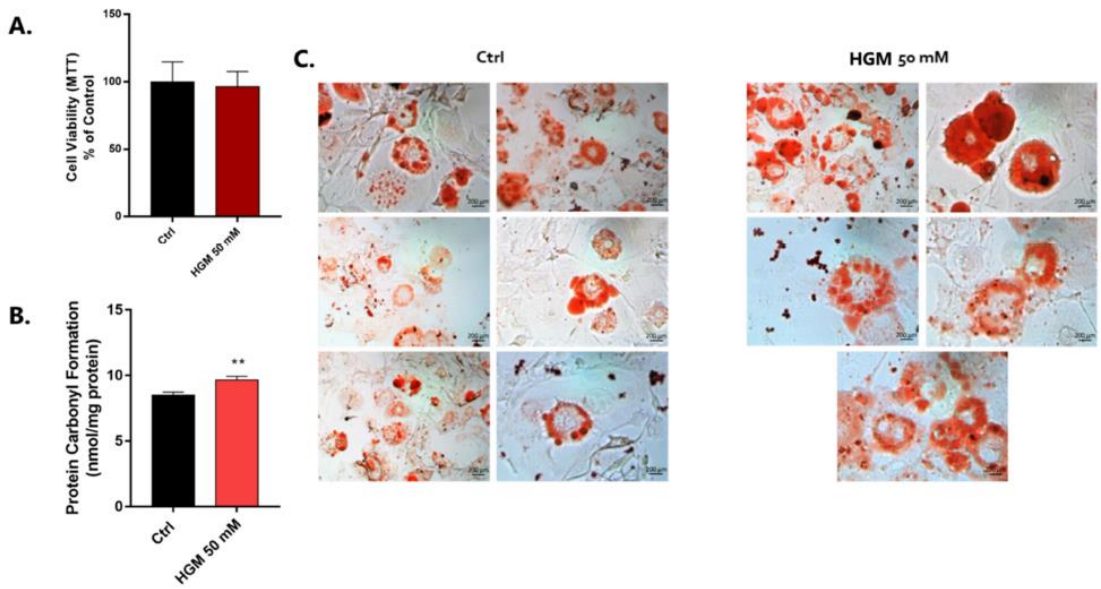

Figure 2. High-glucose medium affects adipocyte differentiation. The 50 mM high-glucose medium was used to expose pre-adipocyte cells for stimulation to differentiation. Firstly, cytotoxicity was measured by using an MTT assay (A). Thereafter, oxidative stress was measured by evaluating the protein carbonylation (nmol/mg protein) by performing a method using DNPH (2,4-dinitrophenylhydrazine derivatizing agent) (B). The data are plotted respecting mean ± SD (n = 3), and the significance was shown using Student's t-test, ** p = 0.0058. Intracellular fat droplets of the pre-adipocytes were acquired using a light microscope (40x magnification) thereafter stained by using Oil Red O Staining (C). HGM: high-glucose medium.

Adipocyte differentiation and inflammation signaling pathways are widely studied regarding obesity concerns. Herein, the gene expression was evaluated by investigating the behavior of the interleukins IL-1, IL-6, IL-13, IL-18, and IL-33 genes. They were significantly higher in cells responding to the adipogenesis model where pre-adipocytes were exposed to the high-glucose medium (HGM) (Figure 3A–E), as well as considering TNF-α gene expression (Figure 3G). Importantly, the expression activity of the PPAR-γ gene was also investigated in this study. It was significantly higher in cells responding to HGM (Figure 3J), while both Myd88 and IL1 receptor genes expression were lower in the HGM group (Figure 3F,I), and NFkB remains unchanged (Figure 3H).

We also investigated the behavior of mitogen-activated protein kinase (MAPKs) genes to infer about cell survival signaling in differentiated adipocytes. Our data show that there is a higher profile of MAPK-ERK proteins in cells responding to HGM (Figure 4A,B), while the MAPK-P38 protein remains unchanged (Figure 4C,D). Finally, the perspective of extracellular matrix (ECM) remodeling was investigated by analyzing the

activities of matrix metalloproteinases (MMPs) through gelatin-based proteolysis assay. Our data show that there is higher activity of both MMP2 and 9 in differentiated adipocytes (Figure 4E–J).

3.2. Angiogenesis-Related Genes Were Evaluated in ECs Responding to High Adipogenesis and Titanium

To analyze the behavior of ECs responding to high-adipogenesis and titanium-enriched mediums, we first evaluated angiogenesis-related genes and viability. The Ctrl group now refers to the adipocyte-conditioned medium subjected to normal conditions, while the H_Adip group refers to the adipocyte-conditioned medium chronically responding to high glucose concentrations (50 mM); furthermore, the DAE and nHA refer to the adipocyte-conditioned medium previously used to incubate titanium discs with respect to the difference on their surfaces: H_Adip + DAE and H_Adip + nHA. The VEGF gene remains unchanged when compared to Ctrl or when the cells were treated with either of the titanium-enriched mediums (Figure 5A). In this way, the VEGFr1 gene remains unchanged when compared to the Ctrl group, but significantly decreases in response to both nHA and H_Adip + nHA groups when compared to H_Adip (Figure 5B).

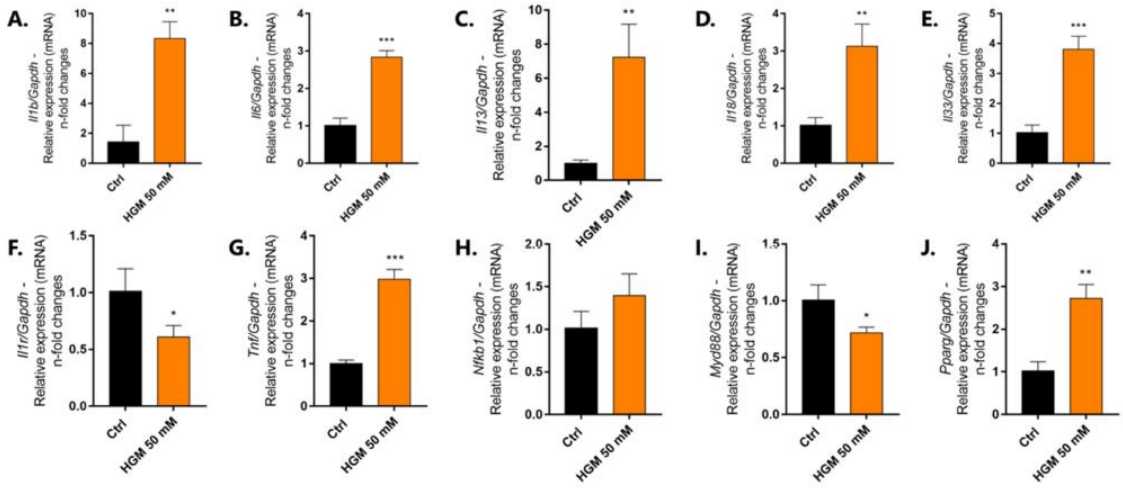

Figure 3. Adipogenesis model recapitulates the inflammation microenvironment and requires PPAR-γ. Pre-adipocytes were differentiated for 10 days using classical model when the cells were harvested and the biological samples forwarded to perform the qPCR technology. A significantly higher expression of IL-1 (A), IL-6 (B), IL-13 (C), IL-18 (D), IL-33 (E), TNF-α (G), and PPAR-γ (J) genes were observed in the adipocytes responding to HGM (50 mM). The graphs bring the n-fold change of the profile of gene expression

normalized to the GAPDH gene (housekeeping gene). Significant differences were considered when * $p < 0.05$, and ** $p < 0.01$, *** $p < 0.001$. HGM: high glucose medium.

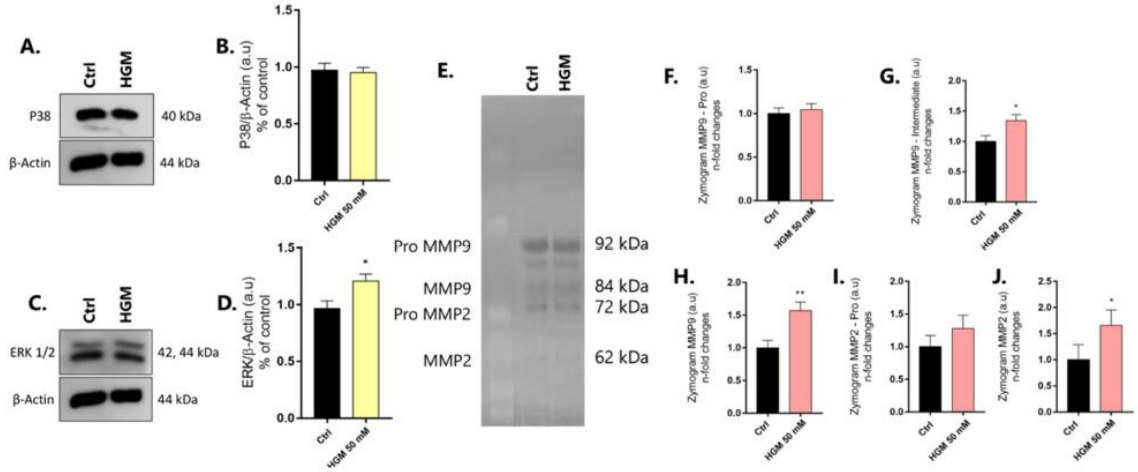

Figure 4. Adipocytes require MAPK and MMP activity. Adipocytes require MAPK-ERK (A,B), while the MAPK-P38 protein remains unchanged (C,D). β-Actin was used as the protein loading control. Additionally, higher activities of MMP9 (F–H) and MMP2 (I,J) were found in adipocytes responding to HGM. Data are plotted as means ± standard deviations (n = 3). Significant differences were considered when * $p < 0.05$, and ** $p < 0.01$. HGM: high glucose medium.

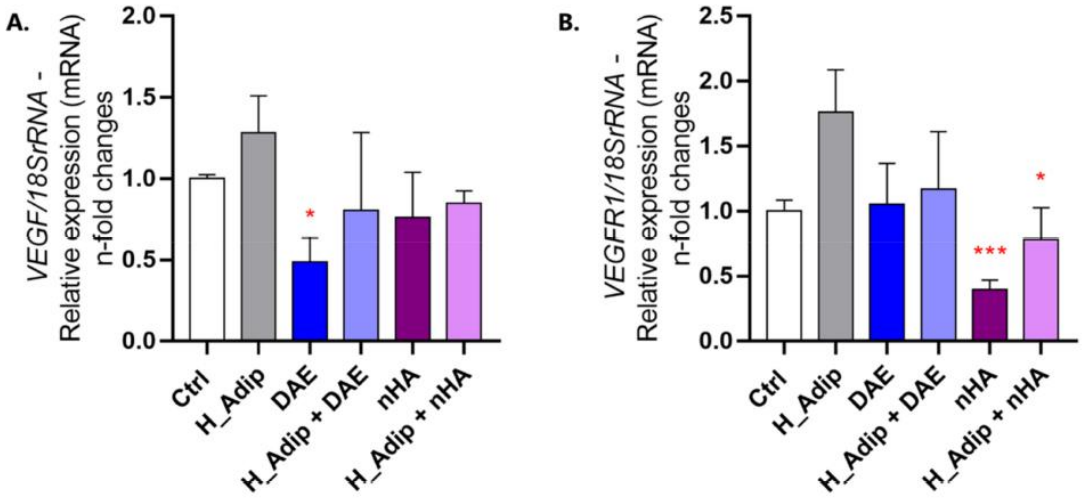

Figure 5. VEGF and VEGFR1 genes are modulated in response to titanium-based surfaces. Both genes are related to EC phenotype as well as to angiogenesis. Their response to H_Adip and the titanium-enriched medium seems to be relevant to the lower angiogenesis profile in adipogenesis. The VEGF gene presented a low expression profile in ECs responding to DAE, while there was no significance when considering the other groups (A). Additionally, the VEGFR1 gene presented a low profile of expression in ECs responding to nHA (B). The data show the n-fold changes in the profile of transcripts normalized to the 18S gene (housekeeping gene). Differences were considered

statistically significant when * $p < 0.05$, and *** $p < 0.001$, represented by red * when compared to the H_Adip group.

3.3. Proliferation and Survival-Related Genes in ECs

The protein kinase B (AKT), cyclin-dependent kinase 2 (CDK2), and CDK4 genes were significantly higher in ECs exposed to adipocyte-conditioned medium (H_Adip) (Figure 6A–C). Thereafter, our data show that there is a significant involvement of the AKT gene in the coupling of adipogenicity and titanium-enriched medium (Figure 6A). Thereafter, the CDK genes presented a very similar profile between DAE and nHA, with CDK2 being higher in nHA (Figure 6B), and CDK4 expressing a very similar profile (Figure 6C).

MAPK genes were also investigated in ECs. Figure 7 shows there is a significant modulation in response to the coupling between high-adipogenicity and titanium-enriched medium. The titanium DAE-enriched medium increased the expression of the MAPK-ERK gene independently of normal or high-adipogenicity conditions (Figure 7A). ECs required MAPK-JNK gene expression when they were exposed to the DAE-enriched medium under normal adipogenesis conditions (DAE) when compared to H_Adip group, but without difference in the H_Adip + DAE group, while cells responding to nHA and H_Adip + nHA remain unchanged (Figure 7B). The MAPK-P38 gene showed involvement but without statistically significant changes when the groups were compared to the Ctrl group, showing an increase only in the DAE group when compared to H_Adip (Figure 7C).

As c-Src kinase is related to the survival mechanism governing the viability of eukaryotic cells, we decided to evaluate whether this protein was involved in response to the titanium-enriched medium under normal and high-adipogenesis conditions. Additionally, our data show that c-Src seems to be required in high-adipogenesis conditions regardless of the presence of the titanium DAE-enriched medium as it remained higher in the group H_Adip + DAE (Figure 8A,B). Moreover, in the titanium nHA-enriched medium, the cells under high adipogenesis showed a significant difference when compared with Ctrl (Figure 8).

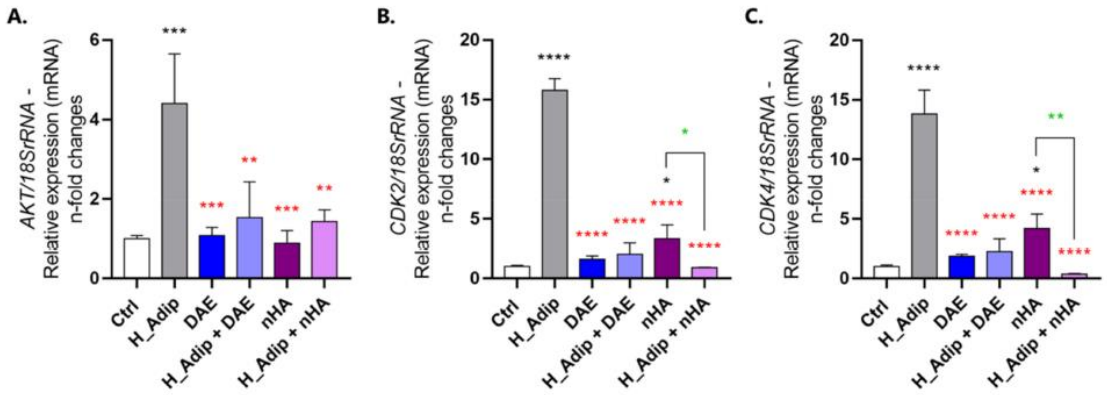

Figure 6. Both survival and cell proliferation progress were investigated in ECs. ECs require an increase in survival and cell cycle-related gene expression even more responding to high adipogenesis condition, observing the behavior of AKT (A), CDK2 (B), and CDK4 (C). Differences were considered statistically when * $p < 0.05$, ** $p < 0.01$, *** $p < 0.001$, and **** $p < 0.0001$, represented by black * when compared to the Ctrl group, by red * when compared to the H_Adip group, and by green * when compared between the groups with nHA.

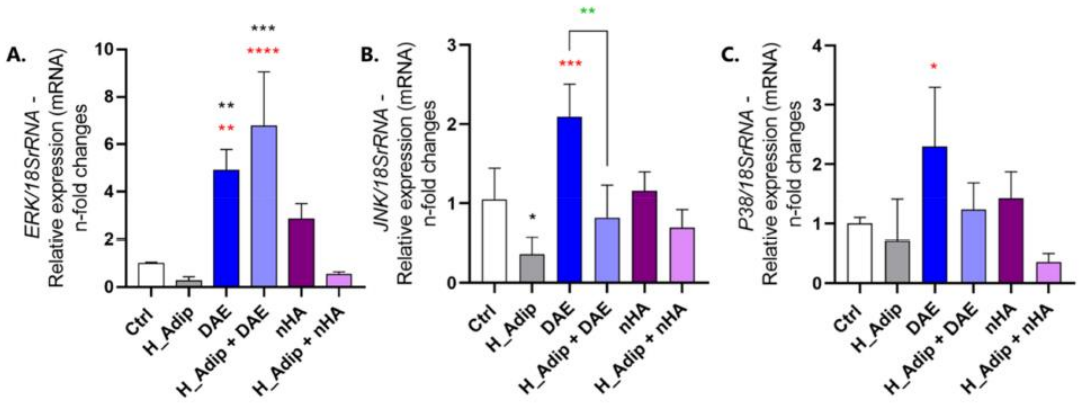

Figure 7. MAPK-related genes were modulated in EC responding to adipogenesis. qPCR shows different modulations of the MAPKs genes in ECs: the MAPK-ERK gene was higher in cells responding to the DAE group, and even higher in the H_Adip + DAE group. However, there was no difference in the H_Adip + nHA group when compared to Ctrl (A). The JNK was down-regulated in the H_Adip group when compared to Ctrl, and higher in response to DAE treatment when compared to H_Adip. Data are reported as means ± standard deviations (n = 3). Comparison by one-way ANOVA. Statistical differences were considered when * $p < 0.05$, ** $p < 0.01$, *** $p < 0.001$, and **** $p < 0.0001$, represented by black * when compared to the Ctrl group, by red * when compared to the H_Adip group, and by green * when compared between the groups with DAE.

3.4. Endothelial Cell Appears to Be Important in Inflammatory Gene Microenvironment

The interleukins IL-6 and IL-1β genes were evaluated using RT-qPCR technology. This revealed an important modulation in ECs responding to different treatments. The IL-6 gene was significantly higher when ECs were treated with titanium DAE and nHA under the high-adipogenesis condition (Figure 9A). The IL-1β gene was also significantly higher in the high-adipogenesis condition, a situation that seems to be controlled in the presence of the titanium-enriched medium, whether considering DAE or nHA (Figure 9B).

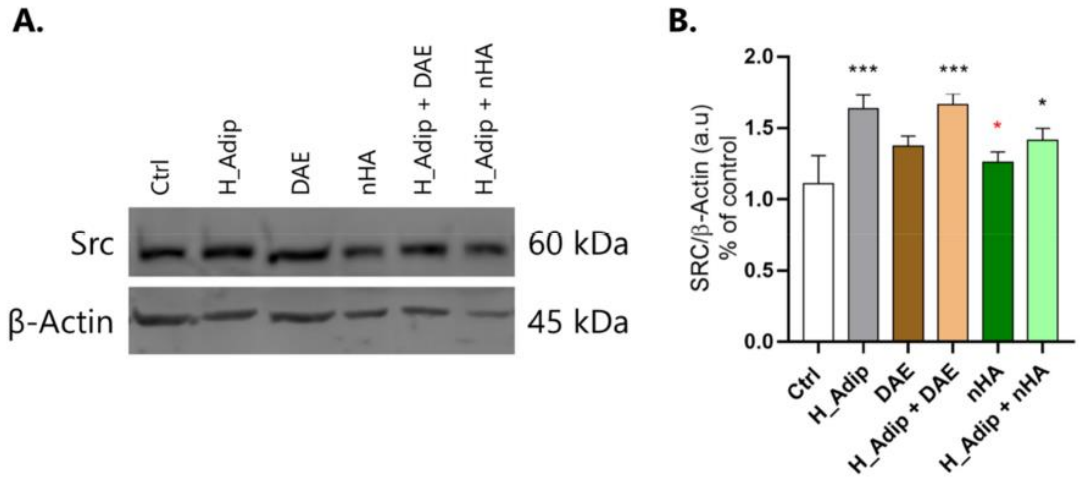

Figure 8. c-Src involvement. After exposing the ECs to different shear-stress treatments for 72 h, the samples were obtained to perform the Western blotting assay and evaluate SRC protein content (A,B). The high adipogenesis condition increased the content of SRC in ECs, significantly in the H_Adip + DAE group, and less significantly in the H_Adip + nHA group. β-Actin was considered the protein loading control. Differences were considered significant when * $p < 0.05$, and *** $p < 0.001$, represented by black * when compared to the Ctrl group, and by red * when compared to the H_Adip group.

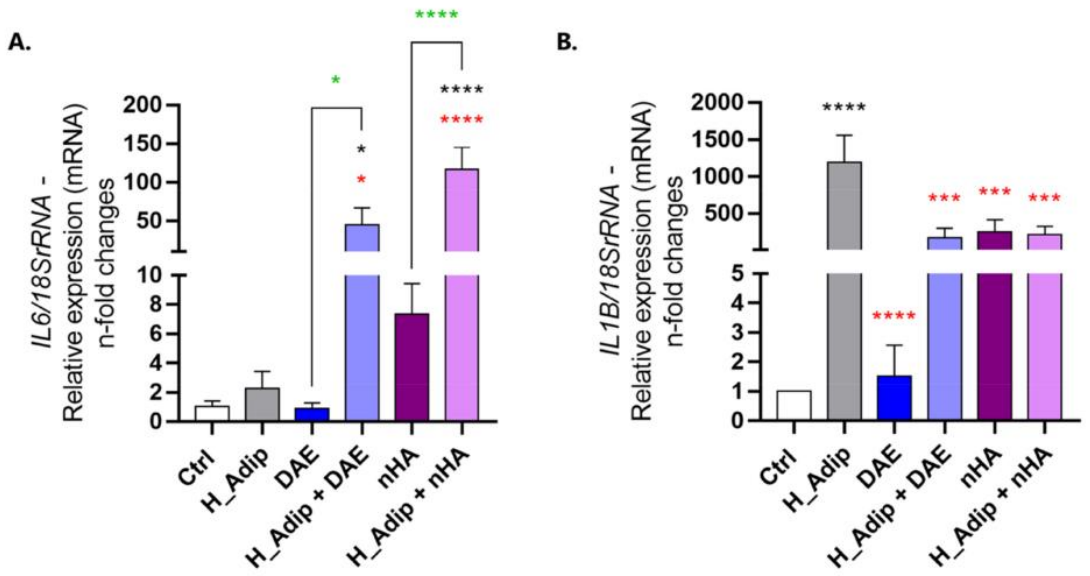

Figure 9. IL6 and IL1B gene expression changed in response to conditioned mediums. The samples were harvested as described earlier and the gene expression was measured using qPCR. To address the inflammatory effect of different conditions on ECs, we evaluated IL-6 (A) and IL-1B (B) genes. The 18SrRNA gene was considered the housekeeping gene and used to normalize the expression values. Data are reported in means ± standard deviations (n = 3). Differences were considered significant when * $p < 0.05$, *** $p < 0.001$, and **** $p < 0.0001$, represented by black * when compared to the Ctrl group, by red * when compared to the H_Adip group, and by green * when compared between the groups with DAE or between the groups with nHA. DAE = titanium with Dual Acid-Etching; nHA = titanium with nano-Hydroxyapatite-coated surface.

4. Discussion

The experimental model proposed in this study permits the evaluation of the effect of high adipogenesis in the ECs responding to a titanium-enriched medium. The adipocyte differentiation under high-glucose conditions has been used as a tool in vitro to understand obesity-related metabolic dysfunctions [32], once the glucose enhances lipid accumulation and adipogenesis [33]. Regarding the validation of this alternative model, the adipocyte exposed to high glucose concentrations in our model significantly modulated specific interleukin gene expression as well as the PPAR-γ gene activation. These genes are related to adipocyte differentiation [34]. Taken together, this validates our biological model for obtaining functional adipocytes. Importantly, the increase in protein carbonylation in obtained adipocytes can be correlated with the high oxidative stress expected in differentiated adipocytes. In general, our proposed adipogenesis model promotes an increase in the intracellular fat droplets during the pre-adipocyte differentiation concomitantly with the increase in the pro-inflammatory profile, as

expected in adipocytes [32,35]. Additionally, MAPK and PPAR are also both involved with adipocyte metabolism [33], which corroborates with our findings. Additionally, we have also shown significant morphological changes in adipocytes and which can explain the higher activities of MMPs and is expected to modulate the ECM remodeling. Considering in vitro studies, this experimental model presents limitations, such as evaluating the crosstalk between cells of different origins, however, it can be overcome by the evolutionarily conserved structure and functions of proteins and genes over 80%.

Although some progress has been made on the way to understanding the etiology of systemic and metabolic dysfunctions such as diabetes and obesity, their relevance to bone-healing peri-implants, which might explain the higher failure of implants in obese patients [36], is barely understood. In fact, it has been hypothesized that angiogenesis is compromised in obese and diabetic individuals. Thus, we have applied an experimental model to better evaluate the impact on ECs responding to a titanium-enriched medium which plays crucial roles during the osseointegration mechanism of angiogenesis, such as interacting with osteoblasts [37,38]. There are important similarities between osseointegration and wound healing, a situation that is harmful in patients with compromised metabolism [39]. To advance with this proposal, we have investigated the effect of two titanium-modified surfaces. Firstly, genes related to the phenotype of endothelial cells were investigated. While VEGF seemed not to be affected, its receptor, VEGFR1, was higher in ECs responding to the titanium-enriched medium. This might be explained by a correlation with its ligand and suggests an autocrine loop in this condition. The increase in the intracellular signaling upon VEGFR1 activation requires the involvement of MAPK upstream, modulating cell survival and proliferative phenotype. This explains the capacity of those cells to involve p38 and CDKs [40]. Additionally, the VEGFR1-related intracellular cascade seems to require Src kinase in this context, and also might be correlated with ECM remodeling by regulating MMP activity.

Lastly, the gene expression of interleukins IL-6 and IL-1 was shown to be sensitive to the response to titanium in an adipogenesis-related metabolic condition once both DAE and nHA promoted their higher expression. It is important that the IL-related cascade also requires the activation of MAPKs and Src. An important aspect is that IL-1β effectively and rapidly induces human mesenchymal stem cells differentiation into osteoblasts [41]. This might be an important axis coupling angiogenesis and osteogenesis during the osseointegration mechanism, meaning nHA is able to improve the capacity of ECs to drive bone healing in obese patients.

5. Conclusions

Taking our data into consideration, it is possible to suggest that nHA-coated surface favor biological events related to angiogenesis and might be an alternative strategy in adipogenesis-related metabolic conditions where usually the percentage of dental implant failure is higher. Altogether, this study gathers valuable information on understanding the higher failure of dental implants in obese individuals.

Author Contributions: Methodology, T.S.P., A.M.G. and P.B.d.M.; Validation, T.S.P.; Formal analysis, A.M.G. and P.B.d.M.; Investigation, T.S.P., A.M.G. and P.B.d.M.; Data curation, P.B.d.M.; Writing—original draft, A.M.G. and W.F.Z.; Writing—review & editing, T.S.P. and P.B.d.M.; Supervision, W.F.Z.; Project administration, W.F.Z.; Funding acquisition, W.F.Z. All authors have read and agreed to the published version of the manuscript.

Funding: Fundação de Amparo à Pesquisa do Estado de São Paulo-FAPESP (FAPESP: 2019/26854-2; 2014/22689-3), Conselho Nacional de Desenvolvimento Científico e Tecnológico (CNPq–Bolsa Produtividade em Pesquisa, 314166/2021-1), and Coordenação de Aperfeiçoamento de Pessoal de Nível Superior (Capes), code 1.

Institutional Review Board Statement: Not applicable.

Informed Consent Statement: Not applicable.

Data Availability Statement: The data that support the findings of this study are available from the corresponding author upon reasonable request.

Conflicts of Interest: The authors declare no conflict of interest.

References

1. Stevens, S.M.; O'Connell, B.P.; Meyer, T.A. Obesity related complications in surgery. Curr. Opin. Otolaryngol. Head Neck Surg. 2015, 23, 341–347. [CrossRef]
2. Adamczak, M.;Wiecek, A. The adipose tissue as an endocrine organ. Semin. Nephrol. 2013, 33, 2–13. [CrossRef]

3. Fuster, J.J.; Ouchi, N.; Gokce, N.; Walsh, K. Obesity-Induced Changes in Adipose Tissue Microenvironment and Their Impact on Cardiovascular Disease. Circ. Res. 2016, 118, 1786–1807. [CrossRef] [PubMed]
4. Wuche, C. The cardiovascular system and associated disorders. Br. J. Nurs. 2022, 31, 886–892. [CrossRef]
5. Givens, C.; Tzima, E. Endothelial Mechanosignaling: Does One Sensor Fit All? Antioxid. Redox Signal. 2016, 25, 373–388. [CrossRef]
6. da Silva, R.A.; Ferreira, M.R.; Gomes, A.M.; Zambuzzi, W.F. LncRNA HOTAIR is a novel endothelial mechanosensitive gene. J. Cell. Physiol. 2020, 235, 4631–4642. [CrossRef]
7. Gomes, A.M.; Pinto, T.S.; da Costa Fernandes, C.J.; da Silva, R.A.; Zambuzzi, W.F. Wortmannin targeting phosphatidylinositol 3-kinase suppresses angiogenic factors in shear-stressed endothelial cells. J. Cell. Physiol. 2020, 235, 5256–5269. [CrossRef] [PubMed]
8. da Silva, R.A.; Fernandes, C.J.d.C.; Feltran, G.d.S.; Gomes, A.M.; de Camargo Andrade, A.F.; Andia, D.C.; Peppelenbosch, M.P.; Zambuzzi,W.F. Laminar shear stress-provoked cytoskeletal changes are mediated by epigenetic reprogramming of TIMP1 in human primary smooth muscle cells. J. Cell. Physiol. 2019, 234, 6382–6396. [CrossRef]
9. Johnson, K.E.; Wilgus, T.A. Vascular Endothelial Growth Factor and Angiogenesis in the Regulation of Cutaneous Wound Repair. Adv. Wound Care 2014, 3, 647–661. [CrossRef] [PubMed]
10. Martins, B.R.; Pinto, T.S.; da Costa Fernandes, C.J.; Bezerra, F.; Zambuzzi, W.F. PI3K/AKT signaling drives titanium-induced angiogenic stimulus. J. Mater. Sci. Mater. Med. 2021, 32, 18. [CrossRef]
11. Pinto, T.S.; Martins, B.R.; Ferreira, M.R.; Bezerra, F.; Zambuzzi, W.F. Nanohydroxyapatite-Blasted Bioactive Surface Drives Shear-Stressed Endothelial Cell Growth and Angiogenesis. BioMed Res. Int. 2022, 2022, 1433221. [CrossRef]
12. Chen, W.; Xu, K.; Tao, B.; Dai, L.; Yu, Y.; Mu, C.; Shen, X.; Hu, Y.; He, Y.; Cai, K. Multilayered coating of titanium implants promotes coupled osteogenesis and angiogenesis in vitro and in vivo. Acta Biomater. 2018, 74, 489–504. [CrossRef] [PubMed]
13. Prasad, K.; Bazaka, O.; Chua, M.; Rochford, M.; Fedrick, L.; Spoor, J.; Symes, R.; Tieppo, M.; Collins, C.; Cao, A.; et al. Metallic Biomaterials: Current Challenges and Opportunities. Materials 2017, 10, 884. [CrossRef] [PubMed]

14. Coelho, P.G.; Granjeiro, J.M.; Romanos, G.E.; Suzuki, M.; Silva, N.R.F.; Cardaropoli, G.; Thompson, V.P.; Lemons, J.E. Basic research methods and current trends of dental implant surfaces. J. Biomed. Mater. Res. B Appl. Biomater. 2009, 88, 579–596. [CrossRef] [PubMed]
15. Rademakers, T.; Horvath, J.M.; van Blitterswijk, C.A.; LaPointe, V.L.S. Oxygen and nutrient delivery in tissue engineering: Approaches to graft vascularization. J. Tissue Eng. Regen. Med. 2019, 13, 1815–1829. [CrossRef]
16. Roseti, L.; Parisi, V.; Petretta, M.; Cavallo, C.; Desando, G.; Bartolotti, I.; Grigolo, B. Scaffolds for Bone Tissue Engineering: State of the art and new perspectives. Mater. Sci. Eng. C Mater. Biol. Appl. 2017, 78, 1246–1262. [CrossRef] [PubMed]
17. Coelho, P.G.; Pippenger, B.; Tovar, N.; Koopmans, S.-J.; Plana, N.M.; Graves, D.T.; Engebretson, S.; van Beusekom, H.M.M.; Oliveira, P.G.F.P.; Dard, M. Effect of Obesity or Metabolic Syndrome and Diabetes on Osseointegration of Dental Implants in a Miniature Swine Model: A Pilot Study. J. Oral Maxillofac. Surg. 2018, 76, 1677–1687. [CrossRef]
18. Di Benedetto, A.; Gigante, I.; Colucci, S.; Grano, M. Periodontal disease: Linking the primary inflammation to bone loss. Clin. Dev. Immunol. 2013, 2013, 503754. [CrossRef]
19. Gottlander, M.; Johansson, C.B.;Wennerberg, A.; Albrektsson, T.; Radin, S.; Ducheyne, P. Bone tissue reactions to an electrophoretically applied calcium phosphate coating. Biomaterials 1997, 18, 551–557. [CrossRef]
20. Meirelles, L.; Arvidsson, A.; Andersson, M.; Kjellin, P.; Albrektsson, T.; Wennerberg, A. Nano hydroxyapatite structures influence early bone formation. J. Biomed. Mater. Res. A 2008, 87, 299–307. [CrossRef]
21. dela Paz, N.G.; Walshe, T.E.; Leach, L.L.; Saint-Geniez, M.; D'Amore, P.A. Role of shear-stress-induced VEGF expression in endothelial cell survival. J. Cell Sci. 2012, 125, 831–843. [CrossRef] [PubMed]
22. Pinto, T.S.; Fernandes, C.J.d.C.; da Silva, R.A.; Gomes, A.M.; Vieira, J.C.S.; Padilha, P.d.M.; Zambuzzi,W.F. c-Src kinase contributes on endothelial cells mechanotransduction in a heat shock protein 70-dependent turnover manner. J. Cell. Physiol. 2019, 234, 11287–11303. [CrossRef]
23. Zambuzzi, W.F.; Bonfante, E.A.; Jimbo, R.; Hayashi, M.; Andersson, M.; Alves, G.; Takamori, E.R.; Beltrao, P.J.; Coelho, P.G.; Granjeiro, J.M. Nanometer scale titanium surface texturing are detected by signaling pathways involving transient FAK and Src activations. PLoS ONE 2014, 9, e95662. [CrossRef]

24. Machado, M.I.P.; Gomes, A.M.; Rodrigues, M.F.; Silva Pinto, T.; da Costa Fernandes, C.J.; Bezerra, F.J.; Zambuzzi, W.F. Cobalt-chromium-enriched medium ameliorates shear-stressed endothelial cell performance. J. Trace Elem. Med. Biol. 2019, 54, 163–171. [CrossRef]
25. da Costa Fernandes, C.J.; Bezerra, F.J.B.; de Campos Souza, B.; Campos, M.A.; Zambuzzi, W.F. Titanium-enriched medium drives low profile of ECM remodeling as a pre-requisite to pre-osteoblast viability and proliferative phenotype. J. Trace Elem. Med. Biol. 2018, 50, 339–346. [CrossRef] [PubMed]
26. Fernandes, C.J.C.; Bezerra, F.; das D do Carmo, M.; Feltran, G.S.; Rossi, M.C.; da Silva, R.A.; Padilha, P.; Zambuzzi, W. CoCrenriched medium modulates integrin-based downstream signaling and requires a set of inflammatory genes reprograming in vitro. J. Biomed. Mater. Res. A 2018, 106, 839–849. [CrossRef]
27. Hartree, E.F. Determination of protein: A modification of the Lowry method that gives a linear photometric response. Anal. Biochem. 1972, 48, 422–427. [CrossRef] [PubMed]
28. Mesquita, C.S.; Oliveira, R.; Bento, F.; Geraldo, D.; Rodrigues, J.V.; Marcos, J.C. Simplified 2,4-dinitrophenylhydrazine spectrophotometric assay for quantification of carbonyls in oxidized proteins. Anal. Biochem. 2014, 458, 69–71. [CrossRef] [PubMed]
29. Lefebvre, V.; Peeters-Joris, C.; Vaes, G. Production of gelatin-degrading matrix metalloproteinases (‘type IV collagenases’) and inhibitors by articular chondrocytes during their dedifferentiation by serial subcultures and under stimulation by interleukin-1 and tumor necrosis factor alpha. Biochim. Biophys. Acta 1991, 1094, 8–18. [CrossRef]
30. Bezerra, F.; Ferreira, M.R.; Fontes, G.N.; da Costa Fernandes, C.J.; Andia, D.C.; Cruz, N.C.; da Silva, R.A.; Zambuzzi, W.F. Nano hydroxyapatite-blasted titanium surface affects pre-osteoblast morphology by modulating critical intracellular pathways. Biotechnol. Bioeng. 2017, 114, 1888–1898. [CrossRef]
31. Fernandes, C.J.C.; Bezerra, F.; Ferreira, M.R.; Andrade, A.F.C.; Pinto, T.S.; Zambuzzi, W.F. Nano hydroxyapatite-blasted titanium surface creates a biointerface able to govern Src-dependent osteoblast metabolism as prerequisite to ECM remodeling. Colloids Surf. B Biointerfaces 2018, 163, 321–328. [CrossRef] [PubMed]
32. Palacios-Ortega, S.; Varela-Guruceaga, M.; Martínez, J.A.; de Miguel, C.; Milagro, F.I. Effects of high glucose on caveolin-1 and insulin signaling in 3T3-L1 adipocytes. Adipocyte 2016, 5, 65–80. [CrossRef] [PubMed]

33. Chuang, C.C.; Yang, R.S.; Tsai, K.S.; Ho, F.M.; Liu, S.H. Hyperglycemia Enhances Adipogenic Induction of Lipid Accumulation: Involvement of Extracellular Signal-Regulated Protein Kinase 1/2, Phosphoinositide 3-Kinase/Akt, and Peroxisome Proliferator-Activated Receptor Signaling. Endocrinology 2007, 148, 4267–4275. [CrossRef] [PubMed]
34. Lefterova, M.I.; Haakonsson, A.K.; Lazar, M.A.; Mandrup, S. PPARγ and the global map of adipogenesis and beyond. Trends Endocrinol. Metab. 2014, 25, 293–302. [CrossRef] [PubMed]
35. Shilpa, K.; Dinesh, T.; Lakshmi, B.S. An In Vitro Model to Probe the Regulation of Adipocyte Differentiation under Hyperglycemia. Diabetes Metab. J. 2013, 37, 176–180. [CrossRef]
36. von Wilmowsky, C.; Stockmann, P.; Harsch, I.; Amann, K.; Metzler, P.; Lutz, R.; Moest, T.; Neukam, F.W.; Schlegel, K.A. Diabetes mellitus negatively affects peri-implant bone formation in the diabetic domestic pig. J. Clin. Periodontol. 2011, 38, 771–779. [CrossRef]
37. Kusumbe, A.P.; Ramasamy, S.K.; Adams, R.H. Coupling of angiogenesis and osteogenesis by a specific vessel subtype in bone. Nature 2014, 507, 323–328. [CrossRef] [PubMed]
38. Ramasamy, S.K.; Kusumbe, A.P.; Schiller,M.; Zeuschner, D.; Bixel,M.G.;Milia, C.; Gamrekelashvili, J.; Limbourg, A.;Medvinsky, A.; Santoro, M.M.; et al. Blood flow controls bone vascular function and osteogenesis. Nat. Commun. 2016, 7, 13601. [CrossRef]
39. de Oliveira, P.G.F.P.; Bonfante, E.A.; Bergamo, E.T.P.; de Souza, S.L.S.; Riella, L.; Torroni, A.; Benalcazar Jalkh, E.B.; Witek, L.; Lopez, C.D.; Zambuzzi,W.F.; et al. Obesity/Metabolic Syndrome and Diabetes Mellitus on Peri-implantitis. Trends Endocrinol. Metab. 2020, 31, 596–610. [CrossRef]
40. Zhang, X.; Simons, M. Receptor tyrosine kinases endocytosis in endothelium: Biology and signaling. Arterioscler. Thromb. Vasc. Biol. 2014, 34, 1831–1837. [CrossRef]
41. Sonomoto, K.; Yamaoka, K.; Oshita, K.; Fukuyo, S.; Zhang, X.; Nakano, K.; Okada, Y.; Tanaka, Y. Interleukin-1β induces differentiation of human mesenchymal stem cells into osteoblasts via the Wnt-5a/receptor tyrosine kinase-like orphan receptor 2 pathway. Arthritis Rheum. 2012, 64, 3355–3363. [CrossRef] [PubMed]

Capítulo 3

Interaction of high lipogenic states with titanium on osteogenesis

Pinto TS[1], van der Eerden BC[2], Schreuders-Koedam M[2], van de Peppel J[2], Ayada I[3], Pan Q[3], Verstegen MM[4], van der Laan LJ[4], Fuhler GM[3], Zambuzzi WF[1,*], Peppelenbosch MP[3,*]

[1] Lab. of Bioassays and Cellular Dynamics, Department of Chemical and Biological Sciences, Institute of Biosciences, UNESP, São Paulo State University, Botucatu, SP, Brazil.
[2] Department of Internal Medicine, Erasmus MC, Erasmus University Medical Center, Rotterdam, The Netherlands.
[3] Department of Gastroenterology and Hepatology, Erasmus MC, Erasmus University Medical Center, Rotterdam, The Netherlands.
[4] Department of Surgery, Erasmus MC, Erasmus University Medical Center, Rotterdam, Netherlands.

*Share senior authorship.

Correspondence: w.zambuzzi@unesp.br

ABSTRACT

As obesity rates continue to rise, so does the prevalence of metabolic dysfunction and alcohol associated steatotic liver disease (MetALD, a new term for Nonalcoholic Fatty Liver Disease - NAFLD). In an aging population, it is crucial to comprehend the interplay between metabolic disorders, such as MetALD, and bone health. This understanding becomes particularly significant in the context of implant osseointegration. This study introduces an *in vitro* model simulating high lipogenesis through the use of human Mesenchymal Stroma Cells-derived adipocytes, 3D intrahepatic cholangiocyte organoids (ICO), and Huh7 hepatocytes, to evaluate the endocrine influence on osteoblasts interacting with titanium. We observed a significant increase in intracellular fat accumulation in all three cell types and a corresponding elevation in metabolic gene expression when compared to control groups. Notably, osteoblasts undergoing mineralization in this high-lipogenesis environment also displayed lipid vesicle accumulation. The study further revealed that titanium surfaces modulate osteogenic gene expression and impact cell cycle progression, cell survival, and extracellular matrix remodeling under lipogenic conditions. These findings provide new insights into the challenges of implant integration in patients with obesity and MetALD, offering a deeper understanding of the metabolic influences on bone regeneration and implant success.

Keywords: Osteogenesis; Titanium implants; Lipogenic states; Metabolic disorders; Bone regeneration

INTRODUCTION

Metabolic disorders such as obesity are in general well-known contributors to implant failure, primarily impairing wound healing, likely due to an exacerbated inflammatory response and an increased risk of peri-implantitis (Cheng et al. 2020; de Oliveira et al. 2020). The global obesity epidemic has led to an alarming number of individuals suffering from hepatic conditions, particularly metabolic dysfunction and alcohol associated steatotic liver disease (MetALD), a new nomenclature for NAFLD (non-alcoholic fatty liver disease) (Rinella et al. 2023), whose prevalence is steadily rising, impacting 30% of the global population and increasing annually (M. V. Machado and Cortez-Pinto 2023). Accompanying this metabolic syndrome, is a constellation of risk factors including high blood pressure, insulin resistance, and dyslipidemia (Rochlani et al. 2017).

In this context, adipose tissue assumes a central role, exerting its recognized endocrine function and secreting bioactive molecules that significantly impact cellular functions in humans (Adamczak and Wiecek 2013). Although the full physiological mechanisms remain elusive, the disproportionate release of adipokines may impair osseointegration of implants by compromising bone growth around them. Studies have indicated that MetALD could also be linked to increased bone loss, raising concerns about its potential connection to osteoporosis and bone fractures (Loosen et al. 2022). However, it is as yet unclear whether this presents as a direct consequence of MetALD or is due to the underlying metabolic syndrome. As the prevalence of metabolic syndrome increases, healthcare practitioners are more likely to treat patients with these complex conditions, particularly with therapies involving titanium implants, a material chosen for its biocompatibility, strength, and durability, capable of withstanding the mechanical stresses of the musculoskeletal system (Coelho et al. 2009, 2018).

The repercussions of these conditions are vast, with compromised wound healing and alveolar bone loss in obese individuals representing a significant concern for orthopedic and dental specialists (Coelho et al. 2018). Despite suggestions of adverse effects of obesity and MetALD on bone health, there remains a knowledge gap, especially regarding their implications for implant success.

This study addresses this gap through a novel *in vitro* model exploring how obesity and MetALD influence the response of osteoblasts derived from human mesenchymal stroma cells (hMSCs) in a titanium-enriched environment. This work incorporates an *in vitro* model that correlates obesity scenarios by employing adipocytes (Pinto et al. 2023). Additionally, it utilizes in vitro steatosis models involving a hepatocyte cell line and 3D

intrahepatic cholangiocyte organoids, as previously suggested (Ayada et al. 2023; L. Wang et al. 2022). Finally, the model builds upon our previous work investigating the impact of various biomaterials on cell adhesion and differentiation (Baroncelli et al. 2019; Bertazzo et al. 2010; Celio J da Costa Fernandes et al. 2018; Célio Junior da Costa Fernandes et al. 2021; G. V. O. Fernandes et al. 2014; R. A. da Silva et al. 2019), and is the first to evaluate cellular and molecular mechanisms of MetALD conditions in response to titanium. These findings aim to fill existing gaps in our understanding, providing valuable insights to inform clinical choices and potentially expedite recovery for people with metabolic dysfunctions.

METHODS

Implants

This experimental protocol involved the utilization of two distinct titanium surfaces: Dual Acid-Etched (DAE) and nanohydroxyapatite-coated (nHA) surfaces. These two sets of titanium discs were generously supplied by S.I.N.—*Sistema Nacional de Implantes*, based in Sao Paulo, SP, Brazil. Additional details of surface characterization are described earlier (Bezerra et al. 2017; C. J. C. Fernandes et al. 2018; Gomes et al. 2023; Gottlander et al. 1997; Meirelles et al. 2008; Pinto et al. 2023).

Reagents

A83-01, alizarin red S, ammonium hydroxide, ascorbic acid, β-glycerophosphate, bovine serum albumin (BSA), calcium chloride (CaCl2.2H2O), dexamethasone, D-Glucose, forskolin, gastrin, indomethacin, 3-isobutyl-1-methylxanthine (IBMX), lactate, N-acetylcysteine, nicotinamide, octanoic acid, oil red O, oleic acid, palmitic acid and pyruvate were obtained from Sigma-Aldrich (St. Louis, MO, USA). α-MEM (without phenol red and calcium chloride), fetal bovine serum (FBS), phosphate-buffered saline (PBS), Penicillin-streptomycin were obtained from Invitrogen - Thermo Fisher Scientific Inc. (Waltham, MA, USA). Advanced DMEM/F12, B27 supplement (minus vitamin A), DMEM, and N2 supplement were obtained from Life Technologies - Thermo Fisher Scientific Inc. (Waltham, MA, USA). Epidermal growth factor (EGF), fibroblast growth factor 10 (FGF-10), and hepatocyte growth factor (HGF) were obtained from R&D Systems (Minneapolis, MN, USA). HEPES was obtained from PROMEGA (Madison, WI, USA), matrigel® was obtained from Corning (Corning, NY, USA), qPCR core kit for SYBR Green I was obtained from Eurogentec (*Seraing*, Belgium), R-spondin1 (produced

by 293TH-RspoI-Fc cell line), and ultraglutamine was obtained from Lonza (Basel, Switzerland).

2D Cell culture

Human bone marrow-derived mesenchymal stroma cells (hMSCs) (tested for surface antigens CD105+, CD166+, CD29+, CD44+, CD14−, CD34−, and CD45−; 750,000 cells per vial; expanded to passage 6) were obtained from Lonza (Basel, Switzerland). Expansion of hMSCs in pre-culture medium was performed as described before (Bruedigam et al. 2011). The hMSC cultures were maintained in 6-well culture dishes in hMSCs medium until reaching confluence and differentiated towards adipocytes or osteoblasts (see below). Huh7, a human immortalized hepatocyte-derived cellular carcinoma cell line, was purchased from the American Type Culture Collection (ATCC, Manassas, VA, USA), which were cultivated in DMEM 10% SFB. Throughout all experimental procedures, a controlled environment was maintained at 37°C with 5% CO_2 and 95% humidity.

3D intrahepatic cholangiocyte organoids MetALD model

Human intrahepatic cholangiocyte organoids (ICO) (Marsee et al. 2021) were isolated and cultured as previously described (Broutier et al. 2016), using ICO Expansion Medium (LEM - *Liver Organoids Expansion Medium*: Advanced DMEM/F12 with 1 M HEPES, ultraglutamine and penicillin-streptomycin as the basic culture medium, supplied with 1:50 B27 supplement [minus vitamin A], 1:100 N2 supplement, 1 mM N-acetylcysteine, 10 mM nicotinamide, 50 ng/ml EGF, 100 ng/ml FGF-10, 50 ng/ml HGF, 5 μM A83-01, 10 μM forskolin, 10 nM gastrin and 10% R-spondin1 [produced by 293TH-RspoI-Fc cell line]).

ICO were cultivated within Matrigel® using the LEM (n = 3), as previously detailed (L. Wang et al. 2022), for a duration of approximately one week. During this period, the medium was replenished every 72 hours. The use of human liver tissues for research purposes was ethically sanctioned by the Medical Ethical Council of Erasmus MC, with informed consent duly obtained (MEC-2014-060).

To induce lipid accumulation, we supplemented the LEM with lactate (L), pyruvate (P), and octanoic acid (O) at concentrations of 10 mM, 1 mM, and 2 mM, respectively, for a duration of 96 hours, like a previous study (Ayada et al. 2023). Following this incubation period, the medium in all experimental groups (Control and Fatty) was replaced with

LEM, devoid of LPO, to prepare the ICO-conditioned medium for 24h. Following that, organoid harvesting was conducted, and the conditioned medium was gathered for future utilization in osteoblast differentiation.

Hepatocytes Huh7 culture and free fatty acid (FFA) treatment

Oleic acid (OA) and palmitic acid (PA) were separately added to DMEM with bovine serum albumin (BSA) and incubated for 30 minutes. To induce steatosis, OA:BSA and PA:BSA complexes were prepared in a 5:1 ratio, resulting in final concentrations of 0.6 mM for both OA and PA (BSA concentration: 0.12 mM). The FFA-treated solution was supplemented with 10% fetal bovine serum and then used to treat Huh7 hepatocytes for 72 hours, inducing lipid droplet formation (Fatty Huh7) (Müller and Sturla 2019; Takahara et al. 2017).

Following the lipid stimulation, the culture medium for both the control (Ctrl) and Fatty Huh7 conditions was replaced with fresh medium containing only 10% fetal bovine serum for 24 hours, yielding Huh7-conditioned medium. Subsequently, cells were harvested, and the conditioned medium was collected for subsequent use in osteoblast differentiation.

Adipocyte differentiation

The hMSCs firstly grew in hMSC medium (Bruedigam et al. 2011)*:* α-MEM without phenol red and calcium chloride, Penicillin-streptomycin, HEPES (molecular biology grade), calcium chloride ($CaCl_2.2H_2O$), 10% fetal bovine serum, 10 M sodium hydroxide (to adjust to pH to 7.5).

Then the adipogenic differentiation was induced by using DMEM with 10% fetal bovine serum, penicillin 100 U/mL, streptomycin 100 mg/mL, 0.1 μM dexamethasone, 60 μM indomethacin and 0.5 mM IBMX.

This differentiation process was performed under two distinct experimental settings. One group was exposed to control conditions (Ctrl Adip), while the other was subjected to a high-glucose medium with a final glucose concentration of 50 mM (High Adip) to promote elevated adipogenesis. These cultures were sustained for a period of up to 14 days, changing the medium every 2 days. After the differentiation period, the culture medium for both the control (Ctrl Adip) and high adipogenic (High Adip) conditions was replaced with a fresh medium containing only 10% of fetal bovine serum for 24 hours, resulting in the creation of the adipocyte-conditioned medium. Following this, the cells

were harvested, while the conditioned medium was collected for subsequent use in osteoblast differentiation - similar to previous work (Pinto et al. 2023).

Preparation of titanium-enriched medium

To prepare the titanium-enriched medium, the conditioned media derived from adipocytes, ICO, and Huh7, were employed in the incubation of two categories of titanium discs, namely DAE (dual acid-etched) and nHA (nano-hydroxyapatite), adhering to ISO 10993:2016 standards (0.2 g/mL w/v), with slight adaptations as recommended by Zambuzzi et al . (Celio J. da Costa Fernandes et al. 2018; M. I. P. Machado et al. 2019; Zambuzzi et al. 2014). The ultimate conditioned medium was then utilized to subject hMSCs during their differentiation towards osteoblasts during a two-week exposure.

Osteogenic differentiation

The hMSCs underwent a two-week differentiation process to transform into mineralizing osteoblasts. This transformation was facilitated using 0.1 μM dexamethasone, 50 μg/mL ascorbic acid, and 10 mM β-glycerophosphate. These supplements were incorporated into the diverse conditioned media previously described for hMSC stimulation.

The resulting experimental conditions were as follows: the hMSCs-derived osteoblasts were subjected to differentiation using the conditions described in **Supplementary figure 1, Figure 4, and Supplementary figure 4.**

Oil red O staining

Oil red O stock solution was prepared by dissolving oil red O dye in isopropanol (3 mg/mL). To create the working solution, 3 parts of the stock solution were diluted with 2 parts of deionized water. The working solution was then filtered through a 0.45 μm syringe filter to remove any remaining particles. This solution was used to stain both adipocytes, intrahepatic cholangiocyte organoids and Huh7 hepatocytes.

Oil Red O Staining and Semi Quantification of Lipid Vesicles: hMSCs-derived Adipocytes and Hepatocytes Huh7

After cell treatments, the medium was removed, cells were washed with warm PBS, fixed in 4% paraformaldehyde at room temperature for 1 hour, washed with 60% isopropanol, and stained with the oil red O working solution for up to 30 minutes at room temperature. The stained cells were washed three times with deionized water and stored in water.

Images were captured using an inverted microscope (Axio Vert.A1, Carl Zeiss microscopy GMBH, Göttingen, Germany). For semi-quantification, water was removed, and the wells were air-dried at room temperature. In each well, 250 µL of isopropanol was added and shaken for 30 minutes on a plate shaker. Subsequently, 100 µL from each well was transferred to a 96-well plate, and the absorbance was measured at 490 nm using a plate reader.

Oil Red O Staining: 3D intrahepatic cholangiocyte organoids

Formed lipids were stained with oil red O after disrupting the Matrigel structure and centrifuging to remove excess Matrigel. In the same tube, the organoids were washed carefully with PBS, followed by a wash with 60% isopropanol. Subsequently, the organoids were stained with the oil red O working solution for up to 30 minutes at room temperature. They were then washed three times with deionized water, with centrifugation after each wash to remove supernatant. The stained organoids were mounted on glass slides using an anti-fading medium and Cellspin® centrifuges. Images were captured using an inverted microscope (Axio Vert.A1, Carl Zeiss microscopy GMBH, Göttingen, Germany).

ELISA

To assess the levels of IL-6 and IL-5 in the conditioned medium from adipocytes, we employed the Invitrogen™ IL-6 Human Uncoated ELISA Kit (Thermo Fisher Scientific, Catalog # 88-7066-88) and the Invitrogen™ IL-5 Human Uncoated ELISA Kit (Thermo Fisher Scientific, Catalog # 88-7056-88), following the instructions provided by the manufacturer.

RT-qPCR

We isolated RNA using the NucleoSpin® RNA Plant Column Set (MachereyNagel, Germany) following the manufacturer's instructions. This RNA was then converted into cDNA through the utilization of either the miScript Reverse Transcription II kit or the PrimeScript RT Master Mix kit (QIAGEN, Hilden, Germany). RT-qPCR analysis was performed using the SYBR Green qPCR assay (Thermo Fisher Scientific, Massachusetts, USA) and gene-specific primers. The relative gene expression levels were determined using the $2^{-\Delta\Delta Ct}$ method, with *RP2* as the internal control for mRNA analysis.

Alizarin Red S Staining

For histological assessment of extracellular matrix mineralization in hMSC-derived osteoblasts, we performed alizarin red S staining. The hMSCs were cultured in 12-well plates, and osteoblast differentiation was conducted as previously described. At the end of the culture period, the cells were washed with PBS and fixed with 10% formalin (700 µl/well) for 15 minutes at room temperature. After fixation, the cells were rinsed with Milli-Q water and stained with 500 µl/well of alizarin red S solution (3 g of alizarin red S in 500 ml Milli-Q water, pH adjusted to 4.2 with ammonium hydroxide) for 20 minutes at room temperature. Subsequently, the cells were washed four times with Milli-Q water, each time for 5 minutes. Finally, the cells were stored in Milli-Q water, and images were captured using an inverted microscope (Axio Vert.A1, Carl Zeiss microscopy GMBH, Göttingen, Germany).

Western blot

hMSCs-derived osteoblasts were collected, and proteins were extracted using 500 µl of Laemmli Buffer, which consists of 4% SDS, 20% glycerol, 120 mM Tris-Cl (pH 6.8), 0.02% (wt/vol) bromophenol blue, and 0.1 M DTT. The protein concentrations were determined using a commercial kit (RC DC Protein Assay by Bio-Rad).

Western blotting was carried out following previously described protocols (Somasundaram et al. 2017; de Sousa et al. 2007). In summary, 40 µg of protein was separated by SDS-PAGE and transferred onto Immobilon FL PVDF membranes from Millipore, Bedford, MA. These membranes were blocked using Odyssey Blocking Buffer (PBS) and left to incubate overnight at 4°C with the appropriate primary antibodies. Afterward, the membranes were incubated with the suitable Alexa-linked secondary antibodies, each at a 1:5000 dilution, in Odyssey Blocking Buffer for 1 hour. Fluorescent bands were detected using the fluorescent Odyssey Imaging System (ODYSSEY® CLx Infrared Imaging System), and densitometric analysis was conducted with ImageJ software (Bethesda, MD, USA) (Schindelin et al. 2015).

In each blot, actin was used as a control to account for equal loading, and the results were normalized, presenting the ratios of the protein of interest over actin levels for each lane.

Analysis of Matrix Metalloproteinases (MMPs) Activities by Zymography

To assess MMPs activity, we collected the conditioned medium from hMSCs-derived osteoblasts cell cultures. This medium was subjected to centrifugation at 14,000 rpm for

15 minutes to remove cellular debris, and the protein concentration was determined using the Lowry method (Hartree 1972). An equal amount of protein was then loaded onto a 12% polyacrylamide gel containing 4% gelatin.

The gelatinolytic activity of MMPs was assessed within the resolved protein bands. To accomplish this, the proteins were first renatured, firstly by washing in a 2% w/v Triton X-100 aqueous solution for 40 minutes, and subsequently, the gels were incubated in a proteolysis buffer (Tris-$CaCl_2$) at 37°C for 18 hours. After this incubation period, the gels were stained with a 0.05% Coomassie Blue R-250 dye solution for 3 hours.

The stained gels were then washed in a solution containing 30% methanol (v/v) and 10% glacial acetic acid (v/v). Areas of gelatinolytic activity, characterized by clear bands, corresponded to MMP2 (~64 kDa) and MMP9 (~84 kDa) activities. These bands were analyzed using ImageJ software (Bethesda, MD, USA), as previously described (Lefebvre, Peeters-Joris, and Vaes 1991).

Statistical analysis

The data was presented as the mean ± standard error of the mean (SEM) for each experiment's replicates (n = 3). The datasets exhibited a normal distribution, and statistical analysis was conducted using a two-tailed Student's t-test, with significance set at $p < 0.05$. In experiments involving more than two groups, we employed either one-way analysis of variance (one-way ANOVA) followed by Bonferroni's correction post-test, or nonparametric analysis. A significance level of $p < 0.05$ was used to determine statistical significance. The statistical software employed for these analyses was GraphPad Prism 7 (GraphPad Software, La Jolla, CA, USA).

RESULTS

Table 1 Description of the experimental assay (n = 3).

Lineage	Treatment			Time		Variable (Group)
hMSCs-derived adipocytes	Adipogenic medium*			2 weeks	24h only DMEM	Ctrl Adip
	Adipogenic medium* + 50 mM glucose					High Adip
Intrahepatic cholangiocyte organoids (ICO)	LEM**			4 days	24h only LEM**	Ctrl ICO
	LEM** + lactate, pyruvate, and octanoic acid (LPO)					Fatty ICO
Huh7	DMEM			3 days	24h only DMEM	Ctrl Huh7
	DMEM + oleic acid and palmitic acid (OA&PA)					Fatty Huh7
hMSCs-derived osteoblasts	Osteogenic medium*** + Adipocytes-conditioned medium	Ctrl Adip medium		2 weeks		Adip
			Titanium DAE			Adip + DAE
			Titanium nHA			Adip + nHA
		High Adip medium				H_Adip
			Titanium DAE			H_Adip + DAE
			Titanium nHA			H_Adip + nHA
hMSCs-derived osteoblasts	Osteogenic medium*** + ICO-conditioned medium	Ctrl ICO medium		2 weeks		ICO
			Titanium DAE			ICO + DAE
			Titanium nHA			ICO + nHA
		Fatty ICO medium				FAT ICO
			Titanium DAE			FAT ICO + DAE
			Titanium nHA			FAT ICO + nHA
hMSCs-derived osteoblasts	Osteogenic medium*** + Huh7-conditioned medium	Ctrl Huh7 medium		2 weeks		Huh7
			Titanium DAE			Huh7 + DAE
			Titanium nHA			Huh7 + nHA
		Fatty Huh7 medium				FAT Huh7
			Titanium DAE			FAT Huh7 + DAE
			Titanium nHA			FAT Huh7 + nHA

* Adipogenic Medium: Dexamethasone, Indomethacin, IBMX (3-isobutyl-1-methylxanthine).

** LEM = Liver Organoids Expansion Medium.

*** Osteogenic Medium: Dexamethasone, Ascorbic acid, and β-glycerophosphate.

Verification of the High-Lipogenesis Model in hMSCs-Derived Adipocytes

We initiated our examination of the high-adipogenesis model (Supplementary figure 1a) by analyzing typical markers of the adipocyte phenotype in the context of heightened glucose levels. It is possible to see the difference in the hMSCs morphology before the differentiation process at time zero (Supplementary figure 1b) and the cells after two weeks of differentiation in adipocytes (Supplementary figure 1c and d). Specifically, we quantified the accumulation of fat droplets as an indicator of adipogenesis. The results underscored a pronounced increase in fat storage within the High Adip group when compared to the standard adipogenic environment as confirmed by visual inspection and semi-quantitative analysis of oil red O-stained intracellular fat droplets (Supplementary figure 1e-g). Reflecting the low-level inflammation seen in obesity, a significant protein elevation of IL-6, but not IL-5, was observed in the High Adip group (Supplementary figure 1h-i). Together, these results indicate that high glucose treatment of hMSCs serves as a model for adipocytes under obese conditions.

Cell adhesion and extracellular matrix remodeling in hMSC-derived osteoblasts

To glean insight into osteoblast function in response to titanium-enriched mediums in both standard and high-adipogenesis co-culture conditions, we investigated focal adhesion kinase (FAK) phosphorylation, a key player in cell adhesion. Phosphorylation of FAK at tyrosine 397 was found to be increased in osteoblasts cultured in high-adipogenesis conditions compared to normal adipocytes (Figure 1a and b). High adipogenesis co-culture increased FAK phosphorylation. The group treated with nHA exhibited increased levels of FAK phosphorylation, although this effect was not observed under conditions of high adipogenesis.

Extracellular matrix (ECM) remodeling was assessed by analyzing matrix metalloproteinase (MMP) activity in osteoblasts (Figure 1c-g). An increase in MMP2 and MMP9 activities was observed under high-adipogenesis conditions compared to normal adipocyte conditioned medium, which remained visible in the presence of DAE titanium, but not in the presence of nHA. This latter was due to an already increased upregulated MMP activity in osteoblasts treated with Adip + nHA conditioned medium. These data suggest that adipogenesis enhances cell adhesion and ECM remodeling in osteoblasts, but that titanium surfaces differentially affect these osteoblast functions.

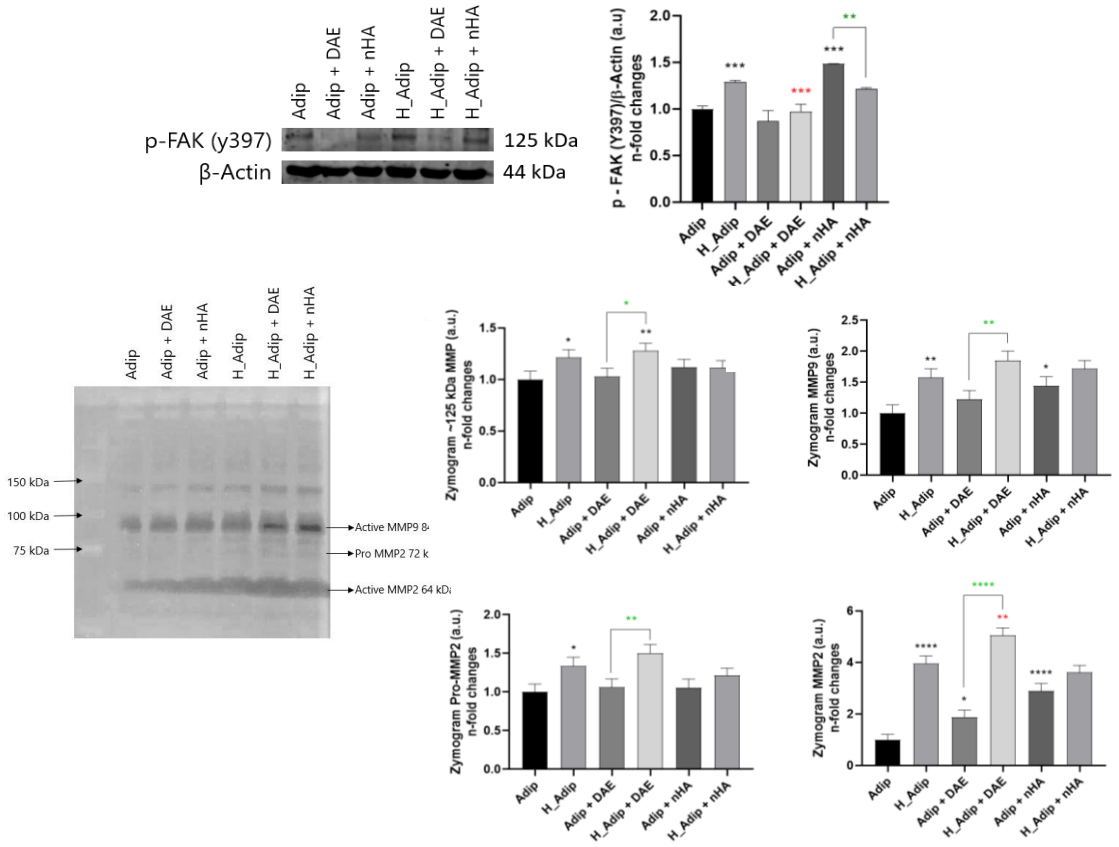

Figure 1: Functional changes in osteoblasts upon coculture with adipocytes and titanium. (a, b) Osteoblasts were harvested after differentiation in the presence of conditioned medium from normal and high glucose adipocytes, with or without titanium exposure. Western blot analysis was performed to phospho-FAK (y397) protein content. β-Actin was considered the protein loading control. (c-g) The results of the zymography technique demonstrate heightened activity of MMP9 (e), Pro-MMP2 (f), and MMP2 (g) in osteoblasts subjected to conditioned medium from high glucose adipocytes. Representative zymography example shown in c, quantification of individual bands shown in d-g. Statistical significance is denoted by asterisks (* $p < 0.05$, ** $p < 0.01$, *** $p < 0.001$, **** $p < 0.0001$), represented by black asterisks in comparison to the Adip group, red asterisks in comparison to the H_Adip group, and green asterisks for comparisons between groups with DAE or between the groups with nHA. The assays were performed in triplicate. DAE = titanium with Dual Acid-Etching; nHA = titanium with nano-Hydroxyapatite-coated surface.

Lipid vesicle accumulation and mineralization upon co-culture of hMSC-derived osteoblasts with adipocyte-derived medium.

Next, we investigated the differentiation of osteoblasts from hMSC in the presence of conditioned media from adipocytes. Visualizing mineralized extracellular matrix (ECM) using alizarin red S staining, we confirmed that cells exposed to both osteogenic medium and adipocyte-conditioned medium successfully underwent mineralization (Figure 2a-f,

upper panels), to a similar extent as cells treated with osteogenic medium alone but not with DMEM alone (Figure 2g and h, panels on the left). Exposure to titanium-enriched medium did not affect this process. We observed an accumulation of intracellular fat droplets upon treatment of osteoblasts with adipocyte-conditioned medium (Figure 2a-f, lower panels), which was not seen when cells were treated with only osteogenic medium or DMEM (Figure 2g and h, panels on the right). This was evident with conditioned media from both normal and high glucose-treated adipocytes, and again titanium exposure did not appear to affect this phenotype.

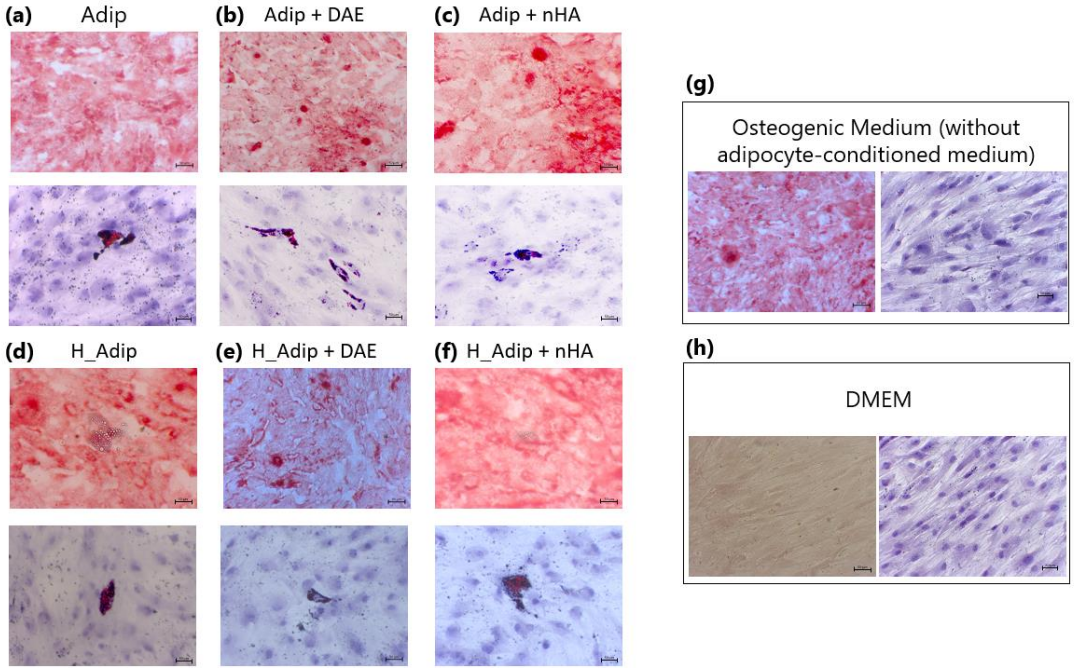

Figure 2. Mineralization and lipid accumulation of osteoblasts derived from hMSCs upon treatment with adipocyte-conditioned medium. Alizarin red S staining of osteoblasts derived from hMSCs, cultured in the presence of conditioned medium from normal adipocytes (Adip, a-c), high glucose adipocytes (H_Adip, d-f) obtained the absence (a and d) or presence of titanium surface DAE (b and e) or nHA (c and f) was performed to determine mineralization of cultures and ensure the osteoblasts differentiation (upper panels). Staining with oil red O and hematoxylin was performed to investigate the ability of the model to trigger lipid droplet accumulation and cell shape, respectively, under these same conditions (a-f) lower panels. As controls, hMSCs exposed solely to osteogenic medium (g), or DMEM alone (h) are shown. The experiments were carried out in three replicates. DAE = titanium with Dual Acid-Etching; nHA = titanium with nano-hydroxyapatite-coated surface.

Gene expression analysis of osteogenesis-related genes in osteoblasts from hMSCs exposed to high adipogenesis and titanium

Having visually confirmed successful osteoblast differentiation in hMSCs in the presence of conditioned media, we next sought to elucidate whether differentiation patterns were quantitatively affected by the presence of titanium. For this analysis, we compared osteoblasts derived from hMSCs under low and high-adipogenesis conditions alongside titanium exposure. Heatmap presentation of a panel of osteoblast-associated genes indicated diverse cellular responses under different treatment conditions (Fig 3a). While not reaching significance, conditioned medium from H_Adip cells reduced expression of the osteogenic markers *RUNX2 (osteoblast transcription factor)*, *BMP7* (a key factor in bone development), *ALP* (pivotal for osteoblastic activity) and *BGLAP*, encoding osteocalcin. Concurrent conditioning with titanium surfaces drastically enhanced the expression of *RUNX2*, *BMP7* and *BGLAP*, but only for H_Adip conditioned media, and most noticeably nHA titanium surface. The *BGLAP* gene demonstrated differential regulation, with a significant upregulation in the presence of titanium DAE and nHA, under both normal and high-adipogenesis conditions with nHA (Fig. 3f). In contrast, the expression of the BMP receptor gene *BMPR1* remained relatively unchanged across all tested conditions (Fig. 3e). Given the accumulation of fat droplets in osteoblastic cells upon co-culture with adipocyte-conditioned medium, we also assessed the expression of *PPARG*, as a measure of adipogenesis. *PPARG* expression was notably diminished in the H_Adip group when further subjected to the DAE and nHA titanium surfaces (Fig. 3g), indicating that differentiation patterns are not skewed towards adipocyte differentiation under these conditions.

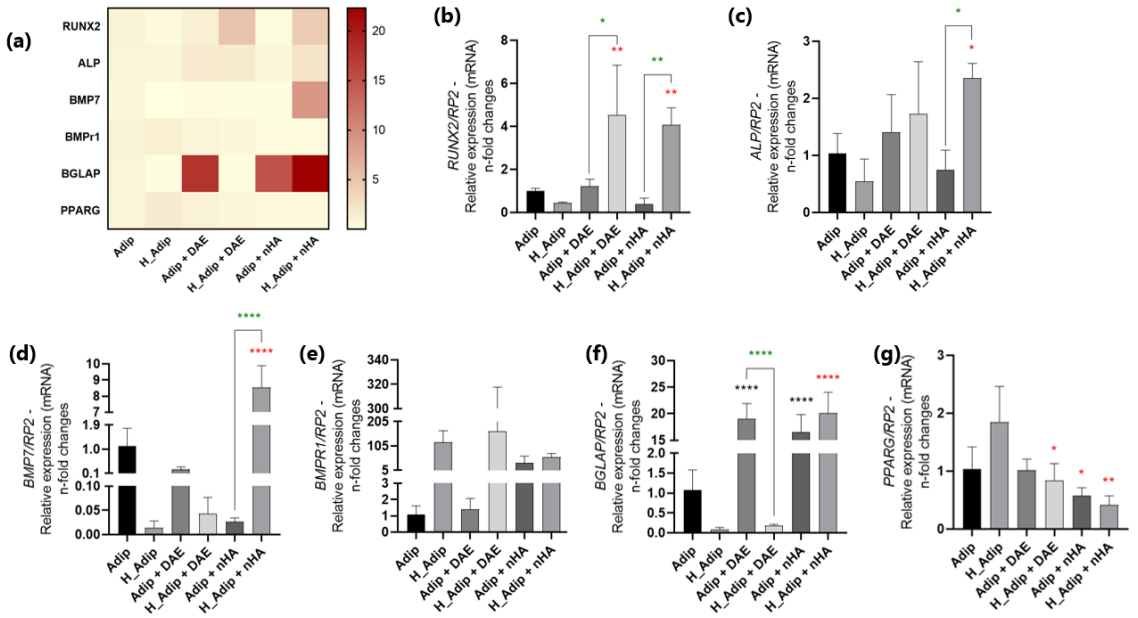

Figure 3. RT-qPCR outcomes of osteogenic cells derived from hMSCs undergoing differentiation in the presence of adipocytes-conditioned medium with or without titanium enrichment. Gene expression analysis of mesenchymal stroma cells (MSCs) differentiated towards osteoblasts in the presence of medium conditioned with normal adipocytes (Adip), high-glucose treated adipocytes (H_Adip) in the absence or presence of titanium surfaces with Dual Acid-Etching (DEA) or nano-hydroxyapatite-coated surface (nHA). (a) Heatmap illustrating the diverse responses of a panel of genes to individual culture conditions. (b-g) Individual expression profiles of *RUNX2* (b), *ALP* (c), *BMP7* (d), *BMPR1* (e), *BGLAP* (f) and *PPARG* (g). Transcript profile changes are depicted as n-fold differences normalized to the *RP2* gene, performed in triplicate, with statistical significance denoted by asterisks (* $p < 0.05$, ** $p < 0.01$, **** $p < 0.0001$), represented by black asterisks in comparison to the Adip group, red asterisks in comparison to the H_Adip group, and green asterisks for comparisons between groups with DAE or between the groups with nHA.

Model utilizing 3D intrahepatic cholangiocyte organoids (ICO)

Having shown a significant effect of adipose conditions in co-culture of osteoblasts with adipocytes, we next examined whether other lipogenic tissues present similar effects. To this end, we first set up a high-lipogenesis model, leveraging 3D ICO (Fig. 4a). Our results seem to reveal an increase in lipid accumulation when organoids were supplemented with lactate, pyruvate, and octanoic acid, as evidenced by oil red O staining (Fig. 4c-d). We analyzed the expression of targeted key markers involved in steatosis and lipid metabolism, such as *PNPLA3*, *TM6SF2*, and *SREBP1*, as well as mitochondrial function genes like *CPT1A*, *CPT1B*, and *CYTB*, and the inflammation marker *TNFA*. The ICO under the high-lipogenesis condition (Fatty Liv.Or.) exhibited a marked increase in the expression of these genes, suggesting an enhanced steatotic state, while the expression of *CIDEB*, *PPARA*, and other related genes remained unaffected (Fig. 4e-m).

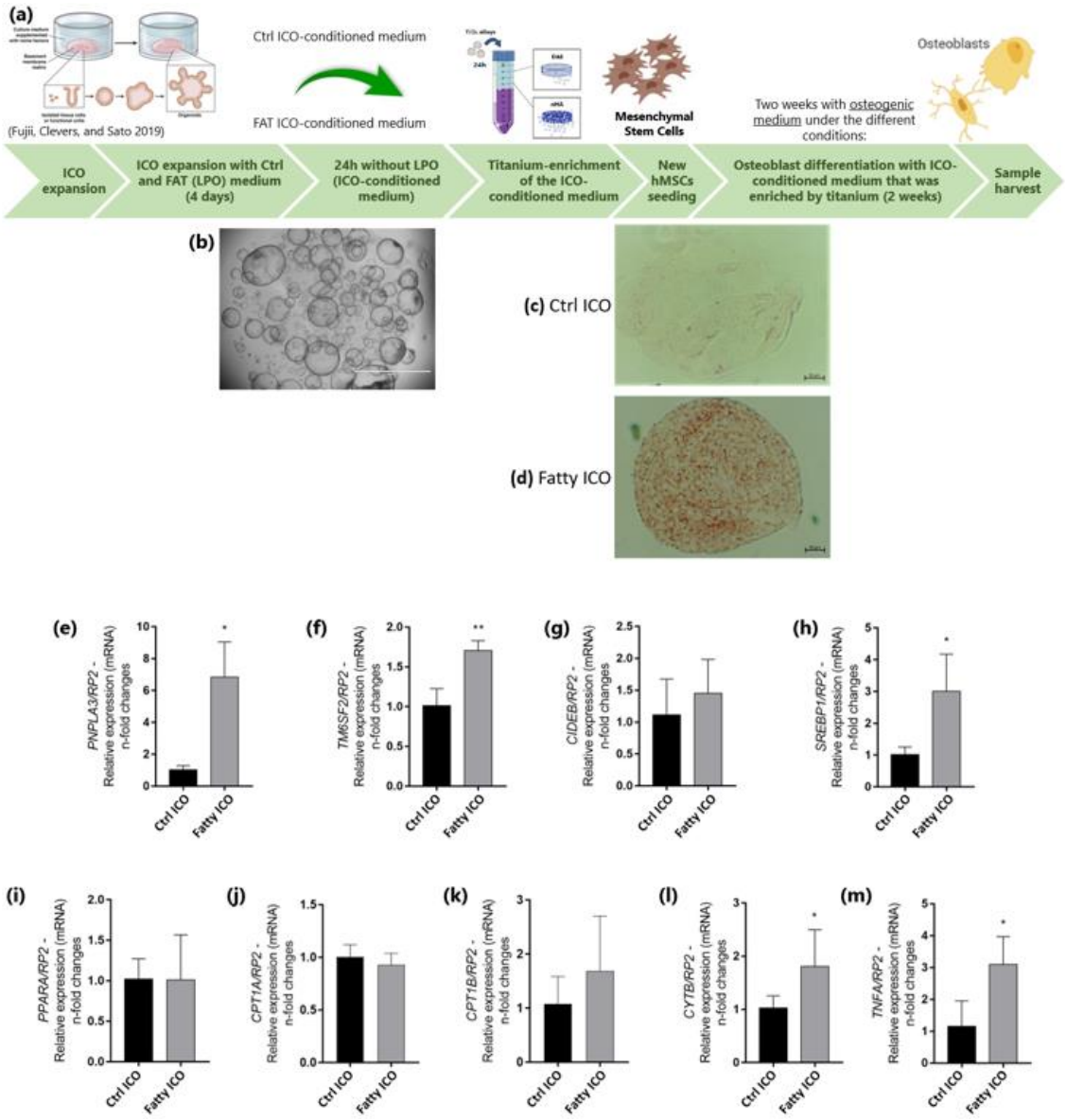

Figure 4. Experimental MetALD model using 3D intrahepatic cholangiocyte organoids (ICO). (a) graphical presentation of the generation of conditioned media from human ICO in the absence or presence of titanium surfaces. Organoids were first cultured in the presence or absence of lactate, pyruvate, and octanoic acid (LPO) for 4 days, after which the culture medium was substituted and organoids were cultured medium without LPO for 24 hours to condition the medium. This conditioned medium underwent titanium enrichment for 24 hours, following ISO 10993:2016 guidelines. Subsequently, this enriched medium was utilized to induce osteoblast differentiation in hMSCs for a two-week period, after which samples were collected for molecular analysis. **C-M.** Verification of organoid MetALD model. The images depict ICO (b) as observed through an EVOS microscope (40x). To validate the high lipogenesis model, ICO cultured in the absence (Ctr liv.org, c) or presence (Fatty Liv.org, d) of LPO underwent oil red O staining. Images of oil red O were captured using an inverted microscope. Gene expression results of ICO after 4 days under normal and LPO conditions. A significantly higher expression of the *PNPLA3* (e), *TM6SF2* (b), *SREBP1* (h), *CYTB* (l), and *TNFA* (m)

genes were observed in ICO responding to LPO. The graphs depict the n-fold change in the gene expression profile, normalized to the RP2 gene (a housekeeping gene). All experiments were performed in three replicates. Statistical significance was determined at * $p < 0.05$, and ** $p < 0.01$.

Evaluation of lipid vesicles and mineralization in hMSC-derived osteogenic cells

In our investigation into the osteogenic capacity of hMSCs treated with ICO-conditioned medium, we again observed intracellular fat vesicles across all test groups, including those subjected to standard and fatty ICO-conditioned mediums, as well as those in contact with titanium surfaces (Supplementary Fig 2a-f, lower panels). This lipid accumulation appeared even more pronounced than when hMSC-derived osteoblasts were treated with adipocyte-conditioned medium. This finding prompted us to verify osteoblast differentiation using the alizarin red S assay, which confirmed successful mineralization of the extracellular matrix in all groups exposed to the osteogenic medium with titanium and ICO-conditioned medium (Supplementary Fig 2a-f, upper panels). This result supports the osteoblast differentiation potential of the cells, even in the presence of high lipid content within the media.

Gene expression and functional analysis of hMSC-derived osteoblasts exposed to fatty ICO and titanium

We delved deeper into the gene expression patterns to understand the osteogenic response of hMSC-derived osteoblasts under the dual influence of high-lipogenesis conditions in ICO and titanium-enriched media. A gene expression heatmap (Fig. 5a) was constructed to depict the nuanced responses of various osteogenesis-related genes to different treatments. Interestingly, while the expression levels of key genes like *RUNX2*, *PPARG*, and *ALP* were not significantly altered under most conditions, the *BMP7* and *BMPR1* genes demonstrated decreased expression in response to fatty liver conditions and normal conditions with titanium DAE, suggesting a complex interplay between lipid content and osteoblastic activity (Fig. 5b-g). Analysis of the activity of MMPs through zymographic assay indicates downregulation of MMP activity of osteoblasts when in the presence of high-lipogenesis conditions (Supplementary figure 3), which could reflect a potential effect of high lipids on ECM remodeling.

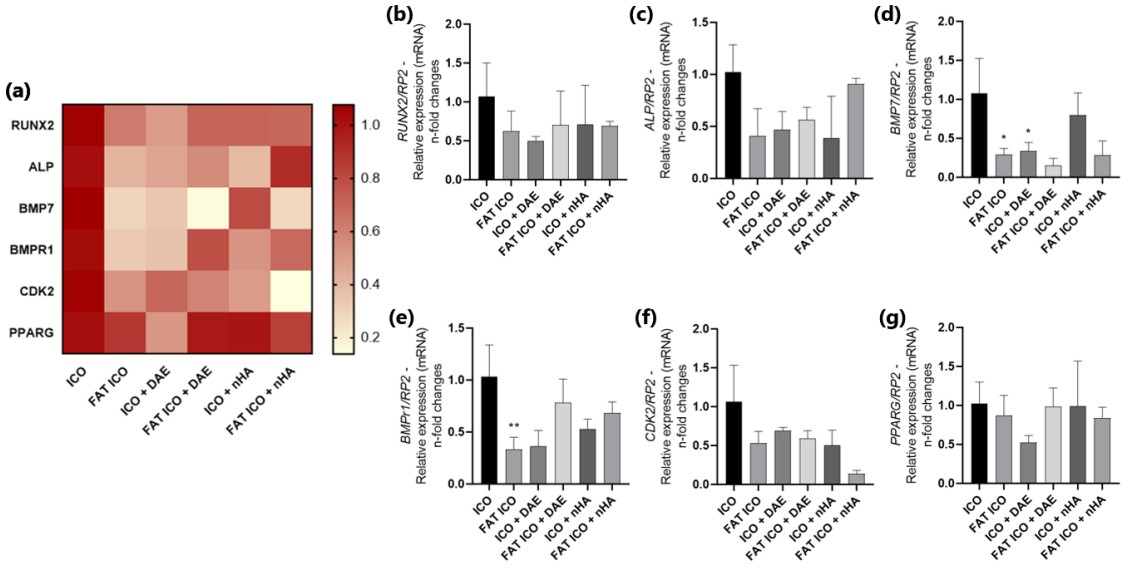

Figure 5. RT-qPCR outcomes of osteogenic cells derived from hMSCs undergoing differentiation in the presence of ICO-conditioned medium with or without titanium enrichment. Gene expression analysis of mesenchymal stroma cells (MSCs) differentiated towards osteoblasts in the presence of medium conditioned with ICO (Liv.Or), LPO treated organoids (FAT Liv.Or) in the absence or presence of titanium surfaces with Dual Acid-Etching (DAE) or nano-Hydroxyapatite-coated surface (nHA). (a) Heatmap illustrating the diverse responses of a panel of genes to individual culture conditions. (b-g) Individual expression profiles of *RUNX2* (b), *ALP* (c), *BMP7* (d), *BMPR1* (e), *CDK2* (f) and *PPARG* (g). Transcript profile changes are depicted as n-fold differences normalized to the *RP2* gene in triplicate with statistical significance indicated by asterisks (* $p < 0.05$, and ** $p < 0.01$). Black asterisks denote comparisons to the Liv.Or. group.

Assessing mineralization in osteoblasts treated with huh7-conditioned medium

Lastly, we created a model system of high adipose hepatocyte conditions, by treating Huh7 cells with oleic acid and palmitic acid (OA&PA) (Supplementary figure 4).

Evaluating osteogenic gene expression and functionality in osteoblasts treated with fatty Huh7 and titanium-enriched medium

As for the other model systems described above, intracellular lipid vesicles as in osteoblasts as well as their successful mineralization, as evidenced by alizarin red S staining (supplementary Figure 5) was observed.

Quantitative analysis of the differential expression of osteogenesis-related genes in response to various treatments with fatty Huh7 and titanium (Fig. 6) indicates a complex osteoblast response. Notably, RUNX2 and BMP2 were oppositely modulated between titanium surfaces and the lipogenic condition (b and d). Additionally, the

BGLAP gene, involved not only in mineralization but also in energetic metabolism, was significantly decreased in all FAT Huh7 groups. Further studies involving these constituents could have far-reaching implications for understanding the molecular underpinnings of bone formation and its potential modulation by metabolic states.

CDK2, a protein crucial for cell cycle progression and with a vital role in osteoblast replication, was evaluated. Its phosphorylation, associated with the advancement of the cell cycle, is essential for osteoblast replication. Interestingly, under the high lipogenesis condition of Huh7 hepatocytes, there was a significant reduction in the content of p-CDK2 (Thr160) in osteoblasts. However, in the presence of nHA titanium, this effect did not occur. A similar pattern was observed with CREB, where phosphorylated p-CREB (Ser133) acts as an activator of genes involved in the cell survival and differentiation of osteoblasts (Fig. 7a-d).

Finally, the changes in ECM dynamics, as revealed by alterations in MMPs activities (Supplementary figure 6), point to a nuanced regulatory environment within osteoblasts that could be influenced by lipid-rich conditions and the presence of titanium.

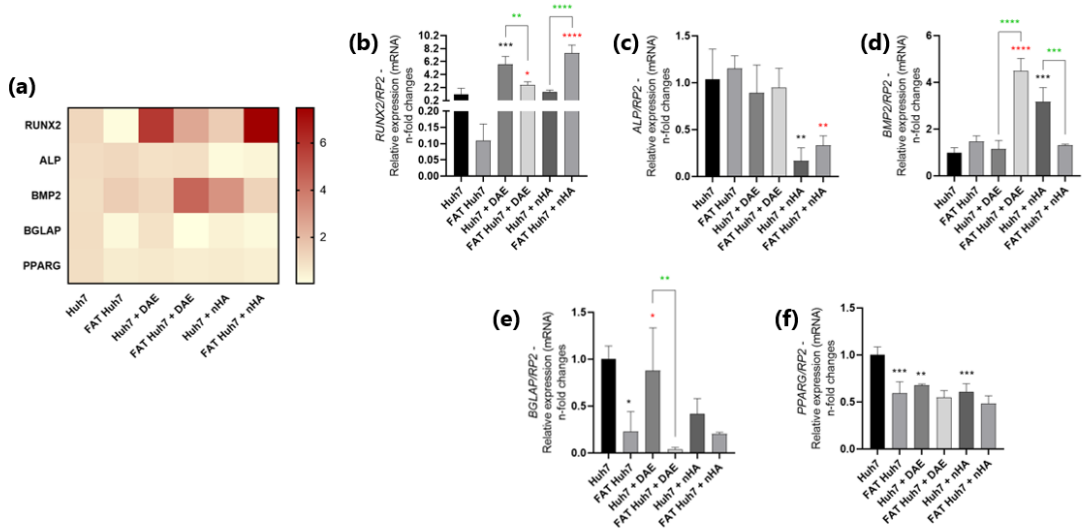

Figure 6. RT-qPCR outcomes of osteogenic cells derived from hMSCs undergoing differentiation in the presence of hepatocyte-conditioned medium with or without titanium enrichment. Gene expression analysis of mesenchymal stroma cells (MSCs) differentiated towards osteoblasts in the presence of medium conditioned with Huh7 cells or OA&PA-treated Huh7 cells (FAT Huh7) in the absence or presence of titanium surfaces with Dual Acid-Etching (DAE) or nano-Hydroxyapatite-coated surface (nHA). (a) Heatmap illustrating the diverse responses of a panel of genes to individual culture conditions. (b-f) Individual expression profiles of *RUNX2* (b), *ALP* (c), *BMP2* (d), and *PPARG* (f). Transcript profile changes are depicted as n-fold differences normalized to the *RP2* gene, performed in triplicate, with statistical significance indicated by asterisks (* $p < 0.05$, ** $p < 0.01$, *** $p < 0.001$, and **** $p < 0.0001$), represented by black

asterisks in comparison to the Huh7 group, red asterisks in comparison to the FAT Huh7 group, and green asterisks for comparisons between groups with DAE or between the groups with nHA.

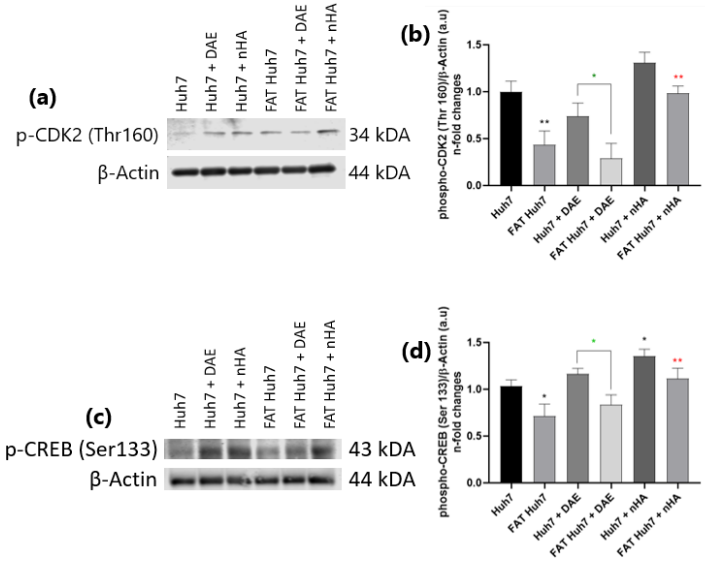

Figure 7. Cell cycle and proliferation of hMSCs after two weeks of differentiation in osteoblasts, treated with hepatocytes Huh7-conditioned medium and titanium-enriched medium. The western blot results show that the phosphorylation profile of CDK2 (Thr160) is subject to modulation by the various treatments, showing a decrease in fatty conditions, although this response is somewhat mitigated by the presence of titanium nHA (a-b). Furthermore, the phosphorylation of CREB (Ser133), which is down-regulated in the FAT Huh7 group, appears to be partially mitigated by both titanium DAE and nHA (c-d). The experiments were performed in triplicate. Significant differences are indicated by asterisks (* $p < 0.05$, ** $p < 0.01$), with black asterisks denoting comparisons to the Huh7 group, red asterisks for comparisons to the FAT Huh7 group, and green asterisks for intergroup comparisons involving DAE.

DISCUSSION

Our investigation delved into the intricate relationship between metabolic disorders and the response of osteoblasts to titanium implants, establishing an in vitro model mirroring the high-lipogenesis conditions characteristic of obesity and MetALD. Our findings reveal compelling insights into the effects of metabolic dysfunction on bone cell behavior and implant integration. We observed that hMSCs-derived adipocytes subjected to elevated glucose levels exhibited not only an increase in intracellular lipid droplets but also an enhanced inflammatory profile, marked by elevated IL-6 content and TNF-alpha expression (Coelho et al. 2018; Palacios-Ortega et al. 2016; Pinto et al. 2023; Shilpa,

Dinesh, and Lakshmi 2013). The increase in intracellular fat droplets triggered by glucose appears to coincide with an increase in cell number in the figure, reminiscent of the conditions of hypertrophy (increase in cell size) and hyperplasia (increase in cell number) observed in the adipose tissue of obese patients (Jung and Choi 2014).

The progression from simple steatosis to steatohepatitis and cirrhosis, as part of the MetALD spectrum, represents a continuum of liver damage associated with metabolic dysfunction (Chalasani et al. 2018; Eslam et al. 2020). By employing intrahepatic cholangiocyte organoids (ICO) and Huh7 hepatocyte models, we closely address these conditions to ascertain their effect on bone cell response to titanium. The implication of cholangiocytes, the epithelial cells lining the bile ducts, in fatty liver disease (Cadamuro et al. 2022; S. Wang et al. 2023) has prompted the proposal of *in vitro* studies utilizing these cells to model steatosis yielding valuable insights into the disease process (Ayada et al. 2023; L. Wang et al. 2022). Our models recapitulated key features of MetALD, including steatosis markers PNPLA3 and TM6SF2, upregulated in our fatty ICO, and SREBP1, a regulator of lipogenesis, demonstrating an increase in expression in line with MetALD (Fabbrini, Sullivan, and Klein 2010; Newberry et al. 2021).

The findings of this study illuminate the potential systemic impact of dysfunctional adipose or liver disease on bone health, likely mediated by hormones, metabolites, fatty acids, and lipoproteins, which may be further influenced by extracellular vesicles from these tissues (Huang-Doran, Zhang, and Vidal-Puig 2017). The presence of lipid droplets within osteoblasts, once considered exclusive to adipocytes, underscores a more dynamic lipid metabolism within bone cells than previously recognized (Enlow, Conklin, and Bang 1965; Rendina-Ruedy, Guntur, and Rosen 2017).

Our discovery of intracellular lipid vesicles in hMSCs-derived osteoblasts across various conditions, including standard treatments, poses new questions about the role of these organelles in osteoblast function. This is particularly relevant as bone marrow adiposity and low bone mass have been linked to lipid accumulation in bone cells, a phenomenon associated with conditions such as aging and alcoholism (Ronis, Mercer, and Chen 2011; S. V. da Silva et al. 2016). Additional quantification studies using this model are essential to assess whether adipocytes and titanium impact osteoblast lipid content and mineralization. This underscores the significance of exploring these cells within co-culture models.

Hydroxyapatite (the mineralized form of calcium phosphate present in bone) has been proposed as a nanoscale bone implant surface coating to induce appropriate

osseointegration (C. J. C. Fernandes et al. 2018). In terms of osteoblast differentiation, the expression of *RUNX2*, a critical transcription factor for osteogenesis, was notably influenced by titanium surfaces. The upregulation of *RUNX2* in the presence of titanium suggests a protective feedback mechanism that may counteract the pro-inflammatory state induced by high-lipogenesis conditions (Salazar, Gamer, and Rosen 2016; R. N. Wang et al. 2014). This protective effect seems to be triggered by nHA under crosstalk with adipocytes by upregulating BMP7, a key agent in osteoblastic differentiation and promoting bone formation (Kanakaris et al. 2009). Moreover, the study's outcomes hint at a significant modulation of osteoblast functionality in response to metabolic states, with variations in gene expression and protein activity that could impact implant integration.

In osseointegration, cell adhesion proteins play a crucial role in ensuring successful implantation. Among these proteins, FAK is pivotal in focal adhesion signaling, essential for cell adhesion, particularly when activated by phosphorylation at Y397 (p-FAK) (Gittens et al. 2014). We observed an influence of the two adipogenic environments on the response of osteoblasts to titanium in cell adhesion signaling pathways. In normal conditions, the titanium nHA-enriched medium led to an increase in the content of p-FAK (y397) in osteoblasts. However, under conditions of high adipogenesis with titanium nHA, the observed increase was less pronounced. Our results corroborate with another study evaluating the pre-osteoblasts MC3T3-E1 upregulating the p-FAK (y397) when in direct contact with the titanium nHA (Bezerra et al. 2017). This data suggests that the high adipogenesis condition is affecting the osteoblast adhesion signaling in response to the titanium nHA.

Crucial mechanisms involved in these processes include the cell cycle and osteoblast proliferation, regulated by the phosphorylation of key constituents. The MetALD model with Huh7 influenced the phosphorylation profile, particularly in CDK2 (whose phosphorylation is associated with cell cycle progression, crucial for osteoblast replication) (Shaikh et al. 2023), and CREB (a regulator of genes involved in cell survival and differentiation into osteoblasts) (Oury et al. 2010).

Osteocalcin is a crucial component of the bone matrix. It plays a vital role in regulating mineralization, contributing to the integrity and structural resistance of bones (Wawrzyniak and Balawender 2022). Also, osteocalcin is often associated not only with improved glucose metabolism but also with benefits in insulin resistance and obesity, demonstrating positive cardiometabolic effects, which highlight its importance in the complex interaction between bones and other metabolic and physiological systems

(Kanazawa 2015). Intriguingly, the observed increase in osteocalcin (*BGLAP*) expression in osteoblasts under high adipogenic conditions and a medium enriched with titanium raises questions about whether titanium may play a protective or attenuating role in mitigating the harmful effects of high lipogenesis in bones by stimulating *BGLAP* gene. This suggests a potential stimulus by titanium in the expression of osteocalcin.

The influence of lipogenesis conditions on the response of osteoblasts to titanium varies across different titanium surfaces. Moreover, it's crucial to recognize that not all lipogenic conditions are uniform; the effects stemming from adipocytes, ICO, and hepatocytes exhibit distinctive patterns. This intricate interplay signifies a complex adaptive response from cells, underscoring the need for further in-depth studies. This suggests a need to consider metabolic health when selecting titanium surface treatments to optimize implant success (Coelho et al. 2018), and also reduce re-implantation and burden on health care due to readmissions of the patients.

Taking our data into account, this study underscores the influence of metabolic conditions on osteoblastic activity and response to implant materials. Future studies are warranted to further elucidate these mechanisms and translate these findings into clinical practice for improved management of bone healing in metabolic disorders.

SUPPLEMENTARY MATERIAL

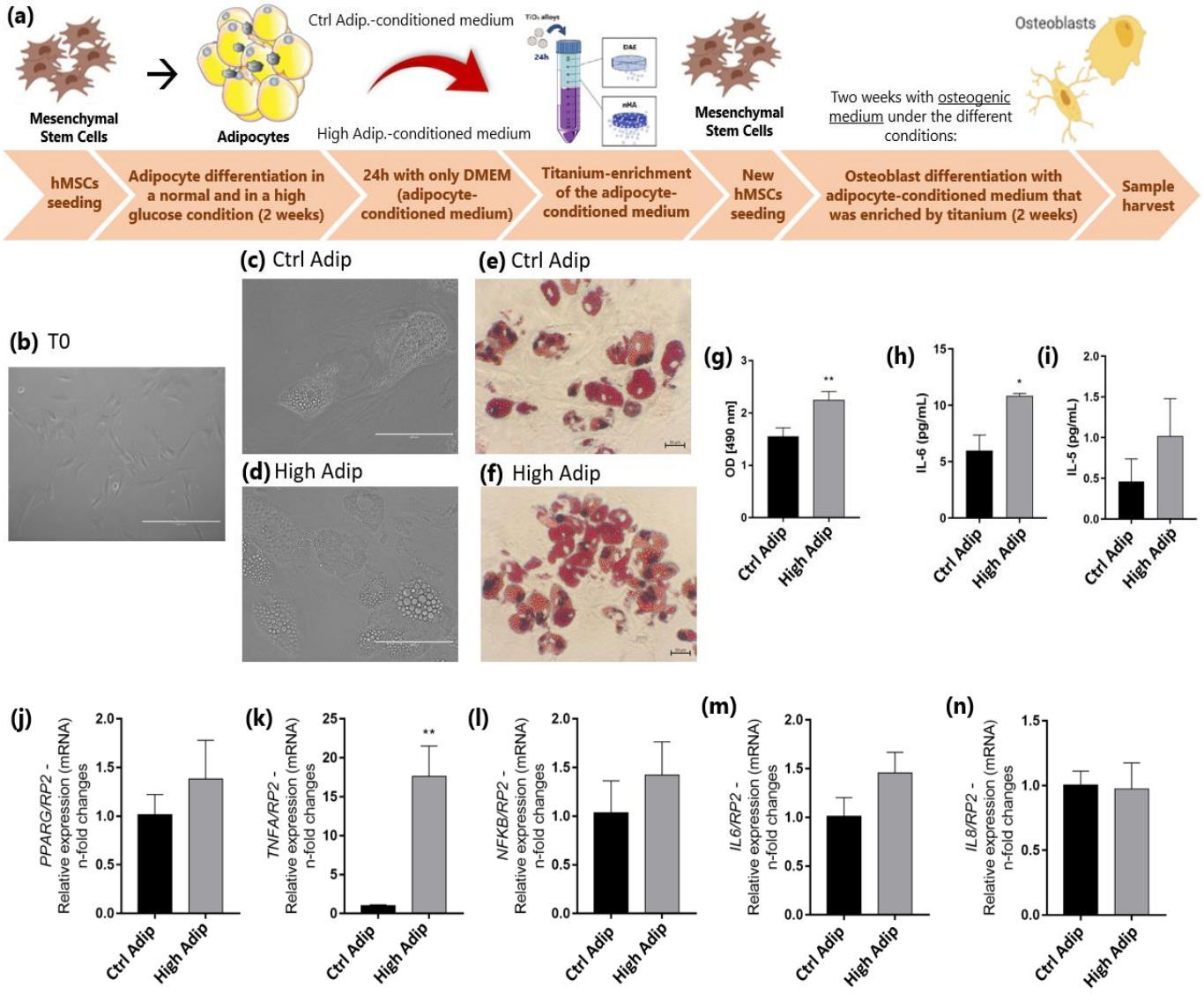

Supplementary figure 1: Experimental Flow for High Adipogenesis Condition. A. Graphical presentation of the experimental set-up. To assess how osteoblast differentiation responds to a titanium-enriched environment in the presence of heightened adipogenesis from adipocytes, we harvested the medium conditioned by adipocytes derived from hMSCs during their differentiation. Subsequently, we changed the culture medium, allowing the cells to incubate in DMEM supplemented with 10% FBS for 24 hours to prepare the conditioned medium. This conditioned medium was then titanium-enriched for 24 hours, adhering to ISO 10993:2016 recommendations. Subsequently, this enriched medium was employed to stimulate hMSCs for a two-week osteoblast differentiation period. After this duration, samples were collected for molecular analysis. **B-N.** Verification of the adipogenesis model. The images show hMSCs at time 0 (b) and after two weeks with adipogenic medium under either normal conditions (Ctrl Adip, c) or high-glucose conditions (High Adip, d) captured using an EVOS microscope (40x). Adipocytes underwent oil red O staining (e and f) with subsequent semi-quantification of lipid droplets (g). Images of the lipid droplets of the adipocytes were acquired using a

light microscope (40× magnification). Additionally, ELISA was performed on the conditioned medium for analysis of secreted IL-6 (h) and IL-5 (i). Finally, gene expression analysis of adipocytes-derived hMSC after 2 weeks differentiation under normal and high glucose medium conditions revealed a significantly higher expression of the *TNFA* (k) The results are presented as mean ± standard deviation (n = 3), and statistical significance was determined using Student's t-test. Significance levels were denoted as * $p < 0.05$ and ** for $p < 0.01$.

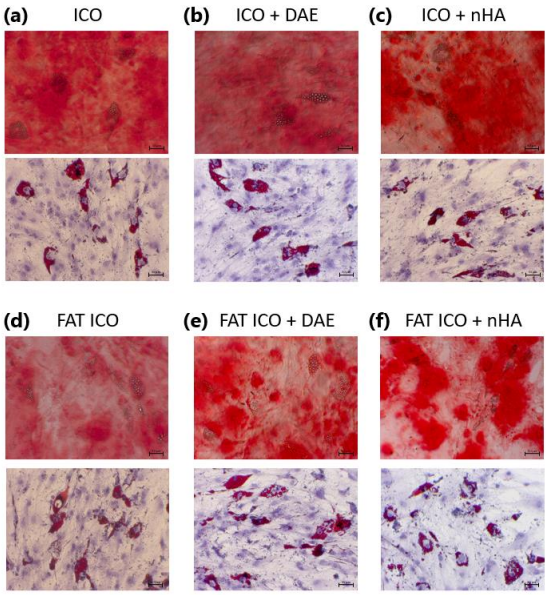

Supplementary figure 2. Osteoblasts originating from hMSCs stained with and alizarin red S staining (upper panels) and oil red O and hematoxylin (lower panels), upon treatment with ICO-conditioned medium. To verify the osteoblast differentiation of mesenchymal cells after exposure to the osteogenic medium and ICO-conditioned medium, we carried out the alizarin red S staining assay. The images demonstrate that mesenchymal stroma cells when treated with the osteogenic medium, including in the presence of titanium-enriched medium and ICO-conditioned medium, underwent effective mineralization. This validation ensures the successful differentiation of osteoblasts in all experimental groups (upper panels, a-f). To visualize lipid vesicles, the application of oil red O was employed. We aimed to explore whether osteoblasts treated with a ICO-conditioned medium would demonstrate the presence of intracellular fat vesicles. The addition of hematoxylin staining aided in the visualization of cell shape and quantity. Our findings indicated the existence of intracellular fat vesicles in all groups subjected to ICO-conditioned medium treatment (a-f, lower panels). DAE = titanium with Dual Acid-Etching; nHA = titanium with nano-hydroxyapatite-coated surface.

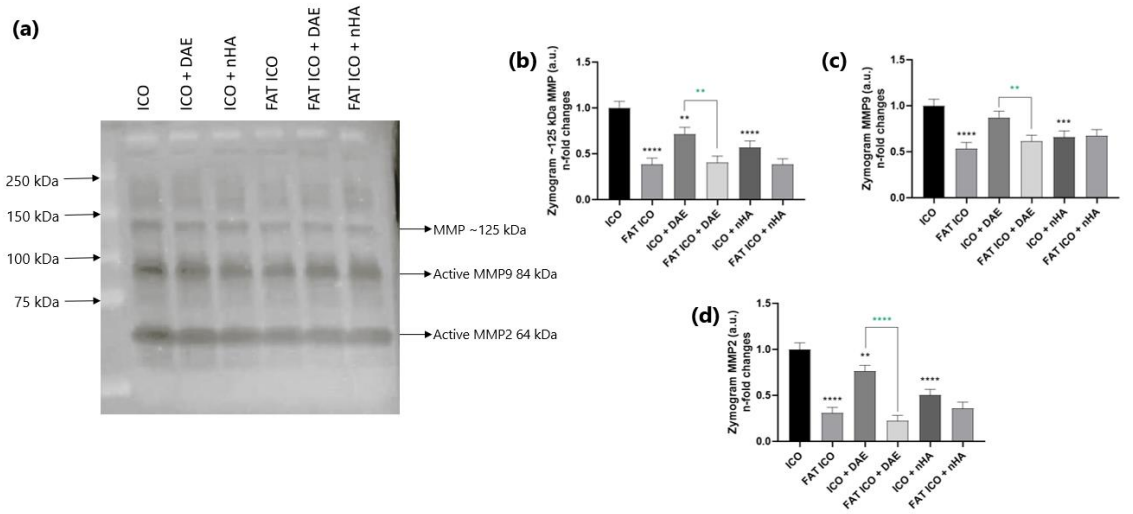

Supplementary figure 3: ECM remodeling of hMSCs after two weeks of differentiation in osteoblasts treated with ICO-conditioned medium. To explore extracellular matrix (ECM) remodeling in osteoblasts under *in vitro* fatty liver conditions and titanium treatments, we employed zymography to assess matrix metalloproteinase (MMP) activity. Our results indicate a decrease in MMPs activity across almost all experimental groups (a-d). MMP9 activity consistently decreased in all groups except the Liv.Or. + DAE group (c), while MMP2 activity exhibited a decrease in all groups (d). Significant differences were observed in the activity of all analyzed MMPs when comparing between the titanium DAE groups, underscoring the impact of normal and high adipogenesis conditions on their modulation. Significant differences are indicated by asterisks (* $p < 0.05$, ** $p < 0.01$, *** $p < 0.001$, and **** $p < 0.0001$), with black asterisks denoting comparisons to the Liv.Or. group, red asterisks for comparisons to the FAT Liv.Or. group, and green asterisks for intergroup comparisons involving DAE.

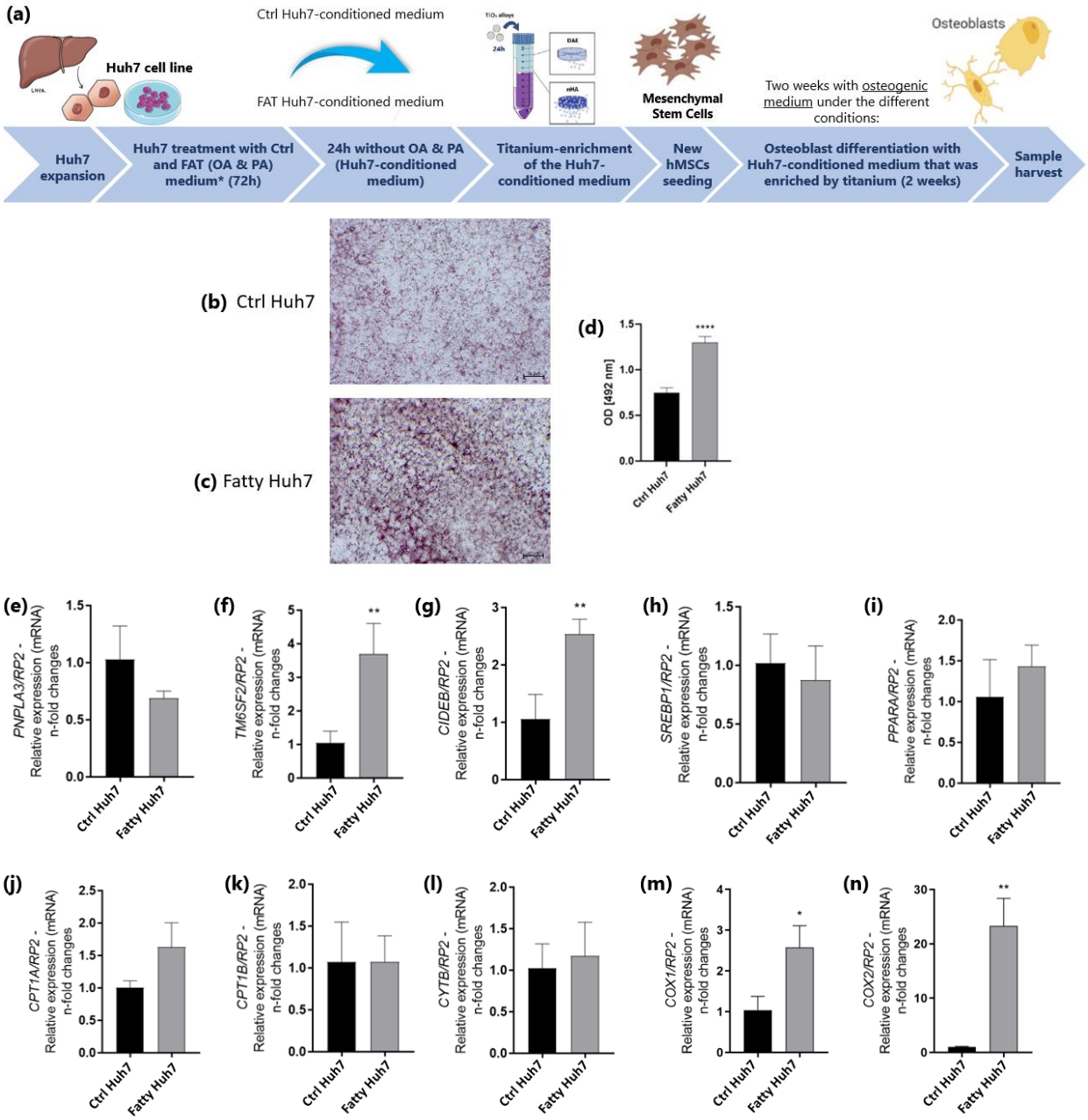

Supplementary figure 4. Experimental MetALD model with Huh7 hepatocytes. (a) the generation of conditioned media from these human hepatocytes Huh7 involved culturing cells with or without oleic acid and palmitic acid (OA&PA) for 72 hours. Afterward, the culture medium was replaced, and the cells were cultured without OA&PA for an additional 24 hours to condition the medium. Following ISO 10993:2016 guidelines, this conditioned medium underwent titanium enrichment for 24 hours. Subsequently, the enriched medium was employed to induce osteoblast differentiation in hMSCs over a two-week period, and samples were collected for molecular analysis. To validate the high lipogenesis model, hepatocytes cultured with or without OA&PA were subjected to oil red O staining (b and c), and semi-quantification was performed (c). The images were captured using an inverted microscope. Additionally, gene expression analysis of Huh7 hepatocytes after 3 days under normal and OA&PA conditions revealed

a significantly higher expression of the *TM6SF2* (f), *CIDEB* (g), *COX1* (m), and *COX2* (n) genes in hepatocytes responding to OA&PA. The graphs depict the n-fold change in gene expression normalized to the *RP2* gene (a housekeeping gene). Statistical significance was determined at * $p < 0.05$, and ** $p < 0.01$ ($n = 3$).

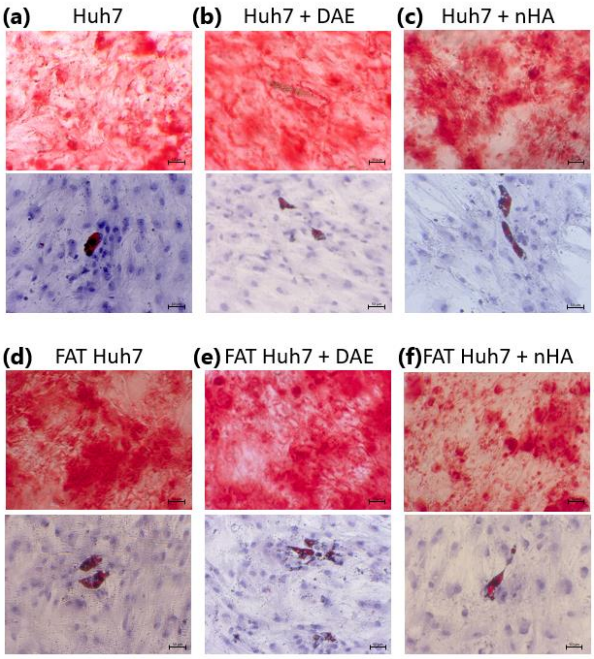

Supplementary figure 5. Osteogenic hMSCs-derived cells stained with alizarin red S (upper), and Staining with oil red O and hematoxylin (lower), after differentiation with Huh7-conditioned medium. To confirm the osteoblast differentiation of mesenchymal cells following exposure to the osteogenic medium, titanium-enriched medium and a medium conditioned by Huh7, the alizarin red S staining assay was employed. The results verified that mesenchymal stroma cells, when treated with the osteogenic medium, even in the presence of titanium and hepatocytes Huh7-conditioned medium, underwent mineralization effectively (a-f, upper panels). For the visualization of lipid droplets and cell number, we performed the staining with oil red O and hematoxylin of hMSCs post two weeks of differentiation into osteoblasts with Huh7 hepatocyte-conditioned medium and titanium-enriched medium (a-f, lower panels). DAE = titanium with Dual Acid-Etching; nHA = titanium with nano-Hydroxyapatite-coated surface.

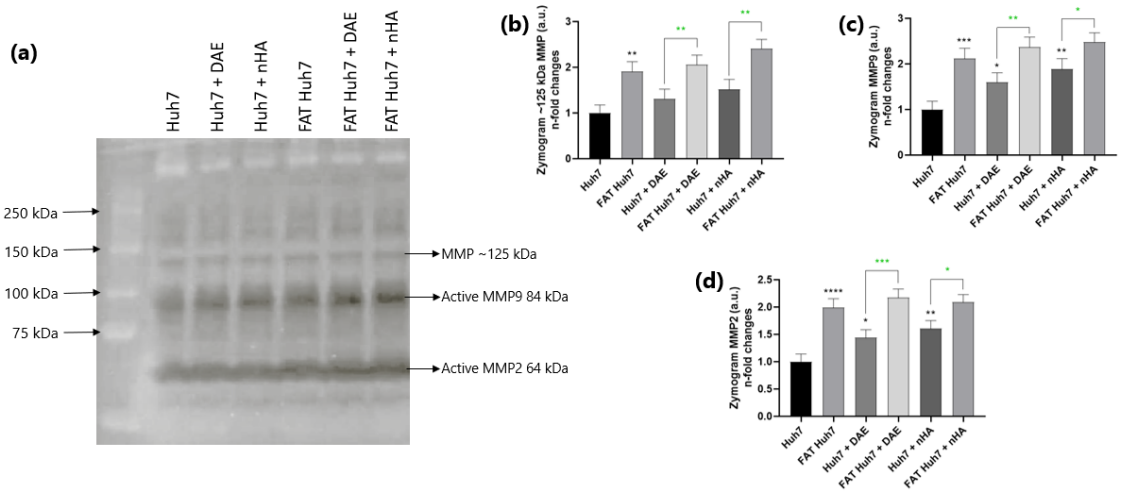

Supplementary figure 6: ECM rearrangement of osteoblasts originating from hMSCs, treated with hepatocytes Huh7-conditioned medium and titanium-enriched medium. The extracellular matrix (ECM) in osteoblasts exposed to Huh7-conditioned mediums and titanium treatments reveal a significant upregulation in MMPs activity in all groups exposed to the fatty Huh7 condition. This elevation seems to be more pronounced in the groups treated with titanium (a-d). Additionally, the data suggests that the presence of titanium increased the activity of both MMP9 (c) and MMP2 (d) under normal conditions compared to the standard Huh7 group. Significant differences are indicated by asterisks (* $p < 0.05$, ** $p < 0.01$, *** $p < 0.001$, and **** $p < 0.0001$), with black asterisks denoting comparisons to the Huh7 group and green asterisks when compared between the groups with DAE or between the groups with nHA. DAE = titanium with Dual Acid-Etching; nHA = titanium with nano-Hydroxyapatite-coated surface.

References

Adamczak, Marcin, and Andrzej Wiecek. 2013. "The Adipose Tissue as an Endocrine Organ." *Seminars in nephrology* 33(1): 2–13.

Ayada, Ibrahim et al. 2023. "Dissecting the Multifaceted Impact of Statin Use on Fatty Liver Disease: A Multidimensional Study." *EBioMedicine* 87: 104392.

Baroncelli, Marta et al. 2019. "Human Mesenchymal Stromal Cells in Adhesion to Cell-Derived Extracellular Matrix and Titanium: Comparative Kinome Profile Analysis." *Journal of cellular physiology* 234(3): 2984–96.

Bertazzo, Sergio et al. 2010. "Hydroxyapatite Surface Solubility and Effect on Cell Adhesion." *Colloids and surfaces. B, Biointerfaces* 78(2): 177–84.

Bezerra, Fabio et al. 2017. "Nano Hydroxyapatite-Blasted Titanium Surface Affects Pre-Osteoblast Morphology by Modulating Critical Intracellular Pathways." *Biotechnology and bioengineering* 114(8): 1888–98.

Broutier, Laura et al. 2016. "Culture and Establishment of Self-Renewing Human and Mouse Adult Liver and Pancreas 3D Organoids and Their Genetic Manipulation." *Nature protocols* 11(9): 1724–43.

Bruedigam, Claudia et al. 2011. "Basic Techniques in Human Mesenchymal Stem Cell Cultures: Differentiation into Osteogenic and Adipogenic Lineages, Genetic Perturbations, and Phenotypic Analyses." *Current protocols in stem cell biology* Chapter 1: Unit1H.3.

Cadamuro, Massimiliano et al. 2022. "The Neglected Role of Bile Duct Epithelial Cells in NASH." *Seminars in liver disease* 42(1): 34–47.

Chalasani, Naga et al. 2018. “The Diagnosis and Management of Nonalcoholic Fatty Liver Disease: Practice Guidance from the American Association for the Study of Liver Diseases.” *Hepatology (Baltimore, Md.)* 67(1): 328–57.

Cheng, Karen Y et al. 2020. “Metabolic Syndrome Is Associated With Higher Risk of Wound Complications After Total Hip Arthroplasty.” *Arthroplasty today* 6(3): 571–77.

Coelho, Paulo G et al. 2009. “Basic Research Methods and Current Trends of Dental Implant Surfaces.” *Journal of biomedical materials research. Part B, Applied biomaterials* 88(2): 579–96.

Coelho, Paulo G et al. 2018. “Effect of Obesity or Metabolic Syndrome and Diabetes on Osseointegration of Dental Implants in a Miniature Swine Model: A Pilot Study.” *Journal of oral and maxillofacial surgery : official journal of the American Association of Oral and Maxillofacial Surgeons* 76(8): 1677–87.

da Costa Fernandes, Celio J. et al. 2018. “Titanium-Enriched Medium Drives Low Profile of ECM Remodeling as a Pre-Requisite to Pre-Osteoblast Viability and Proliferative Phenotype.” *Journal of Trace Elements in Medicine and Biology* 50(July): 339–46.

da Costa Fernandes, Celio J, Marcel Rodrigues Ferreira, Fábio J B Bezerra, and Willian F Zambuzzi. 2018. “Zirconia Stimulates ECM-Remodeling as a Prerequisite to Pre-Osteoblast Adhesion/Proliferation by Possible Interference with Cellular Anchorage.” *Journal of materials science. Materials in medicine* 29(4): 41.

da Costa Fernandes, Célio Junior et al. 2021. “Metabolic Effects of CoCr-Enriched Medium on Shear-Stressed Endothelial Cell and Osteoblasts: A Possible Mechanism Involving a Hypoxic Condition on Bone Healing.” *Materials science & engineering. C, Materials for biological applications* 128: 112353.

Enlow, D H, J L Conklin, and S Bang. 1965. “Observations on the Occurrence and the Distribution of Lipids in Compact Bone.” *Clinical orthopaedics and related research* 38: 157–69.

Eslam, Mohammed et al. 2020. “A New Definition for Metabolic Dysfunction-Associated Fatty Liver Disease: An International Expert Consensus Statement.” *Journal of hepatology* 73(1): 202–9.

Fabbrini, Elisa, Shelby Sullivan, and Samuel Klein. 2010. “Obesity and Nonalcoholic Fatty Liver Disease: Biochemical, Metabolic, and Clinical Implications.” *Hepatology (Baltimore, Md.)* 51(2): 679–89.

Fernandes, Celio J C et al. 2018. “Nano Hydroxyapatite-Blasted Titanium Surface Creates a Biointerface Able to Govern Src-Dependent Osteoblast Metabolism as Prerequisite to ECM Remodeling.” *Colloids and surfaces. B, Biointerfaces* 163: 321–28.

Fernandes, Gustavo V O et al. 2014. “Osteoblast Adhesion Dynamics: A Possible Role for ROS and LMW-PTP.” *Journal of cellular biochemistry* 115(6): 1063–69.

Gittens, Rolando A, Rene Olivares-Navarrete, Zvi Schwartz, and Barbara D Boyan. 2014. “Implant Osseointegration and the Role of Microroughness and Nanostructures: Lessons for Spine Implants.” *Acta biomaterialia* 10(8): 3363–71.

Gomes, Anderson M, Danielle F da Silva, Fábio J Bezerra, and Willian F Zambuzzi. 2023. “Nanohydroxyapatite-Coated Titanium Surface Increases Vascular Endothelial Cells Distinct Signaling Responding to High Glucose Concentration.” *Journal of Functional Biomaterials* 14(4). https://www.mdpi.com/2079-4983/14/4/188.

Gottlander, M et al. 1997. “Bone Tissue Reactions to an Electrophoretically Applied Calcium Phosphate Coating.” *Biomaterials* 18(7): 551–57.

Hartree, E F. 1972. “Determination of Protein: A Modification of the Lowry Method That Gives a Linear Photometric Response.” *Analytical biochemistry* 48(2): 422–27.

Huang-Doran, Isabel, Chen-Yu Zhang, and Antonio Vidal-Puig. 2017. “Extracellular Vesicles: Novel Mediators of Cell Communication In Metabolic Disease.” *Trends in endocrinology and metabolism: TEM* 28(1): 3–18.

Jung, Un Ju, and Myung-Sook Choi. 2014. “Obesity and Its Metabolic Complications: The Role of Adipokines and the Relationship between Obesity, Inflammation, Insulin Resistance, Dyslipidemia and Nonalcoholic Fatty Liver Disease.” *International journal of molecular sciences* 15(4): 6184–6223.

Kanakaris, Nikolaos K, George Petsatodis, Magnus Tagil, and Peter V Giannoudis. 2009. “Is There a Role for Bone Morphogenetic Proteins in Osteoporotic Fractures?” *Injury* 40 Suppl 3: S21-6.

Kanazawa, Ippei. 2015. “Osteocalcin as a Hormone Regulating Glucose Metabolism.” *World journal of diabetes* 6(18): 1345–54.

Lefebvre, V, C Peeters-Joris, and G Vaes. 1991. “Production of Gelatin-Degrading Matrix Metalloproteinases ('type IV Collagenases') and Inhibitors by Articular Chondrocytes during Their Dedifferentiation by Serial Subcultures and under Stimulation by Interleukin-1 and Tumor Necrosis Factor Alpha.” *Biochimica et biophysica acta* 1094(1): 8–18.

Loosen, Sven H et al. 2022. “Non-Alcoholic Fatty Liver Disease (NAFLD) Is Associated with an Increased Incidence of Osteoporosis and Bone Fractures.” *Zeitschrift fur Gastroenterologie* 60(8): 1221–27.

Machado, Mariana Issler Pinheiro et al. 2019. “Cobalt-Chromium-Enriched Medium Ameliorates Shear-Stressed Endothelial Cell Performance.” *Journal of Trace Elements in Medicine and Biology* 54: 163–71. https://www.sciencedirect.com/science/article/pii/S0946672X18306813.

Machado, Mariana Verdelho, and Helena Cortez-Pinto. 2023. “NAFLD, MAFLD and Obesity: Brothers in Arms?” *Nature reviews. Gastroenterology & hepatology* 20(2): 67–68.

Marsee, Ary et al. 2021. “Building Consensus on Definition and Nomenclature of Hepatic, Pancreatic, and Biliary Organoids.” *Cell stem cell* 28(5): 816–32.

Meirelles, Luiz et al. 2008. “Nano Hydroxyapatite Structures Influence Early Bone Formation.” *Journal of biomedical materials research. Part A* 87(2): 299–307.

Müller, Fabrice A, and Shana J Sturla. 2019. “Human in Vitro Models of Nonalcoholic Fatty Liver Disease.” *Current Opinion in Toxicology* 16: 9–16. https://www.sciencedirect.com/science/article/pii/S2468202019300117.

Newberry, Elizabeth P et al. 2021. “Liver-Specific Deletion of Mouse Tm6sf2 Promotes Steatosis, Fibrosis, and Hepatocellular Cancer.” *Hepatology (Baltimore, Md.)* 74(3): 1203–19.

de Oliveira, Paula Gabriela Faciola Pessôa et al. 2020. “Obesity/Metabolic Syndrome and Diabetes Mellitus on Peri-Implantitis.” *Trends in endocrinology and metabolism: TEM*.

Oury, Franck et al. 2010. “CREB Mediates Brain Serotonin Regulation of Bone Mass through Its Expression in Ventromedial Hypothalamic Neurons.” *Genes & development* 24(20): 2330–42.

Palacios-Ortega, Sara et al. 2016. “Effects of High Glucose on Caveolin-1 and Insulin Signaling in 3T3-L1 Adipocytes.” *Adipocyte* 5(1): 65–80.

Pinto, Thaís Silva, Anderson Moreira Gomes, Paula Bertin de Morais, and Willian F. Zambuzzi. 2023. “Adipogenesis-Related Metabolic Condition Affects Shear-Stressed Endothelial Cells Activity Responding to Titanium.” *Journal of Functional Biomaterials* 14(3).

Rendina-Ruedy, Elizabeth, Anyonya R Guntur, and Clifford J Rosen. 2017. “Intracellular Lipid Droplets Support Osteoblast Function.” *Adipocyte* 6(3): 250–58.

Rinella, Mary E et al. 2023. “A Multisociety Delphi Consensus Statement on New Fatty Liver Disease Nomenclature.” *Hepatology (Baltimore, Md.)* 78(6): 1966–86.

Rochlani, Yogita, Naga Venkata Pothineni, Swathi Kovelamudi, and Jawahar L Mehta. 2017. “Metabolic Syndrome: Pathophysiology, Management, and Modulation by Natural Compounds.” *Therapeutic advances in cardiovascular disease* 11(8): 215–25.

Ronis, Martin J J, Kelly Mercer, and Jin-Ran Chen. 2011. “Effects of Nutrition and Alcohol Consumption on Bone Loss.” *Current osteoporosis reports* 9(2): 53–59.

Salazar, Valerie S, Laura W Gamer, and Vicki Rosen. 2016. “BMP Signalling in Skeletal Development, Disease and Repair.” *Nature reviews. Endocrinology* 12(4): 203–21.

Schindelin, Johannes, Curtis T Rueden, Mark C Hiner, and Kevin W Eliceiri. 2015. “The ImageJ Ecosystem: An Open Platform for Biomedical Image Analysis.” *Molecular reproduction and development* 82(7–8): 518–29.

Shaikh, Alisha et al. 2023. “Cell Cycle Regulators and Bone: Development and Regeneration.” *Cell & bioscience* 13(1): 35.

Shilpa, Kusampudi, Thangaraj Dinesh, and Baddireddi Subhadra Lakshmi. 2013. “An In Vitro

Model to Probe the Regulation of Adipocyte Differentiation under Hyperglycemia." *Diabetes & metabolism journal* 37(3): 176–80.

da Silva, Rodrigo A et al. 2019. "HOXA Cluster Gene Expression during Osteoblast Differentiation Involves Epigenetic Control." *Bone* 125: 74–86.

da Silva, Simone Vargas et al. 2016. "Obesity Modifies Bone Marrow Microenvironment and Directs Bone Marrow Mesenchymal Cells to Adipogenesis." *Obesity (Silver Spring, Md.)* 24(12): 2522–32.

Somasundaram, Rajesh et al. 2017. "Analysis of SHIP1 Expression and Activity in Crohn's Disease Patients." *PloS one* 12(8): e0182308.

de Sousa, Roberta R Ruela et al. 2007. "Phosphoprotein Levels, MAPK Activities and NFkappaB Expression Are Affected by Fisetin." *Journal of enzyme inhibition and medicinal chemistry* 22(4): 439–44.

Takahara, Ikuko et al. 2017. "Toyocamycin Attenuates Free Fatty Acid-Induced Hepatic Steatosis and Apoptosis in Cultured Hepatocytes and Ameliorates Nonalcoholic Fatty Liver Disease in Mice." *PloS one* 12(3): e0170591.

Wang, Ling et al. 2022. "Recapitulating Lipid Accumulation and Related Metabolic Dysregulation in Human Liver-Derived Organoids." *Journal of molecular medicine (Berlin, Germany)* 100(3): 471–84.

Wang, Richard N et al. 2014. "Bone Morphogenetic Protein (BMP) Signaling in Development and Human Diseases." *Genes & diseases* 1(1): 87–105.

Wang, Shuang et al. 2023. "An Autocrine Signaling Circuit in Hepatic Stellate Cells Underlies Advanced Fibrosis in Nonalcoholic Steatohepatitis." *Science translational medicine* 15(677): eadd3949.

Wawrzyniak, Agata, and Krzysztof Balawender. 2022. "Structural and Metabolic Changes in Bone." *Animals : an open access journal from MDPI* 12(15).

Zambuzzi, Willian F et al. 2014. "Nanometer Scale Titanium Surface Texturing Are Detected by Signaling Pathways Involving Transient FAK and Src Activations." *PloS one* 9(7): e95662.

Capítulo 4

SHORT COMMUNICATION

Gamma-oryzanol (γOz) rich rice bran promotes osteogenic phenotype of bone marrow-obtained stromal cells in obesity conditions

Thaís Silva Pinto[1], Jéssica Leite Garcia[2], Anderson Moreira Gomes[1], Amanda Fantini de Camargo Andrade[1], Gerson Santos de Almeida[1], Camila Renata Correa[2], Willian Fernando Zambuzzi[1*]

[1]Lab. of Bioassays and Cellular Dynamics, Department of Chemical and Biological Sciences, Institute of Biosciences, UNESP – São Paulo State University, 18618-970, Botucatu, São Paulo, Brazil;

[2]São Paulo State University (UNESP), Medical School, Botucatu, Brazil

Submitted to: Journal of Nutritional Biochemistry

*Corresponding author:

Correspondence to Prof. Willian F. Zambuzzi, Ph.D
e-mail: w.zambuzzi@unesp.br

ABSTRACT

Introduction: Obesity is a complex and multifactorial inflammatory condition responsible to trigger several complications that deserves attention from public health issues. Among obesity-related implications in the bone is the higher risk of fractures. Gamma-oryzanol (γOZ), anti-inflammatory compound present in rice bran (RB), has positive effects on health, but barely is known about its effects on bone-derived cells on this condition.
Purpose: This study was meant to evaluate the outcome of RB supplementation to a high-sugar fat diet experimental obesity model, specifically in the primary culture of bone marrow-obtained mesenchymal stroma cells (MSC) isolated from rat femur marrow.
Methods: Male Wistar rats were separated into three groups: Control (Ctrl), Obese, and Obese complemented with 11% RB (Obese + RB) up to 20 weeks. Then, the MSCs were isolated to allow gene expression analysis.
Results and Discussion: The MSCs from Obese and Obese + RB groups presented higher Runx2 expression, while it was observed downregulation in transcripts levels of the Pparg, Tgfb1, and Osx genes. Specifically, Obese + RB condition promotes higher expression of both Bglap and Tnfr2 genes, while inflammatory-related genes were decreased.
Conclusion: This *ex vivo* experimental model reveals modulations in some bone-related gene expression in MSCs triggered by a high sugar-fat diet and rice bran ingestion. Additionally, the results raised insights about molecular mechanisms that may be involved with the protection promoted by gamma-oryzanol (γOz) rich rice bran on obesity-related bone complications.

Keywords Rice bran; Obesity; Bone; Mesenchymal Stroma Cell; Gamma-oryzanol.

INTRODUCTION

Obesity-related complications have raised concerns in different clinical practices. This is already known that this chronic and multifactorial disease predisposes to other conditions, such as type 2 diabetes mellitus (T2DM), hypertension, and dyslipidemia, among other comorbidities, for example, renal, pulmonary, and musculoskeletal illness (Stevens, O'Connell, and Meyer 2015). Bone mass decreasing has also been related to overweight and obesity, as the adipose tissue has an important role in the metabolism and acts systemically as an endocrine organ, bone might suffer interventions through mechanical, hormonal, and inflammatory signals (López-Gómez, Pérez Castrillón, and de Luis Román 2016). In addition, the adipose tissue can affect bone metabolism in a direct manner or indirectly way by via hypophysis (Greco, Lenzi, and Migliaccio 2015). These obesity-related bone implications have been evidenced as a possible cause for a higher risk of fractures (Shapses, Pop, and Wang 2017).

Patients diagnosed with obesity present an abnormality in the function of the adipose tissue, with an abnormal or excessive accumulation of fat mass in the body, and impaired adipokines releasing profiles, besides an intensification in proinflammatory interleukins secretion (Fuster et al. 2016). This greater amount of circulating and tissue interleukins in obese patients, such as TNF-α, IL-1β, and IL-6, might stimulate osteoclast action and bone resorption as these cytokines can modulate the NFkB(RANK)/RANKL/OPG pathway (Cao 2011). Additionally, regarding the consequence of obesity in bone, the diet patterns, often a cause of this disease, and free fatty acids are related to impairing calcium absorption and then declining calcium disposal for bone formation (Cao 2011); nevertheless, the basis of pathophysiological association regarding obesity and bone is not clear and needs to be better addressed.

The differentiation of mesenchymal stromal cells (MSCs) into osteoblasts, a pivotal process in osteogenesis, is finely orchestrated by a network of genes and signaling pathways that can be significantly influenced by metabolic states such as obesity. Key genes involved in this process include RUNX2, a master transcription factor essential for osteoblast differentiation and skeletal morphogenesis (de Oliveira et al. 2020). Another critical gene is PPARG, which is predominantly known for its role in adipocyte differentiation but can also influence MSC fate decisions, potentially diverting them from osteogenesis to adipogenesis, particularly in the context of obesity (Cao 2011). BGLAP, encoding osteocalcin, plays a crucial role in bone mineralization, and its expression is tightly regulated by RUNX2 (Komori 2020a). The BMP family, with its numerous

members, acts synergistically to promote osteoblast differentiation and bone formation, partly through the activation of RUNX2 and OSX (osterix), another transcription factor critical for bone formation (Wang et al. 2014). Obesity is characterized by a chronic, low-grade inflammation state, leading to altered levels of cytokines, which can disrupt the normal process of MSC differentiation into osteoblasts (Cao 2011).

Both overnutrition and sedentarism have significantly amplified the prevalence of obesity worldwide, being the diet patterns based on high consumption of processed nourishments rich in industrialized sugar and fat (Jezewska-Zychowicz et al. 2018). In this context, diet-based therapeutic strategies have been studied to decrease, prevent and treat obesity-related complications, and the use of plant-related foods, with high content of bioactive compounds, has been proposed to less damaging effects of obesity and its related problems (González 2020).

Globally, the most-consumed grain is wheat, followed by Rice (Oryza sativa L.). Half of the population has rice as a constant diet in the world (Van Nguyen and Ferrero 2006; Sharif et al. 2014). The polish form is the principal way of consumption of rice, called white rice. Nevertheless, it is in the bran layer detached from the rice that comprises the main bioactive compounds (Minatel et al. 2016). The rice kernel polishing, in the rice milling industry, generates a byproduct that is mostly discarded or used as animal feed, the rice bran (RB) (Sharif et al. 2014). Full of several bioactive compounds, such as tocopherols, tocotrienols, and oryzanols, in a smaller amount, carotenoids, lecithin, and long-chain alcohols, the RB is 10% of the rough rice weight. RB is rich in antioxidants, mainly γ-oryzanol and vitamin E, and depending on the growing conditions, γ-oryzanol can be 20 fold changes higher (Sohail et al. 2017; Tung and Ng 2019).

RB presents relevant health care effects, mainly because of the γ-oryzanol, which raised the numbers of studies regarding, for example, its hypocholesterolemic, anti-diabetic, anti-obesogenic, antioxidant, anti-hypertensive, and anti-inflammatory properties (Ha et al. 2005; Minatel et al. 2016; Rao, Sugasini, and Lokesh 2016; Yang et al. 2019; Zou et al. 2020), also the wondering if it could have bone biology effects, mitigating the obesity-related complications. Taking into account the low price and easy obtainability, as well as the advantageous health effects and nutritive values, it becomes pertinent to consider even more the use of RB exploring, mainly by being a possibility of natural therapy that would avoid problems like side effects related to anti-obesogenic drugs (Sharif et al. 2014; Sohail et al. 2017).

Considering that RB has many positive influences on health, its effects on bone biology are barely known in obese patients. Thus, we focused on analyzing the RB supplementation effect in a high-sugar fat experimental obesity model, specifically in the MSC population isolated from rat femur regarding their capacity in driving osteogenic phenotype of those cells.

MATERIAL AND METHODS

Animals and experimental design

Male Wistar rats (±325 g) were obtained from the Animal Center of Botucatu Medical School, Sao Paulo State University (UNESP, Botucatu, SP, Brazil). The animals were separated into three groups (n=8): control diet (Ctrl), high-sugar fat diet-induced obesity (Obese), and high-sugar fat diet-induced obesity complemented with RB (Obese + RB) during 20 weeks. In the Obese groups were also added 25% of sucrose in the drinking water, and the Ctrl group was provided normal drinking water without any supplement. During this time the rats received diets and water ad libitum and were kept in individual cages, with controlled temperature (22±3 ◦C), luminosity (12 h light/ dark cycle), and humidity (60±5%).

At the end of the experimental period, the animals were fasted for 8 h and then anesthetized (thiopental 120 mg/kg/i.p.) and euthanized by decapitation after verification of the absence of foot reflex. The femurs of the rats were collected and followed to Mesenchymal Stem Cells isolation further described. This research was made according to the guidelines for animal research (Kilkenny et al. 2010) and approved by the Ethics Committee on Animal Experiments of the Botucatu Medical School, UNESP (protocol number 1305/2019).

Diet composition

The diets used in this study were nutritionally balanced for micronutrients but the macronutrients were different. All the diets were previously described (Garcia et al. 2022). RB was provided by Brasília Alimentos LTDA. (Santa Cruz do Rio Pardo, São Paulo, Brazil) and obtained from Oryza sativa L. rice processing. The RB was stabilized by heating to deactivate the enzymes responsible for the degradation of its components and to avoid rancidity before being mixed with the other components of the diet (Sharif et al. 2014; Sheflin et al. 2015). The Obese + RB diet was personalized with 11% (wt/wt) of RB (Kahlon et al. 1992).

Cell culture

At the end of the 20 days, the rats were euthanized and their femurs were collected placing them in 15 mL tubes containing Dulbecco's Modified Eagle Medium (DMEM) with 1% penicillin–streptomycin. The femurs were taken to a sterile biosafety space where each femur was cleaned out using a sterile gauze to remove soft tissues. With a pair of sharp surgical side scissors, the epiphysis was cleaved off, to access the marrow cavity of the femur, and then with a sterile 18-gauge needle attached to a syringe, we flushed out the marrow cavity with DMEM onto a 100 mm cell culture dish (final volume of 10 mL). One dish for each femur containing DMEM with 1% penicillin-streptomycin and 10% fetal bovine serum. The dishes were placed into an incubator (37°C, 5% CO_2, humidified) for 24 hours. The following day the nonadherent cells were discarded by aspirating the media and washing the adherent cells twice with prewarmed PBS (Jacobs, van de Vyver, and Ferris 2019). Finally, the adherent cells were harvested for RNA isolation to follow RT-qPCR analysis.

Quantitative PCR assay (RT-qPCR)

Thereafter 24 hours in the incubator, the cells were collected, and the total RNA was extracted using Ambion TRIzol Reagent (Life Sciences – Fisher Scientific Inc, Waltham, MA, USA) and treated with DNase I (Invitrogen, Carlsbad, CA, USA). The cDNA synthesis was achieved with High-Capacity cDNA Reverse Transcription Kit (Applied Biosystems, Foster City, CA) following the manufacturer's instructions and standardized earlier (Rocha Camargo et al. 2021). RT-qPCR was performed in a total of 10 µl, containing PowerUp™ SYBR™ Green Master Mix 2x (5 µl) (Applied Biosystems, Foster City, CA), 0,4 µM of each primer, 50 ng of cDNA and nuclease-free H_2O. The results were expressed as relative amounts of the target gene using β-actin as the inner reference gene (housekeeping), using the cycle threshold (Ct) method. Primers and details are described in **Table 1**.

Table 1. Expression primers sequences and quantitative polymerase chain reaction cycle conditions.

Genes	Primers	5′-3′ Sequences	Reaction's conditions
R - Bglap	Forward	AGCTCAACCCCAATTGTGAC	95°C, 3 s; 55°C, 8 s; 72°C, 20 s

	Reverse	AGCTGTGCCGTCCATACTTT	
R - Bmpr1	Forward	GCTGTCTGTATTGTCGCCATGAT	95°C, 3 s; 55°C, 8 s; 72°C, 20 s
	Reverse	TTCCAAGTCACGGTTGTAACGA	
R - Il1b	Forward	TCAAGCAGAGCACAGACCTG	95°C, 3 s; 55°C, 8 s; 72°C, 20 s
	Reverse	ACTGCCCATTCTCGACAAGG	
R - Il1r1	Forward	GCTGGGTCGACTCACAAGAA	95°C, 3 s; 55°C, 8 s; 72°C, 20 s
	Reverse	ATCCAGCAACCTTTCTCCCG	
R - Il6	Forward	CCGGAGAGGAGACTTCACAG	95°C, 3 s; 55°C, 8 s; 72°C, 20 s
	Reverse	ACAGTGCATCATCGCTGTTC	
R - Il6r	Forward	GTGAGAAACTTGCGTGCCAG	95°C, 3 s; 55°C, 8 s; 72°C, 20 s
	Reverse	GTGAGAAACTTGCGTGCCAG	
R - Nfkb	Forward	ATCAAAGAGCTGGTGGAGGC	95°C, 3 s; 55°C, 8 s; 72°C, 20 s
	Reverse	TGTGGAGGAGGACGAGAGAG	
R - Osx	Forward	CCGGACTGACAAGATGTGCT	95°C, 3 s; 55°C, 8 s; 72°C, 20 s
	Reverse	GGCAGCTCTTGTACCATGGT	
R - Pparg	Forward	GTTCATGCTTGTGAAGGATGC	95°C, 3 s; 55°C, 8 s; 72°C, 20 s
	Reverse	ACTCTGGATTCAGCTGGTCG	
R - Runx2	Forward	GAGCACAAACATGGCTGAGA	95°C, 3 s; 55°C, 8 s; 72°C, 20 s
	Reverse	TGGAGATGTTGCTCTGTTCG	
R - Tgfb1	Forward	CCCATGAACTACCATCCCCG	95°C, 3 s; 55°C, 8 s; 72°C, 20 s
	Reverse	CCAGTAAGCCATGTCCCCTG	
R - Tnfa	Forward	CTTCCAGGACAGCTCACCAG	95°C, 3 s; 55°C, 8 s; 72°C, 20 s
	Reverse	GGTGGGGATCAGGAGAGAGT	
R - Tnfr1	Forward	CGCTACCTGAGTGAGACGCATT	95°C, 3 s; 55°C, 8 s; 72°C, 20 s
	Reverse	GAGGCAACAGCACGGCAGTA	
R - Tnfr2	Forward	GGGACTTTTGTTTGGGACGC	95°C, 3 s; 55°C, 8 s; 72°C, 20 s
	Reverse	CTTTGCCGTGTTCAACCTGG	
R - Actb	Forward	CCACCATGTACCCAGGCATT	95°C, 3 s; 55°C, 8 s; 72°C, 20 s
	Reverse	CGGACTCATCGTACTCCTGC	

Statistical analysis

We used the Shapiro–Wilk for the test for normality and for homogeneity of variance we used Levene's test prior to statistical analysis. The statistical analysis was made by one-way ANOVA followed by Tukey post-hoc test for parametric data or Kruskal–Wallis followed by Dunn's post-hoc test for non-parametric data. Data are

expressed as mean ± standard deviation (SD) or median {minimum [min]–maximum [max]}.

By using a web tool for visualizing the clustering of multivariate data ClustVis we analyzed all numerical biological results [35] for exploring the unsupervised multivariate principal component analysis (PCA) and hierarchical clustering analyses. The correlation matrix with all data was analyzed using a 2-tailed Pearson's correlation test. The analyses were performed using SigmaPlot 12.0 for Windows (Systat Software Inc., San Jose, CA, USA). All graphics were generated using GraphPad Prism 8 (GraphPad Software Inc., San Diego, CA, USA). Differences were considered statistically significant when $p<0.05$.

RESULTS AND DISCUSSION

Bone marrow-derived mesenchymal stem cells (BM-MSCs) are acquiring grow relevance in the regenerative medicine field over the last years (Bhat et al. 2021). Evaluating BM-MSCs outcomes under different conditions is also an effective experimental tool in the study of bone biology (Stamnitz and Klimczak 2021). In this context, for years our group has been working on understanding bone-related biology as well as wound healing by performing different experimental models. Thus, at the end of the experimental period with male Wistar rats separated into different groups the bone marrow cells were harvested end seeded up to 24h then follow by molecular analysis through RT-qPCR (Fig.1).

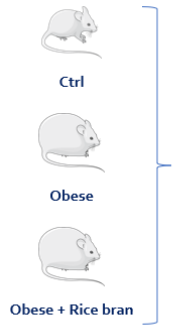

Table. Description of the experimental assay (Lineage: Wistar Rat)

Variable	N	Time	Treatment
Ctrl	8	20 weeks	Standard
Obese	8	20 weeks	HSF chow
Obese + RB	8	20 weeks	Rice bran mixed to the HSF chow in a dose of 11% (w/w).

HSF = High Sugar-Fat Diet; RB = Rice bran.

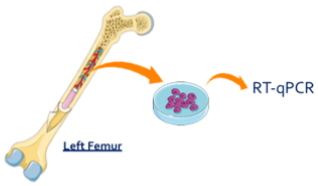

Fig.1. Experimental Design. Male Wistar rats received diets and water *ad libitum*, separated into three groups (n=8): control diet (Ctrl), high-sugar fat diet-induced obesity (Obese), and high-sugar fat diet-induced obesity complemented with RB (Obese + RB) during 20 weeks. In the Obese groups, 25% of sucrose was added to the drinking

water, while the Ctrl group was with normal drinking water. At the end of 20 weeks, the animals were euthanized. The femurs of the rats were collected and taken to a sterile biosafety space where each femur was cleaned and the epiphysis was cleaved off, to access the marrow cavity of the femur. Then with a sterile 18-gauge needle attached to a syringe, the marrow cavity was flushed out with DMEM onto a 100 mm cell culture dish (one dish for each femur). The dishes were placed into an incubator (37°C, 5% CO_2, humidified) for 24 hours. Finally, on the following day, the nonadherent cells were discarded and the adherent cells were harvested for RNA isolation to follow RT-qPCR analysis.

Osteoblasts and adipocytes have a common precursor, mesenchymal stem cells. MSCs can differentiate themselves into several cell types, including osteoblasts and adipose tissue cells (adipocytes) (Pierce et al. 2019). Considering this knowledge, we evaluated the MSCs transcription levels for Pparg and Runx2 genes, as they are key constituents in the adipocyte differentiation and osteoblast differentiation, respectively (Ge et al. 2016). Conversely, our data reveal that the high-sugar fat diet was able to inversely modulate these genes independently of the presence of the rice bran (RB) in the diet, as both Obese and Obese + RB groups were significantly decreased in the Pparg gene expression and significantly higher in the Runx2 transcripts levels when compared to Ctrl group (Fig.2a-b). The Tgfb1 gene is also involved with cell differentiation, as well as proliferation, contributing to cell development (Li and Flavell 2008). Tgfb1 gene expression was similar to the Pparg gene, down-regulating in the Obese and Obese + RB groups (Fig.2c), the similarity was also found in the Osx gene expression (Fig.2d), a transcription factor essential for osteoblast differentiation, bone formation, and mineralization (Liu et al. 2020). Interestingly, the Bglap gene, which encodes an extracellular important constituent (Osteocalcin), is related with the regulation of bone remodeling and energy metabolism (Komori 2020a), and it was significantly higher in the HFS + RB group compared to the other two groups (Fig.2e). Osteocalcin can act systemically, and it has been reported to perform as a hormone that improves glucose metabolism, as well as, induces testosterone synthesis (Komori 2020b).

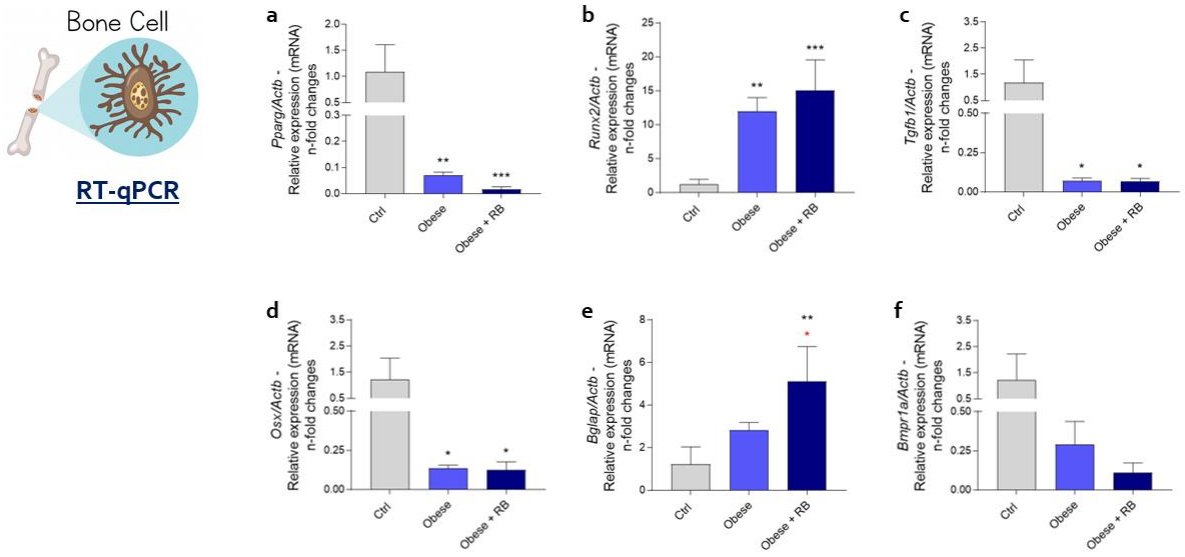

Fig.2. Rice bran promotes preferentially stimulating osteogenic phenotype in bone marrow-obtained adherent cells. The animals were fed with rice bran up to 20 weeks, when they were killed, the femur was dissected and forwarded to a cell culture hood to obtain bone marrow-obtained cells. The primary cells were cultured up to 24 hours when the samples were collected to allow the expression of specific genes by performing qPCR technology. Conversely, the expression of PPAR was downregulated (a) when the RUNX2 gene was significantly higher in animals fed with Obese and Obese + RB (b). Importantly, the osteogenic phenotype was further confirmed by the expression of BGLAP gene (c), which was higher in Obese + RB subjected rats. Additionally, Tgfb1 (c), Osterix (d), and Bmpr1 (f) genes were significantly lower in rats subjected to the experimental food. Actb was considered a housekeeping gene to normalize the expression of specific expressions. Significances were considered when $p < 0.05$ represented by * when compared to the Ctrl group; and red * when compared to the Obese group.

Obesity establishes a systemic proinflammatory state, triggered mainly by alterations in adipokines releasing profiles, an increase in proinflammatory interleukins release, as well as an impairment in cortisol signaling (Ellulu et al. 2017). This makes pertinent the evaluation of inflammatory markers, like TNF and its receptors, also pro-inflammatory interleukins.

TNF receptors involvement shows different patterns of expression among the groups. Thereafter, we have investigated genes with inflammatory landscape, and our data shows Tnfr2 gene was higher in the Obese + RB group when compared to Ctrl and

Obese groups (Fig.3a). In contrast, the Tnrf1 transcript levels significantly decreased in both Obese groups with and without RB (Fig.3b). In turn, TNFR2 is related to decreasing the activities of regeneration like wound healing, in TNFα-TNFR2 axis-dependent regenerative functions (Beldi et al. 2020).

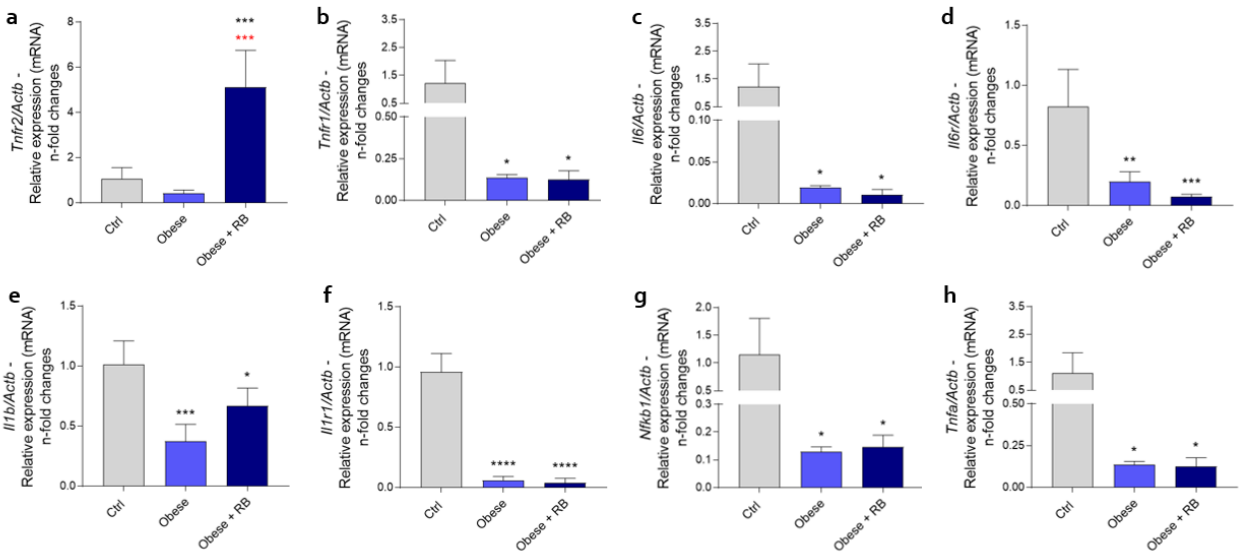

Fig.3. The Tnfr2 gene was higher, while relevant osteogenic phenotype-related cytokines and their receptors were downregulated. To better evaluate the performance of the bone marrow obtained primary adherent cells, we have investigated genes related to the synthesis of cytokines involved with osteogenic. Surprisingly, the Tnfr2 gene was significantly higher in Obese + RB (a; $p = 0.0006$ for Ctrl vs. Obese + RB; and $p = 0.0002$ for Obese vs. Obese + RB), while Tnfr1 (b), Il6 (c), Il6R (d), Il1b (e), Il1r1 (f), Nfkb (g), and Tnfa (h) genes were significantly lower. Actb was considered a housekeeping gene to normalize the expression of specific expressions. Significances were considered when: black * when compared to Ctrl; red * when compared to Obese.

Obesity has been related to wound healing complications (Morris, Ochi, and Winkler 2000), but barely is known about its signals in bone marrow mesenchymal stem cells. In conjunction, this study brings an ex vivo experimental model able to reveal the bone-related gene expression was modulated responding to high sugar-fat diet and rice bran ingestion. Bone regeneration in obese patients is an increasing concern among health professionals and politics, and our data brings insights about molecular mechanisms that

wonder to be involved in these protective mechanisms, opening the perspective to validate these outcomes in preclinical trials.

ACKNOWLEDGEMENTS

The authors are grateful to Fundação de Amparo à Pesquisa do Estado de São Paulo - FAPESP (FAPESP: 2019/26854-2) and Conselho Nacional de Desenvolvimento Científico e Tecnológico (CNPq – Bolsa Produtividade em Pesquisa, 314166/2021-1), and CAPES (Coordenação de Aperfeiçoamento de Pessoal de Nível Superior), code 01.

REFERENCES

Beldi, Ghada et al. 2020. "TNFR2 Is a Crucial Hub Controlling Mesenchymal Stem Cell Biological and Functional Properties." *Frontiers in Cell and Developmental Biology* 8. https://www.frontiersin.org/articles/10.3389/fcell.2020.596831.

Bhat, Samatha et al. 2021. "Expansion and Characterization of Bone Marrow Derived Human Mesenchymal Stromal Cells in Serum-Free Conditions." *Scientific Reports* 11(1): 3403. https://doi.org/10.1038/s41598-021-83088-1.

Cao, Jay J. 2011. "Effects of Obesity on Bone Metabolism." *Journal of orthopaedic surgery and research* 6: 30.

Ellulu, Mohammed S et al. 2017. "Obesity and Inflammation: The Linking Mechanism and the Complications." *Archives of medical science : AMS* 13(4): 851–63.

Fuster, José J, Noriyuki Ouchi, Noyan Gokce, and Kenneth Walsh. 2016. "Obesity-Induced Changes in Adipose Tissue Microenvironment and Their Impact on Cardiovascular Disease." *Circulation research* 118(11): 1786–1807.

Garcia, Jéssica Leite et al. 2022. "Rice (Oryza Sativa L.) Bran Preserves Cardiac Function by Modulating pro-Inflammatory Cytokines and Redox State in the Myocardium from Obese Rats." *European journal of nutrition* 61(2): 901–13.

Ge, Chunxi et al. 2016. "Reciprocal Control of Osteogenic and Adipogenic Differentiation by ERK/MAP Kinase Phosphorylation of Runx2 and PPARγ Transcription Factors." *Journal of cellular physiology* 231(3): 587–96.

González, Sonia. 2020. "Dietary Bioactive Compounds and Human Health and Disease." *Nutrients* 12(2).

Greco, Emanuela A, Andrea Lenzi, and Silvia Migliaccio. 2015. "The Obesity of Bone." *Therapeutic advances in endocrinology and metabolism* 6(6): 273–86.

Ha, Tae-Youl et al. 2005. "Bioactive Components in Rice Bran Oil Improve Lipid Profiles in Rats Fed a High-Cholesterol Diet." *Nutrition Research* 25(6): 597–606. https://www.sciencedirect.com/science/article/pii/S0271531705001028.

Jacobs, Frans Alexander, Mari van de Vyver, and William Frank Ferris. 2019. "Isolation and Characterization of Different Mesenchymal Stem Cell Populations from Rat Femur BT - Pre-Clinical Models: Techniques and Protocols." In ed. Paul C Guest. New York, NY: Springer New York, 133–47. https://doi.org/10.1007/978-1-4939-8994-2_13.

Jezewska-Zychowicz, Marzena et al. 2018. "The Associations between Dietary Patterns and Sedentary Behaviors in Polish Adults (LifeStyle Study)." *Nutrients* 10(8).

Kahlon, Talwinder S, Faye I Chow, Robert N Sayre, and Antoinette A Betschart. 1992.

"Cholesterol-Lowering in Hamsters Fed Rice Bran at Various Levels, Defatted Rice Bran and Rice Bran Oil." *The Journal of Nutrition* 122(3): 513–19. https://doi.org/10.1093/jn/122.3.513.

Kilkenny, Carol et al. 2010. "Improving Bioscience Research Reporting: The ARRIVE Guidelines for Reporting Animal Research." *PLoS biology* 8(6): e1000412.

Komori, Toshihisa. 2020a. "Functions of Osteocalcin in Bone, Pancreas, Testis, and Muscle." *International Journal of Molecular Sciences* 21(20).

Komori, Toshihisa. 2020b. "What Is the Function of Osteocalcin?" *Journal of oral biosciences* 62(3): 223–27.

Li, Ming O, and Richard A Flavell. 2008. "TGF-Beta: A Master of All T Cell Trades." *Cell* 134(3): 392–404.

Liu, Qian et al. 2020. "Recent Advances of Osterix Transcription Factor in Osteoblast Differentiation and Bone Formation." *Frontiers in cell and developmental biology* 8: 601224.

López-Gómez, Juan J, José L Pérez Castrillón, and Daniel A de Luis Román. 2016. "Impact of Obesity on Bone Metabolism." *Endocrinologia y nutricion : organo de la Sociedad Espanola de Endocrinologia y Nutricion* 63(10): 551–59.

Minatel, Igor Otavio, Fabiane Valentini Francisqueti, Camila Renata Corrêa, and Giuseppina Pace Pereira Lima. 2016. "Antioxidant Activity of γ-Oryzanol: A Complex Network of Interactions." *International journal of molecular sciences* 17(8).

Morris, H F, S Ochi, and S Winkler. 2000. "Implant Survival in Patients with Type 2 Diabetes: Placement to 36 Months." *Annals of periodontology* 5(1): 157–65.

Van Nguyen, Nguu, and Aldo Ferrero. 2006. "Meeting the Challenges of Global Rice Production." *Paddy and Water Environment* 4(1): 1–9. https://doi.org/10.1007/s10333-005-0031-5.

de Oliveira, Paula Gabriela Faciola Pessôa et al. 2020. "Obesity/Metabolic Syndrome and Diabetes Mellitus on Peri-Implantitis." *Trends in endocrinology and metabolism: TEM*.

Pierce, J L, D L Begun, J J Westendorf, and M E McGee-Lawrence. 2019. "Defining Osteoblast and Adipocyte Lineages in the Bone Marrow." *Bone* 118: 2–7.

Rao, Y Poorna Chandra, D Sugasini, and B R Lokesh. 2016. "Dietary Gamma Oryzanol Plays a Significant Role in the Anti-Inflammatory Activity of Rice Bran Oil by Decreasing pro-Inflammatory Mediators Secreted by Peritoneal Macrophages of Rats." *Biochemical and biophysical research communications* 479(4): 747–52.

Rocha Camargo, Tavani et al. 2021. "Biological Activities of the Protein Hydrolysate Obtained from Two Fishes Common in the Fisheries Bycatch." *Food Chemistry* 342: 128361. https://www.sciencedirect.com/science/article/pii/S0308814620322238.

Shapses, Sue A, L Claudia Pop, and Yang Wang. 2017. "Obesity Is a Concern for Bone Health with Aging." *Nutrition research (New York, N.Y.)* 39: 1–13. https://pubmed.ncbi.nlm.nih.gov/28385284.

Sharif, Mian Kamran, Masood Sadiq Butt, Faqir Muhammad Anjum, and Saima Hafiz Khan. 2014. "Rice Bran: A Novel Functional Ingredient." *Critical reviews in food science and nutrition* 54(6): 807–16.

Sheflin, Amy M et al. 2015. "Pilot Dietary Intervention with Heat-Stabilized Rice Bran Modulates Stool Microbiota and Metabolites in Healthy Adults." *Nutrients* 7(2): 1282–1300.

Sohail, Muhammad et al. 2017. "Rice Bran Nutraceutics: A Comprehensive Review." *Critical reviews in food science and nutrition* 57(17): 3771–80.

Stamnitz, Sandra, and Aleksandra Klimczak. 2021. "Mesenchymal Stem Cells, Bioactive

Factors, and Scaffolds in Bone Repair: From Research Perspectives to Clinical Practice." *Cells* 10(8).

Stevens, Shawn M, Brendan P O'Connell, and Ted A Meyer. 2015. "Obesity Related Complications in Surgery." *Current opinion in otolaryngology & head and neck surgery* 23(5): 341–47.

Tung, Yu-Hsiang, and Lean-Teik Ng. 2019. "Effects of Nitrogen Fertilization Rate on Tocopherols, Tocotrienols and γ-Oryzanol Contents and Enzymatic Antioxidant Activities in Rice Grains." *Physiology and molecular biology of plants : an international journal of functional plant biology* 25(1): 189–95.

Wang, Richard N et al. 2014. "Bone Morphogenetic Protein (BMP) Signaling in Development and Human Diseases." *Genes & diseases* 1(1): 87–105.

Yang, Suh-Ching et al. 2019. "Rice Bran Reduces Weight Gain and Modulates Lipid Metabolism in Rats with High-Energy-Diet-Induced Obesity." *Nutrients* 11(9).

Zou, Yucheng et al. 2020. "Rice Bran Attenuated Obesity via Alleviating Dyslipidemia, Browning of White Adipocytes and Modulating Gut Microbiota in High-Fat Diet-Induced Obese Mice." *Food & Function* 11(3): 2406–17. http://dx.doi.org/10.1039/C9FO01524H.

Capítulo 5

Nanohydroxyapatite-Blasted Bioactive Surface Drives Shear-Stressed Endothelial Cell Growth and Angiogenesis

T. S. Pinto, B. R. Martins, M. R. Ferreira, F. Bezerra, & W. F. Zambuzzi

Lab. of Bioassays and Cellular Dynamics, Department of Chemical and Biological Sciences, Institute of Biosciences, UNESP - São Paulo State University, 18618-970, Botucatu, São Paulo, Brazil

ARTIGO PUBLICADO:

Pinto TS, Martins BR, Ferreira MR, Bezerra F, Zambuzzi WF. Nanohydroxyapatite-Blasted Bioactive Surface Drives Shear-Stressed Endothelial Cell Growth and Angiogenesis. Biomed Res Int. 2022 Feb 23;2022:1433221. doi: 10.1155/2022/1433221. PMID: 35252440; PMCID: PMC8890866.

ABSTRACT

Nanosized crystalline hydroxyapatite coating (HAnano®) accelerates the osteointegration of dental implants which is hypothesized to drive angiogenesis. In order to test this hypothesis, we have subjected shear-stressed human umbilical vein endothelial cells (HUVECs) to a HAnano®-enriched medium, as well as to surface presenting dual acid etching (DAE) as a control. To note, the titanium implants were coated with 10 nm in diameter HA particles using the Promimic HAnano method. Our data reveals that HAnano® modulates higher expression of genes related with endothelial cell performance and viability, such as VEGF, eNOS, and AKT, and further angiogenesis in vitro by promoting endothelial cell migration. Additionally, the data shows a significant extracellular matrix (ECM) remodeling, and this finding seems developing a dual role in promoting the expression of VEGF and control endothelial cell growth during angiogenesis. Altogether, these data prompted us to further validate this phenomenon by exploring genes related with the control of cell cycle and in fact our data shows that HAnano® promotes higher expression of CDK4 gene, while p21 and p15 genes (suppressor genes) were significantly lower. In conjunction, our data shows for the first time that HAnano®-coated surfaces drive angiogenesis by stimulating a proliferative and migration phenotype of endothelial cells, and this finding opens novel comprehension about osseointegration mechanism considering nanosized hydroxyapatite coating dental implants.

1. Introduction

Advances in metallic based biomaterials were dynamically achieved over the last years and have proposed optimized materials in the biomedical field to replace or sustain a lost bone function [1]. There are many characteristics of metal implants that develop essential functions in the success of biomaterial biocompatibility and performance, and these issues affect several biological processes, such as endothelial cells (EC) and blood platelets, responsible for triggering signaling involved with local inflammation, blood coagulation, angiogenesis, and others [2].

Considering the osseointegration biology of dental implants, this is expected that the biology of the reactional tissue surrounds the implanted devices need to recapitulate principles of osteogenesis in an appositional bone growth manner by requiring a plethora performance of undifferentiated and osteogenic cells and also require specific intracellular pathways to drive the cell adhesion, proliferation, and differentiation [3, 4]. Although titanium alloys have been widely used in dentistry mainly considering their characteristics such as stability, mechanical strength, and corrosion resistance [5], there is constant interest in ameliorating their performance by proposing the most sophisticated surfaces considering more than physicochemical properties, applying the knowledge on the bioactive performance of coatings, as well as nanotechnology and how much these surfaces could be predicted considering the biological responses [6, 7].

As it has been related in other studies, a novel surface blasted with nanosized hydroxyapatite (0.02 μm thin; HAnano®, Promimic, Gothenburg, Sweden) is proposed with already known biological responses [6, 7] mainly based on their superhydrophilic surface without changing the microstructure of the dental implants [8]. It is important to mention that HA is the major inorganic component of the bone, and it seems to favor the success of bone cell interaction and osteogenesis [9], and it seems HAnano® be a bioinspired surface. Recently, we have focused on evaluating the relevance of intracellular signaling pathways in driving the interface of tissue with the implants [10–14], mainly considering the releasing debris/molecules from these materials and whether these materials could affect blood vessels and osteogenesis [15]. Additionally, this is known that the clinical success of the treatment using biomaterials depends on adequate blood apport to deliver important nutrients and biomolecules to the injured tissue during osseointegration and angiogenesis and seems develop a pivotal role maybe coupling osteoblast's differentiation and also enhancing bone healing [16].

Angiogenesis in bone tissue is crucial during development and healing and during its remodeling; it involves a critical interaction with bone cells preceding the onset of osteogenesis by activating a plethora of proangiogenic factors such as vascular endothelial growth factor (VEGF), platelet-derived growth factor (PDGF), transforming growth factor beta (TGF-β), fibroblast growth factors (FGF), and bone morphogenetic proteins (BMPs). In this way, Kusumbe et al. identified a new capillary subtype able to couple angiogenesis to osteogenesis by generating a distinct microenvironment and maintaining perivascular osteoprogenitors [17]. Importantly, these mechanisms seem to require a dynamic extracellular matrix (ECM) remodeling in response to biomaterials and this mechanism is devoted to the matrix metalloproteinase (MMP) activities [18].

Blood vessels play a pivotal role in bone development, remodeling, and homeostasis; its being in the angiogenesis is crucial during the bone healing surrounding the dental implants. In this way, although some progress has been achieved regarding the HAnano® promoting osteogenesis, very few is documented about angiogenesis in this aspect. Thus, we have hypothesized that HAnano® drives angiogenesis surrounding the implants and guarantees the success of its osseointegration when coating titanium-based dental implants. To better address this issue, we have subjected shear-stressed human umbilical vein endothelial cells (HUVECs) to HAnano®-enriched medium up to 24 hours when the biological samples were collected to allow further the molecular analysis. Importantly, the endothelial cells were maintained in vitro considering the shear stress mimicking blood tensional forces [19, 20]. Summarizing, our data shows clearly that HAnano® activates genes related with angiogenesis and promotes the proliferation/migration of endothelial cells by coordinating ECM remodeling and higher expression of genes related with endothelial cell growth and migration.

2. Material and Methods

2.1. Implants and Reagents

2.1.1. Implants. The titanium-based dental implants evaluated in this study presenting DAE surfaces and EPIKUT® with HAnano® surface were obtained from S.I.N. Implant System, Sao Paulo, Brazil, with 3.5 mm in diameter and 10.0 mm in length. HAnano® surface was obtained using the Promimic HAnano method [21, 22]. Briefly, the samples were dipped into a stable particle suspension containing 10 nm in diameter HA particles followed by a heat treatment at 550° C for 5 min in a nitrogen atmosphere. Importantly, the calcium to phosphor ratio is 1.67. The surfactant mediated process allows better

control of the chemical composition of the coating [22], which has a thickness of less than or equal to 150 nm.

2.1.2. Reagents. RPMI medium, fetal bovine serum (FBS), trypsin, penicillin, and streptomycin (antibiotics) were purchased from Nutricell (Campinas, Sao Paulo, Brazil). Trypan Blue (T6146), acetic acid glacial (695092), (3-(4,5-dimethylthiazol-2-yl)-2,5-diphenyltetrazolium bromide) (MTT) (M2128), ethanol (459844), and crystal violet dye (C0775) were purchased from Sigma Chemical Co. (St. Louis, MO, USA). TRIzol™ reagent (15596026), DNase I (18068015), and High-Capacity cDNA Reverse Transcription Kit (4368814) were obtained from Thermo Fisher Scientific Inc. (Waltham, Massachusetts, EUA). GoTaq qPCR Master Mix (A6002) was purchased from PROMEGA (Madison, Wisconsin, EUA). Oligonucleotides for gene expression, microRNA, and promoter methylation were purchased from Exxtend (Campinas, São Paulo, Brazil).

2.2. Cell Culture. In this study, the cell line used was human umbilical vein endothelial cells (HUVECs) (ATCC; CRL-1730; passage < 10). HUVECs were cultivated in RPMI medium (Nutricell, Campinas, Brazil) supplemented with penicillin (100 U/mL) and streptomycin (100 mg/mL) and 10% fetal bovine serum (FBS) and maintained at 37° C with 5% CO_2. HUVECs were seeded in the peripheral area of the modified 100 mm culture dishes to allow the application of shear stress methodology. To note, the modified 100 mm culture dishes were obtained by bonding at the bottom a 60 mm culture dishes into their center using medical silicone, and thereafter, the dishes were sterilized using UV light for 30 min [20, 23–25] (Figure 1).

2.3. Shear Stress Model. HUVECs were previously seeded onto the peripheral area of the modified culture dishes (as described earlier) and then subjected to the orbital shear stress-induced tension force, using an orbital shaker (Scilogex, Rocky Hill, CT) positioned inside of the cell culture incubator, at 37° C in the presence of CO_2 and 95% humidity, as proposed by others [19, 20, 23, 26–28]. The shear stress model performed here uses an orbital shaker respecting the formula of the maximal wall shear stress: $\tau max = \alpha\sqrt{\rho\eta(2\pi f)}3$, in which τ max (Pascal unit) is the shear stress, α is the radius of orbital rotation (12 cm), ρ is the density of the cell culture medium (937.5 kg/m^3), η is the viscosity of the cell culture medium ($7{:}5 \times 10^{-4}$ Pa s), and $\int$ is the frequency of rotation.

The titanium-enriched medium was used to treat monolayers of endothelial cells in this shear stress workflow in a rotation frequency of 100 rpm, respecting the protocol of previous studies, which is within the range of physiological arterial shear stress (~1–4 Pa). Thus, HUVECs remained in this workflow up to 24 h, being subjected to different treatments: HAnano®-enriched medium and dual acid-etched- (W/DAE-) enriched medium; both were compared to the control (when the cultures were maintained without any treatment). The samples of each group were properly collected to allow the molecular analysis, as schematized in Figure 1.

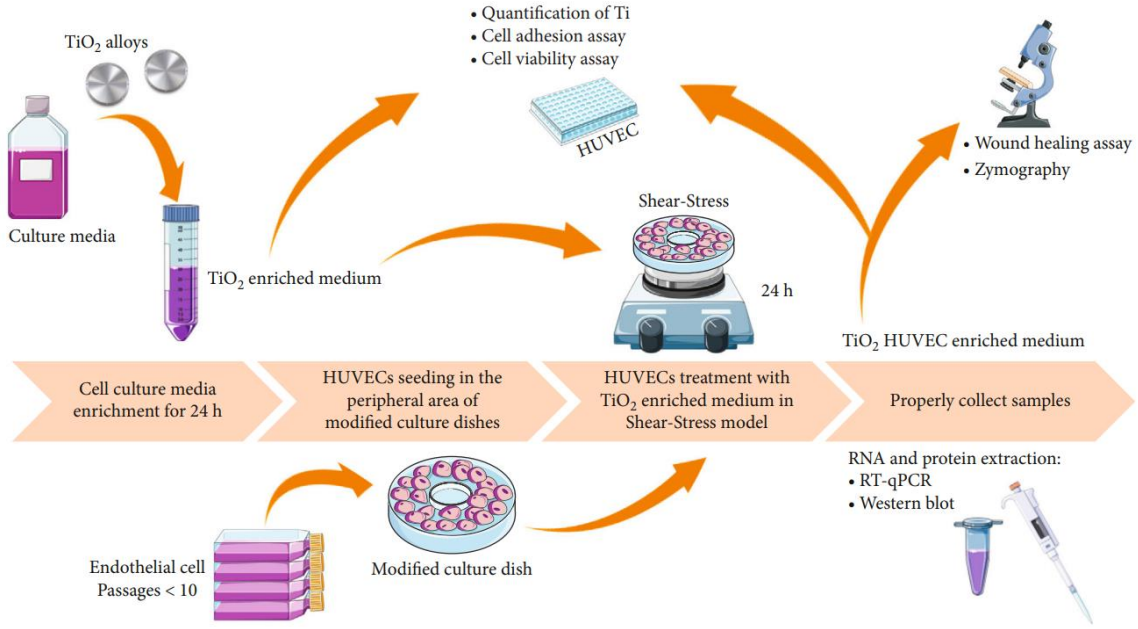

Figure 1: Experimental design of this study. In order to evaluate the endothelial cell (EC) behavior in response to HAnano®, the conditioned medium was obtained in according to ISO 10993:2016 and further used to treat the endothelial cells for 24 h in an in vitro mimicking shear stress model, when the samples were properly collected to allow the molecular analysis.

2.4. Conditioned Medium Obtention. To prepare the titaniumenriched medium, both dual acid-etching (DAE) treating surface (named W/DAE) and the nanohydroxyapatite-blasted surfaces (named HAnano®) were incubated in cell culture media (RPMI) without FBS up to 24 h at 37° C, 5% CO_2, and 95% humidity (0.2 g/mL (w/v); ISO 10993:2016), as we have proposed earlier to evaluate biomaterials [11, 29, 30]. This is expected that the conditioned medium contains molecules released from those metallic alloys and might affect the biology of endothelial cells. The cytotoxic effect of those implants was measured using MTT assay.

2.5. Ti Amount Was Measured by Graphite Furnace Atomic Absorption Spectrometry. The conditioned medium was used to measure Ti element content before and after treating the HUVECs in the shear stress model. Importantly, Ti determination was performed by a graphite furnace atomic absorption spectrometry, in which the graphite tube's heating program optimized for Ti determinations was based on the procedure described by Silva et al. [31].

2.6. Cell Viability Assay. The conditioned medium was prepared using the ISO 10993:2016, as well as it has been used by Zambuzzi et al. [32]. To prepare the conditioned medium, the implants were incubated in RPMI up to 24 hours. Previously, the cells were seeded on 96-well plates (5×10^4 cells/mL) and incubated up to 24 h with the conditioned medium, when the culture media was substituted by 180 μL/well of each sample extract plus 20 μL FBS (resulting a final concentration of 10% of FBS). The control cultures were considered maintaining cells under classical cell culture conditions. The experimental time was 24 hours, when the cell viability was assessed by adding 1 mg/mL of 3-(4,5- dimethyl-2-thiazolyl)-2,5-diphenyl-2H-tetrazolium bromide (MTT) to measure the mitochondrial dehydrogenase activity by MTT reduction up to 3 hours into CO_2 incubator, where there is a conversion of the yellow water-soluble tetrazolium salt MTT into the purple-colored soluble compound of formazan. The formazan was solubilized into ethanol, and the absorbance measured at 570 nm (Synergy II; BioTek Instruments, USA).

2.7. Cell Adhesion Assay. For evaluating cell adhesion performance, endothelial cells were trypsinized, properly counted, and then reseeded (1×10^4 cells per well) in sextuplicate into 96-well plates in implant-conditioned medium supplemented with 10% of FBS and 1% antibiotics up to 24 h. Then, the nonadherent cells were removed by washing with PBS (37° C) and the adherent cells fixed in glacial acetic acid and absolute ethanol solution (3 : 1; v/v) for 10 minutes at room temperature (RT). Thereafter, the cells were stained with 0.1% (w/v) crystal violet for 10 minutes at RT. The excess dye was retained by decanting and washing (2x) with distilled water. Finally, the dye was extracted with 10% acetic acid (v/v) and the optical density measured at 550 nm using a microplate reader (Biotek Co., Winooski, VT). For the positive control, the cells were seeded on

polystyrene surface (control group (Ctrl)). The results were expressed as percent of the control (100%).

2.8. Angiogenesis Assay. The cell migration and angiogenesis were estimated by using a scratch assay, as performed earlier [19]. The scratch assay estimates the cell migration and angiogenesis. Briefly, the cells were cultured in 12-well plates at 4×10^4 cells/cm^2, and after 100% confluence, an introduced area was cleared using a pipet tip [19] and then a monitoring of the angiogenesis and the migration of the ECs up to 12 h and 16 h. Thereafter, the cultures were subjected to fixation with 4% PFA and stained with Alizarin Red S. In the analysis of the angiogenesis in vitro, the wound healing area was measured in an inverted microscope with a coupled digital camera (Zeiss) and the acquired images analyzed using the ImageJ software (NIH, Bethesda, MD).

2.9. Total mRNA Isolation and RT-qPCR Analysis. In order to evaluate the molecular behavior of genes related with angiogenesis and cellular survival in response to HAnano®, the cells were newly subjected to the conditioned medium containing the released molecules and further harvested and total mRNA properly isolated using Ambion TRIzol Reagent (Life Sciences, Thermo Fisher Scientific Inc., Waltham, MA) and treated with DNase I (Invitrogen, Carlsbad, CA). Complementary DNA (cDNA) synthesis was performed with the High-Capacity cDNA Reverse Transcription Kit (Applied Biosystems, Foster City, CA) according to the manufacturer's instructions. Real-Time Reverse Transcriptase qPCR was carried out in a total of 10 μL, containing PowerUp™ SYBR™ Green Master Mix 2× (5 μL; Applied Biosystems, Foster City, CA), 0.4 μM of each primer, 50 ng of cDNA, and nuclease-free H_2O. Results were expressed as relative amounts of the transcripts using 18s as reference gene (housekeeping gene), using the cycle threshold (Ct) method. Primers and work conditions are described in Table 1.

Table 1: Expression *primers* sequences and qPCR cycle conditions.

Gene	Primer	5′-3′ sequence	Work condition
AKT	Forward 1	CAGCGCGGCCCGAAGGAC	95°C -3 s, 55°C -8 s, 72°C -20s
	Forward 2	GGACTCCCGTTTGCGCCAGT	
	Reverse	GACGCTCACGCGCTCCTCTC	
CFL1	Forward	TGTGCGGCTCCTACTAAACG	95°C -3 s, 55°C -8 s, 72°C -20s
	Reverse	TCCTTGACCTCCTCGTAGCA	
P15	Forward	GGGACTAGTGGAGAAGGTGC	95°C -3 s, 55°C -8 s, 72°C -20s
	Reverse	CATCATCATGACCTGGATCGC	
P21	Forward	GCTGCCGAAGTCAGTTCCTT	95°C -3 s, 55°C -8 s, 72°C -20s
	Reverse	ATCTGTCATGCTGGTCTGCC	
CDK2	Forward	CTTTGCTGAGATGGTGACTCG	95°C -3 s, 55°C -8 s, 72°C -20s
	Reverse	GCCTCCCAGATTCCTCATGC	
CDK4	Forward	CTCTCTAGCTTGCGGCCTG	95°C -3 s, 55°C -8 s, 72°C -20s
	Reverse	GCAGGGATACATCTCGAGGC	
VEGF	Forward	TGCAGATTATGCGGATCAAACC	95°C -3 s, 55°C -8 s, 72°C -20s
	Reverse	TGCATTCACATTTGTTGTGCTGTAG	
ENOS	Forward	TATTTGATGCTCGGGACTGC	95°C -3 s, 55°C -8 s, 72°C -20s
	Reverse	AAGATTGCCTCGGTTTGTTG	
P38	Forward	GAGAACTGCGGTTACTTA	95°C -3 s, 55°C -8 s, 72°C -20s
	Reverse	ATGGGTCACCAGATACACAT	
ERK	Forward 1	AACAGGCTCTGGCCCACCCAT	95°C -3 s, 55°C -8 s, 72°C -20s
	Forward 2	CGCCCCTCCAAACGGCTCAA	
	Reverse	GCAGCGCCTCCCTTGCTAGA	
ITGB1	Forward	GCCGCGCGGAAAAGATGAA	95°C -3 s, 55°C -8 s, 72°C -20s
	Reverse	TGCTGTTCCTTTGCTACGGT	
FAK	Forward	TCAGCTCAGCACAATCCTGG	95°C -3 s, 55°C -8 s, 72°C -20s
	Reverse	CTGAAGCTTGACACCCTCGT	
SRC	Forward	CAACACAGAGGGAGACTGGT	95°C -3 s, 55°C -8 s, 72°C -20s
	Reverse	AGCTTCTTCATGACCTGGGC	
18S	Forward	CGGACAGGATTGACAGATTGATAGC	95°C -3 s, 55°C -8 s, 72°C -20s
	Reverse	TGCCAGAGTCTCGTTCGTTATCG	

2.10. Statistical Analyses. Results were represented as mean ± standard deviation (SD). The samples assumed a normal distribution, and they were subjected to Student's t-test (two-tailed) with $p < 0:05$ considered statistically significant. In the experiment where there were more than two groups, we used one-way ANOVA with Tukey's multiple comparisons test, in order to compare all pairs of groups. In this case, the significance level was considered when alpha = 0:05 (95% confidence interval). The software used was GraphPad Prism 7 (GraphPad Software, USA).

3. Results

Firstly, we have focused on evaluating whether the different surfaces of titanium proposed in this study were able to develop some cytotoxicity in endothelial cells. Thus, Figure 2(a) shows that there is no significance effect on mitochondrial activities in response to both surfaces, as well as the cell adhesion, once Figure 2(b) brings the same behavior of endothelial cells responding to the materials, without any changes on the outcomes obtained by shear-stressed endothelial cells. Additionally, we have also investigated whether endothelial cells were able to capture titanium released from the

materials, and our data shows for the first time there is a significant uptake of titanium by shear-stressed endothelial cells responding to HAnano® super hydrophilic surface (Figure 2(c)) and this data could explain some metabolic changes in those cells.

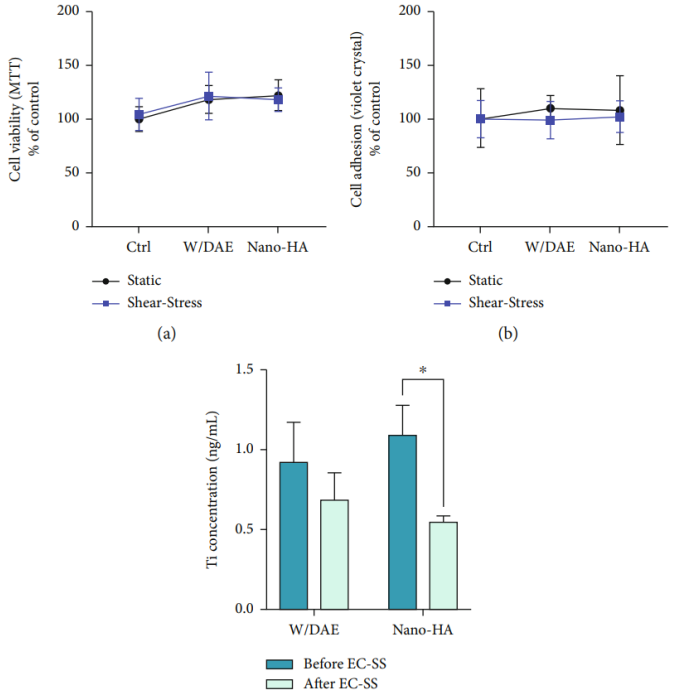

Figure 2: HAnano® cytotoxicity and the capacity of shear-stressed endothelial cell in capturing medium-soluble titanium. The titanium-enriched medium was obtained in according to ISO 10993:2016 by incubating the implants containing DAE (w/DAE) or nanosized hydroxyapatite (HAnano®) coatings up to 24 hours and thereafter used to subject endothelial cell. Our data shows there is no effect on endothelial cell viability (a) and endothelial cell adhesion (b). Additionally, it was confirmed that shear-stressed endothelial cell captures a significant amount of medium-soluble titanium mainly responding to HAnano®. A significant difference was considered when $p < 0:05$.

Thereafter, in order to investigate whether the Ti-enriched medium was able to change the metabolism of shear-stressed endothelial cells, we evaluated genes related with endothelial cells phenotype: importantly, our data shows that shear-stressed endothelial cells responding to HAnano® super hydrophilic surface presents a significant higher expression profile of VEGF (Figure 3(a); about 10- fold changes), eNOS (Figure 3(b); about 4-fold changes), and AKT (Figure 3(c); about 2.5-fold changes).

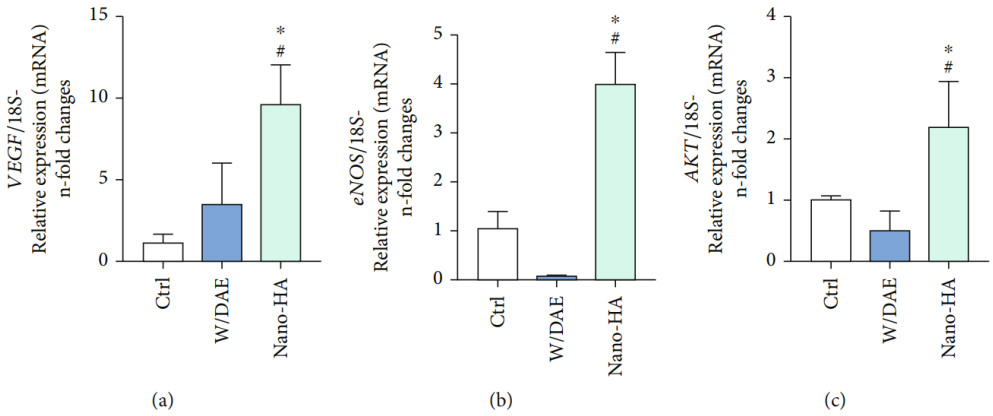

Figure 3: HAnano® upmodulates EC phenotype-related genes. Shear-stressed endothelial cells were subjected to Ti-enriched medium for 24 hours, and the samples were harvested to allow gene expression using RT-qPCR methodology. Our data shows there is a significant higher expression of VEGF (a) and eNOS (b) genes in response to HAnano®, as well as AKT gene (c). The graphs bring the n-fold change of the profile of transcripts normalized to the 18S gene (housekeeping gene). Significant differences were considered when $p < 0:05$, represented by $*$ when compared to the Ctrl group and by # when compared to the W/DAE group.

In addition, this data prompted us to better evaluate the behavior of shear-stressed endothelial cells by considering a well-accepted in vitro methodology. In general, shear stressed endothelial cells responding to Ti-enriched medium presented a better performance in cell migration and angiogenesis in vitro than control cultures (Figures 4(a)–4(j)), with better outcomes obtained in response to HAnano® superhydrophilic surface in 16 hours (Figure 4). Figure 4(k) brings the analysis of the wounding area; considered here, the capacity of endothelial cells migrate responding to the specific treatments.

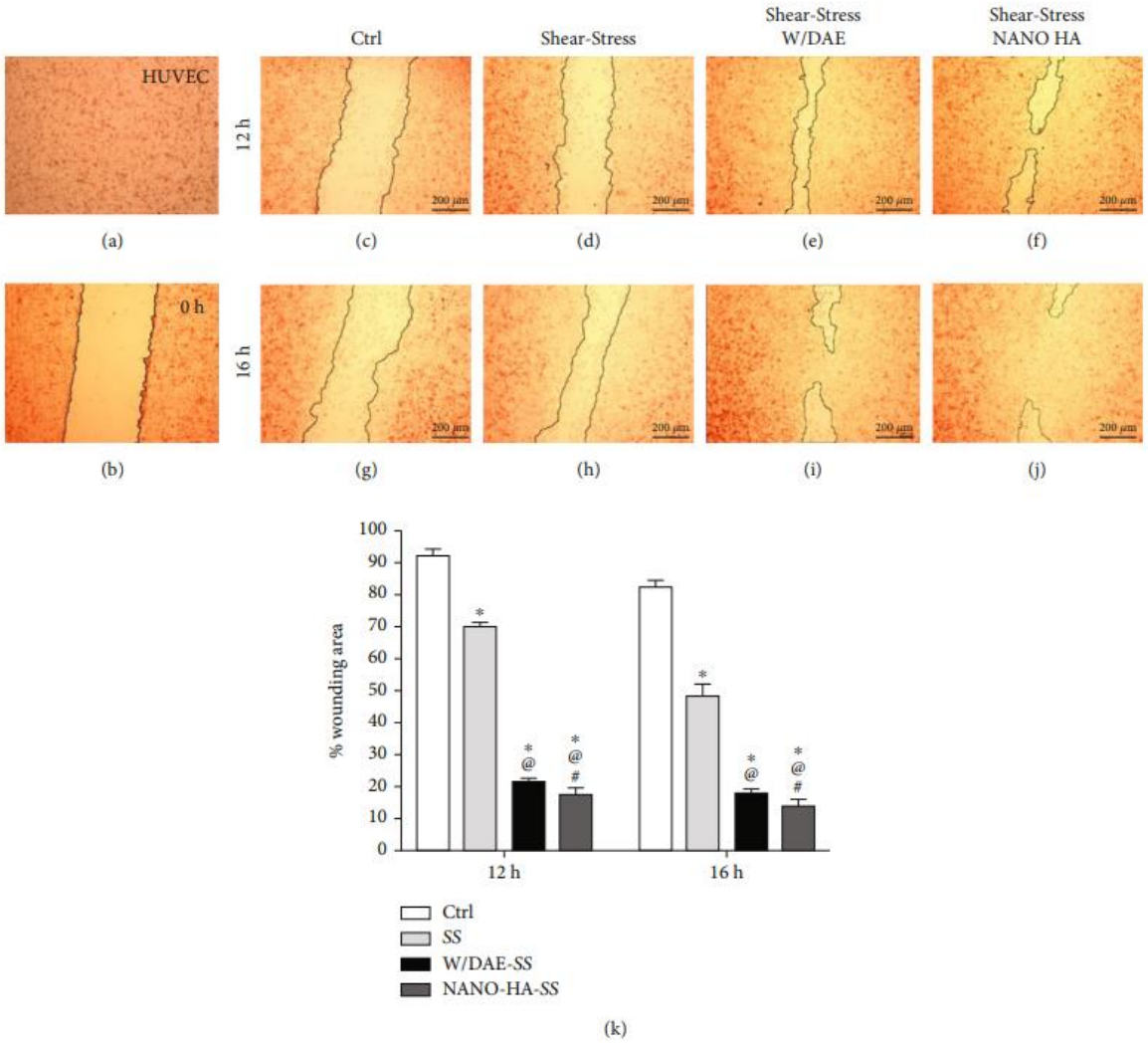

Figure 4: The angiogenic effect of HAnano® was measured by a wound healing assay. (a) Endothelial cell forming a confluent monolayer. (b) In vitro "wound" was created by a straight-line scratch across the endothelial cell monolayer (T0). At time 0 (T0), the endothelial cell were scratched and subjected to conditioned medium, respecting the culture groups, as follows: Ctrl: RPMI (c, g); shear stress: endothelial cell in shear stress model (d, h); shear stress W/DAE: shear-stressed endothelial cell subjected with Ti-enriched medium by DAE (w/DAE) (e,i); shear stress HAnano®: shear-stressed endothelial cell subjected with Ti-enriched medium by HAnano® (nano-HA) (f, j). The scratch wound assay was used to assess the migration capacity of the endothelial cells under different conditioned media. The wound area was estimated by calculating the cell-free area in captured images using the ImageJ software (NIH, Bethesda, MD). The migration rate is expressed in percentage as the change in the wound area over time, the scratch area at time point 0 hours was set to 100%, and the other ones are represented as wound closure expressed as the remaining area uncovered by the cells in percentage. (k) The statistically significant changes are represented by ∗ when compared with the Ctrl group, by @ when compared to the SS group, and by # when compared to the W/DAE SS group. Significant differences were considered when $p < 0:05$.

As migration and proliferation actions of the cells requires a dynamic mechanism of extracellular matrix (ECM) remodeling, we also investigated the behavior of matrix metalloproteinase (MMP) activities, and our data supports that shear-stressed endothelial cells responding to the Ti-enriched medium promoted a higher activity of MMP2 (Figures 5(a)–5(d)). Here, we need to consider the limitation of the experimental model used in this study, and the data supports a significant stimulus of Ti-enriched medium on remodeling ECM in endothelial cells.

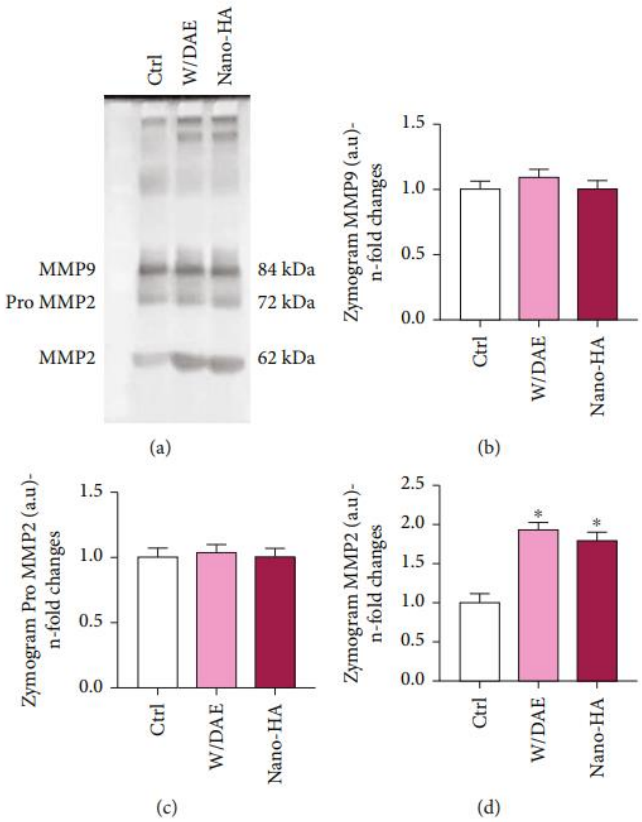

Figure 5: Both Ti-related surfaces with DAE or HAnano® promote higher activity of MMP2 enzyme. The ECM remodeling was evaluated by checking the activities of MMPs in response to titanium-enriched media indirectly obtained by 2 different surfaces DAE (w/DAE) and nanohydroxyapatite-blasted titanium surface (HAnano®) applying zymography technology (a). MMP2 activity showed different activities profiles, mainly observed higher in response to both treatments when compared to Ctrl (b–d). Differences were considered significant when $p < 0{:}05$, represented by $*$ when compared with the Ctrl group. MMP: matrix metalloproteinase.

To better understand the behavior of shear-stressed endothelial cells responding to Ti-enriched medium obtained by surfaces DAE and HAnano®, we now investigated the relevance of genes related with cell proliferation. Our data shows there is a significant downregulation of genes of MAPKs p38 and ERK in endothelial cells responding to Ti-

enriched medium, and it does not matter the kind of surface evaluated (Figures 6(a) and 6(b)). In addition, specific genes related with cell cycle progression were also investigated and Figure 6(c) shows there is a significant higher expression of CDK4 gene by shear stressed endothelial cells responding to HAnano® super hydrophilic surface, while CDK2 gene was significant downregulated (Figure 6(d)). These data could explain the findings shown previously here in cell migration and angiogenesis in response to HAnano® surfaces.

Importantly, in this context and considering the regulation of cell cycle activity of endothelial cells, we also investigated the behavior of genes related to negatively control cell proliferation, p15 and p21, and our data shows there is a significant downregulation of the expression profile of these both genes in endothelial cells responding to Ti-enriched medium, mainly considering p21 gene in response to HAnano® (Figures 6(e) and 6(f)).

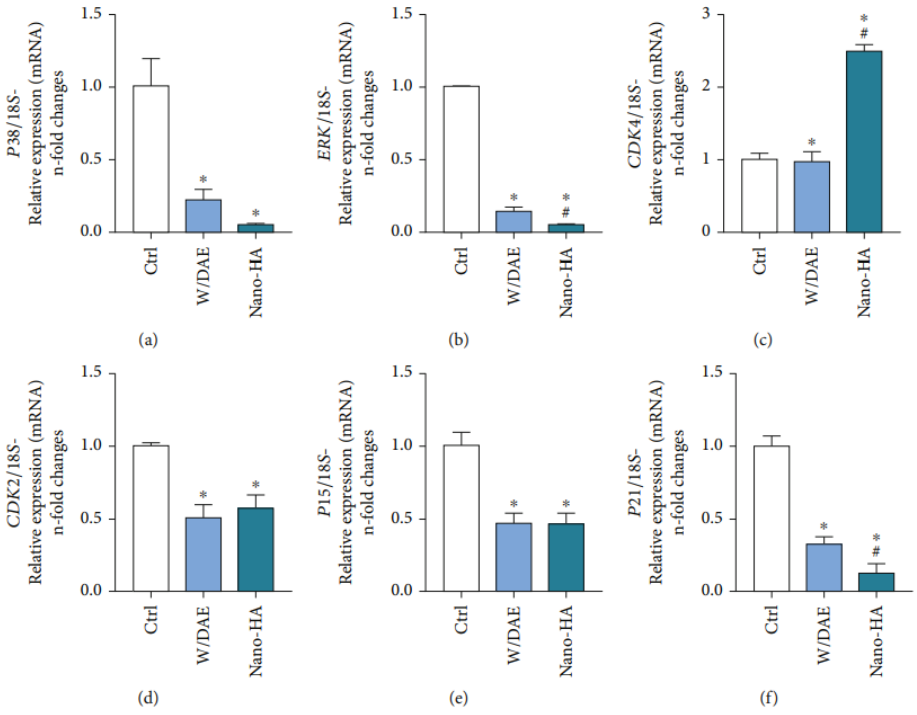

Figure 6: CDK4 is upmodulated in response to HAnano®. Thereafter, understanding its relevance on endothelial cells migration and angiogenesis, we postulated the hypothesis that HAnano® modulates cell cycle-related genes. Although MAPKs p38 (a) and ERK (b) genes were downregulated in response to HAnano®, CDK4 gene expression was significantly higher ((c) approximately 2.5-fold changes), while CDK2 gene was downregulated (d). Importantly, cell cycle suppressor genes, p15 (e) and p21 (f), were downregulated in response to both W/DAE and HAnano®. The graphs bring the n-fold change of the profile of transcripts normalized to the 18S gene (housekeeping gene).

Significant differences were considered when $p < 0.05$, represented by * when compared with the Ctrl group and by $^{\#}$ when compared to the W/DAE group.

4. Discussion

Considering the osseointegration-related microenvironment, angiogenesis is an important biological event to be considered, which plays a pivotal role on supplying cells, nutrients, and gases changes as well as clearing up waste molecules from the cellular metabolism. In addition, the vascularization plays crucial role in bone healing, mainly considering the coupling mechanism between bone cells and endothelial cells by angiocrine signals addressing bone cell activities and further osteogenesis. Once angiogenesis in response to biomaterials is barely understood, we decided to better evaluate the behavior of shear-stressed endothelial cells responding to Ti-enriched medium obtained from 2 different types of modified surfaces, as follows: (1) subjected to DAE (w/DAE) and (2) DAE-modified surfaces coated with nanosized HA (HAnano®). It is important to mention that we have previously shown that HAnano® superhydrophilic surface drives osteoblast performance when modifying dental implants surfaces [33].

In this study, our data shows that dental implants having HAnano® superhydrophilic surfaces generates an adequate microenvironment to drive angiogenesis and this study could explain the success of its clinical application [34]. Firstly, our data shows that shear-stressed endothelial cells significantly uptake titanium released from HAnano®- enriched medium and this data opened a set of question about the behavior of endothelial cells and angiogenesis and, in part, is shown here. Importantly, our data shows that conditioned medium by HAnano® promotes higher expression of important genes related with endothelial cell phenotype: VEGF and eNOS. Importantly, these data bring important evidences to suggest the relevance of angiogenesis during tissue remodeling microenvironment surrounding the dental implants.

This is known that angiogenesis is regulated by many growth factors and molecules, and in this scenario, VEGF and nitric oxide (NO) are potent angiogenic factors. Mechanistically, the capacity of VEGF in promoting bone regeneration and healing has been shown in several biological models [35–37]. VEGF is a very important growth factor in the vascular system driving endothelial cell growth and survival, as well as develops a signaling hub with osteogenesis by regulating the expression of bone morphogenetic proteins (BMPs) [38, 39], and VEGF may be released during matrix

remodeling orchestrated by MMP-mediated matrix breakdown, which induces vascular invasion and angiogenesis [40].

Importantly, we have shown previously that titanium-based devices drive matrix remodeling by upmodulating the activities of matrix metalloproteinases (MMPs) [6, 29, 41] and this recapitulates events are also shown in bone development and healing [27, 42–47]. Importantly, this could be a prerequisite also to favor the angiogenesis process throughout the distraction osteogenesis phase, but to a lesser extent during the phase of consolidation [48], respecting distinct phases of bone repair progress. Another concern evaluated here was the possibility of shear-stressed endothelial cells in expressing eNOS in response to nanosized HA, once the role of the messenger molecule nitric oxide has been evaluated in fracture healing [49], and NO is synthesized by three kinds of nitric oxide synthase (NOS): inducible NOS (iNOS), endothelial (eNOS), and neuronal (nNOS). Regarding eNOS, our data show a very similar profile of VEGF and seems to develop a pivotal role in endothelial cell activity to maintain endothelial homeostasis during bone healing surrounding the implanted devices. As we have also noticed from the data, a higher expression of AKT gene in endothelial cells responds to HAnano®; this seems obvious suggesting that the angiogenic stimulus of HAnano® requires AKT/eNOS axis in shearstressed endothelial cells; once, this is widely related in the literature that AKT activates eNOS via activation of mTOR [50, 51]. Thus, AKT is closely linked to the formation of new blood vessels through the activation of endothelial nitric oxide synthase (eNOS) [52], which is responsible for relaxing vascular smooth muscle and also mediates angiogenesis by controlling the action of VEGF [52–54]. Moreover, Akt also regulates PI3K-mediated cell survival and is sufficient to block cell death induced by a variety of apoptotic stimuli [55, 56] and the importance of PI3K in endothelial cell was shown by using wortmannin as an inhibitor [28].

Finally, we have also investigated whether these molecular mechanisms led to the proliferation and migration of endothelial cells. Thus, we have further investigated angiogenesis in vitro by using a well-accepted functional assay and our data validates this hypothesis; once, endothelial cells subjected to HAnano® presented better cell cycle performance by upmodulating CDK4 gene and ECM remodeling, while both investigated cell cycle suppressor genes p15 and p21 were downmodulated. ECM remodeling seems to be an important hub in endothelial cells responding to HAnano® by favoring as a prerequisite to VEGF expression and also related with the growth of cells during angiogenesis.

Generally, this is reasonable to suggest that HAnano® promotes an ideal microenvironment for osseointegration by regulating genes related with endothelial cell growth, such as VEGF, which could play an autrocrine loop and AKT/ eNOS signaling, culminating with EC proliferation and angiogenesis, which could be coupled to osteogenesis; once, we have shown earlier the osteogenic effect of HAnano®. In conjunction, this study brings sufficient in vitro data to support the angiogenic effect of HAnano®-coated titanium surface by modulating the proliferative and migration phenotype of endothelial cells, and these data partially explain a better performance of the application of HAnano® in vivo [34], maybe by coupling angiogenesis and osteogenesis during its osseointegration processes.

Data Availability

The data that support the findings of this study are available from the corresponding author upon reasonable request.

Conflicts of Interest

The authors declare that they have no conflicts of interest.

Authors' Contributions

Pinto TS and Martins BR contributed equally in this study.

Acknowledgments

The authors are grateful to FAPESP (Fundação de Amparo à Pesquisa do Estado de São Paulo) (grant numbers: 2019/ 26854-2 and 2019/09140-6), Coordenação de Aperfeiçoamento de Pessoal de Nível Superior-Brasil (CAPES, code-01), and CNPq for the financial support (PQ2). Also, we would like to thank Prof. Pedro Padilha for the graphite furnace atomic absorption spectrometry analysis.

References

[1] S. Tharani Kumar, S. Prasanna Devi, C. Krithika, and R. N. Raghavan, "Review of metallic biomaterials in dental applications," Journal of Pharmacy & Bioallied Sciences, vol. 12, pp. S14–S19, 2020.

[2] B. Walkowiak, "Surface-modified metallic biomaterials in contact with blood and endothelial cells," Macromolecular Symposia, vol. 253, pp. 122–127, 2007.

[3] O. Andrukhov, C. Behm, A. Blufstein et al., “Effect of implant surface material and roughness to the susceptibility of primary gingival fibroblasts to inflammatory stimuli,” Dental Materials, vol. 36, no. 6, pp. e194–e205, 2020.

[4] P. G. Coelho, J. M. Granjeiro, G. E. Romanos et al., “Basic research methods and current trends of dental implant surfaces,” Journal of Biomedical Materials Research. Part B, Applied Biomaterials, vol. 88, pp. 579–596, 2009.

[5] A. T. Sidambe, “Biocompatibility of advanced manufactured titanium implants-a review,” Maternité, vol. 7, pp. 8168– 8188, 2014.

[6] C. J. C. Fernandes, F. Bezerra, M. R. Ferreira, A. F. C. Andrade, T. S. Pinto, and W. F. Zambuzzi, “Nano hydroxyapatite-blasted titanium surface creates a biointerface able to govern Src-dependent osteoblast metabolism as prerequisite to ECM remodeling,” Colloids and Surfaces. B, Biointerfaces, vol. 163, pp. 321–328, 2018.

[7] F. Bezerra, M. R. Ferreira, G. N. Fontes et al., “Nano hydroxyapatite-blasted titanium surface affects pre-osteoblast morphology by modulating critical intracellular pathways,” Biotechnology and Bioengineering, vol. 114, pp. 1888–1898, 2017.

[8] R. E. Baier, A. E. Meyer, J. R. Natiella, R. R. Natiella, and J. M. Carter, “Surface properties determine bioadhesive outcomes: methods and results,” Journal of Biomedical Materials Research, vol. 18, pp. 337–355, 1984.

[9] E. Pepla, L. K. Besharat, G. Palaia, G. Tenore, and G. Migliau, “Nano-hydroxyapatite and its applications in preventive, restorative and regenerative dentistry: a review of literature,” Annali di Stomatologia, vol. 5, pp. 108–114, 2014.

[10] M. R. Ferreira, G. A. Santos, C. A. Biagi, W. A. Silva Junior, and W. F. Zambuzzi, “GSVA score reveals molecular signatures from transcriptomes for biomaterials comparison,” Journal of Biomedial Materials Research Part A, vol. 109, pp. 1004–1014, 2021.

[11] M. I. P. Machado, A. M. Gomes, M. F. Rodrigues et al., “Cobalt-chromium-enriched medium ameliorates shear-stressed endothelial cell performance,” Journal of Trace Elements in Medicine and Biology, vol. 54, pp. 163–171, 2019.

[12] W. F. Zambuzzi, P. G. Coelho, G. G. Alves, and J. M. Granjeiro, “Intracellular signal transduction as a factor in the development of “Smart” biomaterials for bone tissue engineering,” Biotechnology and Bioengineering, vol. 108, pp. 1246–1250, 2011.

[13] C. J. da Costa Fernandes, T. S. Pinto, H. R. Kang et al., “Layered double hydroxides are promising nanomaterials for tissue bioengineering application,” Advanced Biosystems, vol. 3, article e1800238, 2019.

[14] S. Gemini-Piperni, E. R. Takamori, S. C. Sartoretto et al., “Cellular behavior as a dynamic field for exploring bone bioengineering: a closer look at cell-biomaterial interface,” Archives of Biochemistry and Biophysics, vol. 561, pp. 88–98, 2014.

[15] B. R. Martins, T. S. Pinto, C. J. da Costa Fernandes, F. Bezerra, and W. F. Zambuzzi, “PI3K/AKT signaling drives titanium-induced angiogenic stimulus,” Journal of Materials Science. Materials in Medicine, vol. 32, 2021.

[16] S. K. Ramasamy, A. P. Kusumbe, M. Schiller et al., “Blood flow controls bone vascular function and osteogenesis,” Nature Communications, vol. 7, pp. 1–13, 2016.

[17] A. P. Kusumbe, S. K. Ramasamy, and R. H. Adams, “Coupling of angiogenesis and osteogenesis by a specific vessel subtype in bone,” Nature, vol. 507, pp. 323–328, 2014.

[18] C. J. da Costa Fernandes, M. R. Ferreira, F. J. B. Bezerra, and W. F. Zambuzzi, “Zirconia stimulates ECM-remodeling as a prerequisite to pre-osteoblast adhesion/proliferation by possible interference with cellular anchorage,” Journal of Materials Science. Materials in Medicine, vol. 29, p. 41, 2018.

[19] N. G. dela Paz, T. E. Walshe, L. L. Leach, M. Saint-Geniez, and P. A. D’Amore, “Role of shear-stress-induced VEGF expression in endothelial cell survival,” Journal of Cell Science, vol. 125, pp. 831–843, 2012.

[20] T. S. Pinto, C. J. . C. Fernandes, R. A. da Silva et al., “c-Src kinase contributes on endothelial cells mechanotransduction in a heat shock protein 70-dependent turnover manner,” Journal of Cellular Physiology, vol. 234, no. 7, pp. 11287–11303, 2019.

[21] M. Gottlander, C. B. Johansson, A. Wennerberg, T. Albrektsson, S. Radin, and P. Ducheyne, “Bone tissue reactions to an electrophoretically applied calcium phosphate coating,” Biomaterials, vol. 18, pp. 551–557, 1997.

[22] L. Meirelles, A. Arvidsson, M. Andersson, P. Kjellin, T. Albrektsson, and A. Wennerberg, “Nano hydroxyapatite structures influence early bone formation,” Journal of Biomedical Materials Research. Part A, vol. 87, pp. 299–307, 2008.

[23] R. A. da Silva, M. R. Ferreira, A. M. Gomes, and W. F. Zambuzzi, “Lnc RNA HOTAIR is a novel endothelial mechanosensitive gene,” Journal of Cellular Physiology, vol. 235, pp. 4631– 4642, 2020.

[24] C. J. da Costa Fernandes, G. S. de Almeida, T. S. Pinto, S. A. Teixeira, F. J. Bezerra, and W. F. Zambuzzi, “Metabolic effects of CoCr-enriched medium on shear-stressed endothelial cell and osteoblasts: a possible mechanism involving a hypoxic condition on bone healing,” Materials Science & Engineering. C, Materials for Biological Applications, vol. 128, p. 112353, 2021.

[25] R. A. da Silva, A. F. de Camargo Andrade, G. da Silva Feltran et al., “The role of triiodothyronine hormone and mechanically-stressed endothelial cell paracrine signalling synergism in gene reprogramming during hBMSC-stimulated osteogenic phenotype in vitro,” Molecular and Cellular Endocrinology, vol. 478, pp. 151–167, 2018.

[26] K.-S. Heo, K. Fujiwara, and J. Abe, “Shear stress and atherosclerosis,” Molecules and Cells, vol. 37, pp. 435–440, 2014.

[27] R. A. da Silva, C. J. D. C. Fernandes, G. D. S. Feltran et al., “Laminar shear stress-provoked cytoskeletal changes are mediated by epigenetic reprogramming of TIMP1 in human primary smooth muscle cells,” Journal of Cellular Physiology, vol. 234, no. 5, pp. 6382–6396, 2019.

[28] A. M. Gomes, T. S. Pinto, C. J. da Costa Fernandes, R. A. da Silva, and W. F. Zambuzzi, “Wortmannin targeting phosphatidylinositol 3-kinase suppresses angiogenic factors in shear-stressed endothelial cells,”Journal of Cellular Physiology, vol. 235, no. 6, pp. 5256–5269, 2020.

[29] C. J. da Costa Fernandes, F. J. B. Bezerra, B. de Campos Souza, M. A. Campos, and W. F. Zambuzzi, "Titanium-enriched medium drives low profile of ECM remodeling as a prerequisite to pre-osteoblast viability and proliferative phenotype," Journal of Trace Elements in Medicine and Biology, vol. 50, pp. 339–346, 2018.

[30] C. J. C. Fernandes, F. Bezerra, M. . D. do Carmo et al., "CoCr-enriched medium modulates integrin-based downstream signaling and requires a set of inflammatory genes reprograming in vitro," Journal of Biomedical Materials Research. Part A, vol. 106, no. 3, pp. 839–849, 2018.

[31] F. A. Silva, C. C. F. Padilha, L. E. Pezzato, M. M. Barros, and P. M. Padilha, "Determination of chromium by GFAAS in slurries of fish feces to estimate the apparent digestibility of nutrients in feed used in pisciculture," Talanta, vol. 69, pp. 1025–1030, 2006.

[32] W. F. Zambuzzi, E. A. Bonfante, R. Jimbo et al., "Nanometer scale titanium surface texturing are detected by signaling pathways involving transient FAK and Src activations," *PLoS One*, vol. 9, article e95662, 2014.

[33] R. A. da Silva, G. da Silva Feltran, M. R. Ferreira, P. F. Wood, F. Bezerra, and W. F. Zambuzzi, "The impact of bioactive surfaces in the early stages of osseointegration: an *In Vitro* comparative study evaluating the HAnano® and SLActive® super hydrophilic surfaces," BioMed Research International, vol. 2020, Article ID 3026893, 11 pages, 2020.

[34] S. C. Sartoretto, J. Calasans-Maia, R. Resende et al., "The influence of nanostructured hydroxyapatite surface in the early stages of osseointegration: a multiparameter animal study in low-density bone," International Journal of Nanomedicine, vol. 15, pp. 8803–8817, 2020.

[35] J. Street, M. Bao, L. de Guzman et al., "Vascular endothelial growth factor stimulates bone repair by promoting angiogenesis and bone turnover," Proceedings of the National Academy of Sciences of the United States of America, vol. 99, pp. 9656–9661, 2002.

[36] H. Eckardt, M. Ding, M. Lind, E. S. Hansen, K. S. Christensen, and I. Hvid, "Recombinant human vascular endothelial growth factor enhances bone healing in an experimental nonunion model," Journal of Bone and Joint Surgery. British Volume (London), vol. 87, pp. 1434–1438, 2005.

[37] T. Tarkka, A. Sipola, T. Jämsä et al.,"Adenoviral VEGF-A gene transfer induces angiogenesis and promotes bone formation in healing osseous tissues," The Journal of Gene Medicine, vol. 5, pp. 560–566, 2003.

[38] C. Maes, S. Goossens, S. Bartunkova et al., "Increased skeletal VEGF enhances beta-catenin activity and results in excessively ossified bones," The EMBO Journal, vol. 29, pp. 424–441, 2010.

[39] W. Yang, D. Guo, M. A. Harris et al., "Bmp 2 in osteoblasts of periosteum and trabecular bone links bone formation to vascularization and mesenchymal stem cells," Journal of Cell Science, vol. 126, pp. 4085–4098, 2013.

[40] C. Colnot, Z. Thompson, T. Miclau, Z. Werb, and J. A. Helms, "Altered fracture repair in the absence of MMP9," Development, vol. 130, pp. 4123–4133, 2003.

[41] C. S. Albano, A. Moreira Gomes, G. da Silva Feltran et al., “Biofunctionalization of titanium surfaces with alendronate and albumin modulates osteoblast performance,” Heliyon, vol. 6, pp. e04455–e04455, 2020.

[42] T. Accorsi-Mendonça, K. B. D. S. Paiva, W. F. Zambuzzi et al., “Expression of matrix metalloproteinases-2 and -9 and RECK during alveolar bone regeneration in rat,” Journal of Molecular Histology, vol. 39, pp. 201–208, 2008.

[43] W. F. Zambuzzi, C. L. Yano, A. D. M. Cavagis, M. P. Peppelenbosch, J. M. Granjeiro, and C. V. Ferreira, “Ascorbate-induced osteoblast differentiation recruits distinct MMP-inhibitors: RECK and TIMP-2,” Molecular and Cellular Biochemistry, vol. 322, pp. 143–150, 2009.

[44] A. C. C. de Oliveira Demarchi, W. F. Zambuzzi, K. B. S. Paiva et al., “Development of secondary palate requires strict regulation of ECM remodeling: sequential distribution of RECK, MMP-2, MMP-3, and MMP-9,” Cell and Tissue Research, vol. 340, no. 1, pp. 61–69, 2010.

[45] C. J. C. Fernandes, M. R. Veiga, M. T. S. Peracoli, and W. F. Zambuzzi, “Modulatory effects of silibinin in cell behavior during osteogenic phenotype,” Journal of Cellular Biochemistry, vol. 120, pp. 13413–13425, 2019.

[46] K. B. S. Paiva, W. F. Zambuzzi, T. Accorsi-Mendonça et al., “Rat forming incisor requires a rigorous ECM remodeling modulated by MMP/RECK balance,” Journal of Molecular Histology, vol. 40, pp. 201–207, 2009.

[47] C. J. da Costa Fernandes and W. F. Zambuzzi, “Fibroblast-secreted trophic factors contribute with ECM remodeling stimulus and upmodulate osteocyte gene markers in osteoblasts,” Biochimie, vol. 168, pp. 92–99, 2020.

[48] R. S. Carvalho, T. A. Einhorn, W. Lehmann et al., “The role of angiogenesis in a murine tibial model of distraction osteogenesis,” Bone, vol. 34, pp. 849–861, 2004.

[49] A. D. Diwan, M. X. Wang, D. Jang, W. Zhu, and G. A. Murrell, “Nitric oxide modulates fracture healing,” Journal of Bone and Mineral Research: the Official Journal of the American Society for Bone and Mineral Research, vol. 15, pp. 342–351, 2000.

[50] J. L. Jewell, Y. C. Kim, R. C. Russell et al., “Metabolism. Differential regulation of mTORC1 by leucine and glutamine,” Science, vol. 347, pp. 194–198, 2015.

[51] X. Cai, C. Zhu, Y. Xu et al., “Alpha-ketoglutarate promotes skeletal muscle hypertrophy and protein synthesis through Akt/mTOR signaling pathways,” Scientific Reports, vol. 6, p. 26802, 2016.

[52] B. Icli, W. Wu, D. Ozdemir et al., “MicroRNA-615-5p regulates angiogenesis and tissue repair by targeting AKT/eNOS (protein kinase B/endothelial nitric oxide synthase) signaling in endothelial cells,” Arteriosclerosis, Thrombosis, and Vascular Biology, vol. 39, pp. 1458–1474, 2019.

[53] S. Hazarika, A. O. Dokun, Y. Li, A. S. Popel, C. D. Kontos, and B. H. Annex, “Impaired angiogenesis after hindlimb ischemia in type 2 diabetes mellitus: differential regulation of vascular endothelial growth factor receptor 1 and soluble vascular endothelial growth factor receptor 1,” Circulation Research, vol. 101, pp. 948–956, 2007.

[54] R. M. Bell and D. M. Yellon, “Bradykinin limits infarction when administered as an adjunct to reperfusion in mouse heart: the role of PI3K, Akt and eNOS,” Journal of Molecular and Cellular Cardiology, vol. 35, pp. 185–193, 2003.
[55] R. Yao and G. M. Cooper, “Requirement for phosphatidylinositol-3 kinase in the prevention of apoptosis by nerve growth factor,” Science, vol. 267, pp. 2003–2006, 1995.
[56] T. F. Franke, S. I. Yang, T. O. Chan et al., “The protein kinase encoded by the Akt proto-oncogene is a target of the PDGF-activated phosphatidylinositol 3-kinase,” Cell, vol. 81, pp. 727–736, 1995.

Capítulo 6

PI3K/AKT signaling drives titanium-induced angiogenic stimulus

Bruna Rodrigues Martins[1], Thaís Silva Pinto[1], Célio Junior da Costa Fernandes[1], Fábio Bezerra[1], Willian Fernando Zambuzzi[1]

[1]Institute of Biosciences of Botucatu, Department of Chemical and Biological Sciences, UNESP – São Paulo State University, Botucatu, São Paulo, Brazil

ARTIGO PUBLICADO:

Martins BR, Pinto TS, da Costa Fernandes CJ, Bezerra F, Zambuzzi WF. PI3K/AKT signaling drives titanium-induced angiogenic stimulus. J Mater Sci Mater Med. 2021 Jan 27;32(1):18. doi: 10.1007/s10856-020-06473-8. PMID: 33506378; PMCID: PMC7840643.

Abstract

Although osseointegration and clinical success of titanium (Ti)-implanted materials depend on neovascularization in the reactional peri-implant tissue, very little has been achieved considering the Ti-molecules release on the behavior of endothelial cells. To address this issue, we challenged endothelial cells (HUVECs) with Ti-enriched medium obtained from two types of commercial titanium surfaces [presenting or not dual-acid etching (DAE)] up to 72 h to allow molecular machinery analysis. Our data show that the Ti-enriched medium provokes significant stimulus of angiogenesis-related machinery in endothelial cells by upexpressing VEGFR1, VEGFR2, VEGF, eNOS, and iNOS genes, while the PI3K/Akt signaling pathway was also significantly enhanced. As PI3K/AKT signaling was related to angiogenesis in response to vascular endothelial growth factor (VEGF), we addressed the importance of PI3K/Akt upon Ti-enriched medium responses by concomitantly treating the cells with wortmannin, a well-known PI3K inhibitor. Wortmannin suppressed the angiogenic factors, because VEGF, VEGFR1, and eNOS genes were downregulated in those cells, highlighting the importance of PI3K/AKT signaling on driving angiogenic phenotype and angiogenesis performance within the peri-implant tissue reaction. In conjunction, these data reinforce that titanium-implantable devices modify the metabolism of surrounding cells, such as endothelial cells, probably coupling osteogenesis and angiogenesis processes in peri-implant tissue and then contributing to successfully osseointegration of biomedical titanium-based devices.

1 Introduction

Titanium-based implants are widely used in dentistry and medical fields contributing to therapies for edentulism and stabilization of bone fractures, respectively, mainly due to their properties including mechanical strength, high corrosion resistance, low toxicity, and adequate biocompatibility acceptance [1–3]. However, current studies have shown that titanium alloys are not inert as once believed, and they dynamically release particles and molecules to their embedding microenvironment affecting the surrounding cell behavior, as osteoblast-like cells, and the vascular endothelium that irrigates the injured tissue and then affects the endothelial cells (ECs) [4, 5]. Because of that and especially considering vascularization, which is an important step to regenerate the tissue surrounding the implants, studies are necessary to address the effect of titanium on ECs. For the biocompatibility and performance of biomaterials, some properties of the biomaterial surfaces should be considered critical issues that trigger signals of host tissue interactions [6]. As previously mentioned, adequate vascularization is required for successful tissue regeneration. Osseointegration is an important process that occurs in the appositional interface between tissue and biomaterial, in which an orchestrated action of bone formation and bone resorption helps to maintain the health of neoformed bone. To improve the osseointegration, reducing patient recuperation time and decreasing implant-associated complications, several modifications on biomaterial surfaces have been widely proposed, such as nanotopographical and acid etching [7, 8]. These physicochemical properties require more investigation about their effects on biological performance for full comprehension of the mechanism underlying wound healing after an implant is introduced [1].

To better address this issue, our group has investigated the interaction between the biomaterial and the host tissue in a direct [9] and indirect way [10], presenting specific signaling cascades triggered by this interface. Although titanium has been considered for decades a resistant and inert material, it can release molecules triggering dynamic responses in its microenvironment and surrounding tissues [9], and it is reasonable to hypothesize that it could compromise the role of blood vessels during bone growth by impairing EC phenotypes. Thus, better understanding the properties of titanium-enriched medium on angiogenesis in wound healing and osseointegration process is urgently required [11, 12]. As important members within the angiogenesis process, EC is housed in the lumen of the vessel, is constantly exposed to the blood flow forces, regulates the blood supplement to tissue, and is crucial in the angiogenesis process [13]. The formation

of new blood vessel supports new bone formation by transporting fundamentals constituents, such as nutrients, regulatory factors, oxygen, and osteoprogenitor cells [12]. Some authors have already reported coupling angiogenesis with osteogenesis, which are both important and dynamic processes to drive bone growth and remodeling during wound healing [14]. In bone development and healing, the angiogenesis and osteogenesis are coupled processes, through complex intercellular signaling, that also exists in the osseointegration and biomedical devices, to ensure an appositional bone development on the implanted device [15]. First, some growth factors are released by extravasate platelets from injured vessels on the alveolar bone site, such as PDGF (platelet-derived growth factor), TGF-β (transforming growth factor beta), FGF (fibroblast growth factor), and VEGF (vascular endothelial growth factor). Among them, VEGF is one of the main factors responsible for angiogenesis promotion and is crucial to osteogenesis [16].

Considering the pivotal role of ECs in wound healing [17], their biological responses to different biomaterials must be investigated. Thus, this study aims to evaluate the behavior of human umbilical vein endothelial cell (HUVEC) exposed to a titanium-enriched medium by exploring molecular approaches focusing on comprehending intracellular pathways involved with angiogenesis and cell survival, and proliferation signaling. The cascade of events for wound healing is complex and involves highly regulated processes, such as angiogenesis. The comprehension of these processes at the cellular and molecular level is far from complete [18]. In this context, genes such as VEGF and its receptors, VEGFR1 and VEGFR2, are relevant as they are closely related to the angiogenesis process and are required for tissue wound healing [19]. Downstream to activate receptor tyrosine kinases, protein kinase B (PKB or Akt) is a multifaceted protein and plays an important role in cell metabolism, growth, proliferation, and survival. Its activation is controlled by a multi-step process, mainly involving phosphoinositide-3-kinase (PI3K) [20–22].

Specifically, we evaluated whether the Ti-enriched medium was able to modulate EC performance. Summarizing, our data show that the Ti-enriched medium requires an upmodulation of PI3K/AKT signaling in ECs to maintain their angiogenic phenotype.

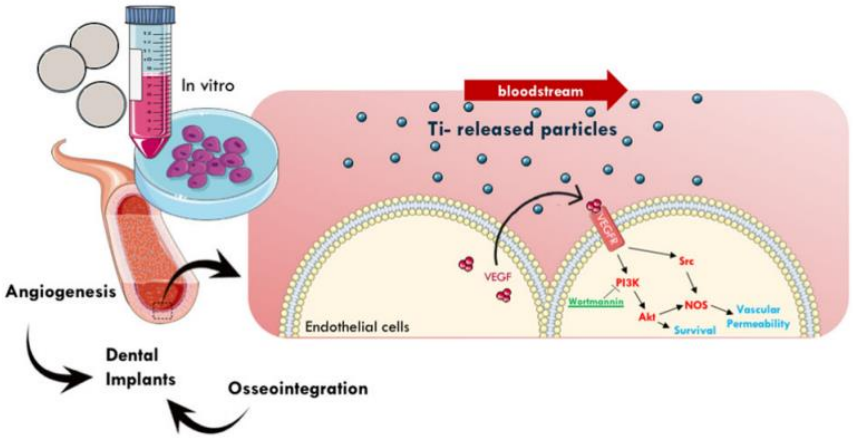

Graphical Abstract

2 Materials and methods

2.1 Reagents, TiO_2 alloys, antibodies, and primers

Two different titanium surfaces (discs) were investigated in this study, distinguished by the surface properties, as follows: Machined (Wo/DAE), and Dual Acid-Etched (W/ DAE). The metallic TiO_2-based alloys were generously donated by the S.I.N. (São Paulo, SP, Brazil). The cell culture flasks were purchased from TPP (Trasadingen, Switzerland), and the cell culture reagents from Nutricell (Campinas, SP, Brazil). Ripa buffer (R0278), Phosphatase inhibitor cocktail 2 (P5726), and bovine serum albumin (A7906) were purchased from Sigma Chemical Co. (St. Louis, MO, USA). Gotaq qPCR master mix (A6002) was purchased from PROMEGA (Madison, WI, USA). The following antibodies were purchased from Cell Signaling (Danvers, MA, USA): Akt Antibody (4691P, 60 kDa); PhosphoAkt (S473) Antibody (4060P, 60 kDa); Anti-Rabbit IgG (7074).

2.2 Cell culture and PI3K inhibition

HUVECs were used in this study. ECs were cultivated in RPMI medium (Nutricell, Campinas, SP, Brazil) supplemented with penicillin (100 U/ml), streptomycin (100 mg/ ml), and 10% fetal bovine serum (FBS), and maintained at 37 °C and 5% CO_2. HUVECs were cultivated in culture flasks until proper amount and then were seeded in traditional culture dishes until adhesion, when the culture medium was exchanged for the different medium treatments as described below, for 72 h. To investigate the role of PI3K

in the signaling behavior of ECs, we again carried out the treatment as described, but using a culture medium containing Wortmannin (5 μM), a PI3K inhibitor.

2.3 TiO_2-enriched medium obtaining

To prepare the TiO_2-enriched medium, dual-acid-etching (DAE) treating surface (named W/DAE) and the machined surfaces (named Wo/DAE), the experimental alloys (n = 6) were incubated in cell culture media (RPMI) without FBS up to 24 h at 37 °C, 5% CO_2, and 95% humidity [0.2 g/mL (w/v); ISO 10993:2016]. The TiO_2-enriched medium contains molecules released from those metallic alloys and might affect the biology of ECs. To test this hypothesis, the TiO_2-enriched medium was further used to treat the ECs.

2.4 Total mRNA isolation and RT-qPCR analysis

After treatment, the cells were harvested and total mRNA isolated using Ambion TRIzol Reagent (Life Sciences, Thermo Fisher Scientific Inc., Waltham, MA, USA) and treated with DNase I (Invitrogen, Carlsbad, CA, USA). Complementary DNA (cDNA) synthesis was performed with High Capacity cDNA Reverse Transcription Kit (Applied Biosystems, Foster City, CA, USA) according to the manufacturer's instructions. Real-Time qPCR was carried out in 10 μl, containing PowerUpTM SYBRTM Green Master Mix 2× (5 μl; Applied Biosystems, Foster City, CA, USA), 0.4 μM of each primer, 50 ng of cDNA, and nuclease-free H_2O. Results were expressed as relative amounts of the transcripts using glyceraldehyde 3-phosphate dehydrogenase (GAPDH) and 18S as reference genes (housekeeping gene), using the cycle threshold (Ct) method. Primers and run details are described in Table 1.

Table 1 Expression primers sequences and qPCR cycle conditions

Gene	Primer	5′-3′ Sequence	Work condition
AKT	Forward 1	CAGCGCGGCCCGAAGGAC	95 °C—3 s; 55 °C—8 s; 72 °C—20 s
	Forward 2	GGACTCCCGTTTGCGCCAGT	
	Reverse	GACGCTCACGCGCTCCTCTC	
VEGFR1	Forward	CAGGCCCAGTTTCTGCCATT	95 °C—3 s; 55 °C—8 s; 72 °C—20 s
	Reverse	TTCCAGCTCAGCGTGGTCGTA	
VEGFR2	Forward	CCAGCAAAAGCAGGGAGTCTGT	95 °C—3 s; 55 °C—8 s; 72 °C—20 s
	Reverse	TGTCTGTGTCATCGGAGTGATATCC	
VEGF	Forward	TGCAGATTATGCGGATCAAACC	95 °C—3 s; 55 °C—8 s; 72 °C—20 s
	Reverse	TGCATTCACATTTGTTGTGCTGTAG	
INOS	Forward	TGGATGCAACCCCATTGTC	95 °C—3 s; 55 °C—8 s; 72 °C—20 s
	Reverse	CCCGCTGCCCCAGTTT	
ENOS	Forward	TATTTGATGCTCGGGACTGC	95 °C—3 s; 55 °C—8 s; 72 °C—20 s
	Reverse	AAGATTGCCTCGGTTTGTTG	
GAPDH	Forward	AGGCCGGTGCTGAGTATGTC	95 °C—3 s; 55 °C—8 s; 72 °C—20 s
	Reverse	TGCCTGCTTC ACCACCTTCT	
18S	Forward	CGGACAGGATTGACAGATTGATAGC	95 °C—3 s; 55 °C—8 s; 72 °C—20 s
	Reverse	TGCCAGAGTCTCGTTCGTTATCG	

2.5 Western blotting

After 72 h of treatment with TiO_2-enriched medium, the challenged HUVECs were washed in ice-cold PBS and protein extracts were obtained using a RIPA lysis buffer (Sigma Aldrich, St. Louis, Missouri, USA) and supplemented with a cocktail of antiproteases and antiphosphatases (Sigma Aldrich, St. Louis, MO, USA) up to 1 h on ice. Protein extracts were cleared by centrifugation 14,000 rpm for 15 min at 4 °C. The precipitate was then resuspended in 100 µL of RIPA lysis buffer (Sigma Aldrich, St. Louis, Missouri, USA). The protein extracts were clarified and the protein concentration determined by the Lowry method [23]. Protein extracts were resolved by SDS-PAGE and later transferred to PVDF membranes (Bio-Rad, Hercules, CA, USA). An equal volume of gel loading buffer [100 mmol L−1 Tris–HCl (pH 6.8), 200 mmol L^{-1} dithiothreitol, 4% SDS, 0.1% bromophenol blue, and 20% glycerol] was added to the samples and boiled for 5 min at 95 °C. Aliquots of the samples (75–100 µg/lane) were resolved into SDS-PAGE (8, 10, or 12% gels) and later transferred to PVDF membranes (Millipore, USA), which were blocked with 5% nonfat dry milk dissolved in trisbuffered saline (TBS)-Tween-20 (0.05%) and then incubated overnight with the appropriate primary antibody (1:1000) at 4 °C. After 1×-washing in TBS–Tween-20 (0.05%) and 2×-washing in TBS, the membranes were incubated with horseradish peroxidase-conjugated secondary anti-rabbit or anti-mouse IgGs antibodies (1:2000), diluted in blocking buffer for 1 h. Immunoreactive bands were detected using Enhance Chemiluminescence (ECL, Pierce, USA).

2.6 Statistical analyses

Results were represented as mean ± standard deviation (SD). The samples assumed a normal distribution with $p < 0.05$ considered statistically significant and $p < 0.001$ considered highly significant. In the experiment with >2 groups, we used one-way ANOVA with multiple comparisons, to compare all pairs of groups. In this case, the significance level was considered when alpha = 0.05 (95% confidence interval). The software used was GraphPad Prism 7 (GraphPad Software, USA).

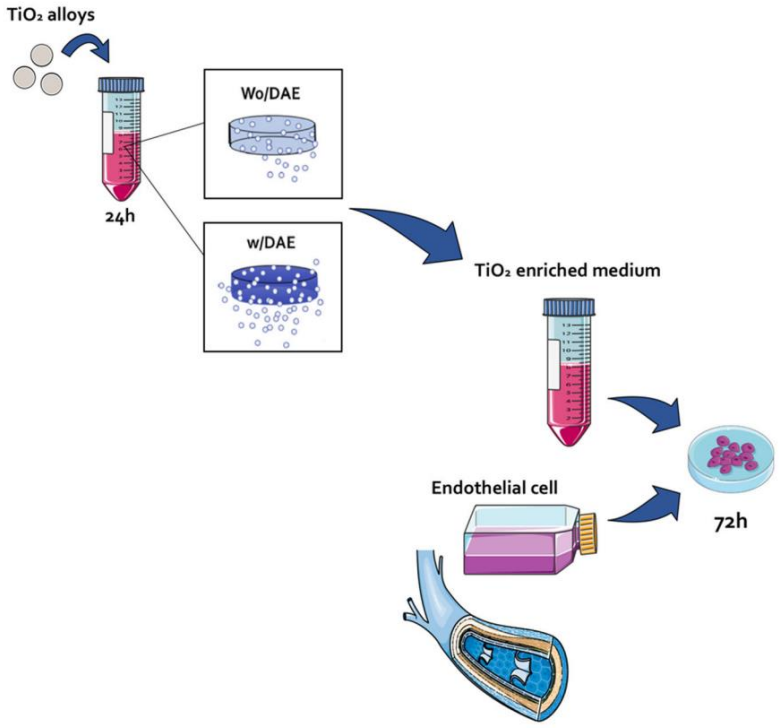

Fig. 1 Experimental design of this study. To evaluate the biological response of endothelial cells to TiO_2, the Ti-enriched medium was obtained by incubating Ti-based materials in the cell culture medium (FBS free), as recommended by ISO 10993:2016 (part 5). Thereafter, the Ti-enriched medium was used to challenge endothelial cells up to 72 h, when the samples were collected for the analysis. The main focus here was to evaluate whether there is some association of survival signaling an angiogenic stimulus of titanium, which could better support comprehension about their biocompatibility and dynamic relationship with the surrounding tissue.

3 Results and discussion

The biological responses of tissue surrounding the implanted metallic biomaterials require a well-coordinated cascade of events involving a coupled network between undifferentiated cells and angiocrine mediators released by ECs. It is known that the correct coupling between endothelium and bone guarantees proper cell differentiation and tissue regeneration, resulting in successful osseointegration. Although endothelium is not properly in close contact with the implanted materials, we have recently reported that titanium-based devices release a considerable amount of titanium and this interferes in cell metabolism [9, 10, 24– 26], which could affect cells away. In this study, to evaluate whether the surface particles released from Ti affect the metabolism of ECs, we previously prepared a Ti-enriched medium and used it to further challenge HUVEC cells up to 72 h (Fig. 1).

We suggest Ti-enriched medium mimics the Ti released when the devices are implanted in a host, covering an indirect and alternative model to study the effect of Ti on eukaryotic and adherent cells, as has been suggested previously. The performance of ECs was estimated by evaluating widely accepted angiogenic biomarkers at the mRNA levels, such as: VEGFR1, VEGFR2, VEGF, eNOS, and iNOS. Within the repertoire of cascading events involved in the biological response to biomaterials, it is expected that viable cells interacting with biomaterials surfaces drive their biocompatibility [27, 28].

The surface modifications, such as DAE of titanium implants, have produced a positive effect on osseointegration in newly formed and native bone [29], triggering different signals in osteoblast-like cells [10], and our data show that these surfaces also trigger distinct responses in ECs. Experimentally, we proposed intracellular signaling pathways to evaluate cell viability mainly by considering PI3K/PKB/Akt upstream stimulus culminating in gene expression related to cell proliferation and survival [30, 31]. In addition, as these protein activities are regulated by phosphorylation, the effectivity of this signaling can be measured by the specific phosphorylation profile [32]. In turn, Akt is a serine/threonine protein kinase that is activated by a number of growth factors and cytokines in an upstream phosphatidylinositol-3 kinase-dependent manner. Here, the PI3K/Akt signaling was evaluated by measuring the phosphorylation profile of Akt at S473. Phosphorylation of Akt at S473 guarantees its activity, leading to additional substrate-specific phosphorylation events in both the cytoplasm and nucleus, including inhibitory phosphorylation of the pro-apoptotic FOXO proteins [33, 34].

Figure 2 shows that the phosphorylation of PKB/Akt was significantly increased in response to Ti-enriched medium, in both evaluated surfaces: w/DAE and wo/DAE. Importantly, our data demonstrated an upexpression of mRNA of Akt in ECs responding to the Ti-Wo/DAE-enriched medium (Fig. 2a). Variations in titanium surfaces can modulate the PI3K/ Akt pathway differently in osteoblast-like cells [35], and we observed that distinct titanium surfaces developed different modulations in this pathway in ECs, seen in the changes to the gene expression and protein AKT phosphorylation pattern. Altogether, these data strongly suggest the importance of this signaling in challenged ECs, maybe modulating their viability and phenotype, as fully active PKB/Akt mediates numerous cellular functions including angiogenesis, metabolism, growth, proliferation, survival, protein synthesis, and transcription [33, 36].

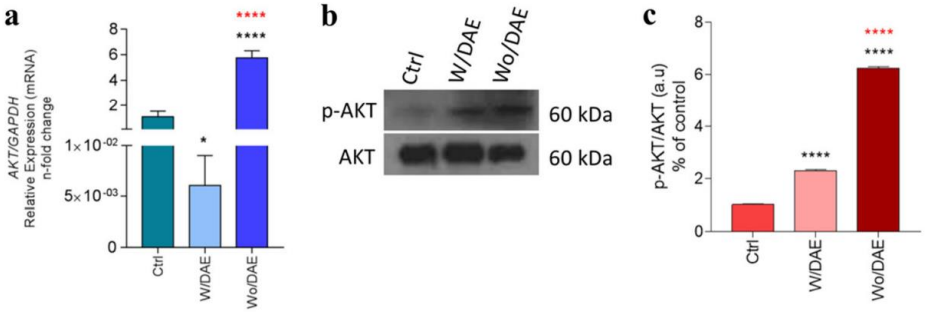

Fig. 2 Survival signaling was evaluated by measuring the phosphorylation profile of AKT. To understand whether survival signaling was required by endothelial cells responding to Ti-enriched medium (72 h), the cells were subjected to Ti-enriched medium obtained by incubating two different conditions of titanium discs [double acid-etching (DAE) treatment (W/DAE) and without DAE (Wo/DAE)] into cell culture medium up to 24 h. After subjecting the cells up to 72 h, the samples were obtained to allow the gene expression of AKT (a) and protein performance (b, c) by evaluating AKT phosphorylation. GADPH was considered a housekeeping gene. Statistics: the value obtained to Ctrl was considered 1, and the relative values obtained to W/DAE or Wo/ DAE are shown in fold-changes. One-way ANOVA with multiple comparisons were applied to compare all pairs of groups. Differences were considered significant when *p = 0.04 and ****p < 0.0001 when compared with the Ctrl; and ****p < 0.0001 when compared with W/ DAE group.

Later, the repertoire of genes involved with angiogenic phenotype was also investigated, and Fig. 3 provides a panorama where Ti medium enriched by Wo/DAE condition requires a significant activity of those genes, such as VEGFR1 (Fig. 3a), VEGFR2 (Fig. 3b), VEGF (Fig. 3c), iNOS (Fig. 3d), and eNOS (Fig. 3e). Importantly,

VEGFR2 (Fig. 3b) and VEGF (Fig. 3c) genes are stimulated by both surfaces investigated here (W/DAE and Wo/DA).

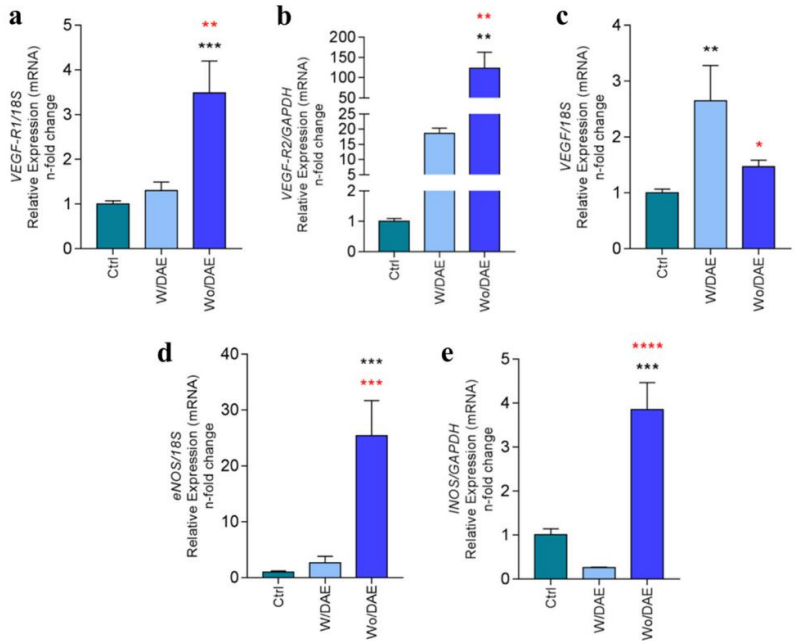

Fig. 3 Angiogenic stimulus of titanium (Ti) on endothelial cells. The samples were collected respecting the already described methodology to allow qPCR technology performance. To address the angiocrine effect of Ti on endothelial cells, we investigated VEGFR1 (a), VEGFR2 (b), VEGF (c), eNOS (d), and iNOS (e) genes. The GADPH gene was considered the housekeeping gene and used to normalize the values. Statistics: One-way ANOVA with multiple comparisons was used to compare all pairs of groups, and the differences were considered significant when a VEGFR1 ***p = 0.0009 and **p = 0.0019; b VEGFR2 **p = 0.0014 and **p = 0.0032; c VEGF **p = 0.004 and *p = 0.02; d eNOS ***p = 0.0006 and ***p = 0.0008; and e INOS ***p = 0.0002 and ****p < 0.0001. Black (*) when compared with Ctrl and red (*) when compared with W/DAE.

This different biological consequences between the surfaces can be explained by the concentration of titanium released into the medium. To date, VEGF has long been recognized as the key regulator of vascular development and function in health [37]. In addition, Kitamura et al. [38] demonstrated that the Akt/ Girdin signaling pathway is essential in VEGF-mediated postneonatal angiogenesis. Nonetheless, they reveal that Girdin knockdown severely impairs cell migration and tube formation by HUVECs, and that Girdin−/− mice display significant defects in postnatal microvascular remodeling in the retina and the sprouting of vessels from aortae [38]. In conjunction, it seems acceptable to suggest that Ti released by implantable devices could also dynamically modulate the phenotype of ECs, which explains, in association with their effect on osteoblasts [9, 10, 25, 26, 39–42], the success of titanium in implantology applications,

since angiogenic factors by ECs are required to drive angiogenesis that modulates the traffic of nutrients, growth factors, and undifferentiated cells to the site where the tissue is regenerate.

We are convinced there is a coupling of mechanisms considering that cells respond to titanium directly (mainly osteogenic cells adhering on the surfaces directly) and indirectly (undifferentiated cells and ECs/angiogenesis), where these devices coordinate the surrounding microenvironment and drive the osseointegration-related mechanism. We noticed a potential involvement of survival signaling in modulating angiogenic stimulus in response to the Ti-enriched medium since there was a probable correlation between PKB/AKT performance and genes related to angiogenic signals, mainly in the Wo/DAE group (see Figs. 2 and 3). Finally, to test the hypothesis that PI3K/AKT drives angiogenic factors in response to the Ti-enriched medium, we subjected the cells to a chemical inhibition of PI3K using well-known Wortmannin, as it is widely proposed by others [43], and further investigated the behavior of VEGF (Fig. 4a), VEGFR1 (Fig. 4b), and eNOS (Fig. 4c) genes.

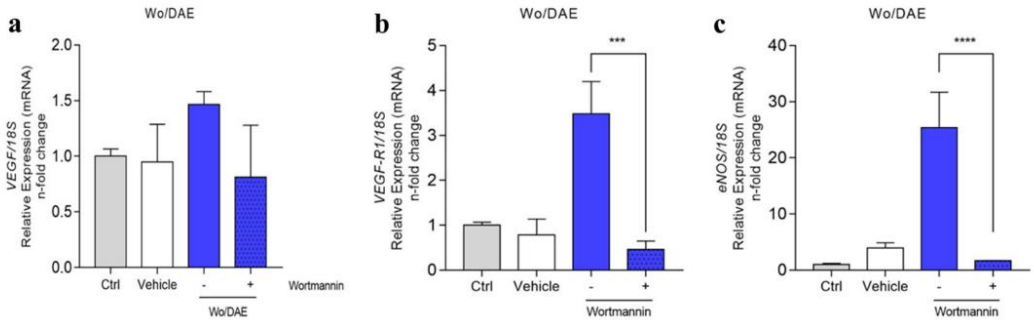

Fig. 4 Wortmannin targeting PI3K suppresses the angiogenic stimulus of titanium (Ti). The samples were collected respecting the already described methodology to allow qPCR technology performance. To address whether PI3K/AKT is involved in endothelial responding to the Ti-enriched medium, we reanalyzed the already known performance of genes, as was shown in Fig. 3, but now treated with wortmannin, a specific chemical inhibitor of PI3K (upstream to AKT). Thus, the suppression of the angiogenic stimulus by Ti is clear since VEGF (a), VEGFR1 (b), and eNOS (c) genes were significantly down expressed when PI3K was inhibited. The 18S gene was considered the housekeeping gene and used to normalize the values. Statistics: The statistical analysis test used was one-way ANOVA with multiple comparisons to compare all pairs of groups, and the figure specifies the differences between the absence (−) and the presence (+) of the Wortmannin. Differences were considered significant when b VEGFR1 ***$p = 0.0002$ and c eNOS ****$p < 0.0001$.

Our data clearly shows that wortmannin suppresses the angiogenic factors because all of these three genes were significantly downregulated (Fig. 4). Altogether these data validate our hypothesis that PI3K/Akt signaling is involved in angiogenic signals triggered by ti-enriched medium. Mechanistically, VEGF induces nitric oxide production and release by nitric oxide synthase (NOS) in isolated vessels and in cultured ECs [44–46], which is attenuated by PI3K inhibitors [47]. Subsequently, it was demonstrated that VEGF stimulates PKB/Akt-mediated eNOS phosphorylation at Ser1177 [36, 48, 49].

Thus, we reasonably suggest that PI3K/AKT signaling participates in the angiogenic phenotype of ECs responding to the Ti-enriched medium. We previously reported that the major mechanotransduction pathway activates PI3K, which plays a pivotal role in guaranteeing EC phenotype and vascular homeostasis [43], and Ti-release displays a very similar effect, mainly in response to Wo/DAE. Peri-implant healing seems to recapitulate conventional regenerative processes involving a coupling of biological systems, which requires a cascade of carefully and precisely regulated steps and events that correlate with the appearance of various cell types during distinct stages of healing [50–54]. Although titanium has been considered a physiologically inert material, we have demonstrated Ti develops dynamic interaction with the microenvironment by releasing particles and active molecules affecting osteoblast biology by positively coordinating proliferative and differentiation mechanisms, and the properties of the surfaces seems to influence this response [16].

These modifications on titanium surfaces aim to optimize the wound healing to reduce the clinical time for patient recovering and has been shown to trigger changes in osteoblast metabolism [24]. A previously published study indicated involvement of a set of genes related with osteogenesis in response to dual-acid-etched surface of titanium in human mesenchymal stromal cells [55]. The involvement of ECs has a pivotal role during crucial phases of wound healing. Their importance on osseointegration success has raised some questions mainly about the response to changes in titanium surfaces [6], and our data address this issue and provides further comprehension. This study reinforces that the titanium-released particles modify differentially the EC behavior emphasizing the importance of survival and angiogenic related intracellular signaling in these responses by upactivating PI3K/AKT signaling, mainly in response to Wo/DAE. In conjunction, these data support that titanium-implantable devices interact dynamically with the host surrounding tissues modulating the activity of osteogenic and ECs, maybe coupling

osteogenesis and angiogenesis processes in peri-implant tissue and then contributing with their successful osseointegration.

Acknowledgements

The authors would like to thank the FAPESP (2014/22689-3 and 2019/09140-6) and CNPq for financial support.

Compliance with ethical standards

Conflict of interest The authors declare that they have no conflict of interest.

Publisher's note Springer Nature remains neutral with regard to jurisdictional claims in published maps and institutional affiliations.

References

1. Coelho PG, Granjeiro JM, Romanos GE, Suzuki M, Silva NRF, Cardaropoli G, et al. Basic research methods and current trends of dental implant surfaces. J Biomed Mater Res B Appl Biomater. 2009;88:579–96. https://doi.org/10.1002/jbm.b.31264
2. Bonfante EA, Coelho PG. A critical perspective on mechanical testing of implants and prostheses. Adv Dent Res. 2016;28:18–27. https://doi.org/10.1177/0022034515624445
3. Dohan Ehrenfest DM, Coelho PG, Kang B-S, Sul Y-T, Albrektsson T. Classification of osseointegrated implant surfaces: materials, chemistry and topography. Trends Biotechnol. 2010;28:198–206. https://doi.org/10.1016/j.tibtech.2009.12.003

4. Raines AL, Berger MB, Patel N, Hyzy SL, Boyan BD, Schwartz Z. VEGF-A regulates angiogenesis during osseointegration of Ti implants via paracrine/autocrine regulation of osteoblast response to hierarchical microstructure of the surface. J Biomed Mater Res A. 2019;107:423–33. https://doi.org/10.1002/jbm.a.36559
5. Chen W, Xu K, Tao B, Dai L, Yu Y, Mu C, et al. Multilayered coating of titanium implants promotes coupled osteogenesis and angiogenesis in vitro and in vivo. Acta Biomater. 2018;74:489–504. https://doi.org/10.1016/j.actbio.2018.04.043
6. An N, Schedle A, Wieland M, Andrukhov O, Matejka M, RauschFan X. Proliferation, behavior, and cytokine gene expression of human umbilical vascular endothelial cells in response to different titanium surfaces. J Biomed Mater Res - Part A. 2010;93:364–72. https://doi.org/10.1002/jbm.a.32539
7. Ferguson SJ, Broggini N, Wieland M, de Wild M, Rupp F, GeisGerstorfer J, et al. Biomechanical evaluation of the interfacial strength of a chemically modified sandblasted and acid-etched titanium surface. J Biomed Mater Res A. 2006;78:291–7. https:// doi.org/10.1002/jbm.a.30678
8. Cochran DL, Buser D, Ten Bruggenkate CM, Weingart D, Taylor TM, Bernard JP, et al. The use of reduced healing times on ITI® implants with a sandblasted and acid-etched (SLA) surface: Early results from clinical trials on ITI® SLA implants. Clin Oral Implants Res. 2002;13:144–53. https://doi.org/10.1034/j.1600-0501.2002.130204.x
9. Rossi MC, Bezerra FJB, Silva RA, Crulhas BP, Fernandes CJC, Nascimento AS, et al. Titanium-released from dental implant enhances pre-osteoblast adhesion by ROS modulating crucial intracellular pathways. J Biomed Mater Res A. 2017;105:2968–76. https://doi.org/10.1002/jbm.a.36150
10. da Costa Fernandes CJ, Bezerra FJB, de Campos Souza B, Campos MA, Zambuzzi WF. Titanium-enriched medium drives low profile of ECM remodeling as a pre-requisite to pre-osteoblast viability and proliferative phenotype. J Trace Elem Med Biol. 2018;50:339–46. https://doi.org/10.1016/j.jtemb.2018.07.015
11. Masaki C, Schneider GB, Zaharias R, Seabold D, Stanford C. Effects of implant surface microtopography on osteoblast gene expression. Clin Oral Implants Res. 2005;16:650–6. https://doi. org/10.1111/j.1600-0501.2005.01170.x
12. Shi B, Andrukhov O, Berner S, Schedle A, Rausch-Fan X. The angiogenic behaviors of human umbilical vein endothelial cells (HUVEC) in co-culture with osteoblast-like cells (MG-63) on different titanium surfaces. Dent Mater. 2014;30:839–47. https:// doi.org/10.1016/j.dental.2014.05.005
13. Ando J, Yamamoto K. Effects of shear stress and stretch on endothelial function. Antioxid Redox Signal. 2011;15:1389–403. https://doi.org/10.1089/ars.2010.3361
14. Ramasamy SK, Kusumbe AP, Schiller M, Zeuschner D, Bixel MG, Milia C, et al. Blood flow controls bone vascular function and osteogenesis. Nat Commun. 2016;7:1–13. https://doi.org/10. 1038/ncomms13601
15. de Oliveira PGFP, Bonfante EA, Bergamo ETP, de Souza SLS, Riella L, Torroni A, et al. Obesity/metabolic syndrome and diabetes mellitus on peri-implantitis. Trends Endocrinol. Metab. (2020). https://doi.org/10.1016/j.tem.2020.05.005.

16. Smeets R, Stadlinger B, Schwarz F, Beck-Broichsitter B, Jung O, Precht C, et al. Impact of dental implant surface modifications on osseointegration. Biomed Res Int. 2016;2016:6285620 https://doi. org/10.1155/2016/6285620
17. Tonnesen MG, Feng X, Clark RA. Angiogenesis in wound healing. J Investig Dermatol Symp Proc. 2000;5:40–46. https:// doi.org/10.1046/j.1087-0024.2000.00014.x
18. de AC, Gonzalez O, Costa TF, de Z, Andrade A, Medrado ARAP. Wound healing—a literature review. Bras Dermatol. 2016;91:614–20. https://doi.org/10.1590/abd1806-4841. 20164741
19. Shibuya M. Vascular endothelial growth factor (VEGF) and its receptor (VEGFR) signaling in angiogenesis: a crucial target for anti- and pro-angiogenic therapies. Genes Cancer. 2011;2:1097–105. https://doi.org/10.1177/1947601911423031
20. Alessi DR. Discovery of PDK1, one of the missing links in insulin signal transduction. Colworth Medal Lecture. Biochem Soc Trans. 2001;29:1–14. https://doi.org/10.1042/0300-5127:0290001
21. Alessi DR, James SR, Downes CP, Holmes AB, Gaffney PR, Reese CB, et al. Characterization of a 3-phosphoinositidedependent protein kinase which phosphorylates and activates protein kinase Balpha. Curr Biol. 1997;7:261–9. https://doi.org/ 10.1016/s0960-9822(06)00122-9
22. Brazil DP, Hemmings BA. Ten years of protein kinase B signalling: a hard Akt to follow. Trends Biochem Sci. 2001;26:657–64. https://doi.org/10.1016/s0968-0004(01)01958-2
23. Hartree EF. Determination of protein: a modification of the Lowry method that gives a linear photometric response. Anal Biochem. 1972;48:422–7. https://doi.org/10.1016/0003-2697(72)90094-2
24. Zambuzzi WF, Bonfante EA, Jimbo R, Hayashi M, Andersson M, Alves G, et al. Nanometer scale titanium surface texturing are detected by signaling pathways involving transient FAK and Src activations. PLoS ONE. 2014;9:e95662 https://doi.org/10.1371/ journal.pone.0095662
25. Bezerra F, Ferreira MR, Fontes GN, da Costa Fernandes CJ, Andia DC, Cruz NC, et al. Nano hydroxyapatite-blasted titanium surface affects pre-osteoblast morphology by modulating critical intracellular pathways. Biotechnol Bioeng. 2017;114:1888–98. https://doi.org/10.1002/bit.26310
26. Fernandes CJC, Bezerra F, Ferreira MR, Andrade AFC, Pinto TS, Zambuzzi WF. Nano hydroxyapatite-blasted titanium surface creates a biointerface able to govern Src-dependent osteoblast metabolism as prerequisite to ECM remodeling. Colloids Surf B Biointerfaces. 2018;163:321–8. https://doi.org/10.1016/j.colsurfb. 2017.12.049
27. Gemini-Piperni S, Takamori ER, Sartoretto SC, Paiva KBS, Granjeiro JM, de Oliveira RC, et al. Cellular behavior as a dynamic field for exploring bone bioengineering: a closer look at cell-biomaterial interface. Arch Biochem Biophys. 2014;561:88–98. https://doi.org/10.1016/j.abb.2014.06.019

28. Zambuzzi WF, Coelho PG, Alves GG, Granjeiro JM. Intracellular signal transduction as a factor in the development of “smart” biomaterials for bone tissue engineering. Biotechnol Bioeng. 2011;108:1246–50. https://doi.org/10.1002/bit.23117
29. Qahash M, Hardwick WR, Rohrer MD, Wozney JM, Wikesjö UME. Surface-etching enhances titanium implant osseointegration in newly formed (rhBMP-2-induced) and native bone. Int J Oral Maxillofac Implants. 2007;22:472–7.
30. Sewduth R, Santoro MM. “Decoding” angiogenesis: new facets controlling endothelial cell behavior. Front Physiol. 2016;7:306 https://doi.org/10.3389/fphys.2016.00306
31. Eichmann A, Simons M. VEGF signaling inside vascular endothelial cells and beyond. Curr Opin Cell Biol. 2012;24:188–93. https://doi.org/10.1016/j.ceb.2012.02.002
32. Yudushkin I. Control of Akt activity and substrate phosphorylation in cells. IUBMB Life. 2020. https://doi.org/10.1002/iub.2264
33. BA Hemmings, DF Restuccia, The PI3K-PKB/Akt pathway, Cold Spring Harb. Perspect. Biol. 2015;7. https://doi.org/10.1101/ cshperspect.a026609.
34. Guertin DA, Stevens DM, Thoreen CC, Burds AA, Kalaany NY, Moffat J, et al. Ablation in mice of the mTORC components raptor, rictor, or mLST8 reveals that mTORC2 is required for signaling to Akt-FOXO and PKCalpha, but not S6K1. Dev Cell. 2006;11:859–71. https://doi.org/10.1016/j.devcel.2006.10.007
35. Gu Y-X, Du J, Si M-S, Mo J-J, Qiao S-C, Lai H-C. The roles of PI3K/Akt signaling pathway in regulating MC3T3-E1 preosteoblast proliferation and differentiation on SLA and SLActive titanium surfaces. J Biomed Mater Res A. 2013;101:748–54. https://doi.org/10.1002/jbm.a.34377
36. Shiojima I, Walsh K. Role of Akt signaling in vascular homeostasis and angiogenesis. Circ Res. 2002;90:1243–50. https://doi. org/10.1161/01.res.0000022200.71892.9f
37. Koch S, Claesson-Welsh L. Signal transduction by vascular endothelial growth factor receptors. Cold Spring Harb Perspect Med. 2012;2:a006502 https://doi.org/10.1101/cshperspect. a006502
38. Kitamura T, Asai N, Enomoto A, Maeda K, Kato T, Ishida M, et al. Regulation of VEGF-mediated angiogenesis by the Akt/PKB substrate Girdin. Nat Cell Biol. 2008;10:329–37. https://doi.org/ 10.1038/ncb1695
39. Gomes OP, Feltran GS, Ferreira MR, Albano CS, Zambuzzi WF, Lisboa-Filho PN. A novel BSA immobilizing manner on modified titanium surface ameliorates osteoblast performance. Colloids Surf B Biointerfaces. 2020;190:110888 https://doi.org/10.1016/j. colsurfb.2020.110888
40. da G, Feltran S, Bezerra F, da Costa Fernandes CJ, Ferreira MR, Zambuzzi WF. Differential inflammatory landscape stimulus during titanium surfaces obtained osteogenic phenotype. J Biomed Mater Res A. 2019;107:1597–604. https://doi.org/10.1002/jbm.a. 36673
41. Baroncelli M, Fuhler GM, van de Peppel J, Zambuzzi WF, van Leeuwen JP, van der Eerden BCJ, et al. Human mesenchymal stromal cells in adhesion to cell-derived extracellular matrix and titanium: Comparative kinome profile analysis. J Cell Physiol. 2019;234:2984–96. https://doi.org/10.1002/jcp.27116

42. Ribeiro AR, Oliveira F, Boldrini LC, Leite PE, Falagan-Lotsch P, Linhares ABR, et al. Micro-arc oxidation as a tool to develop multifunctional calcium-rich surfaces for dental implant applications. Mater Sci Eng C Mater Biol Appl. 2015;54:196–206. https://doi.org/10.1016/j.msec.2015.05.012
43. Gomes AM, Pinto TS, da Costa Fernandes CJ, da Silva RA, Zambuzzi WF. Wortmannin targeting phosphatidylinositol 3- kinase suppresses angiogenic factors in shear-stressed endothelial cells. J Cell Physiol. 2020;235:5256–69. https://doi.org/10.1002/ jcp.29412
44. Ku DD, Zaleski JK, Liu S, Brock TA. Vascular endothelial growth factor induces EDRF-dependent relaxation in coronary arteries. Am J Physiol. 1993;265:H586–92. https://doi.org/10. 1152/ajpheart.1993.265.2.H586
45. Yang R, Thomas GR, Bunting S, Ko A, Ferrara N, Keyt B, et al. Effects of vascular endothelial growth factor on hemodynamics and cardiac performance. J Cardiovasc Pharmacol. 1996;27:838–44. https://doi.org/10.1097/00005344-199606000- 00011
46. van der Zee R, Murohara T, Luo Z, Zollmann F, Passeri J, Lekutat C, et al. Vascular endothelial growth factor/vascular permeability factor augments nitric oxide release from quiescent rabbit and human vascular endothelium. Circulation. 1997;95:1030–7. https://doi.org/10.1161/01.cir.95.4.1030
47. Papapetropoulos A, Garcia-Cardena G, Madri JA, Sessa WC. Nitric oxide production contributes to the angiogenic properties of vascular endothelial growth factor in human endothelial cells. J Clin Investig. 1997;100:3131–9. https://doi.org/10.1172/ JCI119868
48. Fulton D, Gratton JP, McCabe TJ, Fontana J, Fujio Y, Walsh K, et al. Regulation of endothelium-derived nitric oxide production by the protein kinase Akt. Nature. 1999;399:597–601. https://doi. org/10.1038/21218
49. Dimmeler S, Fleming I, Fisslthaler B, Hermann C, Busse R, Zeiher AM. Activation of nitric oxide synthase in endothelial cells by Akt-dependent phosphorylation. Nature. 1999;399:601–5. https://doi.org/10.1038/21224
50. Okan D, Woo K, Ayello EA, Sibbald G. The role of moisture balance in wound healing. Adv Ski Wound Care. 2007;20:35–39. https://doi.org/10.1097/00129334-200701000-00013
51. Strecker-McGraw MK, Jones TR, Baer DG. Soft tissue wounds and principles of healing. Emerg Med Clin North Am. 2007;25:1–22. https://doi.org/10.1016/j.emc.2006.12.002
52. Attinger CE, Janis JE, Steinberg J, Schwartz J, Al-Attar A, Couch K. Clinical approach to wounds: debridement and wound bed preparation including the use of dressings and wound-healing adjuvants. Plast Reconstr Surg. 2006;117:72S–109S. https://doi. org/10.1097/01.prs.0000225470.42514.8f
53. Broughton G II, Janis JE, Attinger CE. Wound healing: an overview. Plast Reconstr Surg. 2006;117:1e-S–32e-S. https://doi. org/10.1097/01.prs.0000222562.60260.f9
54. Rice J. Secondary intention wound healing–pathphysiology and management. Collegian. 2000;7:40–41. https://doi.org/10.1016/ s1322-7696(08)60377-7
55. Mamalis A, Silvestros S. Modified titanium surfaces alter osteogenic differentiation. J Oral Implantol. 2013;39:591–601. https://doi.org/10.1563/ AAID-JOI-D-10-00209

DISCUSSÃO

Implantes metálicos, como os feitos de titânio, são estudados experimentalmente na biotecnologia com o intuito de otimizá-los afim de fornecer terapias baseadas em implantes que sejam mais rápidas e eficazes, devolvendo a qualidade de vida do paciente em menos tempo e com mais excelência (Davis et al., 2022). Apesar da alta taxa de sucesso na utilização de biomateriais metálicos como implantes, muitos pacientes ainda sofrem determinadas complicações relacionadas à sua implantação, como uma demora em demasia na recuperação, sendo que nesse contexto os pacientes com metabolismo comprometido têm chamado atenção (P. G. Coelho et al., 2018). A síndrome metabólica, muitas vezes responsável por esse comprometimento do metabolismo, é composta pelos fatores de risco, diabetes mellitus tipo 2, hipertensão, esteatose hepática, dislipidemia e obesidade (Fahed et al., 2022), sendo que a obesidade quase triplicou o número de casos desde 1975, é uma doença que acomete quase 13% da população mundial, sendo que 40% está com sobrepeso, e esse número vem crescendo cada vez mais e preocupando as diversas áreas médicas devido às complicações que podem advir dessa doença (X. Lin & Li, 2021).

Como afirmado anteriormente, distúrbios metabólicos como a obesidade são amplamente reconhecidos pela sua associação com comprometimento do reparo e regeneração de tecidos, particularmente nas intervenções que envolvem implantes metálicos, gerando um obstáculo significativo à progressão normal dos processos de cicatrização de feridas (Cheng, Ball, Gonzales, Schenk, & Hughes-Austin, 2020).

Em nosso laboratório, pesquisas envolvendo a investigação dos mecanismos de sinalização celular relacionados com as respostas à diferentes biomateriais metálicos vêm sendo desenvolvidas e já trouxeram importantes percepções ao longo dos estudos no que diz respeito aos constituintes intracelulares relacionados com esse cenário (Bezerra et al., 2017; da Costa Fernandes, Ferreira, Bezerra, & Zambuzzi, 2018; C J C Fernandes et al., 2018). Vale ressaltar que mesmo de maneira indireta, o titânio, bem como algumas modificações em sua superfície, desencadeiam diferentes respostas adaptativas celulares, sendo importante avaliá-lo nesse modelo pois diferente do que se acreditava, biomateriais metálicos não são inertes, e sim, liberam partículas em seu microambiente e podem atingir as células em seu ambiente e a circulação sanguínea (Raines et al., 2019).

Durante vários anos, o titânio possui ampla aplicação como dispositivo médico e implante em diversos tecidos, como por exemplo, implante ósseo, na ortopedia e odontologia, e como *stents* tubulares em casos de obstrução no endotélio vascular e no esôfago, por exemplo (Girón et al., 2021). Considerado referência nessas aplicações, o titânio possui atributos essenciais que o tornam um biomaterial metálico altamente adequado, e suas qualidades incluem forte resistência à corrosão, robustez mecânica, biocompatibilidade favorável, baixa toxicidade, entre outras, consequentemente, destaca-se como o implante metálico mais utilizado, apesar da existência de opções alternativas de biomateriais no mercado (Sidambe, 2014).

Como abordado inicialmente, o titânio, apesar de suas qualidades, ainda apresenta desafios em sua utilização como implante, e por isso passa por processos que visam a sua otimização, como por exemplo, modificações em sua superfície (Bezerra et al., 2017; Celio J C Fernandes et al., 2018; Sartoretto et al., 2020). Tais processos de otimização pretendem aprimorar a osseointegração, o contato direto entre tecido e implante e a adaptação do tecido peri-implante, bem como evitar complicações relacionadas, como casos de atraso na recuperação, de rejeição tecidual, de infecção (peri-implantite), e qualquer situação que apresente risco de tratamento (Khosravi, Maeda, DaCosta, & Davies, 2018).

Dos processos que visam a otimização do titânio por meio de técnicas de modificação de superfície, duas metodologias comuns são o duplo ataque ácido (*Dual Acid Etching*, DAE) e o jateamento com nanohidroxiapatita (nHA), que modificam a topografia da superfície e/ou adicionam revestimentos com funções específicas (Bezerra et al., 2017; Celio J C Fernandes et al., 2018; Sartoretto et al., 2020).

No caso do titânio com DAE, o método modifica a sua superfície expondo-o a uma mistura de ácidos fortes, geralmente ácido clorídrico (HCl) e ácido sulfúrico (H_2SO_4), gerando uma superfície microrrugosa, aumentando a energia superficial e aprimorando a molhabilidade. Essa microrrugosidade resultante promove maior adesão proteica, facilita a fixação celular e auxilia os estágios iniciais de osseointegração, sendo assim reconhecidas pela sua capacidade de melhorar a fixação biomecânica do implante e acelerar a cicatrização óssea (Al-Radha, 2016; Hung, Lin, & Feng, 2017).

Já no titânio nHA, o processo envolve jatear o implante com partículas de hidroxiapatita em nanoescala (nanohidroxiapatita) após sofrer o duplo ataque ácido. A hidroxiapatita é o principal constituinte inorgânico do esmalte do dente e do osso, uma forma mineral natural de apatita de cálcio, com a fórmula química $Ca_5(PO_4)_3(OH)$. Este

ambiente biomimético aumenta a osteocondutividade do implante, desencadeando a formação de uma camada de fosfato de cálcio na superfície do implante para mimetizar a composição mineral óssea natural (Bezerra et al., 2017; A. Lin, Wang, Kelly, Gubbi, & Nishimura, 2009).

Tanto implantes de titânio DAE quanto implantes de titânio nHA estão disponíveis comercialmente, e essas ligas de titânio utilizadas nesse trabalho foram gentilmente doadas para pesquisa pela empresa S.I.N. Implant System (São Paulo, SP, Brasil), que é uma empresa de implantes dentários especializada no projeto, fabricação e distribuição de implantes dentários e produtos relacionados (S.I.N. Implant System, 2024). As empresas de implantes dentários frequentemente se envolvem em pesquisa e desenvolvimento para melhorar o desempenho e os recursos de seus sistemas de implantes (Oshida, Tuna, Aktören, & Gençay, 2010). Dada a sua acessibilidade no mercado a um custo razoável e a ampla utilização entre os profissionais, o estabelecimento de uma preferência primária baseada na eficácia comprovada pela investigação tem uma importância considerável. A escolha entre estes métodos pelos profissionais de saúde depende de vários fatores, abrangendo a aplicação específica, a rugosidade superficial desejada e a resposta biológica almejada. Os profissionais de saúde beneficiam de avaliações e ensaios que identificam a abordagem ideal para públicos-alvo específicos, desempenhando assim um papel crucial no refinamento da eficácia e no sucesso duradouro dos implantes de titânio em aplicações biomédicas (Bezerra et al., 2017; da Silva et al., 2020; Celio J C Fernandes et al., 2018; Rossi et al., 2017).

Como foi abordado inicialmente, com esse aumento no número de pacientes com obesidade, espera-se que cresça cada vez mais o número de pessoas diagnosticadas obesas que receberão terapias baseadas em implantes, o que preocupa os profissionais já que a condição pró-inflamatória sistêmica presente nessa doença pode complicar os mecanismos de recuperação e regeneração tecidual (Ootsuka, Nakanishi, & Tsukamoto, 2015; Tükel & Delilbaşı, 2019). Alguns estudos apontam que a síndrome metabólica e a obesidade tem impacto negativo na mineralização e no metabolismo ósseo (Kim et al., 2010), e consequentemente levando a complicações nos tratamentos baseados em implantes, destacando que nesse cenário pode haver o envolvimento de múltiplos ensejos, como o aumento de marcadores inflamatórios circulantes (Monteiro, Pellizzer, Araújo Lemos, de Moraes, & do Egito Vasconcelos, 2019) levando a exposição a metabólitos

tóxicos, disfunção da atividade celular, bem como redução no suprimento sanguíneo secundário a microangiopatias (Guo & Dipietro, 2010).

O osso é um tecido dinâmico com elevada capacidade de regeneração, com ação ativa e equilibrada entre renovação e reabsorção óssea (Florencio-Silva, Sasso, Sasso-Cerri, Simões, & Cerri, 2015), mas a atividade dos osteoblastos na osteogênese é dependente de um apropriado suprimento sanguíneo e é acoplada à atividade do endotélio na angiogênese (Kusumbe, Ramasamy, & Adams, 2014; Ramasamy et al., 2016).

Como nesse cenário um apropriado aporte sanguíneo se faz necessário, onde processos como angiogênese e função endotelial adequada garantem o reparo e regeneração tecidual apropriados, torna-se crucial o entendimento do efeito do contexto de obesidade e síndrome metabólica no endotélio vascular (Everts et al., 2023).

A célula endotelial presente no endotélio vascular exerce função crucial na formação de novos vasos, no controle de vasodilatação e vasoconstrição, sendo essencial no processo de regeneração tecidual (Kitamura et al., 2008; Lehoux & Tedgui, 2003). Sendo a obesidade um fator de risco que pré-dispõe a outras doenças, como doenças cardiovasculares, essa doença pode afetar a regeneração de tecidos indiretamente por intervir na atividade do endotélio vascular e consequentemente no suprimento sanguíneo (M. Li, Qian, Kyler, & Xu, 2021).

O crescimento do tecido adiposo na obesidade, caracterizado por hiperplasia e hipertrofia anormais, leva à sua disfunção. Esta disfunção resulta numa liberação desequilibrada de metabólitos, impactando as células vizinhas dentro do tecido, nomeadamente macrófagos e células endoteliais. Especificamente, os macrófagos sofrem uma mudança fenotípica do estado anti-inflamatório M2 para o estado pró-inflamatório M1. Além disso, tornam-se espumosos à medida que engolfam os lipídios liberados irregularmente pelos adipócitos (Jung & Choi, 2014).

No contexto trazido nesse projeto, o adipócito pode estar se comunicando através de diferentes formas com a célula endotelial e com os osteoblastos, por liberar metabólitos como interleucinas, adipocinas (como adiponectina e leptina), ácidos graxos, lipoproteínas, gotículas lipídicas, entre outros (Thiriet, 2018). Antes considerado apenas um órgão de armazenamento de energia, está agora estabelecido que o tecido adiposo é um tecido metabólico altamente ativo que produz uma série de moléculas sinalizadoras que regulam o metabolismo e a homeostase energética (M. Coelho, Oliveira, & Fernandes, 2013).

Embora o conteúdo primário das gotículas lipídicas liberadas pelos adipócitos seja lipídios, há evidências emergentes de que essas gotículas também podem transportar proteínas em seu interior, contribuindo para a complexidade da função dos adipócitos e seu impacto nos tecidos circundantes (Fujimoto & Parton, 2011). Para desvendar e caracterizar essas moléculas e gotículas liberadas pelas células pode-se utilizar técnicas de cromatografia acoplada ao espectrômetro de massas, como a cromatografia gasosa (GC-MS) e a líquida (LC-MS). São técnicas que contribuem para fenotipagem molecular do metabolismo lipídico, chamada de lipidômica, em que GC-MS é mais utilizado para analisar os ácidos graxos (como o tamanho da cadeia e grau de insaturação), enquanto que LC-MS é mais amplo, avaliando glicerofosfolipídeos, esfingolipídeos, esteróis e as proteínas (proteômica) (Miniewska et al., 2020). As proteínas encontradas dentro das gotículas lipídicas liberadas pelos adipócitos variam, e a composição específica pode depender de fatores como o estado metabólico do adipócito, sinalização celular e outras condições ambientais. No entanto, algumas proteínas comumente identificadas associadas às gotículas lipídicas dos adipócitos incluem: As proteínas da família PLIN, especialmente a perilipina-1 (PLIN1), que desempenham um papel fundamental na membrana das gotículas, regulando a lipólise e o armazenamento lipídico; A família CIDE, e vale destacar aqui a proteína CIDEB pois, no contexto trazido desse projeto, a sua expressão gênica foi analisada nos organoides de fígado e nos hepatócitos por causa da sua ligação com a esteatose hepática (Newberry et al., 2021); Caveolinas; Enzimas do metabolismo lipídico, por exemplo, lipase sensível a hormônios (HSL) e acil-CoA sintetases (ACSLs); Várias Rab GTPases, envolvidas no tráfico de vesículas intracelulares; Chaperonas moleculares, tais como HSP (*Heat Shock Proteins*); Elementos do citoesqueleto como tubulina e vimentina; Proteínas relacionadas ao retículo endoplasmático e às mitocôndrias, como a proibitina e a piruvato carboxilase (Brasaemle, Dolios, Shapiro, & Wang, 2004; Brockman & Chen, 2012; Cho et al., 2007; Konige, Wang, & Sztalryd, 2014).

Além disso, os adipócitos liberam vesículas extracelulares (VEs), que abrangem vários subtipos, como exossomos, microvesículas e corpos apoptóticos, tradicionalmente categorizados com base em seu tamanho e origem. Essas VEs transportam diversas moléculas bioativas, encapsuladas dentro de uma bicamada lipídica protetora, incluindo proteínas solúveis e ligadas à membrana, lipídios, metabólitos, DNA e várias espécies de RNA (por exemplo, mRNA e miRNAs), desempenhando um papel na comunicação

intercelular, podendo ser captados por células vizinhas ou distantes, e assim, influenciando os processos celulares (Huang-Doran, Zhang, & Vidal-Puig, 2017).

O modelo experimental empregado neste estudo dirigiu-se à avaliação do impacto do aumento da adipogênese dos adipócitos em células endoteliais e osteoblastos quando expostos a um meio enriquecido com titânio. A utilização da diferenciação de adipócitos sob condições de alto teor de glicose como uma ferramenta *in vitro* oferece insights sobre disfunções metabólicas associadas à obesidade (Palacios-Ortega, Varela-Guruceaga, Martínez, de Miguel, & Milagro, 2016), visto que níveis elevados de glicose promovem o acúmulo de lipídios e a adipogênese. Ao validar este modelo, nossos resultados indicam um aumento substancial na carbonilação de proteínas em adipócitos expostos a altas concentrações de glicose. A técnica para avaliar a carbonilação de proteínas utilizando 2,4-dinitrofenilhidrazina (DNPH) é um método comum para avaliar o estresse oxidativo e a presença do efeito das espécies reativas de oxigênio (EROS) em amostras biológicas. A carbonilação de proteínas é uma modificação química que ocorre quando as proteínas são oxidadas, muitas vezes como resultado da exposição a EROS (Suzuki, Carini, & Butterfield, 2010). Esta técnica fornece uma medida quantitativa da carbonilação de proteínas, que indica estresse oxidativo e danos proteicos induzidos por EROS em sistemas biológicos. É amplamente utilizado em estudos relacionados ao estresse oxidativo, envelhecimento e diversas condições patológicas onde o aumento dos níveis de EROs pode contribuir para danos celulares (Suzuki et al., 2010).

Ainda sobre a validação do modelo com adipócitos, a avaliação de genes específicos nos adipócitos fornece informações valiosas sobre os mecanismos moleculares associados à obesidade, estados inflamatórios e adipogênese. Alguns genes que foram avaliados nos adipócitos nesse trabalho, como interleucinas (ILs) IL-1β, IL-6, IL-18, TNF-α e IL-8 são citocinas pró-inflamatórias que desempenham um papel crucial na resposta inflamatória. Na obesidade, o aumento da adiposidade pode levar ao aumento dos níveis dessas citocinas, contribuindo para a inflamação crônica associada à disfunção metabólica. Essas moléculas são produzidas pelo tecido adiposo e estão implicadas no desenvolvimento da resistência à insulina. IL-1r é o receptor da IL-1beta e sua expressão pode influenciar a resposta celular à IL-1beta, alterações na sua expressão podem impactar a sinalização inflamatória nos adipócitos (Al-Mansoori, Al-Jaber, Prince, & Elrayess, 2022). Importante mencionar também genes que foram analisados no modelo, a citar: o NFkB, que é um fator de transcrição que desempenha um papel central na regulação da inflamação, e em doenças como obesidade, a ativação do NFkB está ligada

à regulação positiva de genes pró-inflamatórios (T. Liu, Zhang, Joo, & Sun, 2017); o Myd88, codifica uma proteína adaptadora envolvida nas vias de sinalização de vários receptores Toll-like, que desempenham um papel no reconhecimento e resposta a patógenos e pode contribuir para respostas inflamatórias (Cuevas, Clark, & Potter, 2021). E finalmente o gene avaliado nos adipócitos, PPAR-γ, que desempenha um papel crucial na diferenciação dos adipócitos e na sensibilidade à insulina, a sua modulação está associada a alterações na adipogênese (Leonardini, Laviola, Perrini, Natalicchio, & Giorgino, 2009).

A coloração Oil Red O é um método versátil para avaliar o acúmulo de lipídios nos adipócitos (e em outras células, como demonstrado nesse trabalho), tornando-se uma ferramenta valiosa para estudar a adipogênese e as alterações relacionadas à obesidade. Essa técnica costuma ser usada em conjunto com outros ensaios para obter uma compreensão abrangente das alterações moleculares e celulares associadas a distúrbios metabólicos como a obesidade. Esse ensaio de coloração não é apenas qualitativo, mas também pode ser usada para análise quantitativa, pois o corante pode ser eluído das células e a sua absorbância ser medida espectrofotometricamente, onde a intensidade da coloração se correlaciona com a quantidade de lipídios acumulados, oferecendo uma medida quantitativa do conteúdo lipídico nos adipócitos (Kraus et al., 2016). Os adipócitos empregados neste estudo, sejam derivados de camundongos ou diferenciados de células-tronco mesenquimais humanas, exibiram acúmulo substancial de lipídios nos grupos tratados com meio rico em glicose, condição que se assemelha à hipertrofia e à hiperplasia observadas no tecido adiposo de indivíduos obesos. Enfatizar a validação deste modelo é fundamental para garantir a fidelidade das etapas experimentais subsequentes alinhadas ao tema e às condições propostas, principalmente porque o meio condicionado é utilizado como tratamento.

No modelo de alta adipogênese com os adipócitos 3T3-L1, a proteína ERK aumentou no grupo com alta glicose, essa análise foi feita pois ERK é um membro da família das MAPKs (*mitogen-activated protein kinase*) e desempenha um papel crucial nos processos celulares, como proliferação, diferenciação e sobrevivência celular, e nos adipócitos suas vias de sinalização podem ser ativadas em resposta a fatores associados à obesidade, como aumento da disponibilidade de nutrientes ou inflamação, que podem contribuir para diversas respostas celulares, incluindo diferenciação de adipócitos e metabolismo lipídico (Horwitz & Birk, 2023). Além disso, a adipogênese, o processo de diferenciação dos adipócitos, correlacionando com a expansão do tecido adiposo na

obesidade, envolve alterações na matriz extracelular (MEC) para acomodar o aumento do armazenamento de gordura, onde as metaloproteinases de matriz (MMPs), incluindo MMP2 e MMP9, podem desempenhar um papel na remodelação da MEC durante a expansão desse tecido (Ruiz-Ojeda, Méndez-Gutiérrez, Aguilera, & Plaza-Díaz, 2019), corroborando com os resultados encontrados da zimografia (atividade das MMPs no gel de eletroforese) realizada nas amostras coletadas dos adipócitos 3T3-L1.

O tecido adiposo disfuncional, marcado pela liberação desregulada das moléculas e fatores mencionados (ácidos graxos, citocinas, etc.), estende seu impacto à corrente sanguínea e assim a diversos sistemas fisiológicos. Dentro do sistema vascular, os ácidos graxos existem predominantemente em duas formas durante o transporte: ácidos graxos livres não esterificados, associados de forma não covalente à albumina, ou esterificados em triacilgliceróis encapsulados em partículas de lipoproteínas. Independentemente da sua forma, todos os ácidos graxos devem atravessar a barreira endotelial para atingir os tecidos alvo. No entanto, a compreensão de como o endotélio gerencia esses lipídios permanece escassa (Stahl, 2004; van der Vusse, van Bilsen, Glatz, Hasselbaink, & Luiken, 2002). Descobertas recentes revelaram uma biogênese robusta de gotículas lipídicas dentro das células endoteliais quando expostas a quantidades excessivas de ácidos graxos, que inclusive não atuam apenas como reservatórios de energia, mas como organelas dinâmicas que regulam ativamente a função das células endoteliais (Kuo, Lee, & Sessa, 2017). A propósito, propõe-se que o endotélio funcione como um tampão de gordura, utilizando gotículas lipídicas para desempenhar um papel regulador crucial, potencialmente protegendo contra a toxicidade dos ácidos graxos livres através de sua esterificação (Ibrahim & Arany, 2017; Kuo et al., 2017).

A avaliação do endotélio vascular é crucial devido ao seu papel integral em numerosos processos cardiometabólicos. Composto por uma única camada de células altamente especializadas que revestem a superfície interna dos vasos sanguíneos, o endotélio desempenha um papel fundamental na manutenção da saúde cardiovascular. Quaisquer desvios na função endotelial, conhecidos como disfunção endotelial, têm sido associados a diversas doenças cardiovasculares, abrangendo diabetes mellitus, obesidade, hipertensão e aterosclerose (Pellegrinelli, Rouault, Veyrie, Clément, & Lacasa, 2014).

Seria de grande interesse realizar uma avaliação das gotículas lipídicas intracelulares nas células endoteliais tratadas com o meio condicionado pelos adipócitos. Esse aspecto específico é de relevância, podendo proporcionar informações valiosas para a compreensão do impacto do meio condicionado nas alterações lipídicas intracelulares

dessas células. Inclusive porque, Pacia et al. 2020 em seu estudo envolvendo células endoteliais da aorta humana submetidas à exposição a um ácido graxo comum, o ácido oleico, conduzido *in vitro* e *ex vivo*, demonstrou um aumento notável nas gotículas lipídicas intracelulares (Pacia et al., 2020).

O envolvimento da célula endotelial no microambiente peri-implante é relevante de ser estudado e avaliado devido a sua grande contribuição acoplada com a osteogênese no processo de osseointegração e regeneração tecidual (Zhu, Wang, & Li, 2021). O endotélio encontra-se em constante exposição à pressão exercida pelo fluxo sanguíneo, sendo o *shear-stress* a força tangencial paralela à parede do vaso sanguíneo, e possui a notável capacidade de perceber e reagir aos estímulos tanto mecânicos como químicos presentes nesse fluxo, disparando vias de sinalização que desempenham papéis fundamentais, tais como vasodilatação e vasoconstrição (dela Paz, Walshe, Leach, Saint-Geniez, & D'Amore, 2012; Givens & Tzima, 2016; Pinto et al., 2019). A célula endotelial atua disparando cascatas de sinalização de modo a realizar a manutenção do endotélio, como por exemplo, liberando o óxido nítrico (NO), produzido pela enzima Óxido Nítrico Sintase endotelial (eNOS), que age principalmente na vasodilatação (Givens & Tzima, 2016), bem como o fator de crescimento endotelial vascular (VEGF) que atua primariamente na angiogênese através de sinais de proliferação, migração e sobrevivência, com envolvimento das proteínas ERK, P38 e da via PI3K/AKT respectivamente nesse contexto, mas que também estão envolvidos em outros processos celulares (Hang et al., 2013).

O VEGF e o seu receptor, VEGFR1, desempenham um papel fundamental na angiogênese, facilitando a formação de novos vasos sanguíneos (Shibuya, 2011). Sob condições de adipogênese aumentada, torna-se pertinente avaliar se sua expressão pode ser influenciada, impactando a forma como as células endoteliais respondem ao titânio e a vascularização ao redor do implante de titânio. Da mesma forma, destaca-se a AKT, uma molécula sinalizadora essencial envolvida na sobrevivência e proliferação celular. A desregulação da sinalização da AKT pode ter impactos significativos na função das células endoteliais, contribuindo para complicações vasculares. Isso ocorre devido à sua associação com a ativação subsequente da eNOS, previamente desencadeada pela ativação de SRC e FAK. Na célula endotelial, essa cascata de sinalização desempenha papel crucial em processos vasodilatadores, anti-inflamatórios, antitrombóticos e antiaterogênicos (Somanath, Razorenova, Chen, & Byzova, 2006). A proteína SRC demonstrou significativo aumento em seu conteúdo na célula endotelial tratada com a

condição de alta adipogênese, inclusive na presença dos titânios DAE e nHA, mas menos significativo no caso do titânio nHA, sendo esse dado relevante devido ao envolvimento dessa proteína em processos e vias de sinalização de angiogênese, permeabilidade vascular, migração, adesão, além de outros já mencionados nesse parágrafo (Hu, Place, & Minshall, 2008).

Em relação ao ciclo celular, a expressão de CDK2 e CDK4 em células endoteliais pode fornecer informações sobre a modulação da proliferação celular (D. Chen, Walsh, & Wang, 2000). Os genes AKT, CDK2 e CDK4 foram aumentados pela condição de alta adipogênese, mas o titânio parece atenuar essa resposta. Estes dados mostram que a condição de alta adipogênese influencia a resposta das células endoteliais ao titânio nesses processos celulares. E ainda, constituintes como ERK (mencionado anteriormente), JNK (que desempenha um papel na apoptose e inflamação) e P38 (envolvido nas respostas celulares ao estresse e à inflamação) são membros da via de sinalização MAPK, envolvida na proliferação e sobrevivência celular (Yue & López, 2020), também sofreram modulação na expressão gênica, principalmente o gene ERK na presença do titânio DAE que aumentou em ambas as condições, mas ainda mais acentuado na condição de alta adipogênese.

Compreender como a expressão de IL-6 e IL-1β é modulada nas células endoteliais durante a obesidade é crucial para desvendar os mecanismos subjacentes às complicações vasculares relacionadas à essa doença e como isso pode impactar o processo de implantação do titânio. Portanto, a avaliação da expressão gênica de IL-6 e IL-1β em células endoteliais contribui para a compreensão dos processos inflamatórios associados à obesidade e seu impacto na saúde vascular (Larsson et al., 2008), sendo que no modelo apresentado, a célula endotelial apresentou um aumento acentuado na expressão de IL-6 quando exposta à condição de alta adipogênese somada à presença do titânio, tanto DAE quanto nHA, enquanto que o gene IL-1β significativamente aumentou apenas no grupo sob alta adipogênese.

Alterações nessas vias de sinalização podem impactar as respostas das células endoteliais e os processos angiogênicos, podendo contribuir para a disfunção endotelial e inflamação crônica (Larsson et al., 2008). A comunicação entre célula endotelial e osteoblastos no ambiente peri-implante ainda não é totalmente esclarecida, mas sabe-se da relevância de suas atividades em conjunto nos processos de regeneração óssea e de osseointegração frente a um biomaterial metálico, nesse contexto, estudos já vêm sendo realizados para esclarecer os mecanismos de angiogênese e osteogênese que afetam a

peri-implantação (W. Chen et al., 2018). Tais processos são passíveis de sofrer influências sob determinada condição e, no contexto trazido nesse trabalho, a obesidade tem preocupado as práticas odontológicas e ortopédicas (Monteiro et al., 2019).

O crescente número de casos mundial de obesidade está refletindo em um aumento das doenças hepáticas, particularmente da doença hepática gordurosa não alcoólica (DHGNA), cuja prevalência cresce consistentemente a uma taxa anual de 1%, afetando já 30% da população mundial (Machado & Cortez-Pinto, 2023). É fundamental ressaltar que a ocorrência de excesso de gordura no fígado, sem acúmulo simultâneo de tecido adiposo visceral, é relativamente incomum, pois esta condição é mais comumente observada em conjunto com níveis elevados de gordura visceral (Lemieux & Després, 2020). O fígado, um regulador central do metabolismo da gordura, coordena o processamento de ácidos graxos produzidos internamente e obtidos externamente e regula os níveis de lipídios no sangue através da síntese e secreção de lipoproteínas (Green, Pramfalk, Morten, & Hodson, 2015). Estudos recentes propõem uma correlação potencial entre a DHGNA e o aumento da perda óssea, suscitando preocupações sobre a sua possível ligação com osteoporose e fraturas ósseas (Loosen et al., 2022), e dada a discussão em curso sobre o impacto das questões relacionadas com a obesidade na regeneração óssea e tecidual, torna-se pertinente levar em consideração o cenário em ambas as doenças.

Portanto, através de modelos *in vitro*, a presente investigação validou uma estrutura conceitual replicando condições semelhantes não só à obesidade, mas também à DHGNA. Modelos *in vitro* de doença hepática gordurosa têm sido desenvolvidos com o intuito de correlacionar com as condições relacionadas ao metabolismo lipídico e à lipogênese, usando tanto cultura celular 2D com hepatócitos, como cultura 3D com organoides de fígado (Ayada et al., 2023; Müller & Sturla, 2019).

A cultura celular com organoides são estruturas tridimensionais compostas de células cultivadas que se auto-organizam para transcrever a arquitetura e a função de órgãos ou tecidos específicos, com uma proposta de fornecer um ambiente fisiologicamente mais relevante, assemelhando-se à complexidade, à diversidade e organização celular dos tecidos do corpo humano (Zhao et al., 2022). No presente trabalho apresentamos dois modelos *in vitro* separados e estabelecidos de DHGNA, um utilizando organoides de fígado e outro envolvendo hepatócitos Huh7, para examinar como a DHGNA influencia as células ósseas e suas respostas ao titânio.

Resumidamente para esclarecer os termos relacionados com essa doença, que representam diferentes estágios e aspectos da saúde do fígado, DHGNA (doença hepática gordurosa não alcoólica, em inglês *non-alcoholic fatty liver disease* - NAFLD) é um termo genérico que abrange várias doenças hepáticas caracterizadas pelo acúmulo excessivo de gordura no fígado. A esteatose hepática refere-se ao estágio inicial de acúmulo de gordura nas células do fígado que se não tratada progride para inflamação e danos às células hepáticas passando a se chamar esteatohepatite não alcoólica (EHNA, em inglês *Non-Alcoholic Steatohepatitis* – NASH). Essa inflamação prolongada pode progredir para fibrose, que é a formação de tecido cicatricial no fígado e ainda é um estágio reversível. A fibrose avançada pode levar à cirrose, onde cicatrizes extensas perturbam a função hepática, é irreversível e pode levar à insuficiência hepática (Pouwels et al., 2022). O termo doença hepática gordurosa associada ao metabolismo (MAFLD, *Metabolic Associated Fatty Liver Disease*) é um termo recente proposto como alternativa à NAFLD, enfatizando a associação com disfunção metabólica em vez de focar apenas no consumo de álcool (Sangro, de la Torre Aláez, Sangro, & D'Avola, 2023).

O modelo de esteatose *in vitro*, utilizando organoides de fígado e hepatócitos da linhagem Huh7, mereceram sua validação no trabalho apresentado, mesmo sendo modelos pré-estabelecidos na literatura, já que os mesmos sofreram algumas adaptações pertinentes, como: após o período de tratamento para estímulo da alta lipogênese nessas células, a cultura celular ficou 24 horas com novo meio de cultura sem o tratamento lipogênico, para produzir o meio condicionado pelos organoides e pelos hepatócitos (de modo que ao ser utilizado nos osteoblastos apenas fatores liberados pelas células do fígado interferissem na resposta final). Mesmo com essa adaptação, o resultado da coloração com Oil Red O foi conclusivo para ambos modelos 2D e 3D. E ainda, a expressão de genes associados com esteatose hepática e metabolismo lipídico, como PNPLA3, TM6SF2, SREBP1 e CIDEB (Fabbrini, Sullivan, & Klein, 2010; Newberry et al., 2021), estavam elevados nos grupos com alta lipogênese, sendo que CIDEB, envolvida na formação de gotículas lipídicas, foi mencionada previamente por ter relatos na literatura de também ser encontrada em gotículas de lipídeos liberadas pelos adipócitos (Konige et al., 2014).

A intrincada relação entre obesidade, esteatose e saúde óssea envolve múltiplos fatores interconectados, incluindo influências mecânicas, hormonais, inflamatórias e metabólicas. Os efeitos sobre os ossos são complexos e podem variar com base em fatores como a duração e gravidade da obesidade, a presença de distúrbios metabólicos

associados e variações individuais na resposta a estas condições (Gkastaris, Goulis, Potoupnis, Anastasilakis, & Kapetanos, 2020; H. Li, Luo, Zhang, Liu, & Lin, 2022). Compreender estas interações é crucial para o desenvolvimento de intervenções direcionadas para mitigar o potencial impacto negativo na saúde óssea em indivíduos com obesidade e esteatose hepática.

Os osteoblastos são células formadoras de osso especializadas, derivadas de células-tronco mesenquimais, que desempenham um papel crucial na formação e mineralização óssea (Florencio-Silva et al., 2015). Essas células sintetizam e secretam uma matriz orgânica composta principalmente por fibras de colágeno e outras diversas proteínas, que servem como estrutura para a mineralização. Os osteoblastos iniciam o processo de mineralização liberando vesículas contendo íons cálcio e fosfato, tais vesículas nucleiam cristais de hidroxiapatita (a forma mineralizada de fosfato de cálcio) dentro da matriz, e essa matriz mineralizada forma uma estrutura endurecida que contribui para a resistência óssea. Os osteoblastos ficam incorporados na matriz óssea e se diferenciam em osteócitos, formando uma rede de células dentro do osso (Florencio-Silva et al., 2015).

A remodelação óssea envolve um mecanismo de acoplamento que coordena as atividades dos osteoblastos e osteoclastos, um processo dinâmico que mantém a homeostase óssea. Os osteoclastos são células grandes e multinucleadas derivadas de células-tronco hematopoiéticas responsáveis pela reabsorção óssea, os osteoclastos se fixam na superfície óssea e secretam ácidos e enzimas que dissolvem a matriz mineralizada formando lacunas, que são cavidades no osso, e faz parte do processo natural de remodelação óssea (Bolamperti, Villa, & Rubinacci, 2022). Desequilíbrios na remodelação óssea podem levar a condições como a osteoporose. Várias proteínas reguladoras, incluindo osteocalcina, osteopontina e sialoproteína óssea, desempenham papéis na modulação da mineralização e na manutenção da integridade óssea (Bolamperti, Villa, & Rubinacci, 2022).

A presença de gotículas lipídicas nos osteoblastos é um aspecto intrigante da biologia celular óssea. Fisiologicamente, as gotículas lipídicas nos osteoblastos desempenham um papel no armazenamento de energia e no metabolismo, refletindo a natureza dinâmica do tecido ósseo, que requer um equilíbrio entre as funções de formação óssea e de armazenamento de energia. Gotículas lipídicas nos osteoblastos podem servir como reservatório de energia, fornecendo o combustível necessário para o processo de mineralização óssea, que consome muita energia (Nandy, Helderman, et al., 2023). No

entanto, condições patológicas podem perturbar este equilíbrio, onde o acúmulo excessivo de gotículas lipídicas nos osteoblastos tem sido associado a vários distúrbios esqueléticos, incluindo osteoporose, redução na densidade mineral óssea e perda óssea relacionada à idade, já que os desequilíbrios no metabolismo lipídico podem impactar a diferenciação e atividade dos osteoblastos, levando potencialmente ao comprometimento da estrutura e função óssea (Nandy, Richards, et al., 2023).

Todos os meios condicionados testados nesse trabalho, dos adipócitos, dos organoides de fígado e dos hepatócitos, foram capazes de desencadear a formação de gotículas de gordura nos osteoblastos, independente da condição basal normal ou de alta lipogênese, e da presença dos titânios. Os osteoblastos que foram diferenciados sem a presença desses meios condicionados não apresentaram tais gotículas. Esse resultado observado, através da coloração com Oil Red O, se mostrou mais intenso nos osteoblastos tratados com meio condicionado pelos organoides, porém uma limitação importante desse tratamento é a presença dos constituintes do meio de expansão dos organoides (LEM, *liver expansion medium*) que foram mantidos durante as 24 horas de condicionamento do meio, por serem necessários para a sobrevivência e integridade desses organoides de fígado. A presença das gotículas de gordura nesses osteoblastos levantou questões sobre ser algo fisiológico ou patológico como abordado previamente, bem como sobre a possibilidade de se apresentarem em proporções desiguais entre os diferentes grupos (normal ou alta lipogênese, titânio DAE e titânio nHA), e nesse caso, a semi-quantificação dessas gotículas através da leitura da absorbância das células suspensas, traria melhores *insights* a respeito.

A matriz mineralizada produzida pelos osteoblastos durante o processo de diferenciação celular foi analisada através da coloração com *Alizarin Red S*, que é um corante que se liga seletivamente aos íons cálcio formando um complexo com essa matriz, fornecendo uma medida qualitativa da capacidade dos osteoblastos de mineralização. Esse ensaio validou o processo de diferenciação dos osteoblastos nesse projeto, que mesmo utilizando o meio condicionado advindo dos adipócitos, dos organoides hepáticos e dos hepatócitos, e ainda, enriquecido pelos titânios DAE e nHA, os constituintes do meio osteogênico (dexametasona, β-glicerofosfato e ácido ascórbico) foram capazes de estimular a diferenciação das células tronco mesenquimais em osteoblastos. Explorar a variação potencial dessa mineralização entre as condições distintas (normal, lipogênese alta, DAE e nHA) forneceria uma compreensão mais matizada deste fenômeno, algo

possível por meio da semi-quantificação dessa matriz através da leitura de absorbância das células suspensas de acordo com protocolos estabelecidos.

A avaliação de genes chaves do osso em osteoblastos sob condições de alta lipogênese é importante para desvendar os mecanismos moleculares que impactam a saúde óssea. Em um estudo em que adipócitos e osteoblastos foram cultivados em co-cultura após sua diferenciação, a expressão do gene RUNX2, um fator de transcrição chave na diferenciação de osteoblastos, diminuiu significativamente nas células osteoblásticas, ocorrendo concomitantemente, nessas células, um aumento na expressão de PPARγ, integrante crucial na diferenciação de adipócitos (L.-F. Liu, Shen, Zhang, Wang, & Kraemer, 2010).

Afirma-se que a obesidade pré-dispõe a outras doenças e complicações através do desbalanço molecular metabólico abordado que pode atuar sistemicamente e de várias maneiras, por exemplo, o TNF-α, que foi mencionado, está relacionado com a resistência à insulina e com dislipidemia, e nos osteoblastos pode aumentar a expressão de RANK e RANKL (Wang, He, & Yu, 2017), principais constituintes envolvidos no processo de diferenciação e maturação de osteoclastos e consequentemente com a absorção óssea (W. Li et al., 2017). Além disso, estudos apontam uma relação entre a obesidade com osteoporose e mostram que uma dieta altamente calórica pode reduzir a densidade mineral óssea, não só pelo aumento da diferenciação de osteoclastos desencadeado pelo TNF-α e por citocinas pró-inflamatórias (como IL-1β e IL-6), mas também pelo fato de que osteoblastos e adipócitos são derivados da mesma célula progenitora, a célula tronco mesenquimal (MSC), e osteoblastogênese é inversamente associada com adipocitogênese, processos de diferenciação mediados pela expressão de RUNX2 e PPAR-γ respectivamente (Wang et al., 2017).

A ALP (fosfatase alcalina), uma enzima intimamente ligada à função dos osteoblastos e à mineralização da matriz extracelular, foi avaliada em estudos que exploraram os impactos distintos da adiponectina e da leptina – adipocinas liberadas pelos adipócitos – em osteoblastos. Pacheco-Pantoja e colaboradores (2014), mostraram que os osteoblastos SAOS-2 tratados com adiponectina exibiram uma redução notável na atividade da ALP (Pacheco-Pantoja, Fraser, Wilson, & Gallagher, 2014). O panorama da pesquisa revelou consistentemente a importância da adiponectina na modulação do delicado equilíbrio entre a diferenciação dos osteoblastos e dos adipócitos (Forte, Renovato-Martins, & Barja-Fidalgo, 2023). Por outro lado, Li e colaboradores demonstraram que as células-tronco mesenquimais humanas, quando diferenciadas em

osteoblastos na presença de leptina, apresentavam uma atividade elevada de ALP (J. Li et al., 2020). Estas descobertas lançam luz sobre a intrincada interação entre as adipocinas e a função dos osteoblastos, contribuindo com informações valiosas sobre os mecanismos reguladores que regem o metabolismo ósseo.

As proteínas morfogenéticas ósseas (BMPs), parte da superfamília do fator de crescimento transformador (TGF-β), constituem um grupo diversificado de 20 BMPs distintas, e foi demonstrado que as BMPs são agentes-chave na diferenciação osteoblástica de células-tronco mesenquimais e promovem a formação óssea (Kanakaris, Petsatodis, Tagil, & Giannoudis, 2009). As funções multifacetadas das BMPs superam as de outros membros da família TGF. Essas proteínas secretadas estão implicadas em diversas patologias, incluindo obesidade, diabetes e complicações associadas. Além disso, a família BMP desempenha um papel crucial como elo que conecta o metabolismo da glicose ao metabolismo ósseo, destacando sua importância fundamental na intrincada interação entre esses processos fisiológicos (Perera, Ritchie, & Tate, 2020). Em uma revisão sobre os efeitos das BMPs no osso, na obesidade e no metabolismo da glicose, foi demonstrado que BMP2 e BMP7 no osso estimulam a formação óssea, além disso, BMP7 também inibe a formação de osteoclastos (Y. Chen et al., 2021). Na obesidade, a BMP2 está elevada no tecido adiposo subcutâneo e visceral (Guiu-Jurado et al., 2016), e a BMP7 atua ajudando a reduzir ganho de peso por induzir a diferenciação do tecido adiposo marrom (relacionado com termogênese) e o gasto energético (Saini, Duraisamy, Bayen, Vats, & Singh, 2015). E no metabolismo da glicose, a BMP2 está elevada no plasma de pacientes com diabetes tipo 2 e parece atuar diminuindo a resistência à insulina uma vez que essa proteína influencia diretamente a translocação do GLUT4 para a membrana plasmática (Guiu-Jurado et al., 2016; Schreiber et al., 2017), enquanto que BMP7 também reduz a resistência à insulina por melhorar a captação de glicose através da otimização da sinalização da insulina na via PI3K/AKT (Chattopadhyay, Singh, Gupta, & Surolia, 2017).

Na osseointegração, onde o osso se integra ao implante, as proteínas de adesão celular desempenham um papel crucial para assegurar o sucesso da implantação. Dentre essas proteínas, a FAK assume uma função fundamental na sinalização de adesão focal, essencial para a aderência celular e movimento, especialmente quando ativada pela fosforilação em Y397 (p-FAK). Dentro desse cenário, a proteína SRC também desempenha um papel importante, não apenas ativando a FAK, mas também contribuindo para processos como proliferação e diferenciação (Gittens, Olivares-Navarrete, Schwartz,

& Boyan, 2014). O titânio nHA elevou o conteúdo de p-FAK (y397) nos osteoblastos derivados da célula mesenquimal, porém na condição de alta adipogênese esse aumento foi menos significativo, mostrando um efeito dessa condição na resposta dos osteoblastos ao titânio em vias de sinalização de adesão celular.

A CDK2 é uma proteína que desempenha um papel essencial na progressão do ciclo celular, sua fosforilação está associada ao avanço do ciclo celular, crucial para a replicação dos osteoblastos (Shaikh, Wesner, Abuhattab, Kutty, & Premnath, 2023). Curiosamente, a condição de alta lipogênese dos hepatócitos Huh7 reduziu significativamente o conteúdo de p-CDK2 (Thr160) nos osteoblastos, mas na presença do titânio nHA esse efeito não ocorreu, mantendo o conteúdo similar ao da condição normal. Essa alta lipogênese também diminuiu expressivamente o conteúdo de p-CREB (Ser133) nessas células, mas o titânio DAE e nHA parecem atenuar essa redução, inclusive o nHA em condição basal aumentou essa proteína fosforilada significativamente. Quando fosforilada p-CREB (Ser133) atua como um ativador de genes envolvidos na sobrevivência celular e diferenciação nos osteoblastos (Oury et al., 2010).

O sucesso da osseointegração no processo de implantação está intrinsecamente ligado aos processos de cicatrização, que englobam: (i) uma fase inflamatória aguda, destacada pela migração de células inflamatórias e pela liberação de mediadores inflamatórios; (ii) uma fase proliferativa, na qual ocorre a deposição da nova matriz extracelular (MEC); e (iii) uma fase de remodelação, durante a qual a matriz é organizada e sofre remodelação (de Oliveira et al., 2020). A proteína SRC também está associada ao controle da remodelação MEC, desempenhando um papel relevante na regulação da atividade das metaloproteinases de matriz (MMPs) em resposta a biomateriais, inclusive foi mencionado que a interface biológica formada pela superfície de titânio nHA é capaz de modular o metabolismo dos osteoblastos, sendo a atividade da proteína SRC um pré-requisito para a remodelação da MEC nesse cenário (da Costa Fernandes, Bezerra, de Campos Souza, Campos, & Zambuzzi, 2018; Celio J C Fernandes et al., 2018).

As MMP2 e MMP9 são enzimas que desempenham um papel crucial na remodelação da MEC nos tecidos, incluindo osso. Nos osteoblastos, essas MMPs estão envolvidas na degradação e remodelação da MEC durante processos como a formação óssea, reparação e remodelação (Khoswanto, 2023). A técnica de zimografia que permite avaliar a atividade dessas MMPs foi realizada nos osteoblastos nos diferentes modelos

desse trabalho, e é importante levar em consideração que por terem sido tratados com meio condicionado por outras células, esse meio já trazia MMPs advindas das mesmas.

Como demonstrado, os adipócitos 3T3-L1 apresentaram um aumento na atividade das MMPs no grupo de alta adipogênese (Pinto, Gomes, de Morais, & Zambuzzi, 2023), dessa forma, provavelmente os adipócitos derivados da célula tronco mesenquimal humana também apresentem esse perfil. Apesar de que essa afirmação não seja cabível para os meios condicionados pelos organoides de fígado e hepatócitos, necessitando de mais investigação. Em todo caso, após esse meio condicionado ser utilizado para tratar os osteoblastos nas diferentes condições, incluindo grupo enriquecido com titânio, a zimografia foi realizada e demonstrou diferentes perfis de atividades dessas MMPs. Com destaque para os grupos com titânio DAE. Curiosamente, os meios condicionados pelos organoides de fígado e pelos hepatócitos Huh7, e então usados para tratar os osteoblastos, apresentaram resultados opostos, pois enquanto a condição proveniente dos organoides causou uma redução na atividade das MMPs, o meio das células Huh7 causou um aumento na atividade das mesmas, principalmente nas condições de alta lipogênese. Vale lembrar que apesar de se tratarem de modelos *in vitro* de esteatose hepática, os meios condicionados pelos organoides, usados para tratar os osteoblastos, podiam ainda conter fatores e constituintes do LEM (*Liver Organoids Expansion Medium*) que os organoides podem não ter consumido totalmente e assim estariam atingindo e afetando a resposta dos osteoblastos.

A osteocalcina é uma proteína produzida principalmente pelos osteoblastos, é um componente importante da matriz óssea, ajuda a regular a mineralização, contribuindo para a integridade e resistência estrutural dos ossos (Wawrzyniak & Balawender, 2022). Além disso, a osteocalcina é uma proteína multifacetada com funções também na regulação hormonal e processos metabólicos possuindo conexões com a sensibilidade à insulina e o metabolismo da glicose, que destacam sua importância na complexa interação entre os ossos e outros sistemas fisiológicos (Kanazawa, 2015). A osteocalcina atua como um hormônio em que sua forma ativa influencia o metabolismo energético, e estudos sugerem que quando ativa pode aumentar a sensibilidade à insulina, ajudando a regular os níveis de glicose no sangue, pode influenciar a função pancreática, particularmente nas células beta secretoras de insulina e assim apoiar a produção e secreção de insulina (Wei & Karsenty, 2015).

A expressão do gene BGLAP, que codifica a osteocalcina, foi significativamente modulada nas células nos diferentes modelos apresentados nesse trabalho. Inicialmente

nos osteoblastos diferenciados com meio condicionado pelos adipócitos, os grupos mostraram variações, com destaque para as células tratadas com meio enriquecido com titânio nHA, que elevou significativamente a sua expressão. Destaque também nos osteoblastos tratados com meio condicionado pelos hepatócitos Huh7 que reduziu expressivamente nos grupos em condição de alta lipogênese. Por fim, curiosamente a expressão de BGLAP foi elevada nas células tronco do fêmur de ratos obesos tratados com farelo de arroz rico em γ-orizanol, o modelo *ex vivo* avaliado nesse estudo.

Dado que a osteocalcina é frequentemente associada à melhoria do metabolismo da glicose, resistência à insulina, e obesidade, com evidências de seus efeitos cardiometabólicos positivos (Kanazawa, 2015), o aumento observado da osteocalcina nas células-tronco do fêmur de ratos obesos tratados com farelo de arroz rico em γ-orizanol suscita a indagação sobre se esse tratamento pode estar desempenhando um papel protetor ou atenuante nos efeitos prejudiciais da obesidade no osso, através de um estímulo na expressão de osteocalcina.

O farelo de arroz contém uma variedade significativa de fitoquímicos conhecidos por suas propriedades antioxidantes e anti-inflamatórias, e entre esses compostos, destaca-se o γ-orizanol, cuja concentração é de 13 a 20 vezes superior à soma dos tocotrienóis e tocoferóis presentes no farelo de arroz (Garcia et al., 2022). O γ-orizanol (γOz) é uma mistura de ésteres de ácido ferúlico de álcoois triterpênicos e esteróis vegetais, que tem sido estudado por seus potenciais benefícios à saúde, por exemplo, atividade antioxidante, anti-inflamatória, melhora no metabolismo da glicose (resistência à insulina, glicose prejudicada e diabetes) e efeitos antiobesidade (através da diminuição do peso corporal, do colesterol total, dos níveis de colesterol LDL e das concentrações pós-prandiais de insulina e glicose) (Minatel, Francisqueti, Corrêa, & Lima, 2016). Nesse contexto o γOz é principalmente investigado pelas suas potenciais propriedades anti-inflamatórias e antioxidantes, o que contribui para os seus efeitos nas vias metabólicas relacionadas com a obesidade (Francisqueti et al., 2017; Garcia et al., 2022).

A compreensão da farmacocinética (absorção, distribuição, metabolização e excreção) de compostos usados com finalidade de tratamento e prevenção de doenças, bem como a farmacodinâmica das substâncias funcionais no corpo é de extrema relevância, inclusive porque estudos apontam que a maioria dos efeitos do γOz provém do ácido felúrico, álcool triterpênico, esterol vegetal e seus metabólitos, os quais podem ser gerados pela hidrólise do γOz no organismo, no entanto, o próprio γOz pode atuar

como a substância ativa (Sawada et al., 2019). Assim sendo, esclarecer o comportamento do γOz *in vivo*, permitiria uma compreensão clara das razões pelas quais o mesmo exibe uma variedade de efeitos (Sawada et al., 2019).

A compreensão desse fenômeno é crucial, visto que uma pesquisa que investigou a biodisponibilidade integral da molécula de γOz no plasma de ratos não obteve êxito (Gillespie, 2003), no entanto, em um estudo subsequente, ratos que consumiram farelo de arroz e γOz exibiram elevadas concentrações de compostos fenólicos derivados do γOz e do ácido ferúlico no plasma, na urina e nas fezes. Esses resultados sugerem que a ausência de γOz pode ser atribuída à atividade de esterases no intestino delgado e grosso, levando à clivagem do γO (Perez-Ternero et al., 2017). Em contrapartida, um estudo investigou amostras de plasma de camundongos após a administração oral de um concentrado de γOz a partir de óleo de farelo de arroz purificado, e mostrou que o γOz foi identificado no plasma 5 horas após a administração, evidenciando que parte do γOz administrado oralmente é absorvido pela corrente sanguínea e permanece intacto no plasma nesses animais (Kobayashi et al., 2016).

Estudos complementares são imprescindíveis para aprofundar a compreensão do impacto do farelo de arroz rico em γOz na mitigação dos efeitos adversos da obesidade nos ossos. Essas investigações devem incluir a análise da presença específica dessa molécula, bem como esclarecer se os efeitos observados nas células-tronco do fêmur dos ratos resultaram da ação das moléculas derivadas da clivagem do γOz.

Os modelos *in vitro* desse trabalho que foram estabelecidos com condições de alta lipogênese, tiveram a seleção dos grupos baseada na premissa de manter todas as células em condições equivalentes. Nesse contexto, as células endoteliais e os osteoblastos tratados com meio condicionado por outras células foram mantidos em padrões comparativos justos. Para assegurar uma comparação adequada, o grupo controle recebeu um meio condicionado com condições padrões normais, e, por conseguinte, esse grupo não foi designado como controle puro, consistindo apenas no meio de cultura com 10% de soro fetal bovino.

Este estudo também investigou o impacto do meio enriquecido com titânio em células endoteliais, sem a presença de uma condição *in vitro* de alta lipogênese. Essa abordagem permitiu correlacionar os efeitos do titânio com uma condição mais próxima da fisiologia normal das células, sendo crucial para análises, comparações e discussões, mesmo que tais comparações não sigam padrões comparativos estritos.

Como abordado inicialmente, os implantes de titânio não são completamente inertes, pois durante a interação com o ambiente biológico, os implantes de titânio podem liberar partículas em nanoescala no microambiente ao seu redor (L. Chen et al., 2023). Uma vez liberadas, essas partículas de titânio podem interagir com as células vizinhas e entrar na corrente sanguínea que irriga o tecido, podendo desencadear respostas biológicas nas células e sistemas afetados. Além disso, a superfície do titânio tem uma tendência natural a formar uma camada de óxido, que pode interagir com proteínas e moléculas biológicas (Callejas, Gil, Brizuela, Pérez, & Bosch, 2022).

A quantificação do titânio no meio de cultura foi conduzida antes e após o tratamento das células endoteliais. De maneira intrigante, a concentração de titânio no meio de cultura diminuiu após esse tratamento, indicando a absorção desse metal pelas células. Os mecanismos de absorção de titânio não são tão bem compreendidos quanto os de outros metais mais estudados, no entanto, algumas questões podem ser levantadas: as células podem internalizar partículas de titânio através de processos como endocitose e fagocitose, as partículas de titânio podem adsorver na superfície celular (e, eventualmente, serem internalizadas), alguns transportadores nas membranas celulares poderiam permitir a entrada de titânio. Mas estudos adicionais são necessários para compreender completamente os mecanismos subjacentes à absorção de titânio pelas células (Sansone, Pagani, & Melato, 2013).

Nesse contexto, surgiu a questão sobre a possível interação entre as proteínas celulares com o titânio absorvido. Em um estudo *in silico*, buscando avaliar essa interação, a análise de *docking* molecular foi conduzida para identificar a ligação mais eficiente com aminoácidos, onde foi observado uma forte interação com diversas proteínas celulares, e de maneira mais específica, as nanopartículas de titânio demonstraram interações frequentes com prolina, lisina e leucina (Ranjan, Dasgupta, Sudandiradoss, Ramalingam, & Kumar, 2018). Este mesmo estudo também sustenta que, considerando a energia de ligação e intermolecular, é possível afirmar que a proteína ICAM e P38 formam ligações estáveis com o titânio, sendo que os resultados indicam influência da carga e da polaridade dos grupos R dos aminoácidos nos sítios de ligação (Ranjan et al., 2018). Outro estudo, avaliou a captação de nanopartículas de titânio em célula do cólon humano por citometria de fluxo, discutindo outras técnicas para avaliar essa absorção, como microscopia de fluorescência e potencial zeta. Também realizou abordagem computacional de *docking* molecular revelando a interação do titânio com

proteínas envolvidas no estresse oxidativo (Sod1), metabolismo lipídico (VLDLR) e regulação da apoptose (p53) (Verma et al., 2018).

Os resultados abordados e debatidos fornecem *insights* importantes e suscitam indagações sobre a razão e a consequência das proteínas que demonstram efeitos e resultados mais proeminentes. Para obter percepções relevantes, seria crucial investigar a localização intracelular dessas proteínas, possivelmente por meio de microscopia confocal de fluorescência. Além disso, analisar se essas proteínas interagem com o titânio, por meio de técnicas como *docking* molecular, poderia esclarecer se tal interação interfere no fenótipo e na fisiologia celular. Aprofundar o estudo dos resultados encontrados pode ser capaz de pavimentar caminhos significativos para as próximas fases da pesquisa.

Capítulo 8

CONSTATAÇÕES

Os resultados obtidos durante a execução deste projeto nos permitiram constatar que:

1. Modelo de alta adipogênese *in vitro* com adipócitos é adquirido através da diferenciação celular em condição de alta glicose (50 mM);
2. Meio alta glicose aumenta marcador de estresse oxidativo (carbonilação de proteínas) nos adipócitos 3T3-L1, bem como o tamanho e número de gotículas de lipídeos intracelular;
3. Expressão de genes relacionados com a inflamação e com diferenciação celular são elevados nos adipócitos tratados com 50 mM de glicose;
4. Titânio nHA atenua a alta expressão de VEGFr2 desencadeada pela alta adipogenicidade nas células endoteliais;
5. As MAPKs Erk e JNK são moduladas nas células endoteliais em *crosstalk* com adipócitos e com meio enriquecido com titânio;
6. Gene da interleucina inflamatória IL-6 é altamente expresso nas células endoteliais em condição de adipogênese e com titânio DAE e nHA;
7. A presença de um meio com alta concentração de glicose resulta no aumento na liberação de IL-6 pelos adipócitos derivados das células mesenquimais humanas.
8. Os osteoblastos apresentam gotículas de gordura intracelular quando diferenciados em meio condicionado pelos adipócitos, bem como pelos organoides de fígado e pelos hepatócitos Huh7, e esses resultados são mais intensos pelos organoides.
9. O gene RUNX2 é significativamente elevado nos osteoblastos em *crosstalk* com adipócitos em alta adipogênese e com meio enriquecido com titânio DAE e nHA.
10. BMP7 tem sua expressão gênica elevada expressivamente nos osteoblastos tratados com condição alta adipogênica e titânio nHA.
11. Os osteoblastos apresentam aumento significativo na expressão gênica de osteocalcina quando tratados com meios enriquecidos por titânio DAE e nHA, sendo que a alta adipogênese dos adipócitos reduz esse efeito no titânio DAE.
12. Condição de alta lipogênese do modelo *in vitro* de esteatose hepática com a Huh7 reduz a expressão do gene BGLAP nos osteoblastos, e isso é mais expressivo na presença dos titânios DAE e nHA.
13. Fosforilação de FAK é aumentada nos osteoblastos tratados com titânio nHA.
14. Os genes RUNX2 e BMP2 são inversamente modulados pelas condições de lipogênese da Huh7 e pelas superfícies de titânio DAE e nHA.
15. O titânio nHA em alta lipogênese nos osteoblastos eleva a expressão de RUNX2 em *crosstalk* com adipócitos e Huh7.
16. Fosforilação de CDK2 é reduzida nos osteoblastos na condição de esteatose *in vitro* das Huh7, mas o titânio nHA previne essa redução.

17. A matriz extracelular dos osteoblastos tratados com meios condicionados pelos adipócitos, pelos organoides hepáticos e pelo hepatócito, sofre remodelamento em resposta aos titânios DAE e nHA.
18. A dieta rica em açúcar e gordura desencadeia redução na expressão gênica de PPAR-γ em células mesenquimais do fêmur de ratos;
19. Uma elevada expressão de RUNX2 é observada nas células mesenquimais dos ratos tratados com dieta rica em açúcar e gordura, e mais alto ainda quando adicionado farelo de arroz rico em γ-oryzanol na ração;
20. O gene da osteocalcina (Bglap) é altamente expresso nas células mesenquimais de fêmur dos ratos tratados com dieta rica em açúcar e gordura junto com farelo de arroz.
21. A célula endotelial é capaz de responder diferencialmente às diferentes superfícies de titânio;
22. A sinalização de angiogênese da célula endotelial é modulada pelo meio enriquecido com titânio;
23. Titânio com duplo ataque ácido (*dual acid etching* - DAE) estimula expressão gênica e expressão proteica de AKT nas células endoteliais.;
24. O titânio nHA promove maior proliferação nas células endoteliais observado no ensaio de migração (*wound healing*);
25. Estímulo angiogênico do titânio na célula endotelial é dependente da via PI3K/AKT;
26. Titânio aumenta o remodelamento da matriz extracelular através da atividade elevada da MMP2;

CONCLUSÃO

Mapear as moléculas envolvidas em processos biológicos, especialmente na presença de patologias e síndromes, é uma tarefa complexa. Este estudo forneceu informações valiosas sobre as respostas das células endoteliais e dos osteoblastos ao titânio, delineando as etapas iniciais para a seleção entre DAE e nHA. Essa seleção, baseada em cenários de alta lipogênese, visa estabelecer, nas próximas fases da pesquisa, qual dessas superfícies responde de maneira mais eficaz, potencialmente tornando-se a escolha primária de implante para o público-alvo em questão.

Além disso, este estudo representa um passo inicial na exploração do efeito da alta lipogênese, correlacionando-a com obesidade e doença hepática gordurosa não alcoólica, nas células do ambiente peri-implante em resposta ao titânio. Fornecemos percepções do perfil de expressão gênica em células mesenquimais de fêmur murino no cenário de obesidade, propondo estratégias de tratamento nutracêutico com farelo de arroz. A visão de longo prazo dessa pesquisa é identificar alvos moleculares terapêuticos que possam ser modulados por meio de modificações de superfície, técnicas de revestimento, sistemas de liberação de medicamentos e bioengenharia na produção de implantes biomiméticos (*smart biomaterials*), destinados a esse público alvo.

PERSPECTIVAS FUTURAS

Os resultados obtidos e as pesquisas em andamento continuam a inspirar nosso compromisso com a ciência básica, visando aprofundar nossa compreensão e fornecer bases sólidas para as etapas subsequentes da pesquisa pré-clínica. Pretendemos avançar na aplicação desses conhecimentos na otimização de biomateriais metálicos, explorando técnicas de modificação de superfície, revestimentos e/ou impressão 3D. A meta é desenvolver *smart biomaterials* que incorporam elementos com mecanismos de ação nos alvos terapêuticos identificados ao final deste estudo. Dessa forma, almejamos criar materiais capazes de reduzir danos sistêmicos associados à condição de saúde específica do público-alvo, proporcionando uma recuperação mais rápida e eficaz para restaurar a qualidade de vida.

REFERÊNCIAS BIBLIOGRÁFICAS

Al-Mansoori, L., Al-Jaber, H., Prince, M. S., & Elrayess, M. A. (2022). Role of Inflammatory Cytokines, Growth Factors and Adipokines in Adipogenesis and Insulin Resistance. *Inflammation*, *45*(1), 31–44. https://doi.org/10.1007/s10753-021-01559-z

Al-Radha, A. S. D. (2016). The influence of different acids etch on dental implants titanium surface. *IOSR Journal of Dental and Medical Sciences*, *15*, 87–91. Retrieved from https://api.semanticscholar.org/CorpusID:40647436

Ayada, I., van Kleef, L. A., Zhang, H., Liu, K., Li, P., Abozaid, Y. J., … Pan, Q. (2023). Dissecting the multifaceted impact of statin use on fatty liver disease: a multidimensional study. *EBioMedicine*, *87*, 104392. https://doi.org/10.1016/j.ebiom.2022.104392

Bezerra, F., Ferreira, M. R., Fontes, G. N., da Costa Fernandes, C. J., Andia, D. C., Cruz, N. C., … Zambuzzi, W. F. (2017). Nano hydroxyapatite-blasted titanium surface affects pre-osteoblast morphology by modulating critical intracellular pathways. *Biotechnology and Bioengineering*, *114*(8), 1888–1898. https://doi.org/10.1002/bit.26310

Boden, G. (2008). Obesity and free fatty acids. *Endocrinology and Metabolism Clinics of North America*, *37*(3), 635–646, viii–ix. https://doi.org/10.1016/j.ecl.2008.06.007

Bolamperti, S., Villa, I., & Rubinacci, A. (2022). Bone remodeling: an operational process ensuring survival and bone mechanical competence. *Bone Research*, *10*(1), 48. https://doi.org/10.1038/s41413-022-00219-8

Brasaemle, D. L., Dolios, G., Shapiro, L., & Wang, R. (2004). Proteomic analysis of proteins associated with lipid droplets of basal and lipolytically stimulated 3T3-L1 adipocytes. *The Journal of Biological Chemistry*, *279*(45), 46835–46842. https://doi.org/10.1074/jbc.M409340200

Brockman, D., & Chen, X. (2012). Proteomics in the characterization of adipose dysfunction in obesity. *Adipocyte*, *1*(1), 25–37. https://doi.org/10.4161/adip.19129

Callejas, J. A., Gil, J., Brizuela, A., Pérez, R. A., & Bosch, B. M. (2022). Effect of the Size of Titanium Particles Released from Dental Implants on Immunological Response. *International Journal of Molecular Sciences*, *23*(13). https://doi.org/10.3390/ijms23137333

Cao, J. J. (2011). Effects of obesity on bone metabolism. *Journal of Orthopaedic Surgery and Research*, *6*, 30. https://doi.org/10.1186/1749-799X-6-30

Chattopadhyay, T., Singh, R. R., Gupta, S., & Surolia, A. (2017). Bone morphogenetic protein-7 (BMP-7) augments insulin sensitivity in mice with type II diabetes mellitus by potentiating PI3K/AKT pathway. *BioFactors (Oxford, England)*, *43*(2), 195–209. https://doi.org/10.1002/biof.1334

Chen, D., Walsh, K., & Wang, J. (2000). Regulation of cdk2 activity in endothelial cells that are inhibited from growth by cell contact. *Arteriosclerosis, Thrombosis, and Vascular Biology*, *20*(3), 629–635. https://doi.org/10.1161/01.atv.20.3.629

Chen, L., Tong, Z., Luo, H., Qu, Y., Gu, X., & Si, M. (2023). Titanium particles in peri-implantitis: distribution, pathogenesis and prospects. *International Journal of Oral Science*, *15*(1), 49. https://doi.org/10.1038/s41368-023-00256-x

Chen, W., Xu, K., Tao, B., Dai, L., Yu, Y., Mu, C., … Cai, K. (2018). Multilayered coating of titanium implants promotes coupled osteogenesis and angiogenesis in vitro and in vivo. *Acta Biomaterialia*, *74*, 489–504. https://doi.org/10.1016/j.actbio.2018.04.043

Chen, Y., Ma, B., Wang, X., Zha, X., Sheng, C., Yang, P., & Qu, S. (2021). Potential Functions of the BMP Family in Bone, Obesity, and Glucose Metabolism. *Journal of Diabetes Research*, *2021*, 6707464. https://doi.org/10.1155/2021/6707464

Cheng, K. Y., Ball, S. T., Gonzales, F. B., Schenk, S., & Hughes-Austin, J. M. (2020). Metabolic Syndrome Is Associated With Higher Risk of Wound Complications After Total Hip Arthroplasty. *Arthroplasty Today*, *6*(3), 571–577. https://doi.org/10.1016/j.artd.2020.06.010

Cho, S. Y., Shin, E. S., Park, P. J., Shin, D. W., Chang, H. K., Kim, D., … Lee, T. R. (2007). Identification of mouse Prp19p as a lipid droplet-associated protein and its possible involvement in the biogenesis of lipid droplets. *The Journal of Biological Chemistry*, *282*(4), 2456–2465. https://doi.org/10.1074/jbc.M608042200

Coelho, M., Oliveira, T., & Fernandes, R. (2013). Biochemistry of adipose tissue: an endocrine organ. *Archives of Medical Science : AMS*, *9*(2), 191–200. https://doi.org/10.5114/aoms.2013.33181

Coelho, P. G., Pippenger, B., Tovar, N., Koopmans, S.-J., Plana, N. M., Graves, D. T., … Dard, M. (2018). Effect of Obesity or Metabolic Syndrome and Diabetes on Osseointegration of Dental Implants in a Miniature Swine Model: A Pilot Study. *Journal of Oral and Maxillofacial Surgery : Official Journal of the American Association of Oral and Maxillofacial Surgeons*, *76*(8), 1677–1687. https://doi.org/10.1016/j.joms.2018.02.021

Cuevas, A. M., Clark, J. M., & Potter, J. J. (2021). Increased TLR/MyD88 signaling in patients with obesity: is there a link to COVID-19 disease severity? *International Journal of Obesity (2005)*, *45*(5), 1152–1154. https://doi.org/10.1038/s41366-021-00768-8

da Costa Fernandes, C. J., Bezerra, F. J. B., de Campos Souza, B., Campos, M. A., & Zambuzzi, W. F. (2018). Titanium-enriched medium drives low profile of ECM remodeling as a pre-requisite to pre-osteoblast viability and proliferative phenotype. *Journal of Trace Elements in Medicine and Biology*, *50*(July), 339–346. https://doi.org/10.1016/j.jtemb.2018.07.015

da Costa Fernandes, C. J., Ferreira, M. R., Bezerra, F. J. B., & Zambuzzi, W. F. (2018). Zirconia stimulates ECM-remodeling as a prerequisite to pre-osteoblast adhesion/proliferation by possible interference with cellular anchorage. *Journal of Materials Science. Materials in Medicine*, *29*(4), 41. https://doi.org/10.1007/s10856-018-6041-9

da Silva, R. A., da Silva Feltran, G., Ferreira, M. R., Wood, P. F., Bezerra, F., & Zambuzzi, W. F. (2020). The Impact of Bioactive Surfaces in the Early Stages of Osseointegration: An In Vitro Comparative Study Evaluating the HAnano® and

SLActive® Super Hydrophilic Surfaces. *BioMed Research International, 2020*, 3026893. https://doi.org/10.1155/2020/3026893

Davis, R., Singh, A., Jackson, M. J., Coelho, R. T., Prakash, D., Charalambous, C. P., … Lawrence, A. A. (2022). A comprehensive review on metallic implant biomaterials and their subtractive manufacturing. *The International Journal, Advanced Manufacturing Technology*, *120*(3–4), 1473–1530. https://doi.org/10.1007/s00170-022-08770-8

de Oliveira, P. G. F. P., Bonfante, E. A., Bergamo, E. T. P., de Souza, S. L. S., Riella, L., Torroni, A., … Coelho, P. G. (2020). Obesity/Metabolic Syndrome and Diabetes Mellitus on Peri-implantitis. *Trends in Endocrinology and Metabolism: TEM*. https://doi.org/10.1016/j.tem.2020.05.005

dela Paz, N. G., Walshe, T. E., Leach, L. L., Saint-Geniez, M., & D'Amore, P. A. (2012). Role of shear-stress-induced VEGF expression in endothelial cell survival. *Journal of Cell Science*, *125*(4), 831–843. https://doi.org/10.1242/jcs.084301

Engin, A. (2017). The Definition and Prevalence of Obesity and Metabolic Syndrome. *Advances in Experimental Medicine and Biology*, *960*, 1–17. https://doi.org/10.1007/978-3-319-48382-5_1

Everts, P. A., Lana, J. F., Onishi, K., Buford, D., Peng, J., Mahmood, A., … Podesta, L. (2023). Angiogenesis and Tissue Repair Depend on Platelet Dosing and Bioformulation Strategies Following Orthobiological Platelet-Rich Plasma Procedures: A Narrative Review. *Biomedicines*, *11*(7). https://doi.org/10.3390/biomedicines11071922

Fabbrini, E., Sullivan, S., & Klein, S. (2010). Obesity and nonalcoholic fatty liver disease: biochemical, metabolic, and clinical implications. *Hepatology (Baltimore, Md.)*, *51*(2), 679–689. https://doi.org/10.1002/hep.23280

Fahed, G., Aoun, L., Bou Zerdan, M., Allam, S., Bou Zerdan, M., Bouferraa, Y., & Assi, H. I. (2022). Metabolic Syndrome: Updates on Pathophysiology and Management in 2021. *International Journal of Molecular Sciences*, *23*(2). https://doi.org/10.3390/ijms23020786

Feijóo-Bandín, S., Aragón-Herrera, A., Moraña-Fernández, S., Anido-Varela, L., Tarazón, E., Roselló-Lletí, E., … Lago, F. (2020). Adipokines and Inflammation: Focus on Cardiovascular Diseases. *International Journal of Molecular Sciences*, *21*(20). https://doi.org/10.3390/ijms21207711

Fernandes, C J C, Bezerra, F., das D do Carmo, M., Feltran, G. S., Rossi, M. C., da Silva, R. A., … Zambuzzi, W. (2018). CoCr-enriched medium modulates integrin-based downstream signaling and requires a set of inflammatory genes reprograming in vitro. *Journal of Biomedical Materials Research. Part A*, *106 3*, 839–849.

Fernandes, Celio J C, Bezerra, F., Ferreira, M. R., Andrade, A. F. C., Pinto, T. S., & Zambuzzi, W. F. (2018). Nano hydroxyapatite-blasted titanium surface creates a biointerface able to govern Src-dependent osteoblast metabolism as prerequisite to ECM remodeling. *Colloids and Surfaces. B, Biointerfaces*, *163*, 321–328. https://doi.org/10.1016/j.colsurfb.2017.12.049

Florencio-Silva, R., Sasso, G. R. da S., Sasso-Cerri, E., Simões, M. J., & Cerri, P. S. (2015). Biology of Bone Tissue: Structure, Function, and Factors That Influence

Bone Cells. *BioMed Research International*, *2015*, 421746. https://doi.org/10.1155/2015/421746

Forte, Y. S., Renovato-Martins, M., & Barja-Fidalgo, C. (2023). Cellular and Molecular Mechanisms Associating Obesity to Bone Loss. *Cells*, *12*(4). https://doi.org/10.3390/cells12040521

Francisqueti, F. V, Minatel, I. O., Ferron, A. J., Bazan, S. G., Silva, V. D., Garcia, J. L., … Corrêa, C. R. (2017). Effect of Gamma-Oryzanol as Therapeutic Agent to Prevent Cardiorenal Metabolic Syndrome in Animals Submitted to High Sugar-Fat Diet. *Nutrients*, Vol. 9. https://doi.org/10.3390/nu9121299

Frühbeck, G., Méndez-Giménez, L., Fernández-Formoso, J.-A., Fernández, S., & Rodríguez, A. (2014). Regulation of adipocyte lipolysis. *Nutrition Research Reviews*, *27*(1), 63–93. https://doi.org/10.1017/S095442241400002X

Fujimoto, T., & Parton, R. G. (2011). Not just fat: the structure and function of the lipid droplet. *Cold Spring Harbor Perspectives in Biology*, *3*(3). https://doi.org/10.1101/cshperspect.a004838

Garcia, J. L., Vileigas, D. F., Gregolin, C. S., Costa, M. R., Francisqueti-Ferron, F. V., Ferron, A. J. T., … Corrêa, C. R. (2022). Rice (Oryza sativa L.) bran preserves cardiac function by modulating pro-inflammatory cytokines and redox state in the myocardium from obese rats. *European Journal of Nutrition*, *61*(2), 901–913. https://doi.org/10.1007/s00394-021-02691-0

Gillespie, M. S. (2003). *METABOLIC ASPECTS OF ORYZANOL IN RATS by*. (May).

Girón, J., Kerstner, E., Medeiros, T., Oliveira, L., Machado, G. M., Malfatti, C. F., & Pranke, P. (2021). Biomaterials for bone regeneration: an orthopedic and dentistry overview. *Brazilian Journal of Medical and Biological Research = Revista Brasileira de Pesquisas Medicas e Biologicas*, *54*(9), e11055. https://doi.org/10.1590/1414-431X2021e11055

Gittens, R. A., Olivares-Navarrete, R., Schwartz, Z., & Boyan, B. D. (2014). Implant osseointegration and the role of microroughness and nanostructures: lessons for spine implants. *Acta Biomaterialia*, *10*(8), 3363–3371. https://doi.org/10.1016/j.actbio.2014.03.037

Givens, C., & Tzima, E. (2016). Endothelial Mechanosignaling: Does One Sensor Fit All? *Antioxidants & Redox Signaling*, *25*(7), 373–388. https://doi.org/10.1089/ars.2015.6493

Gkastaris, K., Goulis, D. G., Potoupnis, M., Anastasilakis, A. D., & Kapetanos, G. (2020). Obesity, osteoporosis and bone metabolism. *Journal of Musculoskeletal & Neuronal Interactions*, *20*(3), 372–381.

González-Muniesa, P., Mártinez-González, M.-A., Hu, F. B., Després, J.-P., Matsuzawa, Y., Loos, R. J. F., … Martinez, J. A. (2017). Obesity. *Nature Reviews Disease Primers*, *3*(1), 17034. https://doi.org/10.1038/nrdp.2017.34

Greco, E. A., Lenzi, A., & Migliaccio, S. (2015). The obesity of bone. *Therapeutic Advances in Endocrinology and Metabolism*, *6*(6), 273–286. https://doi.org/10.1177/2042018815611004

Green, C. J., Pramfalk, C., Morten, K. J., & Hodson, L. (2015). From whole body to cellular models of hepatic triglyceride metabolism: man has got to know his

limitations. *American Journal of Physiology. Endocrinology and Metabolism*, *308*(1), E1-20. https://doi.org/10.1152/ajpendo.00192.2014

Guiu-Jurado, E., Unthan, M., Böhler, N., Kern, M., Landgraf, K., Dietrich, A., … Blüher, M. (2016). Bone morphogenetic protein 2 (BMP2) may contribute to partition of energy storage into visceral and subcutaneous fat depots. *Obesity (Silver Spring, Md.)*, *24*(10), 2092–2100. https://doi.org/10.1002/oby.21571

Guo, S., & Dipietro, L. A. (2010). Factors affecting wound healing. *Journal of Dental Research*, *89*(3), 219–229. https://doi.org/10.1177/0022034509359125

Hang, T.-C., Tedford, N. C., Reddy, R. J., Rimchala, T., Wells, A., White, F. M., … Lauffenburger, D. A. (2013). Vascular endothelial growth factor (VEGF) and platelet (PF-4) factor 4 inputs modulate human microvascular endothelial signaling in a three-dimensional matrix migration context. *Molecular & Cellular Proteomics : MCP*, *12*(12), 3704–3718. https://doi.org/10.1074/mcp.M113.030528

Hausman, D. B., DiGirolamo, M., Bartness, T. J., Hausman, G. J., & Martin, R. J. (2001). The biology of white adipocyte proliferation. *Obesity Reviews : An Official Journal of the International Association for the Study of Obesity*, *2*(4), 239–254. https://doi.org/10.1046/j.1467-789x.2001.00042.x

Horwitz, A., & Birk, R. (2023). Adipose Tissue Hyperplasia and Hypertrophy in Common and Syndromic Obesity-The Case of BBS Obesity. *Nutrients*, *15*(15). https://doi.org/10.3390/nu15153445

Hu, G., Place, A. T., & Minshall, R. D. (2008). Regulation of endothelial permeability by Src kinase signaling: vascular leakage versus transcellular transport of drugs and macromolecules. *Chemico-Biological Interactions*, *171*(2), 177–189. https://doi.org/10.1016/j.cbi.2007.08.006

Huang-Doran, I., Zhang, C.-Y., & Vidal-Puig, A. (2017). Extracellular Vesicles: Novel Mediators of Cell Communication In Metabolic Disease. *Trends in Endocrinology and Metabolism: TEM*, *28*(1), 3–18. https://doi.org/10.1016/j.tem.2016.10.003

Huang, P. L. (2009). A comprehensive definition for metabolic syndrome. *Disease Models & Mechanisms*, *2*(5–6), 231–237. https://doi.org/10.1242/dmm.001180

Hung, K.-Y., Lin, Y.-C., & Feng, H.-P. (2017). The Effects of Acid Etching on the Nanomorphological Surface Characteristics and Activation Energy of Titanium Medical Materials. *Materials (Basel, Switzerland)*, *10*(10). https://doi.org/10.3390/ma10101164

I, T., Noda, S., Ohba, S., Asahina, I., & Sumita, Y. (2023). First-in-Human Study to Investigate the Safety Assessment of Peri-Implant Soft Tissue Regeneration with Micronized-Gingival Connective Tissue: A Pilot Case Series Study. *Medicines*, Vol. 10. https://doi.org/10.3390/medicines10010009

Ibrahim, A., & Arany, Z. (2017, April). Does Endothelium Buffer Fat? *Circulation Research*, Vol. 120, pp. 1219–1221. https://doi.org/10.1161/CIRCRESAHA.117.310865

Ipsen, D. H., Lykkesfeldt, J., & Tveden-Nyborg, P. (2018). Molecular mechanisms of hepatic lipid accumulation in non-alcoholic fatty liver disease. *Cellular and Molecular Life Sciences : CMLS*, *75*(18), 3313–3327. https://doi.org/10.1007/s00018-018-2860-6

Jung, U. J., & Choi, M.-S. (2014). Obesity and its metabolic complications: the role of adipokines and the relationship between obesity, inflammation, insulin resistance, dyslipidemia and nonalcoholic fatty liver disease. *International Journal of Molecular Sciences*, *15*(4), 6184–6223. https://doi.org/10.3390/ijms15046184

Kanakaris, N. K., Petsatodis, G., Tagil, M., & Giannoudis, P. V. (2009). Is there a role for bone morphogenetic proteins in osteoporotic fractures? *Injury*, *40 Suppl 3*, S21-6. https://doi.org/10.1016/S0020-1383(09)70007-5

Kanazawa, I. (2015). Osteocalcin as a hormone regulating glucose metabolism. *World Journal of Diabetes*, *6*(18), 1345–1354. https://doi.org/10.4239/wjd.v6.i18.1345

Khosravi, N., Maeda, A., DaCosta, R. S., & Davies, J. E. (2018). Nanosurfaces modulate the mechanism of peri-implant endosseous healing by regulating neovascular morphogenesis. *Communications Biology*, *1*, 72. https://doi.org/10.1038/s42003-018-0074-y

Khoswanto, C. (2023). Role of matrix metalloproteinases in bone regeneration: Narrative review. *Journal of Oral Biology and Craniofacial Research*, *13*(5), 539–543. https://doi.org/10.1016/j.jobcr.2023.06.002

Kim, H. Y., Choe, J. W., Kim, H. K., Bae, S. J., Kim, B. J., Lee, S. H., … Kim, G. S. (2010). Negative association between metabolic syndrome and bone mineral density in Koreans, especially in men. *Calcified Tissue International*, *86*(5), 350–358. https://doi.org/10.1007/s00223-010-9347-2

Kim, J.-Y., van de Wall, E., Laplante, M., Azzara, A., Trujillo, M. E., Hofmann, S. M., … Scherer, P. E. (2007). Obesity-associated improvements in metabolic profile through expansion of adipose tissue. *The Journal of Clinical Investigation*, *117*(9), 2621–2637. https://doi.org/10.1172/JCI31021

Kitamura, T., Asai, N., Enomoto, A., Maeda, K., Kato, T., Ishida, M., … Takahashi, M. (2008). Regulation of VEGF-mediated angiogenesis by the Akt/PKB substrate Girdin. *Nature Cell Biology*, *10*(3), 329–337. https://doi.org/10.1038/ncb1695

Kobayashi, E., Ito, J., Kato, S., Sawada, K., Matsuki, M., Hashimoto, H., … Nakagawa, K. (2016). Presence of orally administered rice bran oil γ-oryzanol in its intact form in mouse plasma. *Food & Function*, *7*(12), 4816–4822. https://doi.org/10.1039/c6fo01552b

Konige, M., Wang, H., & Sztalryd, C. (2014). Role of adipose specific lipid droplet proteins in maintaining whole body energy homeostasis. *Biochimica et Biophysica Acta*, *1842*(3), 393–401. https://doi.org/10.1016/j.bbadis.2013.05.007

Kraus, N. A., Ehebauer, F., Zapp, B., Rudolphi, B., Kraus, B. J., & Kraus, D. (2016). Quantitative assessment of adipocyte differentiation in cell culture. *Adipocyte*, *5*(4), 351–358. https://doi.org/10.1080/21623945.2016.1240137

Kuo, A., Lee, M. Y., & Sessa, W. C. (2017). Lipid Droplet Biogenesis and Function in the Endothelium. *Circulation Research*, *120*(8), 1289–1297. https://doi.org/10.1161/CIRCRESAHA.116.310498

Kusumbe, A. P., Ramasamy, S. K., & Adams, R. H. (2014). Coupling of angiogenesis and osteogenesis by a specific vessel subtype in bone. *Nature*, *507*(7492), 323–328. https://doi.org/10.1038/nature13145

Larsson, P., Ulfhammer, E., Karlsson, L., Bokarewa, M., Wåhlander, K., & Jern, S.

(2008). Effects of IL-1beta and IL-6 on tissue-type plasminogen activator expression in vascular endothelial cells. *Thrombosis Research*, *123*(2), 342–351. https://doi.org/10.1016/j.thromres.2008.03.013

Lehoux, S., & Tedgui, A. (2003). Cellular mechanics and gene expression in blood vessels. *Journal of Biomechanics*, *36*(5), 631–643.

Lemieux, I., & Després, J.-P. (2020, November). Metabolic Syndrome: Past, Present and Future. *Nutrients*, Vol. 12. https://doi.org/10.3390/nu12113501

Leonardini, A., Laviola, L., Perrini, S., Natalicchio, A., & Giorgino, F. (2009). Cross-Talk between PPARgamma and Insulin Signaling and Modulation of Insulin Sensitivity. *PPAR Research, 2009*, 818945. https://doi.org/10.1155/2009/818945

Li, H., Luo, H., Zhang, Y., Liu, L., & Lin, R. (2022). Association of Metabolic Dysfunction-Associated Fatty Liver Disease and Liver Stiffness With Bone Mineral Density in American Adults. *Frontiers in Endocrinology*, *13*, 891382. https://doi.org/10.3389/fendo.2022.891382

Li, J., Gao, Y., Yu, T., Lange, J. K., LeBoff, M. S., Gorska, A., … Glowacki, J. (2020). Obesity and leptin influence vitamin D metabolism and action in human marrow stromal cells. *The Journal of Steroid Biochemistry and Molecular Biology*, *198*, 105564. https://doi.org/10.1016/j.jsbmb.2019.105564

Li, M., Qian, M., Kyler, K., & Xu, J. (2021). Adipose Tissue-Endothelial Cell Interactions in Obesity-Induced Endothelial Dysfunction. *Frontiers in Cardiovascular Medicine*, *8*, 681581. https://doi.org/10.3389/fcvm.2021.681581

Li, W., Xu, P., Wang, C., Ha, X., Gu, Y., Wang, Y., … Xie, J. (2017). The effects of fat-induced obesity on bone metabolism in rats. *Obesity Research & Clinical Practice*, *11*(4), 454–463. https://doi.org/10.1016/j.orcp.2016.12.001

Lin, A., Wang, C. J., Kelly, J., Gubbi, P., & Nishimura, I. (2009). The role of titanium implant surface modification with hydroxyapatite nanoparticles in progressive early bone-implant fixation in vivo. *The International Journal of Oral & Maxillofacial Implants*, *24*(5), 808–816.

Lin, X., & Li, H. (2021). Obesity: Epidemiology, Pathophysiology, and Therapeutics. *Frontiers in Endocrinology*, *12*. https://doi.org/10.3389/fendo.2021.706978

Liu, L.-F., Shen, W.-J., Zhang, Z. H., Wang, L. J., & Kraemer, F. B. (2010). Adipocytes decrease Runx2 expression in osteoblastic cells: roles of PPARγ and adiponectin. *Journal of Cellular Physiology*, *225*(3), 837–845. https://doi.org/10.1002/jcp.22291

Liu, T., Zhang, L., Joo, D., & Sun, S.-C. (2017). NF-κB signaling in inflammation. *Signal Transduction and Targeted Therapy*, *2*, 17023-. https://doi.org/10.1038/sigtrans.2017.23

Loosen, S. H., Roderburg, C., Demir, M., Qvartskhava, N., Keitel, V., Kostev, K., & Luedde, T. (2022). Non-alcoholic fatty liver disease (NAFLD) is associated with an increased incidence of osteoporosis and bone fractures. *Zeitschrift Fur Gastroenterologie*, *60*(8), 1221–1227. https://doi.org/10.1055/a-1482-9236

Luo, L., & Liu, M. (2016). Adipose tissue in control of metabolism. *The Journal of Endocrinology*, *231*(3), R77–R99. https://doi.org/10.1530/JOE-16-0211

Machado, M. V., & Cortez-Pinto, H. (2023). NAFLD, MAFLD and obesity: brothers in arms? *Nature Reviews. Gastroenterology & Hepatology*, *20*(2), 67–68.

https://doi.org/10.1038/s41575-022-00717-4

Martínez-Martínez, E., Souza-Neto, F. V, Jiménez-González, S., & Cachofeiro, V. (2021). Oxidative Stress and Vascular Damage in the Context of Obesity: The Hidden Guest. *Antioxidants (Basel, Switzerland)*, *10*(3). https://doi.org/10.3390/antiox10030406

Minatel, I. O., Francisqueti, F. V., Corrêa, C. R., & Lima, G. P. P. (2016). Antioxidant Activity of γ-Oryzanol: A Complex Network of Interactions. *International Journal of Molecular Sciences*, *17*(8). https://doi.org/10.3390/ijms17081107

Miniewska, K., Godzien, J., Mojsak, P., Maliszewska, K., Kretowski, A., & Ciborowski, M. (2020). Mass spectrometry-based determination of lipids and small molecules composing adipose tissue with a focus on brown adipose tissue. *Journal of Pharmaceutical and Biomedical Analysis*, *191*, 113623. https://doi.org/https://doi.org/10.1016/j.jpba.2020.113623

Monteiro, J. L. G. C., Pellizzer, E. P., Araújo Lemos, C. A., de Moraes, S. L. D., & do Egito Vasconcelos, B. C. (2019). Is there an association between overweight/obesity and dental implant complications? A systematic review and meta-analysis. *International Journal of Oral and Maxillofacial Surgery*, *48*(9), 1241–1249. https://doi.org/https://doi.org/10.1016/j.ijom.2019.01.015

Müller, F. A., & Sturla, S. J. (2019). Human in vitro models of nonalcoholic fatty liver disease. *Current Opinion in Toxicology*, *16*, 9–16. https://doi.org/https://doi.org/10.1016/j.cotox.2019.03.001

Nandy, A., Helderman, R. C. M., Thapa, S., Jayapalan, S., Richards, A., Narayani, N., … Rendina-Ruedy, E. (2023). Lipolysis supports bone formation by providing osteoblasts with endogenous fatty acid substrates to maintain bioenergetic status. *Bone Research*, *11*(1), 62. https://doi.org/10.1038/s41413-023-00297-2

Nandy, A., Richards, A., Thapa, S., Akhmetshina, A., Narayani, N., & Rendina-Ruedy, E. (2023). Altered Osteoblast Metabolism with Aging Results in Lipid Accumulation and Oxidative Stress Mediated Bone Loss. *Aging and Disease*. https://doi.org/10.14336/AD.2023.0510

Newberry, E. P., Hall, Z., Xie, Y., Molitor, E. A., Bayguinov, P. O., Strout, G. W., … Davidson, N. O. (2021). Liver-Specific Deletion of Mouse Tm6sf2 Promotes Steatosis, Fibrosis, and Hepatocellular Cancer. *Hepatology (Baltimore, Md.)*, *74*(3), 1203–1219. https://doi.org/10.1002/hep.31771

Nuttall, F. Q. (2015). Body Mass Index: Obesity, BMI, and Health: A Critical Review. *Nutrition Today*, *50*(3), 117–128. https://doi.org/10.1097/NT.0000000000000092

Ootsuka, T., Nakanishi, A., & Tsukamoto, I. (2015). Increase in osteoclastogenesis in an obese Otsuka Long-Evans Tokushima fatty rat model. *Molecular Medicine Reports*, *12*(3), 3874–3880. https://doi.org/10.3892/mmr.2015.3811

Oshida, Y., Tuna, E. B., Aktören, O., & Gençay, K. (2010). Dental implant systems. *International Journal of Molecular Sciences*, *11*(4), 1580–1678. https://doi.org/10.3390/ijms11041580

Oury, F., Yadav, V. K., Wang, Y., Zhou, B., Liu, X. S., Guo, X. E., … Karsenty, G. (2010). CREB mediates brain serotonin regulation of bone mass through its expression in ventromedial hypothalamic neurons. *Genes & Development*, *24*(20),

2330–2342. https://doi.org/10.1101/gad.1977210

Pacheco-Pantoja, E. L., Fraser, W. D., Wilson, P. J. M., & Gallagher, J. A. (2014). Differential effects of adiponectin in osteoblast-like cells. *Journal of Receptor and Signal Transduction Research*, *34*(5), 351–360. https://doi.org/10.3109/10799893.2014.898658

Pacia, M. Z., Majzner, K., Czamara, K., Sternak, M., Chlopicki, S., & Baranska, M. (2020). Estimation of the content of lipids composing endothelial lipid droplets based on Raman imaging. *Biochimica et Biophysica Acta (BBA) - Molecular and Cell Biology of Lipids*, *1865*(9), 158758. https://doi.org/https://doi.org/10.1016/j.bbalip.2020.158758

Palacios-Ortega, S., Varela-Guruceaga, M., Martínez, J. A., de Miguel, C., & Milagro, F. I. (2016). Effects of high glucose on caveolin-1 and insulin signaling in 3T3-L1 adipocytes. *Adipocyte*, *5*(1), 65–80. https://doi.org/10.1080/21623945.2015.1122856

Paschos, P., & Paletas, K. (2009). Non alcoholic fatty liver disease and metabolic syndrome. *Hippokratia*, *13*(1), 9–19.

Pellegrinelli, V., Rouault, C., Veyrie, N., Clément, K., & Lacasa, D. (2014). Endothelial cells from visceral adipose tissue disrupt adipocyte functions in a three-dimensional setting: partial rescue by angiopoietin-1. *Diabetes*, *63*(2), 535–549. https://doi.org/10.2337/db13-0537

Perera, N., Ritchie, R. H., & Tate, M. (2020). The Role of Bone Morphogenetic Proteins in Diabetic Complications. *ACS Pharmacology & Translational Science*, *3*(1), 11–20. https://doi.org/10.1021/acsptsci.9b00064

Perez-Ternero, C., Macià, A., de Sotomayor, M. A., Parrado, J., Motilva, M.-J., & Herrera, M.-D. (2017). Bioavailability of the ferulic acid-derived phenolic compounds of a rice bran enzymatic extract and their activity against superoxide production. *Food & Function*, *8*(6), 2165–2174. https://doi.org/10.1039/c7fo00243b

Perseghin, G., Ghosh, S., Gerow, K., & Shulman, G. I. (1997). Metabolic defects in lean nondiabetic offspring of NIDDM parents: a cross-sectional study. *Diabetes*, *46*(6), 1001–1009. https://doi.org/10.2337/diab.46.6.1001

Pinto, T. S., Fernandes, C. J. da C., da Silva, R. A., Gomes, A. M., Vieira, J. C. S., Padilha, P. de M., & Zambuzzi, W. F. (2019). c-Src kinase contributes on endothelial cells mechanotransduction in a heat shock protein 70-dependent turnover manner. *Journal of Cellular Physiology*, *234*(7), 11287–11303. https://doi.org/10.1002/jcp.27787

Pinto, T. S., Gomes, A. M., de Morais, P. B., & Zambuzzi, W. F. (2023). Adipogenesis-Related Metabolic Condition Affects Shear-Stressed Endothelial Cells Activity Responding to Titanium. *Journal of Functional Biomaterials*, *14*(3). https://doi.org/10.3390/jfb14030162

Pouwels, S., Sakran, N., Graham, Y., Leal, A., Pintar, T., Yang, W., … Ramnarain, D. (2022). Non-alcoholic fatty liver disease (NAFLD): a review of pathophysiology, clinical management and effects of weight loss. *BMC Endocrine Disorders*, *22*(1), 63. https://doi.org/10.1186/s12902-022-00980-1

Raines, A. L., Berger, M. B., Patel, N., Hyzy, S. L., Boyan, B. D., & Schwartz, Z. (2019).

VEGF-A regulates angiogenesis during osseointegration of Ti implants via paracrine/autocrine regulation of osteoblast response to hierarchical microstructure of the surface. *Journal of Biomedical Materials Research. Part A*, *107*(2), 423–433. https://doi.org/10.1002/jbm.a.36559

Ramasamy, S. K., Kusumbe, A. P., Schiller, M., Zeuschner, D., Bixel, M. G., Milia, C., … Adams, R. H. (2016). Blood flow controls bone vascular function and osteogenesis. *Nature Communications*, *7*, 1–13. https://doi.org/10.1038/ncomms13601

Ranjan, S., Dasgupta, N., Sudandiradoss, C., Ramalingam, C., & Kumar, A. (2018). Titanium dioxide nanoparticle-protein interaction explained by docking approach. *International Journal of Nanomedicine*, *13*(T-NANO 2014 Abstracts), 47–50. https://doi.org/10.2147/IJN.S125008

Rossi, M. C., Bezerra, F. J. B., Silva, R. A., Crulhas, B. P., Fernandes, C. J. C., Nascimento, A. S., … Zambuzzi, W. F. (2017). Titanium-released from dental implant enhances pre-osteoblast adhesion by ROS modulating crucial intracellular pathways. *Journal of Biomedical Materials Research. Part A*, *105*(11), 2968–2976. https://doi.org/10.1002/jbm.a.36150

Ruiz-Ojeda, F. J., Méndez-Gutiérrez, A., Aguilera, C. M., & Plaza-Díaz, J. (2019). Extracellular Matrix Remodeling of Adipose Tissue in Obesity and Metabolic Diseases. *International Journal of Molecular Sciences*, *20*(19). https://doi.org/10.3390/ijms20194888

Saini, S., Duraisamy, A. J., Bayen, S., Vats, P., & Singh, S. B. (2015). Role of BMP7 in appetite regulation, adipogenesis, and energy expenditure. *Endocrine*, *48*(2), 405–409. https://doi.org/10.1007/s12020-014-0406-8

Sangro, P., de la Torre Aláez, M., Sangro, B., & D'Avola, D. (2023). Metabolic dysfunction-associated fatty liver disease (MAFLD): an update of the recent advances in pharmacological treatment. *Journal of Physiology and Biochemistry*, *79*(4), 869–879. https://doi.org/10.1007/s13105-023-00954-4

Sansone, V., Pagani, D., & Melato, M. (2013). The effects on bone cells of metal ions released from orthopaedic implants. A review. *Clinical Cases in Mineral and Bone Metabolism : The Official Journal of the Italian Society of Osteoporosis, Mineral Metabolism, and Skeletal Diseases*, *10*(1), 34–40. https://doi.org/10.11138/ccmbm/2013.10.1.034

Sartoretto, S. C., Calasans-Maia, J., Resende, R., Câmara, E., Ghiraldini, B., Barbosa Bezerra, F. J., … Calasans-Maia, M. D. (2020). The Influence of Nanostructured Hydroxyapatite Surface in the Early Stages of Osseointegration: A Multiparameter Animal Study in Low-Density Bone. *International Journal of Nanomedicine*, *15*, 8803–8817. https://doi.org/10.2147/IJN.S280957

Sawada, K., Rahmania, H., Matsuki, M., Hashimoto, H., Ito, J., Miyazawa, T., & Nakagawa, K. (2019). Absorption and Metabolism of γ-Oryzanol, a Characteristic Functional Ingredient in Rice Bran. *Journal of Nutritional Science and Vitaminology*, *65*(Supplement), S180–S184. https://doi.org/10.3177/jnsv.65.S180

Schreiber, I., Dörpholz, G., Ott, C.-E., Kragesteen, B., Schanze, N., Lee, C. T., … Knaus, P. (2017). BMPs as new insulin sensitizers: enhanced glucose uptake in mature 3T3-

L1 adipocytes via PPARγ and GLUT4 upregulation. *Scientific Reports*, *7*(1), 17192. https://doi.org/10.1038/s41598-017-17595-5

Shaikh, A., Wesner, A. A., Abuhattab, M., Kutty, R. G., & Premnath, P. (2023). Cell cycle regulators and bone: development and regeneration. *Cell & Bioscience*, *13*(1), 35. https://doi.org/10.1186/s13578-023-00988-7

Shibuya, M. (2011). Vascular Endothelial Growth Factor (VEGF) and Its Receptor (VEGFR) Signaling in Angiogenesis: A Crucial Target for Anti- and Pro-Angiogenic Therapies. *Genes & Cancer*, *2*(12), 1097–1105. https://doi.org/10.1177/1947601911423031

Sidambe, A. T. (2014). Biocompatibility of Advanced Manufactured Titanium Implants-A Review. *Materials (Basel, Switzerland)*, *7*(12), 8168–8188. https://doi.org/10.3390/ma7128168

Somanath, P. R., Razorenova, O. V, Chen, J., & Byzova, T. V. (2006). Akt1 in endothelial cell and angiogenesis. *Cell Cycle (Georgetown, Tex.)*, *5*(5), 512–518. https://doi.org/10.4161/cc.5.5.2538

Stahl, A. (2004). A current review of fatty acid transport proteins (SLC27). *Pflugers Archiv : European Journal of Physiology*, *447*(5), 722–727. https://doi.org/10.1007/s00424-003-1106-z

Suzuki, Y. J., Carini, M., & Butterfield, D. A. (2010, March). Protein carbonylation. *Antioxidants & Redox Signaling*, Vol. 12, pp. 323–325. https://doi.org/10.1089/ars.2009.2887

Thiriet, M. (2018). Hyperlipidemias and Obesity. *Vasculopathies: Behavioral, Chemical, Environmental, and Genetic Factors*, Vol. 8, pp. 331–548. https://doi.org/10.1007/978-3-319-89315-0_5

Tran, V., Brettle, H., Diep, H., Dinh, Q. N., O'Keeffe, M., Fanson, K. V, … Jelinic, M. (2023). Sex-specific effects of a high fat diet on aortic inflammation and dysfunction. *Scientific Reports*, *13*(1), 21644. https://doi.org/10.1038/s41598-023-47903-1

Tükel, H. C., & Delilbaşı, E. (2019). Effects of metabolic syndrome on jawbones and bone metabolic markers in sucrose-fed rats. *Odontology*, *107*(4), 457–464. https://doi.org/10.1007/s10266-019-00422-w

van der Vusse, G. J., van Bilsen, M., Glatz, J. F. C., Hasselbaink, D. M., & Luiken, J. J. F. P. (2002). Critical steps in cellular fatty acid uptake and utilization. *Molecular and Cellular Biochemistry*, *239*(1–2), 9–15. https://doi.org/10.1007/978-1-4419-9270-3_2

Verma, S. K., Jha, E., Panda, P. K., Thirumurugan, A., Parashar, S. K. S., Patro, S., & Suar, M. (2018). Mechanistic Insight into Size-Dependent Enhanced Cytotoxicity of Industrial Antibacterial Titanium Oxide Nanoparticles on Colon Cells Because of Reactive Oxygen Species Quenching and Neutral Lipid Alteration. *ACS Omega*, *3*(1), 1244–1262. https://doi.org/10.1021/acsomega.7b01522

Wang, T., He, C., & Yu, X. (2017). Pro-Inflammatory Cytokines: New Potential Therapeutic Targets for Obesity-Related Bone Disorders. *Current Drug Targets*, *18*(14), 1664–1675. https://doi.org/10.2174/1389450118666170104153512

Wawrzyniak, A., & Balawender, K. (2022). Structural and Metabolic Changes in Bone.

Animals : An Open Access Journal from MDPI, *12*(15). https://doi.org/10.3390/ani12151946

Wei, J., & Karsenty, G. (2015). An overview of the metabolic functions of osteocalcin. *Reviews in Endocrine & Metabolic Disorders*, *16*(2), 93–98. https://doi.org/10.1007/s11154-014-9307-7

Yue, J., & López, J. M. (2020). Understanding MAPK Signaling Pathways in Apoptosis. *International Journal of Molecular Sciences*, *21*(7). https://doi.org/10.3390/ijms21072346

Zhao, Z., Chen, X., Dowbaj, A. M., Sljukic, A., Bratlie, K., Lin, L., … Yu, H. (2022). Organoids. *Nature Reviews. Methods Primers*, *2*. https://doi.org/10.1038/s43586-022-00174-y

Zhu, G., Wang, G., & Li, J. J. (2021). Advances in implant surface modifications to improve osseointegration. *Mater. Adv.*, *2*(21), 6901–6927. https://doi.org/10.1039/D1MA00675D

Capítulo 12

ATIVIDADES DESENVOLVIDAS NO PERÍODO

Estágio no exterior: Programa de Doutorado Sanduíche no Exterior (PDSE) – CAPES. Desde 05 de Setembro de 2022 até 05 de agosto de 2023. ERASMUS MEDICAL CENTER, Rotterdam – Holanda. Orientadores no exterior: Dr. Maikel Peppelenbosch; Drª. Gwenny Fuhler.

Disciplinas cursadas:

- Dinâmica Molecular de Tecidos Mineralizados
- Bioética e Biossegurança
- Microscopia Eletrônica e Ultraestrutura Celular
- Biologia sistêmica: da bioinformática ao wet lab (vetores CRISPR-Cas9 e de super-expressão)
- Biomateriais
- Tópicos especiais em Biotecnologia: Tópicos em Biossegurança e Organismos Geneticamente Modificados (OGMs e AnGMs)
- Bioestatística
- Aspectos Farmacológicos e Bioquímicos da Síndrome Metabólica
- Tópicos Especiais em Genética: Introdução à Bioinformática Genômica de Eucariotos: Como Estudar Genomas Grandes?
- Biologia Celular
- Bioquímica Avançada
- Biologia Molecular
- Farmacologia do Endotélio Vascular
- Química Metabólica da Célula: Carboidratos
- Sinalização Celular
- Citometria de Fluxo: Teoria, Aplicações e Análise de Dados
- Metodologias avançadas e aplicadas em tecidos mineralizados
- Tópicos Especiais em Biotecnologia: 3D-printing: medical applications

Cursos

- Fundamentos da PCR Quantitativa em Tempo Real (qPCR): uma abordagem teórico-prática para as Plataformas QuantStudio 1, QuantStudio 3 e QuantStudio 5. De 11 a 13 de dezembro de 2019. Customer Experience Center da Thermo Fisher Scientific.
- MINICURSO Aplicação de Isótopos Estáveis em áreas biológicas. 10 de agosto de 2020. IBB – UNESP.

- Treinamento Plataforma BATES. Biblioteca da Universidade Nove de Julho. 28 de janeiro de 2021.
- Treinamento Complete Anatomy. Biblioteca da Universidade Nove de Julho. 28 de janeiro de 2021.
- AULA GRATUITA DE HPLC (Introdução à técnica de HPLC com foco em fundamentos da cromatografia; Detalhamento modular; Desenvolvimento analítico e fases estacionárias). 20 de NOVEMBRO de 2021. CIENCO consultoria e capacitação científica.
- Biosafety – working in ML-I and ML-II laboratories. Erasmus MC. 12 de setembro de 2022.

Atuação em Docência

- Estágio Docência na disciplina Química e Bioquímica Animal aos alunos do curso de graduação em Medicina Veterinária. 06 de agosto a 10 de dezembro de 2020 (30 horas). FMVZ – UNESP.
- Aula sobre "Epigenética" para o 3º ano - Noturno do curso de Ciências Biológicas da Faculdade de Ciências – UNESP- Campus Bauru. 02 de novembro de 2020.
- Aula sobre "Epigenética" para o 2º ano - Integral do curso de Ciências Biológicas da Faculdade de Ciências – UNESP- Campus Bauru. 02 de novembro 2020.
- Professora universitária no curso de Farmácia. Universidade Nove de Julho (UNINOVE) de São Manuel (FMR - Faculdade Marechal Rondon). Disciplinas: Microbiologia Clínica, Farmácia Hospitalar, Biotecnologia Farmacêutica, Tecnologia de Cosméticos e Fármacos, Cosmetologia. Setembro de 2020 à abril de 2021.
- Estágio supervisionado remunerado de docência. Disciplina Química e Bioquímica Animal aos alunos do curso de graduação em Medicina Veterinária. 11 de novembro de 2021 a 04 de março de 2022 (120 horas). FMVZ – UNESP.
- Estágio supervisionado remunerado de docência. Módulo: A Célula (Disciplina Bioquímica) aos alunos do curso de graduação em Medicina. 11 de março de 2022 até 12 de agosto de 2022 (120 horas). FMB – UNESP.

Eventos Científicos:

- I Congresso Virtual de Soft Skills – O RESGATE DAS HABILIDADES HUMANAS. 23 de agosto de 2020. CMB educacional.
- I Simpósio de Genética e Biotecnologia da UFJF. 07 a 15 de setembro de 2020.
- VI Jornada Acadêmica Farmácia. UNINOVE - FMR. 23 de novembro de 2020.
- Comissão Organizadora do VI Workshop de Biotecnologia realizado no período de 10 a 12 de agosto de 2021.
- I Encontro de Extensão Universitária no IBB realizado em 02 a 03 de dezembro de 2021.
- Palestra Indicadores de Maturação Óssea - Fundamentos e Aplicações Clínicas nas mais Diversas Áreas. 27 de abril de 2022. Creare educação continuada.

- Brazilian Day at Promega Madison. 30 de maio a 03 de junho de 2022. Promega Corporation, Madison – Wisconsin (EUA).
- Palestra INTRODUÇÃO À TÉCNICA DE CRISPR. 08 de agosto de 2022. Universo da Biologia Molecular.

Resumos em Eventos:

- EPIGENETIC-RELATED CHROMATIN COMPACTION IS REQUIRED ON HYPERTENSIVE-STRESSED ENDOTHELIAL CELL PHENOTYPE (PINTO, T.S., SILVA, R.A., FERNANDES, C.J.C., GOMES, A.M., ZAMBUZZI, W.F.) 48a Reunião Anual da Sociedade Brasileira de Bioquímica e Biologia Molecular. 17 de maio de 2019.

- MODULATORY EFFECT OF TIO_2-ENRICHED MEDIUM ON ENDOTHELIAL CELLS (ALMEIDA,G.S, MARTINS, B.R, PINTO, T.S, ZAMBUZZI, W.F). 48a Reunião Anual da Sociedade Brasileira de Bioquímica e Biologia Molecular. 17 de maio de 2019.

- Adaptive response of endotelial cells in Titanium-enriched Medium *(*Gerson Santos de Almeida, Bruna Rodrigues Martins, Thais Silva Pinto, Willian Fernando Zambuzzi). I Simpósio de Pesquisa e Inovação em Materiais Funcionais" realizado nos dias 23 e 24 de maio de 2019 na Universidade Federal de São Carlos – UFSCar

- MODULAÇÃO EPIGENÉTICA RELACIONADA COM A COMPACTAÇÃO DA CROMATINA É NECESSÁRIA NO FENÓTIPO DE CÉLULAS ENDOTELIAIS ESTRESSADAS DE MODO HIPERTENSO (THAIS SILVA PINTO; ANDERSON MOREIRA GOMES; CELIO JUNIOR DA COSTA FERNANDES; RODRIGO AUGUSTO DA SILVA; WILLIAN FERNANDO ZAMBUZZI). V Workshop de Biotecnologia - WorkBiotech, realizado no(s) dia(s) 11 a 13 de setembro de 2019. IBB – UNESP.

- Coupling of shear-stressed endothelial cell and osteoblasts in responding to Co-Cr-enriched medium (Gerson Santos de Almeida, Célio Junior da Costa Fernandes, Thaís Silva Pinto, Fábio José Bezerra, Willian Fernando Zambuzzi). XX Congress of the Brazilian Society for Cell Biology held online, between January 27th and 29th, 2021.

- MEIO ENRIQUECIDO COM TITÂNIO MODULA VIAS INTRACELULARESRELACIONADAS COM ANGIOGÊNESE EM CÉLULAS ENDOTELIAIS (PINTO, T.S.; MARTINS, B.R.; ZAMBUZZI, W.F.) foi premiado como Melhor Painel no evento VI WorkBiotec, realizado em 10 a 12 de agosto de 2021.

- Meio enriquecido com titânio em condição de alta adipogenicidade modula vias intracelulares relacionadas com angiogênese em células endoteliais (Thaís Silva Pinto; Willian Fernando Zambuzzi), 7° Workshop de Biotecnologia. 27 de setembro de 2022.

- Limonene acts on cell differentiation through modulation of adipogenic factors in 3T3-L1 cells (Assunção, R., Pinto, T.S., Andrade, A.F.C., Emílio-Silva M.T., Zambuzzi, W.F. and Hiruma-Lima C.A.). 54th Brazilian Congress of Pharmacology and Experimental Therapeutics held from 18th-21st October 2022.

Trabalhos submetidos:

- Patente: Pedido de patente de invenção BR 10 2022 026394-9 intitulado "**IMUNOSSENSOR PARA DETECÇÃO DE HEMORRAGIA FETO - MATERNA (HFM) E SEU USO**" perante o INPI. Aline Marcia Marques, Ananda Lini Vieira da Rocha, Andrei Moroz, Elenice Deffune, Ivana Cesarino, Juliana Maziero Azanha, Marjorie de Assis Golim, Marli Leite de Moraes, Martin Kassio Leme da Silva, Pamela Leite da Silva, Sidney José Lima Ribeiro, Suelen de Souza Assunpção Nishio, Thais Silva Pinto, Willian Fernando Zambuzzi.

- Artigo: **Gamma-oryzanol (γOz) rich rice bran promotes osteogenic phenotype of bone marrow-obtained stromal cells**. Thaís Silva Pinto, Jéssica Leite Garcia, Anderson Moreira Gomes, Amanda Fantini de Camargo Andrade, Gerson Santos de Almeida, Camila Renata Correa, Willian Fernando Zambuzzi. *Journal of Nutritional Biochemistry*.

- Artigo: **Contributions of gelatinases-related extracellular matrix remodeling to nuclear mechanisms of gene expression control on endothelial cells.** Gomes, Anderson Moreira; Pinto, Thais Silva; Zambuzzi, Willian Fernando. *Biochemical and Biophysical Research Communications*.

- Artigo: **Epigenetic changes in shear-stressed endothelial cells.** Pinto, Thais Silva; Feltran, Georgia; Fernandes, Célio; Silva, Simone; Abuderman, Abdulwahab; Zambuzzi, Willian Fernando; da Silva, Rodrigo. *Cell Biology International*.

- Artigo: **The biological properties of Co-doped monetite are influenced by thermal treatment.** Almeida, Gerson Santos de; Suter, Luísa Camilo; Pinto, Thais Silva; Feltran, Georgia; Carra, Maria Gabriela Jacheto; Correa, Diego Rafael Nespeque; Saeki, Margarida Juri; Lisboa-Filho, Paulo; Zambuzzi, Willian. *Journal of Biomedical Materials Research: Part B - Applied Biomaterials.*

- Artigo: **Impact of metabolic states on osteoblast response to titanium implants: an in vitro model of high-lipogenesis conditions.** Pinto TS, Schreuders-Koedam M, van der Eerden BC, van de Peppel J, Ayada I, Pan Q, Fuhler GM, Zambuzzi WF, Peppelenbosch MP. *Biomaterials*.

- Artigo: **Effects of intermittent fasting on metabolic dysfunction-associated fatty liver disease are transmissible through fecal transplants.** Junhong Su, Yueying Wang, Ling Wang, Fanglin Li, Kausilia K Krishnadath, Mingfu Ma, Thaís S Pinto, Auke P. Verhaar, Monique M.A. Verstegen, Zhongren Ma, Maikel P. Peppelenbosch. *Nature Metabolism*.

Artigos Publicados:

- **Cobalt-chromium-enriched medium ameliorates shear-stressed endothelial cell performance**. Journal of Trace Elements in Medicine and Biology, 2019. Mariana Issler Pinheiro Machado, Anderson Moreira Gomes, Marcel Ferreira Rodrigues, Thais Silva Pinto, Célio Júnior da Costa Fernandes, Fábio J. Bezerra, Willian Fernando Zambuzzi.

- **Layered Double Hydroxides Are Promising Nanomaterials for Tissue Bioengineering Application**. Advanced Biosystems, 2019. Célio Jr. da Costa Fernandes, Thaís Silva Pinto, Ha Ram Kang, Pedro de Magalhães Padilha, Ivan Hong Jun Koh, Vera Regina Leopoldo Constantino, and Willian F. Zambuzzi.

- **Wortmannin targeting phosphatidylinositol 3-kinase suppresses angiogenic factors in shear-stressed endothelial cells.** Journal of Cellular Physiology, 2019. Anderson M. Gomes, Thais S. Pinto, Célio J. da Costa Fernandes, Rodrigo A. da Silva, Willian F. Zambuzzi.

- **Natural Rubber Latex as Stem Cell Scaffold for Muscle Regeneration.** The FASEB Journal, 2019. Juliana Ferreira Floriano, Carlos Frederico de Oliveira Graeff, Angélica Mércia Pascon Barbosa, João Paulo Marcondes, Thaís Silva Pinto, Willian Fernando Zambuzzi, Marilza Vieira Cunha Rudge

- **Immobilization of paclitaxel on hydroxyapatite for breast cancer investigations**. Langmuir, 2020. Murillo L Martins, Thais S Pinto, Anderson M Gomes, João P R L L Parra, Gilberto C Franchi Jr, Willian F Zambuzzi, Cloves G Rodrigues.

- **PI3K/AKT signaling drives titanium-induced angiogenic stimulus.** Journal of Materials Science: Materials in Medicine, 2021. Bruna Rodrigues Martins, Thais Silva Pinto, Célio Junior da Costa Fernandes, Fábio Bezerra, Willian Fernando Zambuzzi.

- **Metabolic effects of CoCr-enriched medium on shear-stressed endothelial cell and osteoblasts: A possible mechanism involving a hypoxic condition on bone healing**. Materials Science & Engineering C, 2021. Célio Junior da Costa Fernandes, Gerson Santos de Almeida, Thais Silva Pinto, Suelen Aparecida Teixeira, Fábio J. Bezerra, Willian Fernando Zambuzzi.

- **Nanohydroxyapatite-Blasted Bioactive Surface Drives Shear-Stressed Endothelial Cell Growth and Angiogenesis**. BioMed Research International, 2022. T. S. Pinto, B. R. Martins, M. R. Ferreira, F. Bezerra, and W. F. Zambuzzi.

- Artigo: **Adipogenesis-related metabolic condition affects shear-stressed endothelial cells activity responding to titanium.** Journal of Functional Biomaterials, 2023 Thaís Silva Pinto; Anderson Moreira Gomes; Paula Bertin, Fabio Bezerra; Willian F. Zambuzzi.